SPSD II

ATMOSPHERIC NITROGEN INPUT INTO THE NORTH SEA: INORGANIC AND ORGANIC NUTRIENT FLUXES

R. VAN GRIEKEN

PART 2

GLOBAL CHANGE, ECOSYSTEMS AND BIODIVERSITY

- ATMOSPHERE AND CLIMATE
- MARINE ECOSYSTEMS AND BIODIVERSITY
- TERRESTRIAL ECOSYSTEMS AND BIODIVERSITY
- NORTH SEA
- ANTARCTICA
- BIODIVERSITY

.be

SCIENTIFIC SUPPORT PLAN FOR A SUSTAINABLE DEVELOPMENT POLICY
(SPSD II)

FINAL REPORT

Atmospheric Nitrogen Input into the North Sea: Inorganic and Organic Nutrient Fluxes

EV/39

René Van Grieken[1], László Bencs[1,2], Agnieszka Krata[1], Benjamin Horemans[1], Anna Buczynska[1], Alin Dirtu[1,3], Katleen Van Meel[1], Ana F.L. Godoi[1,4], Ricardo H.M. Godoi[1,4], Rodrigo Favoreto[1,4], Sanja Potgieter-Vermaak[1,5], Rob Wuyts[1], Jan Van Loock[1], and Luc Van Vaeck[1]

[1] Micro and Trace Analysis Centre, Department of Chemistry, Campus Drie Eiken, University of Antwerp, Universiteitsplein 1, B-2610, Belgium

[2] Permanent address: Research Institute for Solid State Physics and Optics, Hungarian Academy of Sciences, PO Box 49, H-1525 Budapest, Hungary

[3] Permanent address: Department of Inorganic and Analytical Chemistry, University "Al.I. Cuza" of Iassy, 700506, Romania

[4] Permanent address: Centro Universitário Positivo (UnicenP), Curitiba, Paraná, 81280330, Brazil

[5] Permanent address: Molecular Science Institute, School of Chemistry, University of the Witwatersrand, 2050, Johannesburg, South Africa

BELGIAN SCIENCE POLICY

D/2007/1191/7
Published in 2007 by the Belgian Science Policy
Rue de la Science 8
Wetenschapsstraat 8
B-1000 Brussels
Belgium
Tel: +32 (0)2 238 34 11 – Fax: +32 (0)2 230 59 12
http://www.belspo.be

Contact person: M[r] David Cox

Secretariat: +32 (0)2 238 36 13

Table of content

Acknowledgment 5
Summary 7
1. Introduction 11
2. Inorganic nitrogen: concentrations and fluxes 13
2.1. Experimental ***13***
2.1.1. Sampling campaigns 13
2.1.2. Sampling site description 13
2.1.3. Sampling procedures 13
2.1.3.1. Denuder sampling 13
2.1.3.2. Passive gas-sampling 13
2.1.3.3. Rainwater sampling 14
2.1.3.4. Aerosol sampling 14
2.1.4. Ion-chromatography (IC) 14
2.1.5. Sample preparation for IC analysis 14
2.1.6. Ozone determination 15
2.1.7. Statistical analysis 15
2.1.8. Calculation of air-mass backward trajectories 15
2.1.9. Flux calculations 15
2.1.10. Description of weather conditions 16
2.2. Seasonal/weekly variation of the N-level in gaseous, aerosol and rainwater samples ***17***
2.2.1. Total (inorganic) nitrogen levels in the gaseous and aerosol phases and in rainwater samples 17
2.2.2. N contribution of gaseous compounds in the ambient air 19
2.2.3. Levels of N and other nutrients in size-fractionated particulate matter 21
2.2.4. Weekly N-concentrations from rainwater 22
2.3. Daily variation of the N-level in gaseous phase, aerosol, and rainwater samples ***23***
2.3.1. Total daily N levels from gaseous, aerosol and rainwater samples 23
2.3.2. Daily N contribution of gaseous compounds in the ambient air 24
2.3.3. Daily levels of N-containing compounds and other nutrients in the different size-fractions of particulate matter 25
2.3.4. Evaluation of the daily N-contribution from rainwater 27
2.4. Deposition of nitrogen compounds ***28***
2.4.1 Dry deposition 28
2.4.1.1. Daily average fluxes of gaseous compounds 28
2.4.1.2. Daily average fluxes of aerosols 29
2.4.2. Wet deposition and its comparison with dry fluxes 31
2.4.3. Total (wet+dry) average fluxes 32
2.4.4. Comparison of fluxes with the literature data 33
2.5. Single particle analysis ***33***
2.5.1. Experimental 34
2.5.2. Data interpretation 34
2.5.3. Results and discussion 34
2.6. Literature ***36***
3. Organic nutrient detection 41
3.1. Introduction ***41***
3.1.1. Formation and fate of organic nitrates in the atmosphere; role and occurrence in the environment 41

3.1.2. Analytical procedures for the determination of organic nitrates 43
3.1.3. Limits of detection 44
3.1.4. Purpose of study 44
3.2. Experimental ***44***
3.2.1. Description of the modified high volume (Hi Vol) sampler 44
3.2.2. Sampling and weather data collection procedures 45
3.2.3. Synthesis of reference alkyl nitrate compounds for calibration 46
3.2.4. Extraction and clean-up procedures 46
3.2.5. GC-MS and GC-ECD separation, detection and quantitation 47
3.2.6. Data processing of environmental samples 47
3.2.7. Flux calculations 47
3.3. Results and discussion ***47***
3.3.1. Sampling methodology 47
3.3.2. Analytical methodology 48
3.3.3. Applications to environmental samples 49
3.3.4. Estimation of alkyl nitrate fluxes 50
3.4. Literature ***51***
4. X-ray fluorescence analysis for atmospheric trace metals 55
4.1 Data collection ***55***
4.1.1. Sampling 55
4.1.2. XRF analysis 55
4.1.2.1. Instrumentation 55
4.1.2.2. Statistical treatment 56
4.2. Discussion of the results ***56***
4.2.1. First campaign 56
4.2.1.1. Clustering 56
4.2.1.2. Graphical representations 56
4.2.2 Second Campaign 57
4.2.2.1 Clustering 57
4.2.2.2. Graphical representations 58
4.2.3 Third campaign 59
4.2.3.1 Clustering 59
4.2.3.2 Graphical representations 59
4.2.4 Fourth campaign 60
4.2.4.1 Clustering 60
4.2.4.2 Graphical representations 60
4.3. Conclusions ***61***
4.4. Literature ***61***
Appendix 1 Inorganic nitrogen compoundsTables 63
Appendix 2 Inorganic nitrogen compoundsFigures 77
Appendix 3 Organic Nutrient detectionTables and Figures 143
Appendix 4 X-ray FluorescenceTables and Figures 155

Acknowledgment

The participants of this research gratefully acknowledge the financial support of the Belgian Science Policy (Belspo). They gratefully acknowledge the NOAA Air Resources Laboratory (ARL) for the provision of the HYSPLIT transport and dispersion model and/or READY website (http://www.arl.noaa.gov/ready.html) used in this publication. The participants also wish to thank André Cattrijsse and Frank Broecke (Flanders Marine Institute - VLIZ) for their great help in the sampling and organization of this work, as well as for Francesco Fernandez (VLIZ) for providing the meteorological data from the database of VLIZ. Alin Dirtu acknowledges an EC grant within Marie Curie program HPMT-CT-2001-00310.

Summary

Dry and wet atmospheric fluxes of a large variety of nitrogen-containing inorganic and organic compounds have been studied by means of complementary sampling and analysis techniques applied for gaseous and aerosol phase samples of the ambient air, as well as for the daily precipitation. For this purpose, four sampling campaigns were organized between 2004 and 2006 over various seasons at a coastal site of the Southern Bight of the North Sea at De Haan, Belgium.

On the base of the concentrations of the N-containing nutrients in air, the seasonal/weekly/daily variations in the N-fluxes were evaluated with the assistance of air-mass backward trajectories (BWTs) calculated with the HYSPLIT model and of the meteorological data collected at the sampling site. For this purpose, daily and weekly concentrations and fluxes were classified into different groups of the main air-masses arriving to the sampling site, i.e., (1) continental, (2) North Sea, and (3) Atlantic/Channel/UK.

Inorganic N-containing compounds were detected from the gas phase (i.e., gaseous NO_2, HNO_2, HNO_3, and NH_3), from size-segregated aerosols (NO_2^-, NO_3^-, and NH_4^+), and from rainwater samples (NO_2^-, NO_3^-, and NH_4^+). Organic N-compounds were detected from the gaseous phase (mostly as alkyl nitrates), and also from rainwater samples as dissolved organic nitrogen (DON). Three different size-ranges of aerosols were sampled and analyzed, i.e., with an aerodynamic diameter of >10 μm (coarse), 2.0-10 μm (medium), and 0.4-2.0 μm (fine).

Ammonia has been observed as the highest contributor to the gaseous inorganic nitrogen deposition, comprising around 90 % of the gaseous N-flux, whereas the lowest, negligibly small contribution was found for NO_2. The daily average N-fluxes of HNO_2 and HNO_3 were also relatively low, around 10 % of the gaseous inorganic N-flux.

Outstandingly high N-fluxes of aerosols for the late summer campaign have been observed, with especially high deposition rates of 3.6 and 2.9 mg N/m^2 day for the Atlantic/Channel/UK and North Sea air-masses, respectively. This high level of nutrients at this late summer period, similar to that found for gaseous nitrogen in the same campaign, can be associated with a typical eutrophication event of the coastal region. On the contrary, the other seasons/campaigns experienced average aerosol fluxes of 0.9-1.8 mg N/m^2.day.

For the late summer campaign, the contribution of NH_4^+ to the N-flux from all the three particulate fractions was found to be higher than that of NO_3^-, apart from the North Sea/continental air-mass influenced coarse aerosols, showing about a 5-fold higher flux of NO_3^-.

Over the late winter/spring campaign, the contribution of NH_4^+ to the N-flux was found to be similar to that of NO_3^- in the coarse and medium fractions apart from the continentally influenced aerosols, showing about 2-fold higher contribution.

During the dry mid-summer campaign, the contribution of NH_4^+ to the N-flux was found to be more important in the medium and the fine fractions, whereas NO_3^- was contributing more in the coarse fraction.

Comparing the relative contribution of aerosols observed over various seasons/campaigns, one can see a larger contribution during the late summer campaign from the Atlantic/Channel/UK (48 %) and mixed continental/North Sea (37 %) air-masses, whereas the contribution from North Sea air was found to be low (15 %). For the late winter/spring campaign, continental air contributed more (41 %), while the Atlantic/Channel/UK and North Sea air-masses were contributing equally (~30 %). During the mid-summer campaign, all the three air-masses contributed similarly, each around 33 %.

Thin-window electronprobe microanalysis (TW-EPMA) methods was applied to individual size-segregated aerosol samples of marine and oceanic air-mass origin (assigned with the BWTs) to characterize their morphology and chemical constitution. Since TW-EPMA is able to detect light-Z elements (e.g., nitrogen and oxygen), it could be utilized fruitfully for the identification of the exact composition of sea salt and continental aerosol particles, as well as to draw conclusions on the related atmospheric processes (e.g., sea salt aging, chloride loss/replacement over the continent).

Size-segregated aerosols of continental and marine origin have also been characterized with a sensitive X-ray fluorescence method to assess the concentrations of light, non-metallic elements (e.g., S, Cl), as well as several toxic heavy metals in various air masses. Relative abundancy data suggest that Cl from sea salt and soil dust elements are more abundant in the coarse aerosol fraction. For most samples, S was found to be the most abundant element, followed by Cl. On the other hand, low Cl levels were found in the coarse fraction of aerosols passing over the continent, especially, the industrialized zones. The concentrations of heavy metals (e.g., Pb, Zn, Ti, and V) were found to be increased from aerosol samples that had passed over industial and continental regions compared to marine aerosol, but their levels were found to be lower than 10 ng/m^3.

The average dry and wet fluxes were found to be 2.8 and 3.4 mg N/m^2 day, respectively, over the autumn/early spring, the late winter/spring, and the mid-summer campaigns. However, both the dry and wet fluxes were considerably higher during a typical eutrophication event (e.g., during the late summer (August 2005) campaign), i.e., 5.4 and 5.6 mg N/m^2 day, respectively.

Dry fluxes of N-compounds have been proved to be important contributors to the total N-budget of the coastal sampling site. This rather unexpected result can be explained on the base of the large number of days without any precipitation during the sampling campaigns, which made possible the extent of dry flux approach that of the wet one.

For organic nutrient detection in atmospheric samples, a high volume air sampling method combined with liquid extraction and pre-concentration of the samples, followed by gas-chromatography mass-spectrometry based analytical methods has been elaborated and applied to the separation and quantification of a large set of alkyl nitrate (AN) compounds, generally present at the ultra-trace (pg/m^3) level in the ambient air. The applicability and robustness of the developed analytical methodology has been demonstrated on a large set of air samples, collected at the sampling site, De Haan over various seasons/campaigns.

Over the summer campaigns, eleven ANs have been identified and quantified, but only eight ANs were detected to be present in the late winter/spring samples. From these concentration data of ANs, the extent of their deposition for the Southern North Sea could be estimated.

By comparing the results of the summer and late winter/spring campaigns, a much higher percentage of AN contribution to the N-flux by the Atlantic/Channel/UK air-masses can be experienced during summer (i.e. ~60 % of the total average AN-flux), whereas in the late winter/spring campaign, the fluxes from the North Sea and the continental air-masses were prevailing, i.e., 38 % and 43 %, respectively.

Fluxes of ANs have been found to be more pronounced for the summer periods than for the winter/spring months. Although their contribution to the total (inorganic and organic) N-flux has been found to be low, i.e., ranging between 10-40 ng N/m^2 day, it was high enough to be commensurable with the fairly low fluxes of NO_2 experienced for sea-surfaces.

Over the fairly dry mid-summer period, under continentally influenced air-masses, the dissolved organic nitrogen (DON) content of rainwater samples was found to be a significant contributor (around 45 %) to the total N-budget.

In comparison with the relevant literature data, the overall fluxes of the present study are comparably higher than the waterborne N-inputs from rivers in the catchment area of the North Sea. This fact raises more concern about the atmospheric N-emission originating mostly from traffic and industrialized zones along the coastal regions of the Southern North Sea. The intensive ship traffic through the North Sea contributes to the atmospheric N-deposition as well. This addresses more questions on the impact of atmospheric nitrogen at coastal regions. Moreover, it demands more studies on the atmospheric deposition of nitrogen, including the refinement of both model and experimental approaches, as well as the refinement of the reported emission/depostion data on nitrogen.

The nitrogen flux data offered in this study can be successfully utilized as an input to mathematical models concerning the calculation of dry and wet depositions over the North Sea. These approaches make the estimation of the extent of eutrophication of the North Sea possible, a process, which is proved to imply a significant economic impact on the surrounding countries exploiting this area.

1. Introduction

The Greater North Sea, a regional sea of North Europe, has a surface area of around 775 800 km^2, including the British Channel with an area of 89 620 km^2. It has a long history of multiple uses by people from many nations surrounding this maritime area. The growing anthropogenic activities have significantly increased the input of nutrients to the North Sea during the past decades. Particularly, the biologically available inorganic and organic nitrogen-containing compounds cause proliferation of harmful algal blooms and other eutrophication phenomena, affecting the marine ecosystem, thus fisheries and tourism. Therefore, the atmospheric nitrogen-input, especially at coastal regions, triggers increasing interest in the scientific community. Specifically, the atmospheric nitrogen fluxes, in terms of inorganic and organic nitrogen, is important to be assessed by both experimental and model approaches, particularly, to get an insight into the extent of eutrophication in coastal regions.

Connecting to this central environmental topic, the OSPAR Convention has been formulated, which is a regional convention for the protection of the marine environment of the Northeast Atlantic to which the European Community and several other countries are contracting parties (Bartnicki and Fagerli, 2006). One of the objectives of this convention, organized as "Eutrophication Strategy", is to achieve and maintain a healthy marine environment by 2010, where eutrophication does not occur. This strategy is implemented through measures in reducing anthropogenic emission, discharges, and losses of nutrients in all areas from which nutrient input is possible, c directly, or indirectly, to contribute to inputs to areas with regard to eutrophication. The implementation is supported by the OSPAR Joint Assessment and Monitoring Program (JAMP) of waterborne inputs through the OSPAR Comprehensive Study on Riverine Inputs and Direct Discharges (RID) and of atmospheric inputs though the OSPAR Comprehensive Atmospheric Monitoring Programme (CAMP). This work is also supplemented by gathering information from international bodies out of the OSPAR.

In support of this work a first report on "Atmospheric Nitrogen in the OSPAR Convention Area 1990-2001" (Bartnicki and Fagerli, 2003; 2004) had been prepared. These studies as well as the OSPAR assessment of the CAMP data (OSPAR Commission, 2005a; 2005b) suggest that atmospheric nitrogen inputs appear to play a major role for certain OSPAR Convention waters, including the North Sea.

Emission sources of nitrogen influencing the North Sea are mostly of anthropogenic origin, i.e., national emissions for NO_2 and NH_3. An additional and very important emission source of NO_x is the international ship traffic (Bartnicki and Fagerli, 2006).

The role of atmospheric nitrogen in the total fluxes to the North Sea as well as the related chemical and biological processes has been a subject of several experimental and model studies, documented in the relevant literature of the marine research (e.g., Rendell et al., 1993; Beddig et al., 1997; Hertel et al., 1995, 2002; Peierls and Paerl, 1997; de Leeuw et al., 2003). Most of these studies are related to atmospheric supply of inorganic and organic nitrogen mostly on the base of model studies. They however, do not cover some important species, such as alkyl nitrates, which groups of compounds may play a significant role in atmospheric processes (Roberts, 1990), particularly, by contributing to the nitrogen-flux of coastal regions, as well as to eutrophication. They have also not given an account on the sampling and analysis of size-segregated aerosols; the results acquired could also give an

insight into the chemical processes, taking part at marine and coastal regions of the North Sea. Moreover, the transport of nitrogen compounds from diverse regions surrounding the North Sea has not yet been discussed on the base of using air-mass backward trajectories (BWTs) to assign the various polluted air-masses contributing to coastal eutrophication events.

Considering the above facts, the main objectives of this atmospheric monitoring study were as follows:

- to quantify the fluxes of nitrogen compounds at a coastal site of De Haan in terms of wet and dry deposition from atmospheric samples (gaseous, aerosol, and precipitation);
- to compare and contrast temporal differences in concentrations of nitrogen compounds deposited at De Haan;
- to elaborate analytical chemical methods of high sensitivity and selectivity for the detection and quantification of the most abundant organic compounds (e.g., alkyl nitrates) in coastal/marine regions;
- to quantify the concentration and the contribution of the major nitrogen compounds, such as nitrite, nitrate, ammonium, as well as organic nitrogen, to atmospheric deposition.

2. Inorganic nitrogen: concentrations and fluxes*

2.1. Experimental

2.1.1. Sampling campaigns

Four sampling campaigns were organized over the years 2004-2006, to cover the yearly/seasonal variations in the deposition of nitrogen compounds.
The schedule of the campaigns was the following:

- Autumn/early winter campaign (August 21st, 2004 - January 31th, 2005)
- Late summer campaign (August 8th -21st, 2005)
- Late winter/spring campaign (February 14th - April 30th, 2006)
- Mid-summer campaign (June 12th - August 8th, 2006)

2.1.2. Sampling site description

The sampling site selected for this study, De Haan, Belgium is a small village at the coast of the North Sea located at coordinates 51.172 N, and 3.037 E. The area at which the sampling equipment was deployed is a small research station of VLIZ, located some 300 m of the coast among the sand-dunes, it being characteristic for the region.

Generally, the weather over the Belgian-coast is qualified as moderate with mild winter and summer seasons, and considerable yearly precipitation. The key meteorological parameter, such as air temperature (T_{air}), air pressure (p_{air}), relative humidity, wind-speed, wind direction, and precipitation rate, which play an important role in the air quality, were logged during the sampling campaigns. In the 1st and 2nd campaigns, the meteorological data were obtained from a meteorological database (IVA MDK - afdeling Kust - Meetnet Vlaamse Banken), whereas in the third and fourth campaigns, from a small meteorological weather-station deployed at the sampling site by colleagues from VLIZ. The weather data of this station were logged in every second by a computer.

2.1.3. Sampling procedures

2.1.3.1. Denuder sampling

Gaseous nitric- and nitrous acid, and ammonia, were sampled actively with a URG-2000-01K denuder every day for 6 days of every week during each sampling campaign. The denuder tubes were coated with 1:1 solutions of 2% aqueous sodium carbonate plus 2% glycerine in methanol, and a 1% citric acid in methanol, for the collection of acidic and alkaline gases, respectively. The air flow rate was set to 10 dm^3/min.

2.1.3.2. Passive gas-sampling

Gaseous nitrogen dioxide and sulphur dioxide as well as ozone were sampled passively with diffusion tubes of Radiello 166 and 172, respectively, on a weekly basis for every week of the 2nd, 3rd and 4th campaigns.

* Tables and Figures corresponding to references throughout this section can be found in appendices 1 and 2, respectively.

2.1.3.3. Rainwater sampling

The daily precipitation was sampled with an automatic sequential rainwater sampler (Eigenbrodt, type ARS 721/S) every day of the week for both campaigns. The sampler is programmable for a period of 8 days, using a timer and a multi-valve to direct the rain to one of the 8 different storage vessels. To avoid contamination from dry deposition, a closable funnel is commanded by a rainwater sensor. For comparison, rainwater was also collected with a pluviometer in the 3rd and 4th campaigns.

2.1.3.4. Aerosol sampling

Size-segregated particulate matter was collected with a stacked filter unit in 3 size fractions, i.e. with cut-offs of 0.4, 2 and 10 μm, 6 days of each week, for bulk cationic and anionic (ammonium, nitrite and nitrate) analysis by IC. The filter unit was attached to a vacuum pump. The pump maintained an air-flow rate of around 60 m^3/day.

2.1.4. Ion-chromatography (IC)

A Dionex Model DX-120 ion chromatograph, equipped with Dionex IonPack CS12A cation and AS14 anion exchanger columns and conductivity detection, was applied for the determination of various ionic species. For sample introduction, both the standard and sample solutions were injected through a 20 μl loop. The eluents applied for the anion and cation exchangers were 3.5 mM Na_2CO_3 plus 1.0 mM $NaHCO_3$, and 11 mM H_2SO_4, respectively, with flow rates of 1.2 and 1.0 ml/min. For the detection of ions, the conductivity of the solution was monitored. For the suppression of the conductivity of the eluent, the ASRS-ULTRA and CSRS-ULTRA suppression columns were applied for the anion and cation exchanger, respectively. The retention times of the peaks were used for the assignment of diverse ions in the sample solutions. Calibration was made against two sets of standard solutions, each consisting of five solutions of the measured anions and cations, respectively. Three replicate measurements were performed for each sample/standard solution, from which data the average and the standard deviation (SD) values were calculated.

2.1.5. Sample preparation for IC analysis

Water-soluble fraction of aerosols (ionic compounds) (e.g., ammonium, nitrate and nitrite salts) were quantitatively analysed by means of IC. Filters were exposed to ultrasonic aided aqueous leaching and the leachate solutions were analysed for NH_4^+, NO_2^- and NO_3^-.

For the analysis of gaseous nitric and nitrous acid and ammonia, the absorber-tubes of the denuders were eluted with 10 ml ultrapure water (MILLI-Q) and the solutions were analyzed with IC for their NO_2^-, NO_3^- and NH_4^+ content.

The N-containing compounds in rainwater samples were analyzed for the presence of NH_4^+, NO_2^- and NO_3^- using IC as described above. Moreover, dissolved organic nitrogen (DON) was determined from the rainwater samples by an indirect method, i.e., the organic N-content of rainwater samples was oxidized with an oxidizing agent and the assistance of a microwave oven (Milestone Ethos, Microwave Laboratory Systems, Sorisole, Italy). For this purpose, an oxidizing agent was prepared from 50 g $K_2S_2O_8$, and 30 g H_3BO_3 dissolved in 350 ml of 1.0 M NaOH, and diluted to 1000 ml with ultrapure water. Then, 2.0 ml of this oxidizing agent was added to a 10 ml aliquout of the rainwater sample in a TMF vessel, and exposed to the following microwave oven program: 500 W for 5 min, 600 W for 15 min, 0 W for 15 min and 0 W for 30 min. Then the total (inorganic+organic) N-level as NO_3^- was

determined with IC as above, and the DON was calculated by subtracting the inorganic N-content determined as aforementioned.

2.1.6. Ozone determination

During exposure in a passive diffusion tube, 4,4'-dipyridylethylene is transformed into 4-pyridylaldehyde through ozonolysis. After a Milli-Q water extraction the corresponding yellow-coloured azide is subsequently formed by adding 3-methyl-2-benzothiazolinone hydrazone (MBTH) to the solution. The absorbance is measured by means of a double beam UV/VIS spectrophotometer at 430 nm.

2.1.7. Statistical analysis

The data was statistically treated using the SPSS software package (version 13.0). The discussion of the results throughout this work is mostly based on the nitrogen contribution of various nitrogen-containing compounds to the "total" nitrogen level. We also used the concentrations of individual compounds for comparison with other literature data. The former data represent the appropriate form of summing up the contribution of diverse N-containing compounds from the gaseous and condensed (aerosol) phases of the ambient air, and also make quantitative comparison between these species possible.

2.1.8. Calculation of air-mass backward trajectories

In order to evaluate the movement of air-masses during sampling and/or to assign the possible origin of gaseous and aerosol phase pollutants, air-mass backward trajectories (BWTs) were calculated for each day of the sampling campaign using the Hybrid Single-Particle Lagrangian Integrated Trajectory (HYSPLIT) Model (Draxler and Rolph, 2003). The initial parameters used for the BWT calculations can be seen in Table 1.1.

According to earlier experiences on coastal air-quality monitoring, it was expected that the selection of proper sampling period (days) allows eliminating or at least minimizing the anthropogenic impact of various industrialized zones, e.g., Dunkerque in France close to the Belgian border, and/or those from the United Kingdom, whose emission may considerably influence the composition of aerosols and gases sampled at the selected coastal site (De Haan). This important consideration has to be always taken into account, when one makes an approach to the evaluation of the eutrophication of the Southern Bight of the North Sea on the base of air quality data received at a coastal region.

2.1.9. Flux calculations

The nitrogen deposition (flux) originating from various gaseous and aerosol phase compounds was calculated with the application of experimentally determined deposition rates of each compound and/or aerosol fraction for oceanic area, i.e., air-water interface (Hertel et al., 1995; Cohen, 1998). The daily data were assorted according to the origin of main air-masses, i.e., Atlantic/Channel, North Sea, and continental. From these data, the average fluxes, and their fluctuations (expressed as the standard deviation – SD), and the total N-contributions were calculated.

2.1.10. Description of weather conditions

1st campaign During this autum/early winter campaign, the daily average air-temperature (T_{air}) ranged from -3 ^{o}C to 26 ^{o}C, while the daily average air-pressure (p_{air}) was between 985-1033 hPa. The wind-speed was ranging from 0.2 to 30 m/s, with an average value of 5.3 m/s. The main wind-directions were observed from southwest, west, northwest, north, i.e., air-masses arrived to the sampling site from the North Sea or from the Atlantic Ocean through the Channel and/or the UK. Continental winds were also frequently observed during the campaign from south and east. According to the frequent contribution of humid air from the Ocean, and/or the North Sea, the amount of precipitation was ranging up to 3.8 mm/day.

2nd campaign During this short summer campaign, the daily average air-temperature (T_{air}) ranged from 11 ^{o}C to 24 ^{o}C, and the daily average air-pressure (p_{air}) between 1008 and 1024 hPa. The wind-speed was ranging from 1.1 to 18 m/s with an average value of 4 m/s. The main wind-directions were observed from north-northwest, west and southwest, i.e., air-masses arrived to the sampling site from the North Sea or from the Atlantic Ocean through the Channel and/or the UK/continent. According to the contribution of some humid air-masses from the Ocean, and/or the North Sea, the amount of precipitation was ranging up to 2.5 mm/day with a mean value of 0.8 mm/day.

3rd campaign During the third late winter and spring campaign, the daily average air-temperature (T_{air}) ranged from -1 ^{o}C to 14 ^{o}C, while the daily average air-pressure (p_{air}) was between 986 and 1033 hPa. The relative humidity (RH) was usually high, i.e., it fluctuated daily between 59 and 97 %. The daily average wind-speed was ranging from 0.8 to 4.5 m/s with an average value of 2.3 m/s. The main wind-directions were from southwest and south-southwest, i.e., air movement from the continent and the Atlantic Ocean. According to the frequent contribution of humid air-masses from the Ocean, and/or the North Sea, the extent of precipitation was ranging up to 13 mm/day with a mean value of 1.5 mm/day.

4th campaign During this summer campaign, the daily average air-temperature (T_{air}) ranged from 13 ^{o}C to 26 ^{o}C, and the daily average air-pressure (p_{air}) between 1005 and 1030 hPa. The relative humidity (RH) was usually high, i.e., it being fluctuated daily between 55 and 83 %. The daily average wind-speed was ranging from 0.8 to 11 m/s with an average value of 3.2 m/s. The main wind-directions were south, southeast, and southwest, i.e., air movement from the continent and the Atlantic Ocean. Only low levels of precipitation have been observed during this dry sampling period, i.e., the amount of rain was ranging up to 12 mm/day with a mean value of 0.5 mm/day.

The amounts of precipitation found for all campaigns are somewhat lower compared to those from former studies over Flanders (Van Grieken et al., 2003). In this earlier study, a considerable extent of precipitation was observed for two subsequent sampling campaigns from September 2001 till April 2003, at six different sampling location over the Flanders, i.e., 2.25 mm/day (observation of 285 days), and 2.05 mm/day (observation through 284 days), respectively. An overview of the meteorological parameters is presented in Tables 1.2 and 1.3, while the variation in these parameters is depicted on Figs. 2.1-2.4.

2.2. Seasonal/weekly variation of the N-level in gaseous, aerosol and rainwater samples

2.2.1. Total (inorganic) nitrogen levels in the gaseous and aerosol phases and in rainwater samples

The overview of the weekly variation in the total average N concentration, - obtained from the denuder (gaseous HNO_2, HNO_3, and NH_3), filter (NO_2^-, NO_3^-, and NH_4^+), and rainwater (NO_2^-, NO_3^-, and NH_4^+) sampling, - is depicted on Figs. 2.5-2.8. We attempted to assign the variation in the N level in the ambient air and in the rainwater samples on the base of BWTs. For this purpose, the weekly air-masses were qualified to different groups, (1) continental, (2) North Sea, and (3) Atlantic/Channel/UK. The assignment of the third group needs some explanation. The air-masses arriving from the Atlantic Ocean through the British Channel are generally passing over land (coastlines of North France and/or the UK). Thus, for these air-masses, some anthropogenic influence, hence elevated pollutant levels are, usually expected. Certainly, there were some exceptional days of the sampling with Atlantic influenced air-masses only.

1st campaign The weekly values of total gaseous and rainwater N (inorganic) ranged up to 3.7 $\mu g/m^3$ and 1.4 mg/l, respectively (Fig. 2.5). It is to be noted here that NH_3 was sampled till the 7^{th} week of the campaign.

The 2^{nd} to 4^{th} weeks of the sampling campaign experienced air-masses from the Atlantic/UK/Channel. Accordingly, the total levels of gaseous N nutrients did not show considerable fluctuation, ranging between 2.7-2.9 $\mu g/m^3$, whereas the total N-level in the rainwater samples fluctuated from 0.17 to 1.4 mg/l. The 5^{th} week of the sampling was characterized by similar Atlantic/continental air-masses and with similar weekly nutrient loadings as the former weeks, and low level of total N in the rainwater (0.28 mg/l). The 6^{th} week of the sampling has shown a mixed Atlantic/continental/North Sea influence, with higher total N loading in gaseous and rainwater samples, 3.9 $\mu g/m^3$ and 0.75 mg/l, respectively. The 8^{th} and 9^{th} weeks were characterized with dry Atlantic/UK/North Sea air-masses, and thus with higher total gaseous acid levels than the previous weeks. The 10^{th} to 12^{th} weeks of the sampling was characterized by Atlantic/UK/North Sea/continent mixed air-masses, which brought low levels of N-nutrients in rainwater samples, varying between 0.34-0.96 mg/l. The last weeks of the sampling were characterized with continental and/or Atlantic/continental/North Sea air-masses and with low levels of total gaseous (acidic) N-nutrients.

2nd campaign The weekly values of total gaseous, aerosol and rainwater N (inorganic) ranged between 2.4-3.3, 1.7-1.9 $\mu g/m^3$, and 1.0-25 mg/l, respectively, with average values of 2.8, 1.8 $\mu g/m^3$, and 13 mg/l, respectively (Table 1.4).

On the first week of this campaign, a mixture of Atlantic/Channel/UK and North Sea air-masses was mostly observed with only a little influence of the continent (i.e., North France). This period was found to be with a fairly high gaseous and aerosol contribution, and experienced some daily precipitation as well, which is manifested in the high N-levels in the rainwater samples.

On the other hand, during the 2^{nd} week of the campaign increasing levels of total N-nutrients were observed, due to the dry period and continental influence. The decrease in their total N-level also occurred, when the winds brought clearer marine (North Sea) air to the observation site.

3rd campaign The weekly concentrations of total gaseous, aerosol and rainwater N (inorganic) were ranging between 1.3-4.2, 0.6-3.0 $\mu g/m^3$, and 0-2.8 mg/l, respectively, with average values of 2.1, 1.6 $\mu g/m^3$, and 1.3 mg/l, respectively (Table 1.5).

The 1st and 4th weeks of the sampling campaign mostly corresponds to the influence of the Atlantic/Channel air-masses. The average concentrations of N from gaseous compounds and aerosols were observed to range between 1.2-2.5 and 0.7-0.9 $\mu g/m^3$, respectively, whereas for rainwater samples values around 0.95 mg/l were obtained. Apart from the N level originating from gases, these data are somewhat lower than the weekly average values obtained for the sampling campaign as above (Table 1.5). The higher N contribution from gases indicates some small influence of anthropogenic emission from the continent and/or UK on Atlantic/Channel air-masses (Fig. 2.9).

The 2nd and 5th weeks of the sampling were characterized with a purely continental influence of air-mass movements, together with a drier weather, and a lower quantity of precipitation (Table 1.2). This was manifested by a significantly enhanced level of N-nutrients in aerosols for both weeks, i.e., 2- and 3-fold, respectively, compared to those of the first week (Table 1.5). Also a 2.7-fold increase was found for N in rainwater collected on the 2nd week compared to that of the 1st week. The level of N from gaseous compounds, however, only slightly increased (up to 2.8 $\mu g/m^3$ in 2nd week) or decreased (to 1.6 $\mu g/m^3$ on 5th week). This is likely due to the dry weather conditions during these weeks, which promotes the secondary aerosol formation of nitrates from NO_2. The 2-fold increase of the N levels in the total aerosol fraction, compared to the weekly average, supports this assumption.

For the 3rd, 4th and 10th weeks of the campaign, the BWTs showed rather mixed air-mass movements, mostly from the Atlantic Ocean/Channel, with air-masses also from the North Sea and/or the continent. Thus, effects of some anthropogenic sources from these sites on the air-quality at the observation site might also be possible. Accordingly, the level of N from gases (denuder) decreased to half of the value found in the 2nd week with pure continental influence. The total N levels in the rainwater samples for the 3rd and 4th weeks scored at almost the same level (~1.25 mg/l) as calculated for the first week with some Atlantic/Channel/UK influence.

The 7th, 8th, 9th, and 11th weeks were characterized with air-mass movements from the Atlantic/Channel/UK. The total N concentrations from gases decreased, whereas those of aerosols increased. Apart from the 11th week, the N level was also significant in the precipitation (1.7-2.8 mg/l).

The 5th, 10th and 11th weeks of the sampling were characterized by dry air-masses without any significant precipitation. As known from the literature, precipitation plays an important role in the removal of both gases and suspended particulates from the ambient air through wash-out and scavenging (Ravindra et al., 2003). Thus, its absence usually leads to an increase in the level of air-pollutants. Accordingly, a rather drastic, around 4-fold increase of N concentration in the airborne suspended matter was observed for the 5th week (i.e., 3.0 $\mu g/m^3$). However, the N level in gases only slightly increased compared to the levels found for the third and fourth weeks.

Surprisingly, for the 6th week of the campaign, the total contribution of N from gases considerably increased (i.e., by 2.6-fold). This week was also characterized by fairly mixed air-mass movements from the Atlantic Ocean and/or the continent. It is very likely that the rather high N level, found in the gaseous phase (4.2 $\mu g/m^3$) and rainwater (2.0 mg/l) samples, was due to the higher influence of nearby emission sources (e.g. the industrial area of Dunkerque in France) from the prevailing wind-direction on this week (Table 1.2), and the wash-out of air pollutants by precipitation, compared to the other weeks of the campaign.

4th campaign During this campaign, the weekly concentrations of total gaseous, aerosol and rainwater N (inorganic) were ranging between 1.1-3.6, 0.3-1.5 μg/m^3, and 0-7.0 mg/l, respectively, with average values of 2.6, 0.9 μg/m^3, and 1.8 mg/l, respectively (Table 1.6).

Continental and mixed continental-marine air-masses generally provided higher total N-levels in the gaseous and aerosol phases than the Atlantic/Channel air-masses. This was characteristic for the 1st, 3rd, 4th, 5th and 6th weeks of this campaign. Although the 7th week was also with a mixed continental-Atlantic-Channel influence, it has shown the lowest total N-concentration of the gaseous and aerosol N-compounds. Low N-levels were also observed for the second week of the campaign with Atlantic/Channel/UK influence. Due to the observed low weekly levels of precipitation, the N-level of rainwater samples were also fairly high.

2.2.2. N contribution of gaseous compounds in the ambient air

1st campaign Weekly concentrations of gaseous HNO_2, HNO_3, and NH_3 from the denuder sampling were found to be between 0.1-0.6, 0.02-0.36, and 2.4-4.2 μg/m^3, with average values of 0.28, 0.09 and 3.0 μg/m^3, respectively (Fig. 2.10). It is to be noted here that NH_3 was sampled till the 7th week of the campaign.

The 1st to 4th weeks of the sampling campaign experienced air-masses from the Atlantic/UK/Channel. Accordingly, the levels of gaseous N nutrients did not show considerable fluctuation, ranging between 2.4-2.7 and 0.25-0.44 μg/m^3 for NH_3 and HNO_2+HNO_3, respectively. The 5th week of the sampling was characterized by similar Atlantic/continental air-masses and with similar weekly nutrient loadings as the former weeks. The 6th week of the sampling has shown a mixed Atlantic/continental/North Sea influence, and an increased NH_3 level (3.7 μg/m^3). The 8th to 11th weeks were characterized with Atlantic/UK/North Sea air-masses, which supplied higher gaseous acid levels than the previous weeks, ranging from 0.35 to 0.55 μg/m^3 for HNO_2+HNO_3. Similarly increased gaseous acid levels were observed during the 12th, 13th and 16th weeks of the sampling with Atlantic/continent/North Sea, and Atlantic/UK/continent mixed air-masses. Interestingly, low levels of these gases (0.23 μg/m^3) were observed on the 14th week of the campaign, despite the continental air-masses influence. Similarly low concentrations (0.22-0.39 μg/m^3) were observed on the rest weeks of the campaign, although these weeks were all characterized with mixed air-mass movements from the Atlantic/continent/North Sea. This is possibly due to the dry and colder weather conditions, which does not favour the formation of these acidic gases.

2nd campaign The weekly levels of gaseous HNO_2, HNO_3 and NH_3 from the denuder sampling were found to be between 0.25-0.29, 0.29-0.30, and 1.81-2.67 μg/m^3, respectively. The weekly average NH_3 levels were found to be 6-7-times higher than the acidic gases detected with the denuder. The 1st week of the campaign experienced less NH_3 level, due to scavenging by precipitation. However, the first part of the 2nd week experienced an increased level of N, due to the influence of some dry and polluted air from the continent.

The weekly concentrations of NO_2 for the 1st and 2nd weeks of the sampling were 8.6 and 12.6 μg/m^3, respectively. These data are in line with the higher extent of anthropogenic influence (i.e. mixed continental-marine air-masses) experienced for the 2nd week of sampling.

3rd campaign The weekly variations in the concentrations of gaseous HNO_2, HNO_3, and NH_3 from the denuder sampling together with the total (denuder) N levels are depicted in Fig. 2.12.

The weekly concentration of N (NO_2) was varying from 0.8 to 7.8 μg/m^3 with an average value of 3.5 μg/m^3. The level of NO_2 has shown good correlation with that of ozone, the latter being ranged from 1.3 to 7.8 μg/m^3 with an average value of 3.6 μg/m^3.

The contribution of gaseous acids to the total N level is generally one order of magnitude lower than the N contribution from NH_3. This finding can be explained on the base of former studies conducted in Flanders (Van Grieken et al., 2003). In this region, the ambient air is characterized with a higher level of NH_3 (daily average: 2-6 μg/m^3), mainly originating from agricultural activities (animal husbandry and fertilization), compared to the levels of gaseous HNO_2 and HNO_3 (typically: 0.3-4.0 and 0.2-1.0 μg/m^3, respectively, Van Grieken et al., 2003). Moreover, NH_3 is not transported to long distances in the ambient air, and rapidly converted to NH_4^+ aerosols with a rate of 30 % h^{-1} (Asman and Van Jaarsveld, 1991). Thus, it may react with the acidic components of the ambient air (e.g., HNO_2 and HNO_3), and may significantly contribute to the secondary aerosol formation over the site. So, it is expected that the presence of NH_3 in the air should be lower, when the air-masses reach the sampling location from the Ocean, and/or the North Sea, since the NH_3 emission from the marine environment is significantly lower than that from the continent, e.g., 0.07 μg/m^3, typically for the North Sea under calm sea conditions, although some ship-board campaigns have shown a concentration of 0.06-2.4 μg/m^3 (Lee et al., 1998). These findings indicate that the North Sea may be a source, but more often represents a sink for NH_3 as expected from the literature (Lee et al., 1998).

A comparison between the weekly N levels of gaseous HNO_2 and HNO_3 (cumulative data of 6 days with denuder sampling) and that of NO_2 (diffusion tube sampling on weekly base) is shown on Fig. 2.13. As can be seen, a quite low level N from the gaseous acids was found i.e., ranged up to 1.1 μg/m^3 during the whole sampling period, whereas the N level from NO_2 was generally observed to be significantly higher (between 1.3-9.0 μg/m^3). Only exception was the first week, when the N concentrations from acidic components were found in the same range as that from NO_2. This is possibly due to the channel (Oceanic air-mass movements, which are not affected by the production of ammonium salts from NH_3 and the acidic components of the air in the coastal region). It was also observed that the level of HNO_2 and HNO_3 follows the weekly trend in the change of NO_2 level, which may be a proof on the precursor role of the latter compound in those processes producing the gaseous acids concerned.

Comparison of the presently achieved mean HNO_2 and HNO_3 levels (0.44 and 0.48 μg/m^3, respectively) with the data of former observations (Van Grieken et al., 2003) at the rural site of Wingene for the spring campaign in 2002, (i.e., average of 0.5 and 0.3 μg/m^3, respectively), reveals a fairly good agreement.

4th campaign The weekly average N-levels from gaseous HNO_2, HNO_3, and NH_3 from the denuder was found to be fluctuating between 0.03-0.14, 0.12-0.26, and 0.85-3.2 μg/m^3, respectively (Fig 2.14). The weekly concentration of N (NO_2) was varying from 0.8 to 7.8 μg/m^3 with an average value of 3.5 μg/m^3. From passive diffusive sampling, the weekly level of N (NO_2) was ranging between 2.3 and 10.3 μg/m^3 with an average value of 7.3 μg/m^3, whereas SO_2 level from 0.8 and 7.8 μg/m^3 with an average value of 3.5 μg/m^3. The level of NO_2 has shown anti-correlation with that of ozone, the latter being ranged from 6.9 to 13.2 μg/m^3 with an average value of 9.6 μg/m^3. This higher level of ozone was also expected due to the more intense solar radiation during this sampling period compared to the winter/spring (3rd) campaign.

Low levels of NH_3 were observed for the 2nd and 7th weeks of sampling mostly with Atlantic/Channel/UK or mixed continental-Atlantic air-masses, whereas continental and/or

North Sea air-masses supplied enhanced N-concentrations over the site. This campaign was in a summer period without any considerable amount of precipitation, thus the weekly levels of pollutants have not shown any considerable temporal change, even though the changes in the origin of air-masses.

2.2.3. Levels of N and other nutrients in size-fractionated particulate matter

The weekly average N levels for the different size-fractions of aerosol particles sampled with the three-stage filter unit are depicted on Figs. 2.15-2.17. The diverse size-fractions represent airborne particles with an aerodynamic diameter (AD) of >10 μm (coarse), 10 μm >AD> 2.0 μm (medium), and 2.0 μm >AD> 0.4 μm (fine).

2nd campaign In the late summer campaign, the weekly contribution of various size-fractions to the total N level in aerosols is depicted in Fig 2.14. It can be seen that the medium and the coarse fractions contributed to the total N to a rather high extent, i.e., their weekly level varied between 0.8-1.0 and 0.4-0.8 $\mu g/m^3$. The fine fraction of aerosols contributed less significantly to the total N content of aerosols, i.e., its weekly level was ranging between 0.3-0.4 $\mu g/m^3$. Apart from the coarse fraction, the contribution of NH_4^+ to the total N-loading of each particulate fraction is always significantly higher (about 2-fold) than the N contribution from NO_3^- (Fig. 2.18)

3rd campaign During the late winter/spring campaign, generally, the coarse fraction contributed to the total aerosol N only to a small extent (i.e., 16 % of the total aerosol N), i.e., its level varied between 0.04-0.37 $\mu g/m^3$, as can be seen on Fig. 2.16. On the other hand, the medium and fine fractions of aerosols contributed significantly to the total N content of aerosols, i.e., 33 and 51 %, respectively. The N levels from these two fractions varied to a large extent, i.e., between 0.18-0.64 $\mu g/m^3$ and 0.17-1.9 $\mu g/m^3$, respectively. Generally, the contribution to the total N level was higher from continental and/or North Sea aerosols, although the Atlantic/Channel air-masses also contributed to the N level, mostly to the finer fractions.

The weekly concentration variation and the distribution of N-containing compounds between the diverse aerosol fractions are depicted on Fig. 2.19. The contribution of NH_4^+ to the total N loading of each particulate fraction is always significantly higher than the N contribution from NO_3^-. These findings are in line with the results of former near coast sampling campaigns (Eyckmans, 2003). The results for a near coast region (Adinkerke), however, are significantly lower than the data from former campaigns over some non-coastal regions of Flanders (Van Grieken et al., 2003). The reason for that could be the much lower level of NO_2 in the coastal region (weekly range: 1.3-9.6 $\mu g/m^3$, with a weekly average of 4.0 $\mu g/m^3$ – in De Haan) than those of the non-coastal (range: 31-61 $\mu g/m^3$, mean: 43 $\mu g/m^3$ – urban, suburban, and industrial sites – Van Grieken et al., 2003.). Some data from Flanders considered to be rural was around 21 $\mu g/m^3$ (Deutsch et al., 2001), which is certainly an estimate of the "background" NO_2 level by diffusion tube sampling. Indeed, it is difficult to find a "real" rural site over Flanders, even at the coastal zone.

4th campaign During the mid-summer campaign, a high weekly contribution of the fine particulate fraction to the total aerosol N has been observed, ranging between 0.2-0.8 $\mu g/m^3$ (Fig. 2.17). This was due to the dry weather and the low level of precipitation during this sampling period, which conditions support the secondary aerosol formation processes with aerosol products in the fine particulate mode. The medium and the coarse fractions also contributed to the N-levels, but with a full amount of about 30-50 % to the total aerosol-N.

The weekly N levels from the medium and coarse fractions have shown lower values i.e., between 0.05-0.38 μg/m^3 and 0.06-0.4 μg/m^3, respectively, than those for the 3rd (winter-spring) campaign.

Comparing the weekly N-level of NO_3^- to that of NH_4^+, the latter more significantly contributed to the fine and medium particulate fractions. On the other hand, apart from the 5th week, the contribution of NO_3^- was higher than that of NH_4^+ in the coarse fraction (Figs. 2.19 and 2.20).

Comparing the present results (Tables 1.7-1.8) with the data of former monitoring periods at Adinkerke, a site located some 3 km of the Belgian coast (Tables 1.9-1.10, - Eyckmans, 2003), it can be seen that the nutrient concentrations from Adinkerke are higher, which is due to presence of some anthropogenic source influencing the pollutant content of air at this site.

2.2.4. Weekly N-concentrations from rainwater

1st campaign During the first part of this campaign, the weekly amount of precipitation was considerably high. This was manifested in the relatively moderate N-nutrient levels from NO_3^- and NH_4^+, ranging from 0.08 to 0.39 mg/l and from 0.1 to 0.95 mg/l, with average values of 0.12 and 0.22 mg/l, respectively. NH_4^+ contributed generally more to the N-levels than NO_3^-.

2nd campaign This short, summer campaign experienced precipitation mostly during the 1st week. According to this, an extremely high average level of NO_3^- (33 mg/L) and a low NH_4^+ (0.9 mg/l) were found for this week. Interestingly, the 2nd week experienced precipitation only for one day, but this event significantly contributed to the N-flux from NH_4^+. Accordingly, the weekly total fluxes have also shown high fluctuations as listed in Table 1.11.

3rd campaign The weekly concentrations of N in rainwater samples are indicated on Fig. 2.21. Apart from the 5th, 10th and 11th weeks of the campaign, which experienced no precipitation, both NO_3^- and NH_4^+ significantly contributed to the total level of N in these samples, i.e., they being ranged from 0.2 to 1.2 and 0.6 to 1.8 mg/l, respectively.

The weekly deposition, i.e., the wet N-flux, was calculated from the week-based summing of the daily concentrations of nutrients found in the rainwater samples and the amount of daily precipitation (Table 1.12). The extent of weekly average wet deposition was found to be significant for the 1st, 3rd, 4th, 7th and 9th weeks of the sampling period, i.e., the weekly values of NO_3^- and NH_4^+ were ranging up to 2.0 and 5.2 mg N/m^2.day respectively. These five-week values account for around 90 % of the total wet deposition. For the 5th, 10th and 11th weeks of the sampling, there was not any precipitation observable.

4th campaign The weekly concentrations of N in rainwater samples are indicated on Fig. 2.22. Apart from the 3rd, 5th and 6th weeks of the campaign, which experienced no precipitation, both NO_3^- and NH_4^+ significantly contributed to the total level of N in these samples, i.e., they being ranged from 0.01 to 5.1 and 0.4 to 1.9 mg/l, respectively (Table 1.13).

Only relatively low levels of nutrients were found during the 1st, 2nd, 4th, and 7th weeks of the sampling, whereas an extremely high level was found on the 8th week with the values of NO_3^- and NH_4^+ ranging up to 22 and 9.0 mg N/m^2.day^{-1}, respectively (Table 1.13). The levels of other ions, like SO_4^{2-}, Cl^-, Na^+, K^+, Mg^{2+}, and Ca^{2+} were also found to be high. These highly enhanced concentrations observed for 8th week accounted for around 90 % of the total

wet nutrient levels of the campaign, and were attributed to the mixed Atlantic/Channel-North Sea air-masses dominating during this week.

Interestingly, the average wet deposition for some ions (NH_4^+, NO_3^-, Na^+, and Cl^-) is observed to be higher than those received from former studies at Adinkerke (Table 1.14), despite the lower levels of nutrients in the ambient air for this sampling period compared to that of Adinkerke (Eyckmans, 2003). This is due to the higher extent of precipitation experienced during the 3rd sampling (on average 1.5 mm/day), compared to that of the Adinkerke (1.0 mm/day in the winter campaign). It should be noted, however, that the distribution of the rainy periods during the sampling campaign may also play a crucial role in the degree of the wet deposition flux. The uneven distribution of rain over the sampling period (e.g. heavy rain events only occurring on few days of the sampling) may also cause a low degree of wash-out for air-pollutants, resulting in a lower wet N-flux to the coastal region and/or to the Southern Bight of the North Sea.

It can be summarized from the above results that the total concentration of N in the air (both the gaseous and aerosol phases) and rainwater samples varies significantly during the weekly-based observation period. Although the weekly concentration data shows some important trends between the air-mass movements and the corresponding air-quality changes, it is rather difficult to separate the influence of various areas contributing to the N-fluxes of the sampling-site and/or the North Sea on the weekly-base. Therefore, for a better understanding of the nitrogen contribution of different areas surrounding the North Sea, it is necessary to evaluate the daily variation of the N-containing pollutants, and partly, to correlate them with the most decisive meteorological conditions on a daily base as follows below.

2.3. Daily variation of the N-level in gaseous phase, aerosol, and rainwater samples

2.3.1. Total daily N levels from gaseous, aerosol and rainwater samples

The overview on the daily variation in the total average N concentration, - from the diverse means of sampling, i.e., denuder (gaseous HNO_2, HNO_3, and NH_3), filter (NO_2^-, NO_3^-, and NH_4^+), and rainwater (NO_2^-, NO_3^-, and NH_4^+), - is depicted on Figs. 2.23-2.34.

2nd campaign The daily average concentration of total gaseous nitrogen from the denuder was fluctuating between 0.5 and 4.7 μg/m^3 with an average value of 2.8 μg/m^3, while the total N level from aerosols fluctuated between 0.6 and 3.2 μg/m^3 with a mean value of 1.8 μg/m^3. For rainwater samples, the total N concentration ranged up to 54 mg/l with an average of 13 mg/l.

This period has experienced days with mixed influence of the Atlantic Ocean/Channel/UK, as well as some influence of the North Sea and the continent Generally, the Atlantic Ocean/Channel/UK air-masses brought more N-nutrients during this period, although the North Sea and continental (mixed) air-masses were also contributing significantly to the total N-loading of the sampling site.

3rd campaign The daily average concentration of total nitrogen from the denuder was fluctuating between 0.16 and 9.9 μg/m^3 with a mean value of 2.1 μg/m^3, while in the aerosol phase it fluctuated between 0.25 and 4.0 μg/m^3 with a mean value of 1.6 μg/m^3. For rainwater samples, the total N concentration ranged up to 10 mg/l with an average of 1.4 mg/l.

The days on which the weather conditions allowed to assess the impact of the Atlantic Ocean to the North Sea showed relatively lower values of the total N concentration in gases

and aerosols, compared to the values achieved on days with continental (anthropogenic) influence. These days were assigned on the base of the BWTs as follows: 15th - 16th of February, 8th and 25th of March (Figs. 2.30-2.32). For these days, the total N level from gases, aerosols and rainwater samples ranged between 0.5-4.5 μg/m^3, 0.4-0.9 μg/m^3, and 0.8-1.1 mg/l, respectively. The air-masses moving from the direction of the North Sea (on 27th February and 20th – 21st March) were also characterized by similar total N-loadings for gases, and aerosols, i.e., 1.2-3.9 μg/m^3 and 0.7-1.3 μg/m^3, respectively. For rainwater, significantly higher values (1.7-6.9 mg/l) were scored compared to the former data. This may be the consequence of the rather uneven distribution of rainy days, and the accumulation of pollutants in the ambient air before these rainy periods.

4th campaign The daily average concentration of total gaseous nitrogen was fluctuating between 0.2 and 5.6 μg/m^3 with an average value of 2.6 μg/m^3, while the total N level from aerosols ranged up to 2.5 μg/m^3 with a mean value of 0.9 μg/m^3. For rainwater samples, the total N concentration ranged up to 24 mg/l with an average of 1.8 mg/l.

As was expected from former campaigns, this sampling period has also shown a larger contribution of gaseous N to the total N-levels in the air. Generally, more total gaseous and aerosol N-levels were recorded on days with influence of continental air-mass movements. It should be noted that for some days under either Atlantic/Channel or North Sea influence, the contributions were similar to that of the continent, it being indicative of the extensive mixing of continental and marine air-masses.

2.3.2. Daily N contribution of gaseous compounds in the ambient air

1st campaign In this sampling campaign, daily level of N from HNO_2 varied between 0.01-1.0 μg/m^3 and that of HNO_3 ranged up to 0.6 μg/m^3 with average values of 0.3 and 0.08 μg/m^3, respectively. The daily N contribution from NH_3 varied up to 5.3 μg/m^3 with an average of 2.9 μg/m^3 (Table 1.15). It is noted that NH_3 was monitored till the end of October, 2004 in this campaign, while the two acidic gases till the end of the campaign (Figs. 2.35-2.40).

2nd campaign The daily levels of N from HNO_2 and HNO_3 varied between 0.1-0.4 μg/m^3 and 0.06-0.7 μg/m^3, with average values of 0.27 and 0.3 μg/m^3, respectively (Fig. 2.41). The daily N contribution from NH_3 varied up to 4.4 μg/m^3 with an average of 2.8 μg/m^3 (Table 1.15).

During this campaign, the North Sea and North Sea/Continental air-masses have shown the highest NH_3 and HNO_3. Only slightly lower daily N (NH_3) contributions were recognized from UK/Atlantic/Channel air-masses, indicating that all these air-masses are all mixed with some air carrying pollution, possibly from Northern France or Southern UK industrial regions.

Although NO_2 was sampled with diffusion tubes in weekly periods, its daily level was estimated over the campaign by taking into account the contribution of the different air-masses on a daily base to the total weekly NO_2 level. The NO_2 levels for the UK/Atlantic/Channel and the North Sea influence were estimated to be 1.45 and 1.32 μg/m^3, respectively, whereas for North Sea/Continental air-masses around 1.65 μg/m^3.

3rd campaign The daily variations in the concentrations of NH_3 and gaseous HNO_2, HNO_3 from the denuder sampling together with the total N levels are depicted in Figs. 2.42-2.44. As can be seen, the daily contribution of gaseous acids to the total N level is generally one order of magnitude lower than the N contribution from NH_3. The daily levels of N from HNO_2 and HNO_3 varied up to 0.33 μg/m^3 and 0.3 μg/m^3, with averages of 0.13 μg/m^3 and 0.11 μg/m^3,

respectively. The daily N contribution from NH_3 varied up to 9.6 μg/m^3, with an average of 2.1 μg/m^3.

The daily levels of N from the gaseous components were found to be relatively high in those days, when the air-masses were moving from the Atlantic Ocean through the Channel and partly touching the northern coastal line of France (e.g., between 15th and 19th of February). This is partly due to the presence of the highly industrialized zones at the northern part of France (Dunkerque). Similarly high concentrations of N were observed for those days, when the air-mass movements were characterized as Continental and/or North Sea with Scandinavian origin. The air-masses arriving from the Atlantic/Channel/UK (e.g., between 6th and 11th of March), were generally characterized with high amounts of precipitation, which certainly decreased the level of gaseous pollutants as explained above.

The days with an important influence of the Atlantic Ocean (i.e., 15th - 16th of February, 8th and 25th of March), were found to be with relatively varying N levels of gaseous components. For example, NH_3 was not detected on 15th of February with the applied analytical method. This day may be considered to be with a "pure" oceanic characteristic with a negligibly small impact of NH_3 emission from the Ocean (see explanation above). The NH_3 level showed an increase on the subsequent day. On the other hand, the levels of HNO_2 and HNO_3 were significantly higher during these days, due to the absence of rain, and the possible oxidization of NO_x to gaseous acids. Then again, the extent of precipitation significantly decreased the level of these gaseous phase pollutants, (e.g., see the data for 8th of March on Fig. 2.43).

4th campaign The daily levels of N from HNO_2 and HNO_3 ranged up to 0.4 μg/m^3 and 0.6 μg/m^3, with average values of 0.1 and 0.2 μg/m^3, respectively, whereas the daily N contribution from NH_3 varied up to 5.2 μg/m^3 with an average of 2.3 μg/m^3 (Figs. 2.45-2.46; Table 1.15).

Peak levels of gaseous-N were observed under the influence of continental and mixed North Sea air-mass influence. Although the Atlantic/Channel/UK air-masses have shown about 30-40 % of the highest levels, some of these days were also manifest similarly high daily nutrient levels as the former air-masses. Continental air-masses also demonstrated higher N (HNO_3) levels compared to that of N (NO_2), although their levels were far below to that of N (NH_3).

2.3.3. Daily levels of N-containing compounds and other nutrients in the different size-fractions of particulate matter

The daily average N levels for the different size-fractions of aerosol particles sampled with the three-stage filter unit are depicted on Figs. 2.47-2.52.

1st campaign In this campaign, some "baseline" levels of pollutants are attempted to characterize by selecting proper days with the influence of the Atlantic/Channel only. The discussion on these data is presented with the corresponding N-fluxes (see Section 2.4).

2nd campaign In this short summer campaign, both the medium and coarse fractions of aerosols significantly contributed to the total aerosol N-levels, ranging between 0.1-1.9 μg/m^3 and 0.3-0.9 μg/m^3 with average values of 0.9 and 0.6 μg/m^3, respectively. These amounts correspond to 80-90 % of the total aerosol fraction. The coarse aerosol fraction was especially dominant for Atlantic/Channel/UK and North Sea influences, amounting up to 40-60 % mostly in the form of NO_3^-. The contribution of NH_4^+ was negligibly small in both the coarse and medium fractions; its level varied between 1-4 % of the total aerosol-N. Interestingly, for

mixed North Sea/continental influence the N-contribution from the medium aerosol fraction dominated in the total aerosol N-level, as well as the fine fraction also contributed significantly, which must be the consequence of intensive secondary aerosol formation during this dry (summer) sampling period. During the rainy period (first week of the sampling), low N-levels of the fine aerosol fraction have been observed, possibly due to the scavenging of fine particles by the relatively low amount of daily rain (0.1-2.5 mm/day with an average of 0.8 mm/day).

3rd campaign In this campaign, the coarse fraction contributed to the total daily N level only to a small extent, i.e., it varied between 0.04-0.7 $\mu g/m^3$, with an average value of 0.25 $\mu g/m^3$. On the other hand, the medium and fine fractions of aerosols contributed significantly to the total N content of aerosols. Their N levels ranged between 0.09-2.0 $\mu g/m^3$ and 0.02-2.9 $\mu g/m^3$ with average values of 0.5 and 0.8 $\mu g/m^3$, respectively.

It can be seen that on the rainy days, the total N-loading of the fine and ultra-fine fraction is significantly decreased compared to that of the coarse fraction. This is due to the rather decreased extent of secondary aerosol formation (i.e., the intensive wash-out of gaseous phase components and reduced sunlight radiation for photochemical reactions) as well as the wash-out of the fine fractions of aerosols. Interestingly, the N level showed an increase in the coarse fraction, which may be due to some coagulation processes during non-rainy hours with high RH in the ambient air.

The distribution of N-containing compounds between the diverse aerosol fractions is depicted on Fig. 2.53. From this, it can be seen that the contribution of NH_4^+ to the total N loading of each particulate fraction is significantly higher than the N contribution from NO_3^-, which is in accordance to the findings of a former sea-side aerosol monitoring study (Eyckmans, 2003).

Air-masses originating from the Atlantic Ocean (generally passing via the Channel and the coastal zones of NW France) were observed to be with relatively low N levels of nutrients (between 14th and 18th of February). Similarly low N nutrient levels were observed from air-masses from the North Sea (20th and 21st of March). The presented data demonstrates the formation of N-containing secondary aerosols over the Sea, but to a much lower extent compared to the atmospheric processes over the continent.

The air-masses of continental origin were characterized with considerably higher N-loadings of each size fraction, both for NO_3^- and NH_4^+, i.e., 5-10-fold increase in the concentrations of these nutrients were detected. A very similar observation was also true for air-masses moving through the UK without any precipitation (from 28th February till 5th of March).

4th campaign For this campaign, the contribution of the coarse and the medium fractions to the total daily N-level was found to be low, i.e., their levels were ranging between 0.01-0.6 and 0.02-1.1 $\mu g/m^3$, respectively, with average values of 0.23 and 0.23 $\mu g/m^3$, respectively. In contrast, the fine fraction of aerosols contributed significantly to the total N content of aerosols, showing N levels ranging from 0.09 to 2.1 $\mu g/m^3$ with an average value of 0.6 $\mu g/m^3$. These results were expected for this sampling period, due to the dry and warm summer period and more intense sunlight, which promotes the secondary aerosol formation reactions in the atmosphere, thus leads to the enrichment of N-compounds in the fine aerosol fraction.

Generally, the highest N-contribution of the fine fraction has been observed for the air-masses approaching from the Atlantic/Channel and/or North Sea. It is noted, however, that the continental air-masses have also shown peak values for this fraction on some certain days of this campaign.

The contribution of NO_3^- to the total N-level was observed to be 3- and 4-times higher in the fine and medium fractions, respectively, compared to that of NH_4^+. On the other hand, NO_3^- contributed 2-fold more to the coarse fraction than NH_4^+.

2.3.4. Evaluation of the daily N-contribution from rainwater

The daily concentration of N in rainwater samples are indicated on Figs. 2.54-2.63. It can be seen that the distribution of rainwater is rather uneven throughout the sampling campaigns and/or periods. Some days experienced significant amounts of rain. The air-masses arriving from the Ocean and the North Sea generally transported more precipitation than those from the continent.

1st campaign This period frequently experienced rain events throughout the first part of the sampling (weeks 1-11). Accordingly, the total daily inorganic N-level in rainwater samples reached a maximum value of 5.3 mg/l with a mean of 0.35 mg/l,. As regards the level of N-containing nutrients, NH_4^+ species contributed more to the total level of N than NO_3^-, i.e., their levels ranged up to 3.5 and 2.0 mg/l with average values of 0.23 and 0.13 mg/l, respectively (Table 1.15). The lower average values are indicative of the rather dry second period of the sampling from weeks 12-17.

2nd campaign This period experienced rain events only on the first week, apart from the first day of the 2nd week. Accordingly, the rainwater was characterized with relatively significant levels of nutrients, as listed in Table 1.16. Extremely high concentrations of N (NO_3^-), i.e., 32-53 mg/l were observed between 10th and 13th of August, 2004, possibly due to the dry days before the sampling, which can promote the accumulation of pollutants. On the other hand, the wet N-flux was extremely high (52 mg N/m^2.day) only on 13th of August. This day was characterized with mixed Atlantic/Channel/UK and continental influence and with fairly high amounts of rain (1.5 mm/day), which might take place as a summer shower, i.e., within a relatively short period, but with large intensity. These conditions certainly could cause the drastic increase of the nutrient levels in rainwater, which was not experienced for the former days of sampling with less rainy events, when N (NO_3^-) ranged between 1.8-4.4 mg N/m^2.day.

3rd campaign The total daily inorganic N-level reached as high value as 10 mg/l with a mean value of 1.4 mg/l. Concerning the level of N-containing nutrients, both NO_3^- and NH_4^+ species significantly contributed to the total level of N in the rainwater samples, i.e., their level ranged up to 3.8 and 7.0 mg/l with average values of 0.4 and 0.9 mg/l, respectively (Table 1.15).

4th campaign This campaign experienced only a few rainy events, distributed quite evenly during the sampling period. Accordingly, the concentrations of nutrients were found to be higher in the rainwater samples than those observed during the winter/spring campaigns. These peak concentrations of nutrients in the rainwater samples can be explained by certain washout events. Before any rainy event, the concentration of nutrients increases in the ambient air. During the first hour of a rainy period, the concentration of nutrients is increasing in the rainwater samples, due to their continuous washout for this period. After a while, however, this concentration starts to decrease, since the ambient air becomes clean, i.e., "washed-out", but the new rain dilutes the former wet-precipitate.

The total daily inorganic N-level reached as high value as 24 mg/l with a mean value of 1.8 mg/l, higher than for the 3rd campaign. Regarding the level of N-containing nutrients, both NO_3^- and NH_4^+ species significantly contributed to the total level of N in the rainwater

samples, i.e., their level ranged up to 17.6 and 8.8 mg/l with average values of 1.1 and 0.8 mg/l, respectively (Table 1.15). The contribution from NO_2^- was negligibly low (0.002 mg/l), similar to that of the 3rd campaign (0.001 mg/l).

Especially significant N-concentrations were observed from NO_3^- during Atlantic/Channel air-mass influence, whereas for continental influenced air, the NH_4^+ was slightly more contributing to the N-levels than the former species. The daily precipitation i.e., the wet deposition flux was estimated from the daily concentrations of nutrients found in the rainwater samples and the amount of daily precipitation as follows below.

2.4. Deposition of nitrogen compounds

2.4.1 Dry deposition

2.4.1.1. Daily average fluxes of gaseous compounds

1st campaign In the autumn/early winter campaign in 2004, some representative days were selected on the base of daily BWTs, which were meant to represent the contribution of different air-masses (e.g., Atlantic, North Sea, and continental), arriving to the coast of Southern North Sea at the sampling point. On the base of the daily concentration data, the "baseline" flux of the "clean", oceanic air-masses has been attempted to be calculated.

When comparing the gaseous N-fluxes during Atlantic air-mass movements with continental, a relatively large increase in the N-loading can be seen for the latter (Table 1.19). This is manifested in both the gaseous and aerosol phase compounds as well. The fluxes of both HNO_2 and HNO_3 are significantly (2.0-2.7-times) increased, which is the direct consequence of their increased formation from anthropogenic NO_x. The flux of NH_3 showed only a slighter, 1.8-fold increase, since its homogeneous release and distribution over Flanders, due to animal farming, even in the coastal region, could be expected. The values for the average fluxes of gaseous compounds over the season are a bit higher than that observed for the late winter/spring campaign (see Tables 1.19 and 1.21).

2nd campaign In this late summer campaign, the daily average N-fluxes of HNO_y compounds were relatively low, compared to that of NH_3, they ranging from 0.08 to 0.2 mg/m^2 day. The lowest, negligibly small contribution to the total gaseous N-flux was found from dry deposition NO_2, varying between 0.0002-0.0003 mg/m^2.day. The main contributor of the gaseous N-flux was found to be NH_3 comprising around 90 % of the total gaseous N-loading. A low NH_3 flux was observed from mixed North Sea-Continental air-masses, possibly due to dilution of air and the fast conversion rate of NH_3 as observed by Asman and Van Jaarsveld (1991).

Comparing the average fluxes of various gaseous N-compounds for this campaign from UK/Atlantic/Channel air-mass movements to those originating from the North Sea and mixed North Sea/continental air-masses, ratios ranging between 0.7-1.9 and 1.1-5.8, respectively, have been observed (Table 1.20).

3rd campaign In this winter-spring campaign, the average N-fluxes of HNO_y compounds were ranging from 0.05 to 0.11 mg/m^2.day. Then again, the lowest, negligibly small contribution to the total gaseous N-flux was found from dry deposition of NO_2, varying between 0.00007-0.00014 mg/m^2.day. This compound is generally homogeneously released and distributed over Flanders mainly from animal husbandry, thus it is evenly distributed over coastal regions as well.

Comparing the average fluxes of various gaseous N-compound from continental air-mass movements with those originating from the Atlantic/Channel and North Sea air-masses, generally ratios ranging between 1.2-2 and 0.9-2.0, respectively, have been observed (Table 1.21).

4th campaign During this mid-summer campaign, the average N-fluxes of HNO_y compounds were ranging from 0.04 to 0.14 mg/m^2.day, while that of NO_2 varied between 0.00018-0.00023 mg/m^2.day (Table 1.22). Continental air-masses certainly contributed more to the gaseous flux, as expected. However, a very similar contribution was observed for air-masses approaching from the North Sea, whereas the lowest N-fluxes were observed from Atlantic air-masses.

Comparing the average fluxes of various gaseous N-compounds from continental air-mass movements with those originating from the Atlantic/Channel and North Sea air-masses, generally, ratios ranged between 0.8-1.2 and 1.0-2.0, respectively, have been observed. This means that the contribution of the Atlantic/Channel/UK air-masses were higher during this campaign compared to the late winter/spring campaign.

During each campaign, ammonia has been observed to be as the highest contributor to the gaseous inorganic nitrogen deposition, comprising around 90 % of the gaseous N-flux, whereas the lowest, negligibly small contributor was found to be NO_2 (Tables 1.19-1.22). The daily average N-fluxes of HNO_2 and HNO_3 were also relatively low, amounting around 10 % of the gaseous inorganic N-flux.

Comparing the average gaseous N-fluxes over various seasons/campaigns, outstandingly high deposition rates were observed for the late summer campaign, with values of 4.8 and 2.7 mg N/m^2 day for the Atlantic/Channel/UK and North Sea air-masses, respectively. On the contrary, the other campaigns experienced average gaseous fluxes ranging between 1.2-2.1 mg N/m^2 day.

When comparing the gaseous flux data observed during various seasons, one can see a larger contribution from the Atlantic/Channel/UK and the North Sea than the Continent/North Sea during the late summer (August) campaign. On the other hand, for the winter-spring and the early/mid-summer (June-July) campaigns, the average fluxes of gaseous N-compunds were the highest for continental air-masses, whereas decreased fluxes were observed for the North Sea, and more for the Atlantic/Channel/UK air-masses.

2.4.1.2. Daily average fluxes of aerosols

1st campaign In the autumn/early winter campaign, on the selected representative day under oceanic influence, NO_3^- was present mostly in the medium and coarse fractions of aerosols (Table 1.19), which is due to the less active secondary aerosol formation and the coagulation of fine particles in coarse mode. The NH_4^+ contributed equally to the N-flux in each fraction of Atlantic air, whereas its significantly increased flux was observed in continental air-masses. During continental air-mass movements, secondary aerosol formation becomes significant, which is manifested in the enrichment of N-species in the fine and medium particulate fractions. The total aerosol flux for Atlantic air was found to be 4-times lower than that of continental. The average N-flux of aerosols over the autumn/early winter season was an average of 2.75 mg N/m^2 day, which is a rather comparable value to that observed for the

late winter/spring campaign (see Tables 1.19 and 1.21). Also, similar aerosol contribution to the total dry flux (40 %) has been found.

The ratio of aerosol to gaseous N compounds is inversely changing for oceanic and continental air-masses. During continental air-mass movements, the fluxes originating from aerosols dominate over the gaseous fluxes, whereas the opposite is true for air-masses approaching from the Atlantic Ocean. As a result, the total dry deposition rate was demonstrated to be 4-times higher during air-mass movements from the continent than from the Atlantic/Channel.

2nd campaign For the late summer campaign, the highest average daily deposition for the total aerosol N was found for UK/Atlantic/Channel air-masses (3.6 mg/m^2 day), followed by lower values for North Sea/continental (2.9 mg/m^2 day), and North Sea air-masses (1.0 mg/m^2 day). During mixed North Sea/continental influence, the contribution of coarse and fine fractions to the average aerosol N-flux has been found to be less significant, 25 % and 15 %, respectively, than that of the medium fraction (60 %). On the other hand, for the North Sea influenced air, the coarse fraction was enriched up to 73 % contribution to the total aerosol-N levels. For Atlantic/Channel/UK influenced air, the contribution of medium and coarse fractions was similar (45-50 %), whereas very low N-contribution was observed from the fine fraction (6 %) (Table 1.20). The percent of aerosols in the dry fraction was found to be between 30-43 %, apart from that of the North Sea/continental air-mass ranging up to 70 %.

The contribution of NH_4^+ to the N-flux from all the three particulate fractions was found to be higher than that of NO_3^- apart from the North Sea/continental influenced coarse aerosols, showing about 5-fold higher flux of NO_3^- (Table 1.20). The Atlantic/Channel/UK to North Sea and/or North Sea/continental ratios of total aerosol N flux were found to be 3.1 and 1.3, whereas the total dry N-fluxes were 2.5 and 2.2, respectively, indicating the significant contribution of UK/Atlantic/Channel air-masses to the N-loading of the Southern Bight of the North Sea.

3rd campaign During the late winter/spring campaign, the largest average daily deposition for total aerosol N was found for continental air-masses (1.8 mg/m^2 day), followed by lower values for the North Sea and Atlantic/Channel/UK air, 1.3 and 1.4 mg/m^2 day, respectively.

During continental influence, the average contribution of coarse fraction to the total aerosol N-flux is less significant (10%) than those of either the medium (58 %) or fine (32 %) fractions, due to enrichment of N in finer fractions by secondary aerosol formation, as well as combined with the coagulation of coarser particles in the medium fraction followed by their fall-out with wet air-masses. These led to the enrichment of N-species in the finer particulate fractions, and less abundance of N in the coarse fraction. On the other hand, during oceanic and North Sea air-mass movements the contribution was found to be very similar in all the three fractions, which is due to the less active secondary aerosol formation, and the coagulation of fine particles in medium and coarse mode by the assistance of the marine air of higher humidity (Table 1.21).

The contribution of NH_4^+ to the N-flux was found to be similar to that of NO_3^- in the coarse and medium fractions apart from the continental influenced aerosols, showing about 2-fold higher contribution. Somewhat higher contribution of NH_4^+ was also observed for the fine fractions. The percent of aerosol N-fluxes from the three diverse air-masses to the dry N-flux was around 50 % for all three air-masses. The continental to marine ratios of total aerosol, and total dry flux were found to be always higher, as expected by the more pollutants from continental air-masses (Table 1.21).

4th campaign For the mid-summer campaign, the daily deposition flux of total aerosol N was found to be relatively similar for the three main air-masses. The contribution of coarse fraction to the total aerosol N-flux was a little bit more significant (30-40 %) than those of either the medium or fine fractions, due to the dry period, promoting the coagulation of particles in the coarse fraction (Table 1.22).

The contribution of NH_4^+ to the N-flux was found to be more intensive in the medium and the fine fractions, whereas NO_3^- was contributing more in the coarse fraction. The percent of aerosol-N to the dry N-flux was found to be around 41 % for Atlantic/Channel/UK air-masses, whereas lower values (32-35 %) were observed for continental and North Sea influenced air. Surprisingly, the continental-to-marine ratios of total aerosol and total dry flux were found to be lower than unity, which is an indicative of the higher pollution content of the Atlantic/Channel/UK air-masses during the summer period. This is also a proof of the mixing of oceanic and continental air in the air-masses arriving from the Atlantic Ocean.

Comparing the average N-fluxes of aerosols over various seasons monitored, one can see an outstandingly high values for the late summer campaign, especially, with high deposition rates of 3.6 and 2.9 mg N/m^2 day for the Atlantic/Channel/UK and mixed-continental-North Sea air-masses, respectively. On the contrary, the other campaigns has shown average aerosol fluxes ranging between 0.9-1.9 mg N/m^2 day. The high level of nutrients at the late summer period, similar to that found for gaseous nitrogen (Table 1.20) can be associated with a typical eutrophication event in the coastal region studied

When comparing the relative contribution of aerosols observed over various seasons/campaigns, one can see a larger contribution during the late summer campaign from Atlantic/Channel/UK (48 %) and mixed continental/North Sea (37 %) air-masses, whereas the contribution from North Sea air was found to be low (15 %). For the late winter/spring campaign, continental air contributed more (41 %), while the Atlantic/Channel/UK and North Sea air-masses were contributing equally (~30 %). During the mid-summer campaign, all the three air-masses contributed similarly, each around 33 %.

2.4.2. Wet deposition and its comparison with dry fluxes

Despite the relatively low amounts of rain, experienced during the campaigns, the wet deposition was found to be the more considerable contributor to the total N budget of the North Sea. On the other hand, the dry flux also played an important role in some campaigns.

1st campaign In the autumn/winter campaign, the wet deposition flux was proved to be a more significant contributor (60 %) to the total N-deposition compared to the dry N-flux. Though on the representative day under continentally influenced air (1st October, 2004) its contribution was found to be lower (15 %). As a general observation for this campaign, its contribution was more emphasised for Atlantic/Channel/UK air-mass movements than for either continental, or North Sea air-masses (Table 1.19).

2nd campaign During the late summer campaign, the Atlantic/Channel/UK air-masses contributed more to the wet N-flux (78 %) than those of North Sea (22 %) and North Sea-continentally influenced air (Table 1.20). The contribution of NO_3^- to the wet N-flux was found to be outstandingly high (12 mg N/m^2 day) than that of NH_4^+ for Atlantic/Channel/UK air-masses, whereas both species scored similar values (1.8-1.9 mg N/m^2 day) for the North Sea influenced air. Accordingly, the wet-to-dry ratios were found to be 2-fold higher for UK/Atlantic/Channel air-masses than that for North Sea, indicating the important N-contribution of (wet) N-fluxes from mixed air movements from the Atlantic passing through

the UK and the Channel. For North Sea air-masses, a just about unity wet to dry ratio has been found.

3rd campaign Over the late winter/spring campaign, Atlantic air-masses generally more contributed to the wet N-flux (3.5 mg N/m^2 day) than those of continental and North Sea (Table 1.21). The contribution of NH_4^+ to the N-flux was found to be about 2-fold higher than that of NO_3^- for all the three air-masses. However, the wet to dry ratio was found to be higher than unity for Atlantic air-masses, indicating the more important contribution of dry N-fluxes from continental and North Sea air-masses.

The average DON content of rainwater samples was proved to be a less significant contributor to the N-flux, it amounted up to 0.4, 0.2 and 0.01 mg N/m^2.day, for continental, Atlantic and North Sea air-masses. It is to be mentioned here that the relevant literature generally associates DON with a large set of organic N-containing compounds present in the atmosphere, such as urea, peroxyacetyl nitrate (PAN), alkyl nitrates, aliphatic amines, amino acids, N-PAH, methyl cyanide, etc. (Cornell et al., 2003). Although the exact composition of DON in rainwater is not known, the listed species is to be investigated due to their bioavailability and/or toxicity.

4th campaign For the mid-summer campaign, despite the relatively low amounts of rain experienced, the wet deposition was found to be a considerable contributor to the total N budget of the sampling site (Table 4). For Atlantic air-masses, the wet deposition flux has been proved to be a more significant contributor (~80 %) to the total N-deposition flux compared to the dry N-flux. On the other hand, an equal contribution of the dry and wet fluxes has been found for continental air-masses. As observed in the former campaigns, Atlantic/Channel/UK air-masses generally contributed more to the total N-flux than those of continental and North Sea.

The contribution of NO_3^- to the wet N-flux was found to be about 2-fold higher than that of NH_4^+ for Atlantic/Channel/UK air-masses, whereas for continental air, a similar contribution of these species has been observed. The wet-to-dry ratio was found to be higher than unity for Atlantic and continental air-masses, indicating that in the dry summer period the continental air-masses can also more significantly contribute to the N-flux than in the late winter/spring campaign.

In the mid-summer campaign, the average DON content of rainwater samples was also proved to be a significant contributor to the N-flux. It amounted up to 3.5, and 0.3 mg N/m^2 day, for continental and Atlantic/Channel/UK air-masses. The high contribution of the DON from continental air-masses was associated with the possibly high anthropogenic impact as well as the long and dry mid-summer period, which promoted the accumulation of pollutants in the ambient air. This certainly allows a higher DON content in rainwater samples, even during short, shower-like rain periods.

2.4.3. Total (wet+dry) average fluxes

In the late winter/spring, and the mid-summer campaigns, the relative contribution of diverse air-masses to the dry flux was found to be very similar, ranging between 28-39 %. However, for the late summer campaign, a high contribution was observed from Atlantic/Channel/UK air-masses (52 %), whereas similar contributions were found for continental and North Sea air (each 24 %).

In the late summer campaign, the relative nitrogen contribution to the total (dry plus wet) N-flux was the most considerable from the UK/Atlantic/Channel air-masses (65 %)

followed by the North Sea (23 %) and the North Sea/continental (12 %) air-masses. Compared to this campaign, the relative contributions for the mid-summer campaign in 2006 has only slightly been changed for Atlantic/Channel/UK (54 %) air-masses, but significantly for continental (34 %) and North Sea (12 %) air-masses. In the late winter/spring campaign, the relative contribution to the total flux of was significantly decreased for the Atlantic/Channel/UK air-masses (38 %), whereas it was increased for North Sea air-masses (28 %).

2.4.4. Comparison of fluxes with the literature data

From the above data of individual fluxes, the overall average dry and wet fluxes for the coastal region of De Haan have been calculated, yielding 2.8 and 3.7 kg N/km^2 day, respectively. When comparing these results with the existing literature (model) values of 0.5 and 2.1 kg N/km^2 day in 1999 for the whole area of the sea for dry and wet deposition, respectively (Hertel et al., 2002), a higher extent of N-deposition is evident at least for the Southern Bight of the North Sea. Nevertheless, it is to be mentioned that due to the intensive anthropogenic activities, the atmospheric N-contribution at a coastal sampling site is always higher than that of the northern part of the North Sea, being opened to the Atlantic Ocean. Interestingly, due to the drier periods, experienced during the years sampled in this project, the wet to dry deposition ratio has also been significantly decreased.

The calculated annual dry and wet fluxes for De Haan are 1010 and 1357 kg N/km^2, respectively, which corresponds to a total deposition of 2.4 t N/km^2 (Table 7). This data is in the range of the predicted values by the ACDEP model for 1999 (Hertel et al., 2002), reporting 1.8-3.0 t N/km^2 for this coastal region of Belgium.

Comparing the obtained total annual atmospheric fluxes with the riverine inputs, one can seen that the former ones are higher than the riverine N-input reported either for the German Bight for the 1990s (150 kt N/year; Beddig et al., 1997), or for the total North Sea catchment area (745 kt N/year, Spokes and Jickells, 2002).

According to the latest observation of OSPAR contracting parties on waterborne (direct and riverine) inputs, a total waterborne input of 807 kt N/yr has been reproted for 2004 (Bartnicki and Fagerli, 2006). This value is rather commensurable with the presently observed data on atmospheric inputs, even the latters are more intesive.

2.5. Single particle analysis

Single particle analyses were performed on 24 aerosol samples taken on a weekly basis, with a time resolution of 1 day, using two stages of a May cascade impactor, with aerodynamic diameter cut-offs of 2-8, and 0.5-2.0 mm for stages 3-4, and 5-6, respectively, at a sampling flow-rate of 20 l/min.

Since the number concentration of smaller particles in the air is larger than that of bigger particles, it is necessary to collect small particles in shorter sampling duration, not to create artificial agglomerates while overloading the sample. The sampling time varied between 30 (for stage 5-6) and 60 (for stage 3-4) minutes, to obtain the best loading of particles in the impacted spots. Since uncoated collecting substrates were used, it is possible that some size misclassification could have occurred owing to particle bounce-off. The collected samples were put in plastic carriers, sealed, and stored in a desiccator. Particles collected at stages 5-6 and 3-4 were analysed by Thin-Window EPMA, and some 400 particles for each stage sample were analysed totalling some 800 in each complete sample set.

2.5.1. Experimental

The measurements were carried out on a JEOL JXA- 733 electron probe X-ray microanalyser equipped with an OXFORD Link energy-dispersive X-ray detector (EDX) with a super atmospheric thin window (SATW, 133 eV resolution for Mn K_α X-rays). The recording of the spectra was controlled by software developed in house, and the measurements on individual particles were carried out manually in point analysis mode. To achieve optimal experimental conditions, such as a low level of the spectrum background and a high sensitivity for light element analysis, a 10 kV accelerating voltage was chosen, while the beam current was set at 0.5 nA for all measurements. In order to obtain statistically enough counts in the X-ray spectra and to minimize the beam damage effect on the sensitive particles, a typical measuring time of 20 s was used. Many particle compounds are very volatile, and their structure and composition is unstable under vacuum conditions and intensive electron bombardment. Since the use of a liquid-nitrogen-cooled sample stage can drastically reduce these beam damage effects, a cold stage of the electron microprobe cooled down all particulate samples to -193 ^{0}C. The optimization of the analytical conditions and the cold stage method have been described elsewhere (Ro et al., 1999; Osán et al., 2000; Szalóki et al., 2001; Worobiec et al., 2003). The size and shape of each individual particle was measured and estimated from a high-magnification secondary electron image (M>10,000 x).

2.5.2. Data interpretation

The estimated geometrical data were set as input parameters for the earlier optimized quantification procedure, also described in detail elsewhere (Ro et al., 1999; Osán et al., 2000; Szalóki et al., 2000; Ro et al., 2003). The required net X-ray intensities for the elements were obtained by non-linear least-square fittings of the collected spectra using the AXIL programme (Vekemans et al., 1994). Afterwards, the new concentration calculation method was applied to calculate the elemental concentrations for each individual particle.

For obtaining information on the possible sources of the aerosol and the possible chemical interactions between gaseous and particulate pollutants, the particles were classified into representative groups using the chemical and morphological data obtained by EPMA. For the comparison of the sample sets collected at a different location and time, all particles for each impactor stage (size fraction) were classified into 7 groups using the hierarchical clustering. For simplifying the graphical representation, some similar clusters were taken together into one group afterwards (e.g. several, slightly different clusters of aluminosilicates were considered as one group). The 7 groups were named according to major chemical species in the groups identified on the basis of elemental concentration data of the groups. The optimization of the cluster and multivariate analysis techniques for handling low-Z data was described elsewhere (Osán et al., 2001).

2.5.3. Results and discussion

In this work, we would like to show the impact of marine and continental influences on the different samples, as well as the possible atmospheric reaction of such aerosols, which is linked in some way with the nutrient deposition and consequently to the eutrophication. The 240 h BWTs give us a first indication for this study. Figure 2.64 shows two representative air mass backward trajectories, obtained the HYSPLIT model.

The trajectory in Fig. 2.64a shows that the air-mass sampled had travelled about 120 hours over the ocean before reaching the sampling point. The back-trajectory in Fig. 2.64b

shows that the air mass sampled had travelled about 144 hours over Europe, 30 hours over the ocean, 42 hours over England and other 24 hours over the Channel before it finally was sampled in De Haan.

The results for these two meaningful samples after clustering are illustrated in Figure 2.65a-b. The Table 1.23 reports the relative abundance of the obtained particle types, combined groups, in size fraction of the sampling days.

Table 1.23 shows that sodium chloride (sea salt) particles are abundant on the coarse stage in both samples, which is indeed a fingerprint for the important marine influence on the sampled aerosol. The so-called bubble bursting or sea spray process transports water drops from bursting white caps into the air, after which crystallization takes place and some salts remain airborne. Therefore, sea-salt should be the main constituent among the coarse particle fractions in marine aerosols, except during episodes of continental dust transport (Fitzgerald, 1991). Sodium and magnesium chloride are known to react with other compounds in the atmosphere like nitric and sulphuric acid. This result in chloride loss, since the resulting hydrochloric acid evaporates, while the formed nitrates and sulphates stay behind as sodium nitrate and sulphate salts (together with some remaining chloride if the particle did not react completely).

TW-EPMA is able to detect nitrogen and oxygen, so we were able to clearly identify sodium nitrate (Ro et al., 2001b, 2002, 2005). Although we only used ‘‘$NaNO_3$’’ as the name for the particle type identification, small sodium sulphate crystals were often observed to be connected to the surface of larger sodium nitrate particles.

A possible reason for this effect is the inhomogeneous crystallization at the impacting surface, since sodium sulphate crystallizes at higher relative humidity (Storms et al., 1984).

Nitric and sulphuric acid in the air find their origin in transformations and reactions of nitrogen and sulphuric oxides. In urban environments, these compounds are mostly found as exhaust gases from combustion processes (domestic heating, industrial processes, traffic).

Since the sea is a continuous source of fresh sodium chloride, and since the sea salt in air masses travelling over land has more chance to react with anthropogenic nitrogen and sulphur oxides, we could say that relatively high abundances of (progressive) sea salt aging is an indication for continental influences.

The presence of aged or completely transformed sea salt, like sodium nitrate, was also significant in continentally influenced sample.

A considerable amount of aged sea salt particles was observed in the continental sample (as ‘‘$NaCl+NaNO_3$’’ group). This result is somewhat puzzling while considering that this air mass spent most of its time above Europe.

Organic particles and biogenic particles (recognized by their relatively higher potassium or phosphorus content) were detected with TW-EPMA in the coarse and fine fractions. However, we must mention that these particles are difficult to characterize more in detail, since only elemental concentrations can be determined with TW-EPMA (for elements with $Z>5$; so excluding hydrogen).

For the samples influenced by marine sources, we see a lower abundance of organic / biogenic particles, while they are also abundant in continental sample. The amount of organic and biogenic particles is considerably higher in continental samples, which seems logical taking into account the possible continental sources of these particle types (traffic, industrial processes, domestic heating; vegetation, other bioactivity).

In urban aerosols, most organic particles originate from combustion processes, so these sources must certainly be involved.

The marine bubble bursting process might contribute to the organic fraction, since it also causes (bio)organic materials from the sea water to be transported into the atmosphere.

The fact that numerous sea salt particles also appeared to contain certain amounts of carbon and oxygen (maybe as an organic layer on top of the sodium chloride crystals), is probably a result of this process. Even a mixed particle type of sea salt and organic compounds was found in these samples (''NaCl+Organic'' or "$NaSO_4$ + Organic").

The presence of organic coatings was demonstrated earlier for particles suspended in seawater by using an indirect method (Ru-staining method for organic carbon) (Jambers, 1997), but with TW-EPMA we could determine the existence of these layers directly in the X-ray spectra.

Ammonium sulphate and nitrate particles originate from transformations and reactions of nitrogen and sulphur oxides in the air and, like for sea salt aging, the presence of ammonium particles can be related to continental influences. TW-EPMA has extended the capabilities of conventional EPMA, since it was able to specify the origin of sulphur-rich particles ''Organic+S''.

The aluminosilicates frequently encountered in the continental samples are expected to have their origin in soil dust. Large soil dust particles are not often transported over large distances because of their fast deposition rates, and, therefore, their abundance is expected to be only very high on coarse stage if the analysed samples would have been strongly influenced by continental sources as observed in our case. This is indeed not the case for the marine samples, although the coarse stage contains other soil dust particles like metal oxides, but to a lesser extent.

The contribution of mineral particles, like aluminosilicates or oxides, to the aerosol composition was much higher for the continental sample, which again proves the evident fact that soil dust is more abundant above the continent.

Iron oxide and other metal oxides showed to be more abundant than in the more marine samples, which could also partly be explained by the presence of the intense metallurgic industry over Europe (Van Malderen et al., 1992).

2.6. Literature

Asman, W., Van Jaarsveld, H., A variable-resolution transport model applied for NH_x in Europe. Atmos. Environ. 1991, 24A (2), 445-464.

Bartnicki J., Fagerli H., (2003) Atmospheric supply of nitrogen to the OSPAR Convention Waters. Summary Report for UBA. EMEP Technical Report MSC-W 4/2003. Norwegian Meteorological Institute. Oslo, Norway.

Bartnicki J., Fagerli H., (2004) Atmospheric in the OSPAR Convention Area in the period 1990 - 2001. Summary Report for the German Environmental Agency (Umweltbundesamt UBA). EMEP Technical Report MSC-W 4/2004. Norwegian Meteorological Institute. Oslo, Norway.

Bartnicki J., Fagerli H., (2006) Atmospheic Nitrogen in the OSPAR Convention Area in the period 1990-2004, EMEP/MSC-W Technical Report 4/2006, Oslo, ISSN 0804-2446.

Beddig, S., Brockmann, U., Dannecker, W., Körner, D., Pohlmann, T., Puls, W., Radach, G., Rebers, A., Rick, H.J., Schatzmann, M., Schlünzen, H., Schulz, M., Nitrogen Fluxes in the German Bight, Marine Pollut. Bull., 1997, 34 (6) 382-394.

Cohan Y., Dry deposition model, Multimedia Environsoft Corp., Los Angeles, Ch. 12., 1998.

Cornell SE, Jickells TD, Cape JN, Rowland A.P., Duce R.A., Organic nitrogen deposition on land and coastal environments: a review of methods and data, Atmos. Environ. 2003, 37 (16) 2173-2191.

De Leeuw G., Ambelas Skjøth C., Hertel O., Jickells T., Spokes L., Vignati E., Frohn L., Frydendall J., Schulz M., Tamm S., Sørensen L.L., Kunz G.J., Deposition of nitrogen into the North Sea, Atmos. Environ., 37 (2003) S145-S165.

Deutsch F., M. Stranger, V. Kontozova, P. Joos, A.F.L. Godoi, R. Van Grieken, Studieovereenkomst onderzoek luchtvervuiling Wilrijk, Hoboken, Peer en Antwerpen-Stad, Final report, LUC/99/229, Department of Chemistry, University of Antwerp, 2001. November 30.

Draxler, R.R. and Rolph, G.D., 2003. HYSPLIT (HYbrid Single-Particle Lagrangian Integrated Trajectory) Model access via NOAA ARL READY Website (http://www.arl.noaa.gov/ready/hysplit4.html). NOAA Air Resources Laboratory, Silver Spring, MD.

Eyckmans K., Atmospheric Deposition of Nutrients to Aquatic Ecosystems, PhD Thesis, 2003, University of Antwerpen.

Fitzgerald J.W, 1991. Marine aerosols: a review. Atmospheric Environment 25A, 533–545.

Hertel O., J. Christensen, E.H. Runge, W.A.H. Asman, R. Berkowicz, M.F. Hovmand, Ø. Hov, Atmos. Environ., 29 (1995) 1267.

Hertel O., C. Ambelas Skjøth, L.M Frohn, E. Vignati, J. Frydendall, G. de Leeuw, U. Schwarz, S. Reis, Assessment of the atmospheric nitrogen and sulphur inputs into the North Sea using a Lagrangian model, Phys. Chem. Earth, 27 (2002) 1507-1515.

Jambers W., 1997. Characterization of individual aquatic suspended particles using electron probe X-ray microanalysis and scanning transmission electron microscopy. Ph.D. Thesis, University of Antwerp.

Lee D.S, C. Halliwell, J.A. Garland, G.J. Dollard, R.D. Kingdon, Exchange of ammonia at the sea surface – a preliminary study, Atmos. Environ., 32 (1998) 431-439.

Osán J., J. de Hoog, A. Worobiec, C.-U. Ro, K.-Y. Oh, I. Szalóki, R. Van Grieken, Application of chemometric methods for classification of atmospheric particles based on thin-window electron probe microanalysis data. Anal. Chim. Acta 446 (2001) 211–222.

Osán J., I. Szalóki, C.-U. Ro, R. Van Grieken, Light element analysis of individual microparticles using Thin- Window EPMA. Mikrochim. Acta 132 (2000) 349–355.

OSPAR Commission (2005a), Atmospheric nitrogen in the OSPAR Convention area and agreed international reduction measures, London, 2005, OSPAR publication 232/2005.

OSPAR Commission (2005b), Assessment of trends in atmospheric concentration and deposition of hazardous pollutants to the OSPAR maritime area – Evaluation of the CAMP network. London, 2005, OSPAR publication 234/2005.

Peierls B.L., Paerl H.W., Bio-availability of atmospheric organic nitrogen deposition to coastal eutrophication, Limnol. Oceanography, 42 (1997) 1823-1828.

Rendell A.R., Ottley Ch.J., Jickels T.D., Harrison R.M., The atmospheric input of nitrogen species to the North Sea, Tellus B, 45 (1993) 53-63.

Ravindra K., S. Mor, Ameena, J.S. Kamyotra, C.P. Kaushik, Variation in spatial pattern of criteria air pollutants before and during initial rain of monsoon, Environ. Monit. Assess., 87 (2003) 145-153.

Ro, C.-U., Hwang, H., Kim, H., Chun, Y., Van Grieken, R., 2005. Single-particle characterization of four ‘‘Asian Dust’’ samples collected in Korea, using low-Z particle electron probe X-ray microanalysis. Environ. Sci. Technol., 39, 1409–1419.

Ro, C.-U., Kim, H., Oh, K.-Y., Yea, S.-K., Lee, C.-B., Jang, M., Van Grieken, R., 2002. Single-particle characterization of urban aerosol particles collected in three Korean cities using low-Z electron probe X-ray microanalysis. Environ. Sci. Technol., 36, 4770–4776.

Ro, C.-U., Oh, K.-Y., Kim, H., Kim, Y.P., Lee, C.B., Kim, K.H., Kang, C.H., Osán, J., de Hoog, J., Worobiec, A., Van Grieken, R., 2001b. Single-particle analysis of aerosols at Cheju island, Korea, using low-Z electron probe X-ray microanalysis: a direct proof of nitrate formation from sea salts. Environ. Sci. Technol., 35, 4487–4494.

Ro, C.-U., Osán, J., Szalóki, I., de Hoog, J., Worobiec, A., Van Grieken, R., 2003. A Monte Carlo Program for quantitative electron-induced X-ray analysis of individual particles. Anal. Chem., 75, 851–859.

Ro, C.-U., Osán, J., Van Grieken, R., 1999. Determination of low-Z elements in individual environmental particles using windowless EPMA. Anal. Chem., 71, 1521–1528.

Roberts J.M., The atmospheric chemistry of organic nitrates, Atmos. Environ. A, 24 (1990) 243-287.

Rolph, G.D., 2003. Real-time Environmental Applications and Display sYstem (READY) Website (http://www.arl.noaa.gov/ready/hysplit4.html). NOAA Air Resources Laboratory, Silver Spring, MD.

Spokes, L.J., Jickells, T.D., Is the atmosphere really an important source of reactive nitrogen to coastal waters? Continent. Shelf Res., 25 (2005) 2022-2035.

Storms, H., Van Dyck, P., Van Grieken, R., Maenhaut, W., 1984. Electron microprobe observations of recrystallization affecting PIXE-analysis of marine aerosol deposits. J. Trace Microprobe Technol., 2, 103–117.

Szalóki, I., Osán, J., Worobiec, A., de Hoog, J., Van Grieken, R., 2001. Optimization of experimental conditions of thin window EPMA for light-element analysis of individual environmental particles. X-Ray Spectrom., 30, 143–155

Van Malderen, H., Rojas, C., Van Grieken, R., 1992. Characterization of individual giant aerosol particles above the North Sea. Environ. Sci. Technol., 25, 750–757.

Van Grieken, R., de Hoog, J., Bencs, L., Spolnik, Z., Khaiwal, R., Stranger, M., Deutsch, F., Berghmans, P., Bleux, N. Final report; *PM2.5 Measurements in Flanders (2001-2003)*; Vlaamse Milieumaatschappij, Flanders, Belgium, 2001-2003.

Vekemans, B., Janssens, K., Vincze, L., Adams, F., Van Espen, P., 1994. Analysis of X-ray spectra by iterative least squares (AXIL): new developments. X-Ray Spectrom., 23, 278–285.

Worobiec, A., de Hoog, J., Osán, J., Szalóki, I., Ro, C.-U., Van Grieken, R., 2003. Thermal stability of beam sensitive atmospheric aerosol particles in electron probe microanalysis at liquid nitrogen temperature. Spectrochim. Acta B 58, 479–496.

3. Organic nutrient detection[†]

3.1. Introduction

3.1.1. Formation and fate of organic nitrates in the atmosphere; role and occurrence in the environment

Photochemical processes and oxidant chemistry in the atmosphere are significantly influenced by the presence of a variety of different gases including nitrogen oxides, ozone, hydrocarbons, organosulpfur species, etc (Crutzen, 1979; Logan *et al.*, 1981; Liu *et al*., 1983; Altshuller, 1986; Toon *et al*., 1987). Amongst these gases, alkyl nitrates (ANs) are of particular interest within the ozone/nitrogen oxide system, because their formation and degradation plays an important role in the tropospheric ozone production (Atkinson *et al*., 1982, Singh, 1987; Luke and Dickerson, 1988; Roberts and Fajer, 1989; Roberts, 1990). Since ozone and organic nitrates are formed through the same reaction, therefore, measurements of organic nitrates can provide information on the role of the different peroxy radicals in photochemical ozone formation (Flocke *et al.*, 1991).

The existence of organic nitrates was first suggested, after comparison of results of NO_y measurements with the summing up of individual species belonging to NO_y family which is called "odd nitrogen". An unidentified fraction ranging from 5 to 40% of the NO_y was observed. The missing fraction was significantly higher in summer than in fall thus indicating the photochemical production of the unknown species (Flocke *et al*., 1991). First direct evidence for the existence of alkyl nitrates in the troposphere was provided by Atlas in 1988, after measurements over the North Pacific Ocean. With the development of sampling procedures and detection techniques more and more of organic nitrates were successfully identified in the ambient air samples. Subsequently the contribution of organic nitrates to the total amount of NO_y was tried to be precisely defined. The input of organic nitrates to the budget of NO_y was investigated by Flocke *et al.* (1991) on Schauinsland and found to be 1% on the average with the maximum value of 2% (however this value is too small to account for the missing fraction of NO_y). This deficit may be explained with peroxyacyl-nitrates $RC(O)OONO_2$, peroxy nitrates $ROONO_2$, higher alkyl nitrates, multifunctional nitrates, carbonyl nitrates and α-hydroxy alkylnitrates not yet well identified part of pool of missing NO_y compounds (Luxenhoffer *et al*., 1996)

Odd nitrogen family (NO_y) is constituted from inorganic nitrogen compounds (nitrogen oxides, acids, inorganic aerosol nitrates, nitrate radicals, chlorine nitrates) as well as from different types of organic nitrates; this means they are important NO_y reservoir species. Since organic nitrates have much longer lifetimes than other inorganic NO_y species, they have a prominent influence on the geographic distribution of NO_y (Roberts, 1990).

Organic nitrates are formed in secondary reactions through the atmospheric oxidation of organic compounds initiated by O_3, OH, NO_3. The products of OH-, O_3-, NO_3- and *hv*-initiated oxidation of organic compounds are the oxy ($RO^{\bullet}$) and peroxy ($RO_2^{\bullet}$ = ROO•) radicals. However oxy-radicals react rapidly with oxygen and form peroxyradicals (Turberg *et al.* 1990). Therefore reactions of $RO_2^{\bullet}$ radicals with NO are thought to be the most important sources of atmospheric alkyl nitrates (Atkinson *et al*, 1982; Roberts, 1990). Tropospheric ozone is produced in this process (hydrocarbon oxidation during which NO is oxidized to NO_2) (O'Brien *et al*, 1997). Organic radicals can derive from alkanes, olefines, especially

[†] Tables and Figures corresponding to references throughout this section can be found in appendix 3.

from the biogenically important isoprenes and terpenes, as well as from low molecular weight alkenes as well as aldehydes (Luxenhofer and Ballschmiter, 1994). The occurrence of alkyl nitrates in the urban atmosphere mainly reflects the occurrence of those alkanes which originate from automobiles exhaust gases to a high extent. Hydrocarbons that derive from natural terrestrial sources are characterized by a maximum in C_{18}-C_{24}, with the uneven carbon numbers, while marine atmosphere is marked by a maximum between C_{12}-C_{15} which originate from bioactivity in the ocean water (Luxenhofer and Ballschmiter, 1994). The rate of formation of alkyl nitrates increase with the size of the straight chain alkylperoxy radical (Turberg *et al.* 1990). For typical atmospheric conditions, the yield of alkyl nitrates increases from <1.4% for ethane to 33% for octane (Atlas and Schauffler, 1991). However, the $RO_2^{\bullet}$ radical, especially in a low NO_x environment, may undergo reactions forming other than alkyl nitrates products, thus can limit organic nitrate formation (Roberts, 1990). Thus, NO content is a parameter that regulates the formation of alkyl nitrates. NO is the primary reaction product of N_2 and O_2 at very high temperatures, but it is also formed by the photolysis of NO_2 (Luxenhofer and Ballschmiter, 1994).

A possible source of organic nitrates is formation in combustion effluents. The extent of formation of $RONO_2$ compounds in combustion effluents depends critically on the combination of gas composition and temperature, and nitrate formation may occur upon mixing of the exhaust with the ambient air. However alkyl nitrates have not been observed in exhaust from internal combustion engines (Jonsson, 1985). During biomass burning experiments conducted at Max-Planck Institute für Chemie, Mainz (Flocke *et al.*, 1991), methylnitrate was observed, however 4 orders of magnitude lower relative to the yield of NO_x. Thus it was concluded that industrial and combustion processes are unlikely to constitute a major source of organic nitrates.

Short-chain ANs (with 2-5 C-atoms) have a relatively long lifetime in the atmosphere. Specifically, the half-life of pentyl nitrate and ethyl nitrate is estimated to be from weeks to several days, respectively (Roberts and Fajer, 1989; Clemitshaw *et al*., 1997). Therefore they may behave as temporary reservoirs for reactive nitrogen and promote ozone production, by undergoing long-range transport in the troposphere to release NO_x ($NO+NO_2$) in regions remote from their formation (Clemitshaw *et al*., 1997). The lifetime is assumed to decrease further for ANs with chain lengths above 5 carbon atoms. The ANs are more stable than peroxyacyl nitrates and therefore, are more susceptible to removal by wet and dry deposition to the surface of the earth (Roberts, 1990).

The processes responsible for the degradation of organic nitrates are reaction with OH radicals (> C5), photolysis, and thermal decomposition. Processes of potential importance are uptake by cloud water, aerosols, or precipitation, and deposition on ground surfaces.

The most significant atmospheric loss mechanism appears to be the photolysis through the absorption of the solar radiation near-UV region (<330 nm) (Roberts, 1990). Probably, it occurs mainly by the breakage of the RO-NO_2 bond since the energy of this bond is approximately equal to the activation energy observed in the thermal decomposition of alkyl nitrates; such breakage is energetically allowed at all wavelengths through absorption spectra (Turberg *et al*., 1990). A pronounced temperature dependence was observed in the photolysis rates of ethyl, n-propyl and 2-butyl nitrates which yielded doubled rate between 6-26 °C (Turberg *et al*. 1990) estimates a lifetime of 1-100 days for $RONO_2$ and $ROONO_2$ and most certainly would exhibit strong altitude dependencies. Turberg *et al*. (1990) estimated the photo-dissociation rate coefficients of methyl, ethyl-, n-propyl-, n-butyl- and isopropyl-nitrates, which showed a strong dependency on altitude. The photolytic rates were observed to vary not only with altitude and temperature but with the total column O_3 concentration as well (Roberts, 1990).

Thermal decomposition is an important process because it constitutes the major atmospheric loss mechanism of $ROONO_2$ compounds and can limit the extent to which $RONO_2$ compounds can survive in combustion sources. Conclusions were made that $RONO_2$ compounds are stable at atmospheric temperatures; however they can decompose at significant rates in exhaust streams and at temperatures present in instrumentation used to make chemical measurements, such as NO_2 reduction and GC injection ports (Roberts, 1990).

The degree of adsorption on solid particulate matter would seem to be governed by the vapour pressure of a compound, hence its size. On this basis, compounds having vapour pressure <0.01 torr can be expected to be significantly partitioned onto solid particles. Therefore, organic nitrates of ~7 carbons or more may be found on solid particles to some extent.

The ANs are believed to play an important role for the nitrogen flux, especially when related to the marine environment. Several studies have investigated their temporal variations and geographical distributions (Simpson *et al.*, 2006). First detailed measurements of short chain alkyl nitrates were done by Atlas *et al*, 1988. It was found that the sum of C3-C5 had a mean concentration of 3.3 ppt (v) in marine air (Atlas and Schauffler, 1991). In polluted and heavily polluted areas, concentrations of short-chain alkyl nitrates range from 40 to 105 ppt(v) (Flocke *et al.*, 1991; Luxenhofer *et a*l., 1994). Atlas *et al*. (1993) have monitored the concentrations of ethyl and propyl nitrates above the equatorial Pacific Ocean as a function of height and has concluded that both continental and oceanic sources are responsible for their presence. The research group at the University of Ulm (Germany) has published studies on ANs in the North and South Atlantic Ocean, vicinity of Ulm, several sites in California and the lower troposphere of the Antarctica (Luxenhofer *et a*l., 1994; Luxenhofer and Ballschmiter, 1994; Luxenhofer *et al*., 1996; Schnieder *et a*l., 1998; Fischer *et al*., 2002). Luxenhoffer *et al*. (1996) found concentrations of 44.2-56.7 ng N m^{-3} or 5,7-7,8 ppt (v) for the sum of C_6-C_{14} in the air collected near Ulm. No alkyl nitrates with a chain longer than C_{17} were observed. Also research cruise campaigns have been conducted across the Atlantic Ocean (Schneider and Ballschmiter, 1999; Fischer *et al*., 2000). Additional data are available for sampling at the coast of South Africa, for the Athens basin and a rural sampling site in Denmark Copenhagen (De Kock and Anderson, 1994; Nielsen *et al*., 1998; Glavas and Moschonas, 2001). The low concentrations of ANs and the complexity of the atmospheric system in terms of organic gas phase and aerosol components with a wide range of polarity make sampling, direct detection and quantification of ANs in the ambient air a challenging task.

3.1.2. Analytical procedures for the determination of organic nitrates

Sampling of the gas phase has been performed in several ways, using Tenax adsorption columns (Luxenhofer *et al*., 1994; Fischer *et al*., 2000 and 2002), a combination of Tenax cartridges and polyurethane (PU) foam (Luxenhofer *et al*., 1994), silicagel and PU foam (Luxenhofer *et al*., 1996), silicagel and Tenax (Schneider *et al*., 1998; Schneider and Ballschmiter, 1999) or even charcoal (Atlas, 1988; Atlas and Schauffler, 1991; De Kock and Anderson, 1994).

The first identifications of organic nitrates in laboratory photooxidation systems were made by Stephens *et al*. (1956). Generally organic nitrates have been measured by high-resolution gas chromatography (GC) with electron capture detection (ECD) (De Kock and Anderson, 1994; Moschonas and Glavas, 2000; Glavas, 2001; Glavas and Moschonas, 2001; Fisher *et al*., 2002) and a combination of GC-ECD and GC-MS (Luxenhofer *et al*., 1994; Luxenhofer *et al*., 1996; Schneider *et al.*, 1998; Schneider and Ballschmiter, 1999; Fisher *et al*., 2000). A gold converter used in combination with NO-chemiluminescence detector

(CLD) was used by Flocke *et al.* (1991). The above mentioned detection technique was 1-2 orders of magnitude less sensitive than ECD detection. However, the authors underline its high specificity for components of the NO_y family in contrary to ECD, which places high demands on the resolving power of the GC column because of its sensitivity to halogenated hydrocarbons and other electro-negative compounds. Both traditional injections from an extract (De Kock and Anderson, 1994; Luxenhofer *et al*., 1994 and 1996; Schneider *et al*., 1998; Schneider and Ballschmiter, 1999) as well as thermal desorption of the gas adsorption traps and cryo-trapping have been applied (Flocke *et al.*, 1991, Fischer *et al*., 2000; Moschanos and Glavas, 2000; Fisher et al., 2002). Still, preseparation is critical and diverse procedures have been described such as liquid chromatography on silicagel (Luxenhofer *et a*l., 1996; Schneider and Ballschmiter, 1999) or normal-phase high-performance liquid chromatography (NP-HPLC) with an organonitrate stationary phase (Fischer *et a*l., 2000).

3.1.3. Limits of detection

Various limits of detection have been reported through the literature, depending on the techniques used for sampling, proceeding of samples and quantification. The detection limit of the system reported by Flocke *et al*. (1991) (cryogenic concentration and detection by GC-CLD) was 1 ppt in a sample volume of 3 l. Authors were able to detect C_1-C_8 nitrates in ambient air measurements in Germany. Atlas and Schauffler (1991), reported limit of detection of approximately 4 pg/compound, in a 10 l sample this amounts corresponds to < 0.1 ppt(v) for the $\geq C_3$ and halocarbons. Fischer *et al*. (2002), reported limits of detection for 30 l sample, equal to 0.3 ng/m^3 (or 0.05 ppt(v)). The detection limit reported by Moschonas and Glavas (2000), varied from 0.02 to10 ppt(v) depending on the compound.

3.1.4. Purpose of study

Within the framework of the present project, aiming also at the characterisation of organic nitrogen compounds in the marine environment, it appeared to be necessary to develop a sensitive and robust analytical procedure to the determination of ANs, particularly with the application of GC-MS to replace the routine application of GC-ECD. The latter method provides intrinsically high sensitivity and easy operation, but can be subjected to interferences (Glavas, 2001) to be identified with the aid of the highly specific MS detection. The different steps going from sampling to extraction, clean-up and instrumental analysis have been systematically optimised for ANs with 3 to 9 carbons.
We report here an adapted set-up for low and high volume sampling, extraction and minimised clean-up, identification and quantification capabilities resulting from the complementary use of GC-ECD and GC-MS methods. The preparation of suitable standards for instrumental calibration of the signal intensities is discussed. Also, the levels of gas phase ANs together with identification of the possible sources of these compounds in the air are the goals of this study. Seasonal trends were also investigated by conducting the sampling campaigns during the spring, summer and winter time.

3.2. Experimental

3.2.1. Description of the modified high volume (Hi Vol) sampler

A common Hi-Vol sampler has been redesigned for combined collection of aerosol and gas phase components of the ambient air using either a low-or-high-capacity gas adsorption trap. Particular attention has been paid to redesign the shape of the housing in

order to reduce the effect of the wind direction on the sampling and to improve protection during sample exchange. Furthermore, a rugged pump system and rotameter control of the sampling rate have been incorporated to ensure reliable and maintenance-free operation over long periods without the need to calibrate the flow rate as a function of the under-pressure over a calibrated orifice.

Figure 3.1, shows the design principle of the set-up. Figure 3.2, shows photographs of the inlet of the samples (a) and overall view of the sampler (b). The particles are collected on a filter with a diameter of 11 cm in a stainless steel filter holder with separate pressing and tightening rings to avoid filter damage during mounting. A Viton O-ring is used for sealing. The filter is mounted on the top of a cylindrical manifold with length of 30 cm and inner diameter of 9 cm. The large capacity adsorption trap with internal diameter of 70 mm and height of 50 mm can be inserted in the cylinder and is sealed by a Vitron O-ring of which the groove is calculated for dynamic sealing. The adsorption trap can take up about 175 cm^3 of adsorbent, corresponding to 100 g of silicagel (35-70 mesh). The cylinder is also fitted with four aspiration tubes for the 4 low capacity adsorption traps. The tube diameters are calculated to maintain isokinetic sampling in order to avoid turbulences in the system. The low capacity traps consist of glass tubes (ID: 8 mm, length: 95 mm), mounted in stainless steel protection tubes with the aid of 2 external O-rings. Screw connections of generous dimensions allow the tubes to be mounted leak free with finger tightening only. Connections and protection tubes are again sealed by O-rings and the pressing rings are separated from the turning fittings. The exits of the 4 gas traps are connected to a housing of which the internal design allows combination of the flows into one exit under laminar conditions. The flow (about 3 $m^3\ h^{-1}$) through the four gas traps together is measured by a rotameter (RAGH02-D2ST-G161A-PP16, Rota Yokogawa, Wehr, Germany) and directed to another housing where it is combined with the flow through the main aspiration line at the bottom of the manifold cylinder. Also here the bottom of the cylinder is conically shaped inside to avoid any turbulence. To compensate for the hydrodynamic resistance of the gas traps, a 2 inch diameter ball valve is fitted between the manifold and the second connection housing. From that housing the flows goes through a large rotameter (Model RAGH06-D2ST-G471A-PPN45, Rota Yokogawa, Wehr, Germany) to the pump (max. flow rate 40 $m^3\ h^{-1}$, DT4.40 Becker GmbH, Wuppertal, Germany) with constant flow characteristics over a wide range of low-pressure conditions.

Except the pump, the sampling system is mounted in an aluminium housing (50x50x100cm) with a pyramidal roof (height: 40 cm). The pyramidal shape avoids the asymmetry of the roof section in the common Hi-Vol sampler (with two vertical and two angles surfaces) and thereby avoids the effect of the wind direction on the sampling characteristics. The sampler is mounted on lightweight rods extending at an angle of 45^o with lead-filled supports to ensure stable positioning without the aid of additional means. The housing has a door and opening section on two opposite sites so that sample can be exchanged either side and thereby under protection against wind and rain (as opposed to the common Hi-Vol sampler).

3.2.2. Sampling and weather data collection procedures

In order to check the applicability of the analytical method, samples have been taken during 24 h, four days in a week, on a coastal region, De Haan, Belgium ($51^o17'$ N, $3^o04'$ E) during two weeks in August and three months (February-April) in 2006. The information provided by the meteorological station (wind direction and speed, rain, ambient temperature) were acquired once of each second for all period of sampling and for the calculations the average values were considered. Also, air-mass backward trajectories were specifically

calculated for the sampling periods by Hybrid Single-Particle Lagrangian Integrated Trajectory (HYSPLIT) Model and were considered for determine the influence of the Atlantic Ocean, the North Sea and the continent as possible sources of the ANs (Draxler and Rolph, 2003; Rolph, 2003).

A glass fibre filter (Whatmann GF 25) has been fitted to collect the particles from total volume. Gas phase sampling with the low capacity adsorption traps has been achieved using 2 g of Tenax-TA® (60-80 mesh, Buchem, Apeldoorn, the Netherlands) in each of the four tubes. The adsorbent has been pre-extracted with acetone in a Soxhlet for 8 h. A total volume of less than 20 m^3 has been sampled at a flow rate of 3 m^3 h^{-1} over the four traps. Alternatively, the high capacity adsorption trap has been filled with 100 g silicagel (35-70 mesh, Sigma Aldrich NV/SA, Bornem, Belgium) for the collection of the gas phase components. Silicagel was washed before sampling with a 4:1 (v/v) mixture of pentane-dichloromethane, dried and activated in oven by heating to 160 ^oC for 24 hours. A volume of typically 250 m^3 was sampled at a flow rate of 10 m^3 h^{-1} during 24 h periods.

3.2.3. Synthesis of reference alkyl nitrate compounds for calibration

Apart from isopropyl and isobutyl nitrates, which are commercially available (99 % purity, Aldrich Chem. Co., Steinheim, Germany), the other ANs had to be synthesised to calibrate the signal intensity in GC-MS of GC-ECD as a function of the injected amount. The corresponding halides (iodides used for methyl and 2-butyl nitrates and corresponding bromides for other ANs synthesised) were dissolved in acetonitrile at a concentration in the range of 10^{-3} M, then mixed with a solution of $AgNO_3$ in acetonitrile, containing two-fold excess of the equivalent amount needed in the reaction, and stirred for 24 hours in the dark at room temperature (RT) (Luxenhofer *et al*., 1994). During reaction, the ANs were separated as a separate phase at the top of the solution. Once recovered, separated in an extraction funnel, the ANs were washed with water, dried on Na_2SO_4 and afterwards recovered from the drying agent with dichloromethane. Table 3.1 lists the reaction yields, estimated from the weight of the silver halide precipitate formed during reaction, together with the nomenclature used for the ANs (Schneider and Ballschmiter, 1996; Fischer *et al*., 2002).

3.2.4. Extraction and clean-up procedures

Subsequent Soxhlet extraction with 150 ml acetone and pentane (8 h each) was applied for the recovery of the adsorbed gas phase components from the Tenax TA® samples. The extract was concentrated to 0.5 ml at RT under a gentle nitrogen flow. The further sample clean-up used a glass column with ID of 10 mm containing 4 g of Florisil (100-200 mesh, Fluka, Buchs, Switzerland), heated before use at 120^oC for 12 h. Pentane was used as eluent and the fraction between 9 and 27 ml was kept for analysis. Subsequently, the volume was reduced to about 0.5 ml under a nitrogen steam at RT and 2-fluoro-toluene was added as an internal standard. The samples were stored in the refrigerator at 0^oC prior to injection.

The organic compounds were eluted from the silicagel samples with a 400 ml aliquot of 4:1 (v/v) mixture of pentane-dichloromethane in a water-cooled glass column. Before extraction, 2-fluoro-toluene was added as an internal standard and left for 5 minutes for the evaporation of the solvent. The extract was concentrated to 150 µl at RT under a gentle nitrogen flow. The method is based on combined extraction of the analytes with a clean-up step.

3.2.5. GC-MS and GC-ECD separation, detection and quantitation

The analysis was performed with a Saturn 2000 GC-MS (Varian Inc., Lake Forest, CA) featuring an ion-trap MS and electron ionisation (EI). A VF-1ms capillary column (100% dimethylpolysiloxane, Varian Inc.) with a length of 30 m, an ID of 0.25 mm and a film thickness of 1 µm was used with a He flow rate of 1 ml min^{-1}. Splitless injection of 1 µl of sample aliquot was applied. The temperatures of injector, transfer line and ion-trap were set at 250, 220 and 240 ^{o}C, respectively. The applied temperature programme is given in Table 3.2. Table 3.3 lists elution order and relative retention time of alkyl nitrates on VF-1ms capillary column.

Multi-level calibration curves were created for the quantification and good linearity (correlation coefficient - R>0.9989) was achieved for the whole concentration range found for the samples. The analyte identification was based on relative retention times and ion chromatograms. A deviation of the ion intensity ratios within 20% of the mean values of the calibration standards was considered acceptable. Peak area ratios (analyte response/internal standard response) were plotted against the concentration ratios (analyte concentration/internal standard concentration). Calibration curves were measured daily.

The analysis of ANs by mass selective detection following electron impact ionisation (EI) was based on the formation of an intense ion at m/z 46 corresponding to the NO_2^+ fragment.

Additionally, a Hewlett-Packard 5890 Series II GC (Hewlett-Packard, Palo Alto, CA) with electron capture detector (ECD) was used. The injector and detector temperatures were kept at 250 ^{o}C and nitrogen was used as carrier gas at a flow rate of 1.5 ml min^{-1}. Also there, 1 µl aliquot of sample solutions was applied with splitless injection. The temperature programme is given in Table 3.2.

3.2.6. Data processing of environmental samples

The air-mass backward trajectories were specifically calculated on a daily-base for the coastal sampling station. The HYSPLIT Model was used together with the meteorological information collected at the sampling site. A clustering procedure using the SPSS software for Windows (11.0) was applied on all data, in order to reveal correlations between all samples.

3.2.7. Flux calculations

The relevant literature has not yet reported deposition rates for alkyle nitrates. Therefore, in order to make an estimate of the AN-fluxes, the data of peroxyacyl nitrate (PAN) was selected (Hertel et al., 1995). Analogous to the inorganic nitrogen compounds, the daily data were assorted according to the origin of main air-masses, i.e., Atlantic/Channel, North Sea, and Continental. From these data, the average fluxes of individual ANs and the total AN-contributions were calculated.

3.3. Results and discussion

3.3.1. Sampling methodology

Use of adsorption tubes is the most common method to collect organic compounds from the gas phase. A critical parameter to be considered is the breakthrough volume of the adsorption system: on the one hand, the sampled volume should be as high as possible to

facilitate the detection of low level components. On the other hand, it should be kept small enough to ensure the volatile, already adsorbed compounds on the adsorbent do not undergo losses. It is common practice to determine the limiting volume by connecting two adsorption tubes in series (Atlas and Schauffler, 1991; Luxenhofer and Ballschmiter, 1994). However, in that case, the detection limit of the analytical method determines how much the breakthrough volume of the first column must be exceeded. Therefore, we have used an alternative approach based on isothermal adsorption chromatography

Basically, a conventional glass column is packed with the known weight of adsorbent and the retention volume in isothermal elution on a GC-ECD system is measured at different temperatures. Plotting the logarithm of the corrected retention volume as a function of the reciprocal temperature gives a linear relationship, which can be extrapolated with a good accuracy to derive a realistic value for the breakthrough volume. Table 3.2 gives the breakthrough volumes for ANs from C3 to C7 for Tenax TA® and for C3 on Silicagel. For the latter adsorbent only the breakthrough volume for the most volatile compound has been determined as the retention time becomes too long (at the maximal allowable column temperature) for the higher analogues. Specifically, whenever correct sampling of C3 is aimed at, the sampling volume should be kept within 0.26 and 103 m^3 per g of Tenax TA® and silicagel, respectively. Besides the substantially higher retention capacity of silicagel, it is also less expensive than Tenax TA® and, therefore, it can be used in large adsorption traps without the need of recovering the adsorbent after extraction and analysis. Therefore, for practical application to ambient air sampling, 100 g of silicagel has been used.

3.3.2. Analytical methodology

The small amounts of adsorbens in Tenax TA® sampling makes Soxhlet extraction the most adequate. The extraction efficiency has been checked by spiking 8 g Tenax TA® with a 10 µl of a reference mixture containing all ANs (cf. Table 3.1) in acetone at a concentration of 50 µg ml^{-1}. The recovery values for extraction of the reference compounds using the described method ranged from 85 % for C3 to 95% for C9. In contrast, the large gas trap containing 100 g of silicagel has needed another method. Specifically, the adsorbent is flushed with 400 ml of pentane and dichloromethane in a cooled column. The extraction efficiency has been determined in the same way as for the Tenax TA® and yielded a recovery of 93 to 97% for silicagel. Solvent desorption after adsorptive sampling combines the advantages of multiply injections with various detection methods in GC, including sample pre-separation to reduce the complexity of the analytes (Luxenhoffer et al, 1996).

In spite of the cleaning procedure applied to the adsorbent before use, both materials still contained significant concentrations of trace contaminants. However, the specificity of the GC-MS and GC-ECD methods used in this study was sufficiently high to avoid further pre-cleaning. Fig. 3.3 (a) and (b) illustrate the GC-Ms results of a blank sample. The total ion chromatogram (TIC) contained several major peaks, most of which refer to phthalates. However, the use of the mass chromatogram at m/z 46 (due to NO_2^+) for the selective detection of ANs allows the problem of contaminants to be circumvented.

Fig. 3.3(a) and 3.3(b) show the typical results for GC-MS analysis of reference mixtures and the extract of an environmental sample. The mass chromatogram at m/z 46 for the reference mixture shows the adequate separation with a resolution well above 1, even for the isomers with the same chain length. For quantification, the mass chromatogram at m/z 46 has been as the best compromise between specificity and intensity. The calibration of the intensity as a function of the relative abundance of the AN to 2-fluorotoluene is linear over 1.5 decades, while the precision with 5 injections is within 6 % and the LOD is around 30 pg injected (cf. Table 3.4). Substantial differences in the sensitivity for each analogue are

noticed, requiring separate calibration curves to be constructed. Also, shown in Fig. 3.3(c) is the application of the method to an ambient sample. The TIC clearly shows the presence of many major components, of which the identification will not be discussed here. The ANs are only minor trace constituents, visible in the selective mass chromatogram at m/z 46. The high abundance of C7 in this sample relative to the other ANs shows the need to have a sufficiently wide linear range. Also, the chromatographic separation is clearly maintained, indicating that the major components of the column are not overloading the system.

Fig. 3.3 (c) illustrates the application of GC-ECD to a reference mixture and an environmental sample. Chromatographic separation of the reference mixture on the same column presents no particular problem. As to the analytical parameters, most are comparable with those in GC-MS except the LOD, which is 10 times better in GC-ECD than in GC-MS. Therefore, the method is preferred to be used for routine measurements of environmental samples, however with the back up of GC-MS to overcome the lower specificity of GC-ECD and to verify the absence of interferences in samples with (largely) different matrices. As in GC-MS, also GC-ECD requires calibration curves for each analogue individually as the sensitivity varies with the length and branching. The application to environmental sample clearly illustrates the reduced specificity of GC-ECD in that several (major) peaks from compounds other than ANs are indeed detected. Still, the ANs can be readily traced back easily and quantified separately from the matrix.

3.3.3. Applications to environmental samples

The application of the developed analytical methodology has been demonstrated on a set of 71 diurnal (24h) samples, taken at the Belgian coast over a period of two weeks in the summer 2005 (August), nine weeks in winter/spring 2006 (February-March) and 8 weeks in summer 2006 (June-August); mostly there were four samples taken per week. The results are shown in Fig. 3.5. In the samples from the summer campaigns, 11 ANs have been identified and quantified, but only 8 ANs were detected in the winter/spring samples.

As the AN levels are in the range of a few to 7400 pg m^{-3} of sampled air, the LOD with GC-MS are sufficient for most samples on the condition of a sample volume of 250 m^3.

The AN fraction of the ambient gas phase consists of primarily the 2C4, C5 and C6 isomers, which contribute largely to the total sum.

However, both the levels and the relative abundances of ANs are found to exhibit strong variations as a result of their generation most likely by different sources of which the input varies over time (cf. later on). Therefore, Fig. 3.4 gives the concentration ranges for the different isomers of the different analogues for the three sampling campaign. The fluctuating levels require the latter data to be presented on a logarithmic scale. For the convenience of the reader, the middle of the range is explicitly indicated, but it must be stressed that no averaging is involved in this figure. In a first approximation, the levels look somewhat lower in the 1st campaign while the third one (essentially during a summer period again) yield ranges extending to higher values.

Fig. 3.5 summarises the data in the form of the summed concentrations for all alkyl nitrates detected for each sample. It is to be noted, however, that the distribution over the different analogues and isomers is largely fluctuating between samples. Considering the latter variability, it is preferred to interpret the data as essentially constant levels except for a few samples, i.e., 21st February (6470 pg/m^3) and 22 February (6520 pg/m^3), 15th of June (8700 pg/m^3) and 20th of June (9020 pg/m^3). For more detailed analysis of the fluctuating levels, in our opinion it is scientifically better to make such graphs for individual compounds. Fig. 3.6 gave such plots for two selected analogues, 3C5 and 2C6. No correlation could be found with the average temperature during sampling.

The 24h data were treated with hierarchical clustering using the between-groups linkage with the squared Euclidean distance as an interval. Then it was attempted to relate the groups in the resulting dendrograms with the main information from the BWTs and meteorological information. Fig. 3.8 summarises the main information for the 1st and 2nd campaign using the summed AN concentrations as an input. A first grouping occurs depending on the wet precipitation, yielding classes I and II. Specifically most of the samples in groups A and B were characterized by a wet precipitation of less than 10^{-3} l per m^2 per day. Furthermore, a quite distinct group A was traced back by clustering. These samples showed for high levels of C6 and C7 ANs and occurred for air-masses coming from deep inside Eastern Europe, like Ukraine, and Russia. The majority of samples do not show yet a clear correlation with the BWTs. It looks like there is a variety of (local) anthropogenic sources with time-variable contributions or importance to be considered when the air passed even for a short distances over the UK or France.

Other attempts to increase the data set and change the input to concentrations of individual analogues of summed isomers led to the same conclusion up to now : no conclusive evidence could be obtained yet from multivariate statistical treatment that would be obvious point to an unambiguous relationship between the AN levels and a given processes, source or parameter. As a result, the role of the different natural sources for ANs, that are believed to be operative in the North Sea and North Atlantic Ocean, cannot be readily traced back from the limited data set at this moment.

3.3.4. Estimation of alkyl nitrate fluxes

2nd campaign As expected from the analytical results, the highest average daily deposition has been observed for the 3C5 alkyl nitrate. The highest average daily deposition of 3C5 has been found for UK/Atlantic/Channel air-masses (1.8 ng N/m^2 day), followed by lower values for the North Sea/continental (0.76 ng N/m^2 day), but below the detection limit for the North Sea air-masses (0.18 ng N/m^2 day). The contribution of 2C4 was also significant for the UK/Atlantic/Channel air-masses (i.e., 1.7 ng N/m^2 day), whereas lower contributions were found from 1C3, 1C4, 2C5, 1C5, 3C6, 2C6, 1C6 and 1C8 alkyl nitrates with similar fluxes (0.25 ng N/m^2 day). For the North Sea influenced air-masses, the contributions from 2C4 and 2C5 were found to be significant, both with a deposition value of 0.44 ng/m^2 day. Moreover, the 1C4, 1C5, 3C6 and 1C6 ANs also contributed to the flux, each with ~0.2 ng N/m^2 day. Under mixed continental-North Sea influence, the contribution was significant from 1C4, 3C5, and 2C5 compounds, with deposition rates of 0.35, 0.76, and 0.46 ng N/m^2 day, respectively. The 1C5, 1C6, 1C7, 1C8, and 1C9 compounds also contributed to the N-flux, each with around 0.2 ng N/m^2 day deposition flux.

The average fluxes of ANs for the UK/Atlantic/Channel, North Sea and the mixed continental-North Sea air-masses were found to be 5.3, 1.4, and 2.9 ng N/m^2 day, corresponding to an overall AN flux of 9.6 ng N/m^2 day for this short summer campaign.

3rd campaign In this early winter/spring campaign, a high average daily flux of 3C5 has also been found for all the three main air-masses, ranging from 3.8 to 10.7 ng N/m^2 day. For the Atlantic/Channel/UK air-masses, the contributions of 3C5 was about 55 % of the total AN flux, followed by the 2C5 (0.98 ng N/m^2 day), 2C6 and 1C8 (each with 0.5 ng N/m^2 day), whereas the fluxes of 1C4, 1C5, 1C6, and 1C9 were much lower, i.e., 0.15, 0.22, 0.37, and 0.34 ng N/m^2 day, respectively.

For continental air-masses, intensive fluxes of 3C5, 1C6, and 1C7 AN compounds, i.e., 4.4, 5.7, and 4.6 ng N/m^2 day, respectively, have been observed. The 2C5 has also shown a fairly high value of 1.5 ng N/m^2 day. The 1C8 and 1C9 ANs has only contributed with negligibly low fluxes of 0.37 and 0.15 ng N/m^2 day, respectively. For air-masses, arriving

from the North Sea, the flux of 3C5 was extremely high, i.e., with an average value of 10.7 ng N/m^2 day, corresponding to about 80 % of the total average AN-flux. The other AN fluxes characteristic for this air-mass, were 2C5, 1C5, 2C6 and 1C6 with low fluxed, ranging between 0.5-0.73 ng N/m^2 day, and also negligibly low fluxes of 1C4, 1C8 and 1C9 ANs were also found with values of 0.16-0.27 ng N/m^2 day.

The average fluxes of ANs for the Atlantic/Channel/UK, continental and North Sea air-masses were found to be 6.9, 15.6, and 13.8 ng N/m^2 day, corresponding to an overall AN-flux of 36.3 ng N/m^2 day for this campaign. It can be concluded that the most contribution of AN-fluxes originate from air-masses approaching from the continent and the North Sea.

4th campaign In this longer summer campaign, similarly to the short (2nd) campaign, the AN-fluxes were the most significant from the Atlantic/Channel/UK air-masses. The highest N-flux was observed again by 3C5 with an average value of 12.9 ng N/m^2 day, although the 1C4 flux was also very pronounced (6.5 ng N/m^2 day). The 1C6, 1C7, 1C8 and 1C9 ANs also contributed to the N-flux, but to a much lower extent than the former two ANs, i.e., with depositions ranging between 1.0-1.2 ng N/m^2 day. The fluxes of 2C5, 1C5, and 2C6 were negligibly low, amounting only up to 0.38, 0.6, and 0.57 ng N/m^2 day, respectively.

For continental air-masses, the daily average fluxes of 1C4, 3C5 and 1C8 were found to be the most significant contributors, i.e., 1.0, 2.8 and 2.0 ng N/m^2 day, respectively. The fluxes of 1C5, 2C6, 1C6, and 1C7 were lower, ranging between 0.34-0.46 ng N/m^2 day. For the North Sea air-masses, also the flux of 3C5 was the most decisive with an average value of 4.5 ng N/m^2 day, followed by the 1C5 flux (0.9 ng N/m^2 day). The 1C4, 2C6, 1C6, 1C7, 1C8 and 1C9 compounds contributed to the N-flux to a low and varying extent, i.e., 0.5, 0.3, 0.67, 0.36, 0.45, and 0.18 ng N/m^2 day, respectively.

The average fluxes of ANs for the Atlantic/Channel/UK, continental and North Sea air-masses were found to be 25.3, 7.5, and 7.9 ng N/m^2 day, corresponding to an overall AN-flux of 40.7 ng N/m^2 day for this campaign. Comparing this campaigns data with those observed for the 3rd (spring) campaign, a much higher percentage of AN contribution to the N-flux by the Atlantic/Channel/UK air-masses can be experienced (i.e. ~60 % of the total average AN-flux), whereas in the 3rd campaign the fluxes from the North Sea and the continental air-masses were prevailing (i.e., 38 % and 43 %, respectively). The N-fluxes by ANs are more pronounced for the summer periods than for the winter/spring months, although their contribution to the total (inorganic and organic) N-flux is still low.

3.4. Literature

Altshuller, A.P., 1986. The role of nitrogen oxides in nonurban ozone formation in the planetary boundary layer over N. America, W. Europe and adjacent areas of ocean. Atmos. Environ. 20, 245-268.

Atkinson, R., Aschmann, S.M., Carter, W.P.L., Winer, A.M., Pitts Jr., J.M., 1982. Alkyl nitrate formation from NO_x-air photooxidations of C_2-C_8 n-alkanes. J. Phys. Chem. 86, 4563-4569.

Atlas E., 1988. Evidence for ≥ C3 alkyl nitrates in rural and remote atmospheres. Nature 331, 426-428.

Atlas, E., Schauffler, S., 1991. Analysis of alkyl nitrates and selected halocarbons in the ambient atmosphere using a charcoal preconcentration technique. Environ. Sci. Technol. 25: 61-67

Atlas, E., Pollock, W., Greenberg, J., Heidt, L., Thompson, A.M., 1993. Alkyl nitrates, nonmethane hydrocarbons and halocarbon gases over the equatorial Pacific-Ocean during SAGA-3. J. Geophys. Res.-Atmos., 98: 16933-16947

Clemitshaw, K.C., Williams, J., Rattigan, O.V., Shallcross, D.E., Law, K.S., Cox, R.A., 1997. Gas-phase ultraviolet absorption cross-sections and atmospheric lifetimes of several C_2-C_5 alkyl nitrates. J. Photochem. Photobiol. A: Chem. 102, 117-126.

Crutzen, P.J., 1979. The role of NO and NO_2 in the chemistry of the troposphere and stratosphere. Ann. Rev. Earth Planet. Sci. 7, 443-472.

De Kock, A.C., Anderson, C.R., 1994. The measurement of C3-C5 alkyl nitrates at a coastal sampling site in the southern hemisphere. Chemosphere, 29, 299-310.

Draxler, R.R., Rolph, G.D., 2003. HYSPLIT (HYbrid Single-Particle Lagrangian Integrated Trajectory) Model access via NOAA ARL READY Website (http://www.arl.noaa.gov/ready/hysplit4.html). NOAA Air Resources Laboratory, Silver Spring, MD.

Fischer R.G., Kastler, J., Ballschmiter, K., 2000. Levels and pattern of alkyl nitrates, multifunctional alkyl nitrates and halocarbons in the air over the Atlantic Ocean. J. Geophys. Res. 105, 14473-14494

Fischer, R., Weller, R., Jacobi, H.W., Ballschmiter, K., 2002. Levels and pattern of volatile organic nitrates and halocarbons in the air at Neumayer Station (70°S), Antarctic. Chemosphere 48, 981-992.

Flocke, F., Volz-Thomas, A., Kley, D., 1991. Measurements of alkyl nitrates in rural and polluted air masses. Atmos. Environ., 25A, 1951-1960

Glavas, S., 2001. Analysis of C2-C4 peroxyacyl nitrates and C1-C5 alkyl nitrates with a non-polar capillary column. J. Chromatogr. A 915, 271-274.

Glavas, S., Moschonas, N., 2001. Determination of PAN, PPN, PnBN and selected pentyl nitrates in Athens, Greece. Atmospheric Environment 35: 5467-5475

Hertel, O., Christensen, J., Runge, E.H., Asman, W.A.H., Berkowicz, R., Hovmand, M.F., Hov, Ø., Atmos. Environ., 29 (1995) 1267.

Liu, S.C., McFarland, D., Kley, D., Zafiriou, O., Huebert, B., 1983. Tropospheric NO_x and O_3 budgets in the equatorial Pacific. J. Geophys. Res. 88, 1360-1368.

Logan, J.A., Prather, M.J., Wofsy, S.C., McElroy, M.B., 1981. Tropospheric chemistry: A global perspective. J. Geophys. Res. 86, 7210-7254.

Luke, W.T., Dickerson, R.R., 1988. Direct measurements of the photolysis rate coefficient of ethyl nitrate. Geophys. Res. Lett. 15, 1181-1184.

Luxenhofer, O., Ballschmiter, K., 1994. C4-C15 alkyl nitrates as organic trace compounds in air. Fresenius J. Anal. Chem., 350: 395-402

Luxenhofer, O., Schneider, E., Ballschmiter, K., 1994. Separation, detection and occurence of (C2-C8)-alkyl- and phenyl-alkyl nitrates as trace compounds in clean and polluted air. Fresenius J. Anal. Chem. 350, 384-394.

Luxenhofer, O., Schneider, M., Dambach, M., Ballschmiter, K., 1996. Semivolatile long chain of C6-C17 alkyl nitrates as trace compounds in air. Chemosphere 33: 393-404

Moschonas, N., Glavas, S., 2000. Simple cryoconcentration technique for the determination of peroxyacyl and alkyl nitrates in the atmosphere. J. Chromatogr. A 902: 405-411

Nielsen, T., Platz, J., Granby, K., Hansen, A.B., Skov, H., Egelov, A.H., 1998. Particulate organic nitrates: Sampling and night/day variation. Atmos. Environ. 32: 2601-2608

O'Brien, J.M. , Shepson, P.B., Wu, Q., Biesenthal, T., Bottenheim, J.W., Wiebe, H.A., Anlauf, K.G., Brickell, P, 1997. Production and distribution of organic nitrates and their relationship to carbonyl compounds in an urban environment. Atmos. Environ., 31, 2059-2069

Roberts, J.M., Fajer, R.W., 1989. UV Absorption cross sections of organic nitrates of potential atmospheric importance and estimation of atmospheric lifetimes. Environ. Sci. Technol. 23, 945-951.

Roberts, J.M., 1990. The atmospheric chemistry of of organic nitrates. Atmos. Environ., 24A, 243-287.

Rolph, G.D., 2003. Real-time Environmental Applications and Display System (READY) Website. (http://www.arl.noaa.gov/ready/hysplit4.html). NOAA Air Resources Laboratory, Silver Spring, MD.

Schneider, M., Ballschmiter, K., 1996. Separation of diastereomeric and enantiomeric alkyl-nitrates – systematic approach to chiral discrimination on cyclodextrin LIPODEX-D. Chem. Eur. J. 2, 539-544.

Schneider, M., Luxenhofer, O., Deissler, A., Ballschmiter, K., 1998. C1-C15 alkyl nitrates, benzyl nitrate and bifunctional nitrates: Measurements in California and South Atlantic air and global comparison using C2Cl4 and CHBr3 as marker molecules. Environ. Sci. Technol., 32: 3055-3062

Schneider, M., Ballschmiter, K., 1999. C3-C14 alkyl nitrates in remote South Atlantic air. Chemosphere 38: 233-244

Simpson, I.J., Wang, T., Guo, H., Kwok, Y.H., Flocke, F., Atlas, E., Meinardi, S., Rowland, F.S., Blake, D.R., 2006. Long term atmospheric measurements of C1-C5 alkyl nitrates in the Pearl River Delta region of southeast China. Atmos. Environ. 40: 1619-1632

Singh, H.B., 1987. Reactive nitrogen in the troposphere. Environ. Sci. Technol. 21, 320-327.

Toon, O.B., Kasting, J.B., Turco, R.P., Liu, S.M., 1987. The sulfur cycle in the marine atmosphere. J. Geophys. Res. 92, 943-964.

Turberg, M.P, Giolando, D.M., Tilt, C., Soper, T., Mason, S., Davies M, Klingensmith, P. and Takacs G.A., 1990. Atmospheric photochemistry of alkyl nitrates. J. Photochem. Photobiology, A, 51, 281-292

4. X-ray fluorescence analysis for atmospheric trace metals[‡]

4.1 Data collection

4.1.1. Sampling

Sampling for X-ray Fluorescence (XRF) was done by means of a stacked filter unit connected to a medium volume pump. The sampling arrangement is shown in Figure 4.1. The Millipore unit is shown on the top of the picture. There are two units, one for XRF sampling and one for ion chromatography (IC). The sample unit is covered with a cap, which prevents particles larger than 10 µm to penetrate. Once the particles are in the plastic tube, they will impact on the filter. Instead of the usual one filter, they will, however, however three filters. The first filter has a pore-size of 10 µm and, therefore, collects the coarse fraction. The filter fixed below this one has a pore-size of 2 µm and collects the medium fraction (2-10 µm). The last filter has a pore-size of 0.4 µm, and collects the fine fraction (0.4-2 µm). Using this kind of set-up, a size-segregation is easily accomplished. Air is sucked through the three filters during 24 hours, after which they are stored in a box for further treatment and replaced. The exact amount of air passing the filters is recorded by means of a gas-counter; usually around 60 m^3 per day is pumped. The gas-counter and the pump are stored in the box shown on the picture. During a campaign, aerosol filters were collected on 5 days each week, starting on Monday and ending when the last filters were removed on Saturday. Once a week members of our research group went to pick up the material. The everyday handling was performed by a local contact person. The filters were then stored in the refrigerator until analysis.

4.1.2. XRF analysis

4.1.2.1. Instrumentation

For the XRF analysis, the Epsilon 5 instrument (PANalytical, Almelo, The Netherlands) was used. Epsilon 5 is a high-energy EDXRF using a polarizing beam; it is equipped with a 600 W Gd-anode with a voltage ranging from 25 to 100 kV and a current from 0.5 to 24 mA. There are 13 secondary fluorescencers (Al, CaF_2, Ti, Fe, Co, Ge, KBr, Zr, Mo, Ag, CsI, CeO_2 and W) and two barklascatterers (Al_2O_3 and B_4C). It is possible to use a primary beam filter between tube and target; the following filter materials are present: Al 100 µm, Al 500 µm, Cu 250 µm, Zr 125 µm and Mo 250 µm. Detection is performed with a high purity Ge-detector (HPGe) in the energy range from 0.7 to 200 keV and a resolution at Mn K_α of < 165 eV and it needs cooling down to liquid nitrogen temperature. Tube, target, sample and detector are arranged in a Cartesian geometry in order to obtain polarization. For this research vacuum atmosphere was applied in the measurement chamber. To compensate for possible problems with inhomogeneity, a sample spinner was used. The spectrometer is equipped with an autosampler consisting of four trays, each containing room for 8 sample cups; two additional trays can be added if necessary. The complete measuring process is computer controlled. In the software package (Epsilon 5 software) the complete sample quantification process is built in going from acquiring the spectrum and the spectrum fitting over to the calibration and the quantification.

[‡] Tables and Figures corresponding to references throughout this section can be found in appendix 4.

The different measuring conditions for each element are summarized in Table 4.1. For each target a measuring time of 300 s was applied, hence the total time for analysis will be around 40 min. More information about the optimization of the used procedure can be found elsewhere (Spolnik et al., 2005). Up to 20 elements can be quantified, including several heavy metals such as Cd, Pb and Sb. The calibration is made in $\mu g/cm^2$, when taking in account the deposited filter area (in this case a circle with a diameter of 4.5 cm), this can be converted to µg per filter. Since volume of airmass passed through the filter is being recorded by the gas-counter, this can again be converted to ng/m^3, which is the regular unit of air pollution. These values were used in further data processing.

4.1.2.2. Statistical treatment

A clustering procedure was applied on all the information from XRF (i.e. all 20 elements) for each sample in order to find correlation between the samples. The SPSS for Windows (version 13) program was used to do the clustering. Hierarchical clustering using the between-group linkage was used with the squared Euclidean distance as an interval. The clusters present on the dendrograms were compared to the backward trajectories (BWTs), in order to evaluate them. On the shown dendrograms, the number code stands for the date in "ddmmyy" format. The letters R, B and W stand for red, black and white respectively, which is the used color code to indicate the different fraction. The black fraction is the coarse fraction, the red fraction the medium one and the white one is the fine fraction. Based on the found groups per campaign, one sample from each group will be chosen to investigate in more detail. Since the samples are clustered based on their concentration, the composition within one cluster should be similar. This provides a way to reduce the dataset and yet to give an objective overview of the complete sampling campaign. The BWTs from these samples will be shown, together with the absolute abundance per fraction. Comparison between the groups found per campaign will be made.

4.2. Discussion of the results

4.2.1. First campaign

4.2.1.1. Clustering

The clustering results for the coarse fraction are shown in Figure 4.2. The connection between the groups and the BWTs was very strong and the clusters were easy to explain. The smaller two fractions on the contrary were more difficult and will not be shown here, as will also be the case in the other campaigns. For the fine fraction it was even impossible to find the connection between the clusters and the BWTs. For this reason, the shown samples were each taken from one of the four identified groups using the coarse fraction.

4.2.1.2. Graphical representations

Backward trajectories The BWTs of the representative samples are shown in Figure 4.3. The backward trajectory for the sample with continental influence (Figure 4.3(a)) shows that the air-mass is passing over Southern Europe (Spain and France). For the sample with oceanic influence (Figure 4.3(b)), the air-mass is passing over the Southern part of the Atlantic Ocean and reaches Belgium through The Channel. On the backward trajectory for the sample with industrial influence (Figure 4.3(c)), it can be seen clearly that the air-mass is passing the Ruhr area in Germany. This area is heavily industrialized and is likely to have its own elemental

composition. The second sample with oceanic influence (Figure 4.3(d)), the airmass is coming from the North Pole (Artic Ocean) and reaches Belgium through the Atlantic Ocean and the North Sea.

Relative abundance On Figures 4.4 to 4.7 the relative abundance of the elements in each fraction is represented for the three influences. For the oceanic influences (Figure 4.4 and Figure 4.7) it is clear that Cl is highly abundant in the coarse fraction. Sea-salt is a very important source of Cl in atmospheric aerosols. These particles are usually present in the coarse fraction. In the samples with continental and industrial influence, the Cl becomes less abundant in the large fraction and seems to be concentrated in the medium fraction. NaCl is usually reacting with acidic gases such as SO_2 and NO_2, resulting in the formation of sodium-sulphate and -nitrate particles through exchange of Cl. NO_2 and SO_2 are mainly from anthropogenic origin, especially from traffic, industry and domestic heating, the original NaCl particles are probably mostly replaced with nitrates and sulphates. For all samples, the concentrations of Fe, Si and Ca are sharply decreasing with decreasing particle size. This can be explained by the fact that they usually originate from soil-erosion, and therefore, they occur in the coarse particulate fraction. S is mostly present in the smaller fractions, which can be explained by secondary aerosol formation resulting in smaller particles. Other elements don't reveal a typical pattern and their distribution seems different in all four cases. The main conclusion from the relative abundances is the same throughout the campaigns: Cl (from sea-salt) and the soil dust elements are more abundant in the coarse fraction. For most other elements, no clear tendency can be observed. For the other campaigns, the relative abundances will not be discussed.

Absolute abundance On Figures 4.8 to 4.14, the absolute abundance for all elements in each fraction is shown. First of all it needs to be stressed that the toxic heavy metals Se, Cr, Cd and Sb were analyzed, but their concentrations remained below the detection limit of the method (few ng/m³). It can be seen that the most abundant element are the (rather harmless) low Z elements. Cl is clearly the major constituent of coarse fraction of the oceanic samples (see Figure 4.8 to 4.9), which is to be expected, and the Cl content is the highest for the samples with air masses coming from the North Pole. The Al, Si, Ca and Fe content in this fraction are the lowest in the oceanic cases, which is logical since these elements are the main components of soil dust and therefore would be more explicitly present in the air-masses travelling over land. The industrial sample in this fraction has the maximum S content. And the metals are elevated for the samples with air mass over land (industrial and continental). The high concentrations for Pb and Ti in the industrial sample are very pronounced. For the medium fraction (Figures 4.10 and 4.11), it can be seen that Cl is now equally abundant in all for samples. As expected from an industrial area, the S content is also significantly higher than the other samples. Pb and Zn concentrations are significantly higher in the continental and industrial sample, which suggests an anthropogenic source; they probably have their sources in car exhaust. For the fine fraction (Figures 4.12 and 4.13) it is clear that S is the dominant element. Contrary to the other fraction, the oceanic samples now have the higher S content. Like in the medium fraction, Zn and Pb are the dominant metals.

4.2.2 Second Campaign

4.2.2.1 Clustering

Clustering results are not shown here, since the procedure to obtain them was identical in each campaign. Similar to the first campaign, a sample with an air-mass travelling over the Ruhr-

area in Germany is separated from the others in the early beginning. The samples with mainly oceanic influence are again grouped together. A new cluster with air-masses crossing England from top to bottom are also easily recognized. The last cluster contains a sample with a somewhat weird turn above the North Sea, which apparently yields deviating compositions. For the medium fraction fewer groups can be distinguished but the England group is still there and another sample is standing alone this time. We can see a complete group now around the sample which was standing alone in the coarse fraction, all of them were influenced by the North Sea. The sample standing alone this time also has a BWT similar to them, but the air-mass is also travelling above Iceland and along the Dutch-Belgian coast in the last couple of days. As was the case in the first campaign, the link between the BWTs and the clusters is less clear. For the fine fraction, the only cluster linked to the BWT is the one with the air-masses crossing England, which was also distinguished in the other fractions. The oceanic cluster, which was missing in the medium fraction, is showing up again here. The last cluster is new, but the two samples in it have been grouped together as well in the medium fraction. For the further discussion four samples have been chosen: one from the oceanic cluster, one from the cluster crossing England, the industrial sample (in comparison to the one in the first campaign) and the sample with the North Sea turn, which is separated in the coarse fraction and representing the North Sea cluster in the medium fraction.

4.2.2.2. Graphical representations

Backward trajectories On Figures 4.14(a) to 4.14(d) the backward trajectories of the chosen samples are shown. The sample with industrial influence (Figure 4.14(a)) is again as in the first campaign passing the Ruhr area in Germany. For the sample with oceanic influence (Figure 4.14(c)), the air-mass is travelling the Atlantic Ocean, like it was in the first campaign. There is a new group with the air-mass crossing England (Figure 4.14(b)) and a sample having a big contribution from the North Sea (Figure 4.14(d)) since the air-mass is making a turn there for several days.

Absolute abundance When checking the absolute concentrations (Figures 4.15 to 4.20, it is clear that the level of S for the sample crossing England in all fractions is very low compared to the others. Another remarkable thing is the low concentration of Cl in the coarse fraction of the oceanic sample (see Figure 4.15). The level of Cl in the industrial sample is extremely high; both compared to the other samples as compared to the highest levels of Cl found in the first campaign (see Figure 4.8). The North Sea sample gives the expected pattern, with Cl being the most abundant element in the coarse fraction; however the absolute concentration of Cl is higher than in the first campaign. However expected differently, Si, Ca and Fe in the coarse fraction are most elevated in the case of the oceanic samples. Those elements are the main constituents of soil dust and therefore the highest levels are expected in air masses travelling mostly over land, while the BWT (see Figure 4.14(c)) clearly shows that this didn't happen in the past 10 days. For most elements it can be stated that the found concentrations for all elements in the medium and fine fraction are smaller than in the first campaign. In the coarse fraction they are comparable to the first campaign, except for Cl. In the medium fraction (Figures 4.16 to 2.18) it can be noticed that the industrial sample and the North Sea sample have similar concentrations. This explains why they are grouped together in the clustering of this fraction, although the BWTs are definitely different in this case.

4.2.3 Third campaign

4.2.3.1 Clustering

In contrary to the previous two campaigns, no cluster containing samples with industrial influence are separated. Detailed investigation of the BWTs learned that there are indeed no air masses found that clearly travel the Ruhr area in Germany. As usual a cluster containing samples with an air-mass mainly travelling over the ocean is separated. Another cluster with trajectories mainly over the continent is also found, linked together in one group with the oceanic samples on a higher level. A new group strongly influenced by England, France and the Channel is found. It is slightly unexpected that the group with the more continental influence is closely correlated with the oceanic group. The results of the medium fraction are not so similar to the ones in the coarse fraction as usual. The two main groups, however, remain the same, i.e. the one with oceanic and continental versus the one influenced by England, France and The Channel. The further clustering within them is however altered. The only group which is still more or less similar is the continental group. Similar results can be found for the fine fraction is represented. When choosing the samples, the different groups in the coarse fraction have been taking in account. It was tried to choose the representing sample from these groups in such a way that also one representative from the clusters in the other fractions is present. In this way, a complete overview of the third sampling campaign can still be given.

4.2.3.2 Graphical representations

Backward trajectories In Figure 4.21 to 4.22 the backward trajectories of the chosen samples are shown. Figure 4.21 (a) shows a BWT with a pure oceanic trajectory. Figure 4.21(b) shows a trajectory with a continental influence passing Scandinavia and Eastern Europe. The trajectory that is mainly oceanic but passes England (Figure 4.21(c)) represents a group in the coarse fraction, but can also be found in the first cluster of the other two fractions. The sample passing The Channel and France (Figure 4.21(d)) represents another group in the coarse fraction and the first cluster of second (big) group in the other fractions. Figure 4.22(a) is influenced by The Channel and England and represents the last cluster of the second group in all the fractions. The last trajectory is crossing Scotland (4.22(b)) and represents the lonely cluster in the coarse and medium fractions, but also the small cluster (containing three samples) the fine fraction.

Absolute abundance The absolute abundance of all elements above the detection limit is presented in Figures 4.23 to 4.28. The sample with influence from The Channel and France (Figure 4.22), no Cl is noticed in the coarse fraction. This is somewhat unexpected since the trajectory is still strongly influenced by the Atlantic Ocean. The trajectory passing England on the contrary has a substantial amount of Cl. Inspection of the other samples in the cluster where the sample crossing France belongs to, show an average Cl concentration of 134 ± 112 ng/m³, which is definitely lower than expected. The sample crossing Scotland shows the expected pattern, with Cl being the most abundant element. In the two other samples crossing England (Channel-England and Oceanic England on Figure 4.23), Cl and S have approximately the same abundance. Similar behaviour has been found in the first campaign (See Figure 4.8) for the continental sample and in the second campaign (See Figure 4.15) in case of the oceanic sample. The concentrations, however, are quite different: 60 ng/m³ in the first campaign, 150 ng/m³ in the second campaign and now more than 700 ng/m³. Except for S, Cu and Zn the concentrations of the oceanic sample are every time the lowest in the coarse

fraction. In the sample crossing Scotland, the concentrations are every time the highest, except for Fe, Ti, Mn and Al (Al being only present in the continental sample). The concentrations for all potentially harmful metals are below 10 ng/m³. In the medium fraction (Figures 4.23 to 4.24), S is the most abundant element for all samples except for the sample influenced by The Channel and England. Similar results have been found in the second campaign (see Figure 4.17), but in the first campaign the S and Cl concentrations were more or less similar (See Figure 4.10). Pb is present in the continental sample (Figure 4.26), but the concentration is low (around 5 ng/m³). In the fine fraction, Cl is no longer present, as usual. Furthermore Pb is again present in this fraction (See Figure 4.28) in the continental sample, but in low concentration (around 5 ng/m³).

4.2.4 Fourth campaign

4.2.4.1 Clustering

For this campaign there were no similar clusters in the three fractions at all. Hence the samples will be chosen in order to have a representative for all clusters in every fraction. In this campaign there is again no cluster with a sample crossing the Ruhr area in Germany as was the case in the third campaign.

A cluster with mainly trajectories crossing a continental region is distinguished as well as a group passing the North Sea and/or The Channel. As in the second campaign, there is a lonely cluster with a sample from which the airmass makes a turn in the North Sea. Furthermore there are three other clusters (amongst which two lonely clusters) where no clear indication for the separation based on the BWT can be found.

4.2.4.2 Graphical representations

Backward trajectories In Figures 4.29 to 4.30 the BWT of the chosen samples are shown. As discussed above, each sample is representative for a particular cluster.

Absolute abundance In Figures 4.31 to 4.36 the absolute abundance of all elements for the different influences in one fraction is shown. In the coarse fraction (Figures 4.31 to 4.32) S is the most abundant element in most cases, followed by Cl, as has been seen in the other campaigns as well. The lowest Cl level is not coming from the continental sample as expected, but from the sample passing The Netherlands (see trajectory on Figure 4.30(a) above) which is still severely influenced by the ocean. The continental sample also does not have the highest concentration of soil dust elements, but the sample crossing The Netherlands has. As a matter of fact, the continental sample has usually an average concentration for all elements in the coarse fraction. For the medium fraction, contrary to the coarse fraction, the Cl concentration in the sample crossing The Netherlands is the highest of all samples in the medium fraction, so is the case for S, the soil dust elements and most metals (see Figures 4.32 to 4.33). Especially Al is much higher than the others in this case. The fact that the also Pb is high combined with the high amount of soil dust elements (both in the medium as in the coarse fraction) rises the suspicion that this sample is much more influenced by the continent than one would expect just by checking the BWT. After all Pb turned out to be an excellent tracer for continental air mass in all other campaigns. In the fine fraction (represented in Figures 4.34 to 4.35), no Cl is present as usual. Also here, the highest concentration seems to be coming from the sample crossing The Netherlands. Especially in the case of the metals, this is pronounced: V and Ni are twice as high as in the other samples, but for Cu and Ni the

difference is much smaller. The concentrations of the metals are for most samples however below 10 ng/m³.

4.3. Conclusions

The most harmful components to be identified in aerosols with XRF, are the heavy metals. These elements mostly remain below 10 ng/m³ in all fractions. The most important elements in the coarse fraction are S, Cl and the soil dust elements, as expected. The variation in elemental composition within this fraction could be linked to the backward trajectories, but the tendency is not always as expected. The soil dust elements and Cl loose importance when going from larger to finer particles, whereas S gains even more importance; this is as expected. No clear tendency for the concentration to be expected based on season or airmass trajectory can be found throughout the campaigns.

4.4. Literature

Z. Spolnik, K. Belilov, K. Van Meel, E. Adriaenssens, F. De Roeck, and R. Van Grieken. Optimization of measurement conditions of an energy dispersive X-ray fluorescence spectrometer with high-energy polarized beam excitation for analysis of aerosol filters. Appl. Spectrosc., 59(12):1465–1469, 2005.

Appendix 1

Inorganic nitrogen compounds
Tables

Table 1.1 Parameters selected for the calculation of BWTs

Parameter	Condition
Meteorological database	FNL
Trajectory direction	backward
Vertical motion	model vertical velocity
Start time (UTC)	14:00
Total run time (h)	240
Start new trajectory at time (h)	0
Maximum number of trajectories	24
Start latitude (degrees)	51.17233
Start longitude (degrees)	3.03687
Start height (meters AGL)	20
Label interval (h)	6
Vertical plot height units	meters AGL

Abbreviations: AGL – above ground-level; UTC – coordinated universal time

Table 1.2 Weekly average, minimum, and maximum levels of air-temperature (T_{air}), relative humidity (RH) air-pressure (P_{air}), precipitation, wind-speed, and wind-direction for the late winter/spring campaign in 2006

Week	T_{air} (°C)	RH (%)	P_{air} (hPa)	Precipitation (mm day^{-1})	Wind-speed (m s^{-1})	Wind-direction (°)	
1	6 ± 1	88 ± 4	992 ± 7	4.5 ± 4.2	2.2 ± 0.8	182 ± 61	S
2	2 ± 1	77 ± 6	1019 ± 4	0.5 ± 0.7	2.5 ± 0.6	104 ± 37	SE
3	2 ± 1	80 ± 6	1004 ± 5	1.9 ± 4.7	2.4 ± 1.0	253 ± 44	SW
4	3 ± 3	83 ± 11	1012 ± 14	2.5 ± 2.8	2.2 ± 0.8	202 ± 64	E
5	2 ± 2	74 ± 6	1022 ± 6	0.0 ± 0.0	1.4 ± 0.6	99 ± 16	SE
6	7 ± 4	74 ± 11	1007 ± 6	1.8 ± 2.6	1.8 ± 0.4	141 ± 60	SW
7	11 ± 1	80 ± 4	1005 ± 4	2.5 ± 3.2	3.3 ± 1.0	228 ± 32	SW
8	7 ± 2	74 ± 5	1014 ± 4	0.2 ± 0.5	2.6 ± 0.6	233 ± 50	SW
9	9 ± 2	84 ± 7	1012 ± 6	1.8 ± 1.9	2.7 ± 1.2	220 ± 40	SW
10	10 ± 2	76 ± 2	1015 ± 2	0.0 ± 0.0	1.9 ± 0.9	205 ± 56	SW
11	10 ± 2	80 ± 6	1020 ± 3	0.4 ± 0.6	2.0 ± 0.6	207 ± 35	SW
Weekly average	6 ± 3	79 ± 5	1011 ± 9	1.5 ± 1.4	2.3 ± 0.5	188 ± 52	SW
Weekly minimum	2	74	992	0.0	1.4	99	-
Weekly maximum	11	88	1022	4.5	3.3	253	-

Table 1.3 Weekly average, minimum, and maximum levels of air-temperature (T_{air}), relative humidity (RH) air-pressure (P_{air}), precipitation, wind-speed, and wind-direction for the mid-summer campaign in 2006

Week	T_{air} (°C)	RH (%)	P_{air} (hPa)	Precipitation (mm day^{-1})	Wind-speed (m s^{-1})	Wind-direction (°)	
1	16 ± 3	no data	1017 ± 3	1.3 ± 1.8	4.7 ± 2.3	165 ± 26	S
2	16 ± 1	no data	1014 ± 2	0.3 ± 0.8	6.0 ± 1.7	171 ± 45	S
3	19 ± 4	71 ± 0	1021 ± 2	0.0 ± 0.0	1.2 ± 0.2	118 ± 19	SE
4	21 ± 2	74 ± 5	1016 ± 2	0.7 ± 1.7	1.7 ± 0.8	215 ± 53	SW
5	20 ± 1	73 ± 6.	1026 ± 3	0.2 ± 0.6	1.8 ± 0.8	146 ± 56	SE
6	23 ± 2	70 ± 7	1019 ± 2	0.0 ± 0.0	1.5 ± 0.3	176 ± 62	S
7	22 ± 2	73 ± 5	1014 ± 3	0.0 ± 0.0	1.3 ± 0.3	196 ± 53	S
8	18 ± 1	77 ± 4	1013 ± 6	0.0 ± 0.0	2.6 ± 1.5	231 ± 25	SW
9	19 ± 1	no data	1013 ± 6	2.3 ± 4.4	6.9 ± 3.4	276 ± 47	W
Weekly average	19 ± 3	72 ± 6	1017 ± 5	0.5 ± 1.8	3.2 ± 2.6	186 ± 63	S
Weekly minimum	13	55	1005	0.0	0.8	96	-
Weekly maximum	26	83	1030	12.0	11.0	340	-

Table 1.4 Weekly average levels of N from gaseous, aerosol, and rainwater samples for the late summer campaign in 2005

Week	Period	Air-mass contribution	Total N gases ($\mu g\ N\ m^{-3}$)	Total N aerosols ($\mu g\ N\ m^{-3}$)	Total N rainwater ($mg\ N\ l^{-1}$)
1	08-14/08/05	UK/Atlantic/Channel-(North Sea)	3.26 ± 0.75	1.89 ± 0.90	25.3 ± 22.3
2	15-21/08/05	North Sea (UK/Atlantic/Channel)	2.35 ± 1.95	1.76 ± 1.08	0.96 ± 2.55
Weekly average			2.80 ± 0.65	1.83 ± 0.09	13.1 ± 17.2

Table 1.5 Weekly average, minimum and maximum levels of N from gaseous, aerosol, and rainwater samples for the late winter/spring campaign in 2006

Week	Period	Air-mass contribution	Total N gases ($\mu g\ N\ m^{-3}$)	Total N aerosols ($\mu g\ N\ m^{-3}$)	Total N rainwater ($mg\ N\ l^{-1}$)
1	14-19/02/06	Atlantic/Channel/UK-(continental)	2.52 ± 1.83	0.90 ± 0.45	0.95 ± 0.82
2	20-26/02/06	Continental	2.84 ± 0.53	1.84 ± 0.40	2.74 ± 3.66
3	27/02/06-05/03/06	Atlantic/Channel/UK-(North Sea)	1.44 ± 1.49	1.99 ± 0.99	1.28 ± 2.72
4	06-12/03/06	Atlantic/Channel/UK-(continental)	1.28 ± 0.53	0.72 ± 0.53	0.93 ± 0.92
5	13-19/03/06	Continental	1.57 ± 0.35	2.96 ± 0.99	0.00 ± 0.00
6	20-26/03/06	Atlantic/Channel/UK	4.19 ± 3.39	1.54 ± 1.05	1.75 ± 2.47
7	27/03/06-02/04/06	Atlantic/Channel/UK-(continental)	2.52 ± 0.72	0.60 ± 0.28	1.65 ± 1.39
8	03-09/04/06	Atlantic/Channel/UK	1.55 ± 0.94	1.05 ± 0.57	2.57 ± 3.67
9	10-16/04/06	Atlantic/Channel/UK	1.81 ± 0.87	1.69 ± 0.97	2.79 ± 2.36
10	17-23/04/06	Atlantic/Channel/UK-(North Sea)	1.44 ± 0.66	2.12 ± 0.77	0.00 ± 0.00
11	24-30/04/06	Atlantic/Channel/UK	-	1.69 ± 0.57	0.00 ± 0.00
Weekly average			2.12 ± 0.91	1.56 ± 0.70	1.33 ± 1.08
Weekly minimum			1.28	0.60	0.00
Weekly maximum			4.19	2.96	2.79

Table 1.6 Weekly average, minimum and maximum levels of N from gaseous, aerosol, and rainwater samples for the mid-summer campaign in 2006

Week	Period	Air-mass contribution	Total N gases ($\mu g\ N\ m^{-3}$)	Total N aerosols ($\mu g\ N\ m^{-3}$)	Total N rainwater ($\mu g\ N\ m^{-3}$)
1	12-18/06/2006	Continent - North Sea	3.20 ± 1.72	1.50 ± 0.45	0.88 ± 1.13
2	19-25/06/2006	Atlantic/UK/Channel	1.10 ± 0.90	0.94 ± 0.28	2.39 ± 3.15
3	26/06-02/07/2006	North Sea	2.62 ± 1.18	0.99 ± 0.57	0.00 ± 0.00
4	03-09/07/2006	Continent-Atlantic/UK/Channel	3.60 ± 1.26	1.13 ± 0.25	1.67 ± 2.14
5	10-16/07/2006	North Sea-Atlantic/UK/Channel	2.94 ± 1.46	1.25 ± 0.77	0.00 ± 0.00
6	17-23/07/2006	Continent	2.69 ± 1.41	0.73 ± 0.51	2.24 ± 5.92
7	24-30/07/2006	Continent-Atlantic/UK/Channel	1.67 ± 1.94	0.54 ± 0.31	0.37 ± 0.83
8	31/07-06-08/2006	North Sea-Atlantic/UK/Channel	2.77 ± 1.58	0.34 ± 0.15	7.00 ± 9.58
Weekly average			2.58 ± 0.81	0.93 ± 0.35	1.82 ± 2.30
Weekly minimum			1.10	0.34	0.00
Weekly maximum			3.60	1.50	7.00

Table 1.7 Average levels (µg m^{-3}) for the ionic, water-soluble suspended particulate matter content for the late winter/spring campaign in 2006

Component	Minimum	Maximum	Average
NO_3^-	0.43	6.98	2.69 ± 1.85
NH_4^+	0.00	2.93	1.05 ± 0.74
SO_4^{2-}	0.72	4.71	1.94 ± 0.89
Cl^-	0.15	5.68	2.17 ± 1.42
Na^+	0.08	3.54	1.19 ± 0.80
K^+	0.00	1.29	0.28 ± 0.32
Mg^{2+}	0.00	0.35	0.07 ± 0.08
Ca^{2+}	0.00	0.70	0.03 ± 0.10

Table 1.8 Average levels (µg m^{-3}) for the ionic, water-soluble suspended particulate matter content for the mid-summer campaign in 2006

Component	Minimum	Maximum	Average
NO_3^-	0.00	5.19	1.25 ± 1.12
NH_4^+	0.00	1.67	0.75 ± 0.45
SO_4^{2-}	0.00	4.50	1.52 ± 1.28
Cl^-	0.00	3.65	0.78 ± 0.90
Na^+	0.00	2.76	0.96 ± 0.74
K^+	0.00	0.54	0.16 ± 0.10
Mg^{2+}	0.00	0.35	0.07 ± 0.09
Ca^{2+}	0.00	0.80	0.10 ± 0.17

Table 1.9 Average concentrations for each filter-component in µg m^{-3} collected during the Adinkerke campaign (February 2001)

Period	NH_4^+	Na^+	K^+	Mg^{2+}	Ca^{2+}	NO_3^-	SO_4^{2-}	Cl^-
5-8/2/2001	0.1	6.3	0.7	0.5	3.7	3.1	6.5	11.7
9-11/2/2001	0.3	2.0	0.5	0.1	3.7	2.8	4.6	2.4
12-13/2/2001	0.2	5.5	0.5	0.5	2.7	2.2	5.5	11.4
14-16/2/2001	1.3	1.6	0.5	0.1	3.5	2.9	7.2	1.9
17-20/12/2001	0.6	3.0	0.5	0.0	0.0	1.9	2.1	1.0
21/02/2001	0.5	1.3	0.3	0.1	1.4	1.6	2.9	2.3
22/02/2001	0.7	3.0	0.5	0.0	0.0	1.2	3.5	0.9
23/02/2001	0.4	2.7	0.5	0.2	1.5	2.1	3.4	4.5
24/02/2001-2/3/2001	1.1	1.0	0.3	0.1	0.7	2.3	3.8	1.9

Table 1.10 Seasonal variation in the average concentrations of the water soluble aerosol-components (in µg m^{-3}) from a previous campaign in Adinkerke in 2001

Campaign	NH_4^+	Na^+	K^+	Mg^{2+}	Ca^{2+}	NO_3^-	SO_4^{2-}	Cl^-
June - July 2000	0.7	1.9	0.3	0.1	0.7	2.3	3.6	1.9
December 2000	1.5	5.9	1.1	0.3	2.5	4.4	8.4	8.7
February 2001	0.7	2.4	0.4	0.1	1.7	2.3	4.2	3.2
May - June 2001	0.1	3.5	0.4	0.1	1.1	1.8	3.4	2.4

Table 1.11 Weekly average levels for wet deposition (mg m^{-2} day^{-1}) of ionic, water-soluble components during the late summer campaign in 2005

Week	NO_3^-	SO_4^{2-}	NH_4^+	Na^+	K^+	Mg^{2+}	Ca^{2+}	N (NO_3^-)	N (NH_4^+)
1	41.4 ± 83.4	0.69 ± 1.04	0.11 ± 0.24	2.11 ± 3.23	0.12 ± 0.21	0.21 ± 0.31	0.27 ± 0.42	9.35 ± 18.8	0.54 ± 0.81
2	4.02 ± 10.6	2.05 ± 5.42	0.57 ± 1.50	1.64 ± 4.35	0.09 ± 0.23	0.18 ± 0.47	0.26 ± 0.68	0.91 ± 1.59	2.40 ± 4.22
Weekly average	22.7 ± 26.4	1.37 ± 0.96	0.34 ± 0.32	1.88 ± 0.33	0.10 ± 0.02	0.19 ± 0.02	0.26 ± 0.01	5.13 ± 5.97	1.07 ± 0.75

Table 1.12 Weekly average, minimum, and maximum levels for wet deposition (mg m^{-2} day^{-1}) of ionic, water-soluble components during the late winter/spring campaign in 2006

Week	NO_3^-	SO_4^{2-}	Cl^-	NH_4^+	Na^+	K^+	Mg^{2+}	Ca^{2+}	N (NO_3^-)	N (NH_4^+)
1	7.5 ± 8.1	9.9 ± 7.6	14.0 ± 8.2	4.2 ± 3.9	6.6 ± 4.6	0.3 ± 0.3	0.3 ± 0.4	0.4 ± 0.8	1.7 ± 1.8	3.5 ± 3.2
2	2.8 ± 3.2	2.6 ± 2.9	4.6 ± 6.2	1.1 ± 1.5	2.7 ± 3.8	0.2 ± 0.3	0.2 ± 0.2	0.3 ± 0.3	0.6 ± 0.7	0.9 ± 1.2
3	5.5 ± 14.3	4.1 ± 10.6	9.8 ± 25.4	2.4 ± 5.8	9.4 ± 24.9	0.5 ± 1.4	0.3 ± 0.9	0.2 ± 0.6	1.2 ± 3.2	2.0 ± 4.8
4	7.8 ± 9.2	7.9 ± 9.0	10.7 ± 14.6	3.2 ± 4.1	4.0 ± 6.0	0.8 ± 1.2	0.1 ± 0.2	0.0 ± 0.0	1.8 ± 2.1	2.7 ± 3.4
5	0.0 ± 0.0	0.0 ± 0.0	0.0 ± 0.0	0.0 ± 0.0	0.0 ± 0.0	0.0 ± 0.0	0.0 ± 0.0	0.0 ± 0.0	0.0 ± 0.0	0.0 ± 0.0
6	2.0 ± 2.6	3.3 ± 4.6	1.3 ± 1.7	2.8 ± 3.8	5.5 ± 7.9	0.0 ± 0.1	0.0 ± 0.0	0.0 ± 0.0	0.4 ± 0.6	2.3 ± 3.1
7	6.0 ± 7.0	12.7 ± 14.8	26.1 ± 30.5	6.4 ± 7.4	11.9 ± 13.9	1.7 ± 2.0	0.3 ± 0.4	0.2 ± 0.2	1.3 ± 1.6	5.2 ± 6.1
8	0.0 ± 0.0	0.0 ± 0.0	0.0 ± 0.0	0.0 ± 0.0	0.0 ± 0.0	0.0 ± 0.0	0.0 ± 0.0	0.0 ± 0.0	0.0 ± 0.0	0.0 ± 0.0
9	8.8 ± 5.3	11.7 ± 8.6	8.9 ± 9.3	4.8 ± 3.6	5.6 ± 5.3	0.6 ± 0.5	0.1 ± 0.1	0.1 ± 0.1	2.0 ± 1.2	3.9 ± 2.9
10	0.0 ± 0.0	0.0 ± 0.0	0.0 ± 0.0	0.0 ± 0.0	0.0 ± 0.0	0.0 ± 0.0	0.0 ± 0.0	0.0 ± 0.0	0.0 ± 0.0	0.0 ± 0.0
11	0.0 ± 0.0	0.0 ± 0.0	0.0 ± 0.0	0.0 ± 0.0	0.0 ± 0.0	0.0 ± 0.0	0.0 ± 0.0	0.0 ± 0.0	0.0 ± 0.0	0.0 ± 0.0
Weekly average ± SD	3.6 ± 3.5	4.7 ± 5.0	6.8 ± 8.2	2.2 ± 2.2	4.1 ± 4.1	0.4 ± 0.5	0.1 ± 0.1	0.1 ± 0.2	0.8 ± 0.8	1.8 ± 1.8
Weekly minimum	0.0	0.0	0.0	0.0	0.0	0.0	0.0	0.0	0.0	0.0
Weekly maximum	8.8	12.7	26.1	6.4	11.9	1.7	0.3	0.4	2.0	5.2

Table 1.13 Weekly average, minimum and maximum levels for wet deposition (mg m^{-2} day^{-1}) of ionic, water-soluble components during the mid-summer campaign in 2006

Week	NO_3^-	SO_4^{2-}	Cl^-	NH_4^+	Na^+	K^+	Mg^{2+}	Ca^{2+}	N (NO_3^-)	N (NH_4^+)
1	5.17 ± 11	4.36 ± 7.64	6.61 ± 13.1	1.47 ± 2.58	4.67 ± 7.89	2.44 ± 5.39	0.12 ± 0.29	0.18 ± 0.46	1.17 ± 2.48	1.21 ± 2.12
2	3.82 ± 10.1	2.54 ± 6.71	1.09 ± 2.89	1.36 ± 3.59	1.01 ± 2.67	0.11 ± 0.30	0.10 ± 0.26	0.33 ± 0.88	0.86 ± 2.28	1.12 ± 2.96
3	0.0 ± 0.0	0.0 ± 0.0	0.0 ± 0.0	0.0 ± 0.0	0.0 ± 0.0	0.0 ± 0.0	0.0 ± 0.0	0.0 ± 0.0	0.00 ± 0.00	0.00 ± 0.00
4	6.39 ± 16.92	4.19 ± 11.1	1.56 ± 4.12	1.96 ± 5.19	2.04 ± 5.40	0.42 ± 1.11	0.16 ± 0.42	0.43 ± 1.15	1.44 ± 3.82	1.62 ± 4.28
5	0.0 ± 0.0	0.0 ± 0.0	0.0 ± 0.0	0.0 ± 0.0	0.0 ± 0.0	0.0 ± 0.0	0.0 ± 0.0	0.0 ± 0.0	0.00 ± 0.00	0.00 ± 0.00
6	0.0 ± 0.0	0.0 ± 0.0	0.0 ± 0.0	0.0 ± 0.0	0.0 ± 0.0	0.0 ± 0.0	0.0 ± 0.0	0.0 ± 0.0	0.00 ± 0.00	0.00 ± 0.00
7	0.08 ± 0.10	0.58 ± 0.68	0.35 ± 0.41	0.26 ± 0.30	0.74 ± 0.86	0.01 ± 0.01	0.0 ± 0.0	0.0 ± 0.0	0.0 ± 0.0	0.2 ± 0.2
8	97.3 ± 114	84.2 ± 98.2	106 ± 124	10.9 ± 12.7	60.9 ± 71.1	6.53 ± 7.61	7.02 ± 8.19	41.1 ± 48.0	22.0 ± 25.6	9.0 ± 10.5
Weekly average	17.3 ± 9.3	14.8 ± 34.0	18.0 ± 43.2	2.19 ± 4.34	10.6 ± 24.7	1.16 ± 2.63	1.20 ± 2.85	6.93 ± 16.8	3.90 ± 8.86	1.80 ± 3.57
Weekly minimum	0.00	0.00	0.00	0.00	0.00	0.00	0.00	0.00	0.00	0.00
Weekly maximum	97.3	84.2	106	10.9	60.9	6.53	7.02	41.1	1.44	1.62

Table 1.14 Average wet-deposition flux for each component in mg m^{-2} day^{-1}, collected during winter at Adinkerke in 2001

Campaign	NO_3^-	SO_4^{2-}	Cl^-	NH_4^+	Na^+	K^+	Mg^{2+}	Ca^{2+}
Adinkerke								
Dec 4-Jan 3 2000/2001	1.2	5.7	5.6	1.5	4.6	0.4	0.5	2.1

Table 1.15 Overview of daily average, minimum, and maximum levels* of nitrogen-compounds and fluctuations, expressed as standard deviation (±SD) at the coastal region of De Haan during the four campaigns

Compound	Campaign 1			Campaign 2			Campaign 3			Campaign 4		
	Minimum	Maximum	Average ± SD	Minimum	Maximum	Average ± SD	Minimum	Maximum	Average ± SD	Minimum	Maximum	Average ± SD
Gases												
N (HNO_2)	0.01	0.97	0.29 ± 0.19	0.10	0.42	0.27 ± 0.10	n.d.	0.33	0.11 ± 0.08	n.d.	0.38	0.10 ± 0.09
N (HNO_3)	0.004	0.57	0.08 ± 0.09	0.06	0.73	0.30 ± 0.21	n.d.	0.30	0.11 ± 0.07	n.d.	0.58	0.20 ± 0.13
N (NH_3)	0.61	5.29	2.93 ± 1.26	n.d.	4.44	2.24 ± 1.52	n.d.	9.56	1.89 ± 1.52	n.d.	5.19	2.26 ± 1.54
Total gaseous N	*0.08*	*5.58*	*3.30 ± 1.56*	*0.51*	*4.66*	*2.80 ± 1.49*	*0.16*	*9.94*	*2.11 ± 1.57*	*0.22*	*5.57*	*2.56 ± 1.55*
Aerosols												
Coarse												
N (NO_3^-)	0.01	0.57	0.23 ± 0.14	0.26	0.80	0.55 ± 0.23	0.03	0.42	0.12 ± 0.09	n.d.	0.35	0.14 ± 0.10
N (NH_4^+)	0.007	0.45	0.09 ± 0.11	n.d.	0.11	0.07 ± 0.03	n.d.	0.58	0.14 ± 0.12	n.d.	0.31	0.09 ± 0.09
Total coarse particulate N	*0.02*	*0.89*	*0.32* ± 0.21	*0.31*	*0.91*	*0.60 ± 0.24*	*0.04*	*0.71*	*0.25 ± 0.18*	*0.01*	*0.57*	*0.23 ± 0.14*
Medium												
N (NO_3^-)	0.003	0.56	0.13 ± 0.13	0.06	0.61	0.29 ± 0.21	0.01	0.78	0.21 ± 0.13	n.d.	0.31	0.05 ± 0.06
N (NH_4^+)	0.001	1.07	0.31 ± 0.30	0.04	1.34	0.60 ± 0.55	n.d.	1.26	0.30 ± 0.26	n.d.	0.75	0.18 ± 0.18
Total medium particulate N	*0.005*	*1.63*	*0.44* ± 0.40	*0.13*	*1.90*	*0.89 ± 0.75*	*0.09*	*2.04*	*0.51 ± 0.38*	*0.02*	*1.06*	*0.23 ± 0.20*
Fine												
N (NO_3^-)	0.003	0.08	0.02 ± 0.02	n.d.	0.45	0.12 ± 0.15	0.01	1.26	0.29 ± 0.34	n.d.	1.13	0.13 ± 0.25
N (NH_4^+)	0.0004	0.29	0.12 ± 0.07	n.d.	0.47	0.20 ± 0.15	n.d.	1.75	0.51 ± 0.43	n.d.	1.04	0.45 ± 0.26
Total fine particulate N	*0.003*	*0.33*	*0.14* ± 0.08	*n.d.*	*0.92*	*0.33 ± 0.30*	*0.02*	*2.89*	*0.80 ± 0.75*	*0.09*	*2.13*	*0.58 ± 0.46*
Total particulate N	*0.04*	*2.67*	*0.88* ± 0.61	*0.6*	*3.2*	*1.8 ± 0.9*	*0.25*	*3.98*	*1.56 ± 0.95*	*n.d.*	*2.54*	*0.91 ± 0.55*
Rainwater												
N (NO_2^-)	n.d.	0.12	0.0031 ± 0.012	n.d.	n.d.	n.d.	n.d.	0.07	0.001 ± 0.009	n.d.	0.07	0.002 ± 0.010
N (NO_3^-)	n.d.	2.01	0.13 ± 0.30	n.d.	53.35	12.3 ± 19.5	n.d.	3.76	0.42 ± 0.74	n.d.	17.65	1.02 ± 3.00
N (NH_4^+)	n.d.	3.48	0.23 ± 0.57	n.d.	4.29	0.81 ± 1.31	n.d.	6.97	0.94 ± 1.59	n.d.	8.84	0.78 ± 1.73
Total N in rainwater	*n.d.*	*5.33*	*0.35* ± 0.81	*n.d.*	*53.53*	*13.1 ± 19.8*	*n.d.*	*10.11*	*1.36 ± 2.25*	*n.d.*	*23.89*	*1.84 ± 4.55*

* Units: $\mu g/m^3$ (gases, aerosols) and mg/l (rainwater samples)

Table 1.16 Daily average, minimum, and maximum levels for wet deposition (mg m^{-2} day^{-1}) of ionic, water-soluble components during the late summer campaign in 2005

Date	NO_3^-	SO_4^{2-}	NH_4^+	Na^+	K^+	Mg^{2+}	Ca^{2+}	N (NO_3^-)	N (NH_4^+)	Precipitation (mm day^{-1})
10-08-2005	19.3	0.23	0.04	0.81	0.07	0.11	0.18	4.36	0.18	0.10
11-08-2005	19.4	0.19	0.01	0.63	0.04	0.06	0.11	4.37	0.15	0.13
12-08-2005	8.06	0.01	0.00	0.10	0.00	0.01	0.01	1.82	0.01	0.03
13-08-2005	230	2.31	0.64	8.23	0.58	0.80	1.17	51.9	1.80	1.46
14-08-2005	13.5	2.10	0.09	5.00	0.12	0.49	0.42	3.05	1.64	0.61
15-08-2005	28.1	14.3	3.98	11.5	0.60	1.25	1.79	6.35	11.2	2.60
Daily average ± SD	22.7 ± 60.3	1.37 ± 3.82	0.34 ± 1.06	1.88 ± 3.69	0.10 ± 0.21	0.19 ± 0.39	0.26 ± 0.54	5.13 ± 13.6	1.07 ± 2.97	0.35 ± 0.76
Daily minimum	0.00	0.00	0.00	0.00	0.00	0.00	0.00	0.00	0.00	0.00
Daily maximum	230	14.3	3.98	11.5	0.60	1.25	1.79	51.9	11.2	2.60

Table 1.17 Daily average, minimum, and maximum levels for wet deposition (mg m^{-2} day^{-1}) of ionic, water-soluble components during the late winter/spring campaign in 2006

Date	NO_3^-	SO_4^{2-}	Cl^-	NH_4^+	Na^+	K^+	Mg^{2+}	Ca^{2+}	N (NO_3^-)	N (NH_4^+)	Precipitation (mm day^{-1})
15/02/2006	4.9	11.3	21.2	2.9	13.1	0.6	1.0	1.8	1.1	2.4	1.6
16/02/2006	2.8	7.9	14.0	3.7	6.5	0.6	0.0	0.0	0.6	3.0	4.4
17/02/2006	8.7	8.9	15.4	3.8	7.3	0.3	0.5	0.4	2.0	3.1	3.6
18/02/2006	0.2	0.2	0.2	0.1	0.1	0.0	0.0	0.0	0.1	0.1	1.2
19/02/2006	20.8	21.2	19.1	10.6	6.1	0.0	0.0	0.0	4.7	8.7	11.6
20/02/2006	3.3	2.4	7.9	1.3	4.3	0.3	0.3	0.6	0.8	1.1	0.2
21/02/2006	8.8	6.9	6.6	4.1	4.2	0.6	0.3	0.5	2.0	3.4	0.8
22/02/2006	3.8	2.6	1.4	0.6	0.3	0.1	0.1	0.2	0.8	0.5	0.6
26/02/2006	3.7	6.3	16.5	1.6	10.2	0.6	0.5	0.6	0.8	1.3	1.8
27/02/2006	38.0	28.0	67.5	15.5	65.8	3.8	2.3	1.5	8.6	12.8	12.6
28/02/2006	0.6	0.4	1.1	1.6	0.0	0.0	0.0	0.0	0.1	1.3	0.2
7/03/2006	15.9	21.2	20.7	10.4	4.8	2.7	0.0	0.0	3.6	8.6	7.0
8/03/2006	20.2	13.9	4.4	3.4	2.2	0.0	0.0	0.0	4.6	2.8	4.2
9/03/2006	2.2	3.9	11.0	1.7	4.4	0.4	0.0	0.0	0.5	1.4	1.8

10/03/2006	16.4	16.1	38.8	7.2	16.8	2.5	0.5	0.0	3.7	6.0	4.8
23/03/2006	1.3	1.5	0.9	2.0	2.4	0.2	0.0	0.0	0.3	1.6	0.8
24/03/2006	5.2	8.8	3.4	9.0	11.6	0.0	0.0	0.0	1.2	7.4	4.6
25/03/2006	5.4	9.5	3.3	5.9	18.7	0.0	0.0	0.0	1.2	4.8	5.6
28/03/2006	35.2	71.6	156.5	37.8	69.2	10.5	1.8	0.9	7.9	31.1	8.8
29/03/2006	1.1	2.1	3.4	0.7	1.6	0.4	0.0	0.0	0.3	0.5	0.6
30/03/2006	0.8	1.0	0.5	1.1	0.6	0.1	0.0	0.0	0.2	0.9	1.4
31/03/2006	3.3	8.3	12.9	2.9	7.1	0.5	0.1	0.2	0.7	2.4	2.2
1/04/2006	1.3	5.8	9.6	2.2	4.8	0.3	0.1	0.1	0.3	1.8	1.0
10/04/2006	30.2	30.3	6.5	12.1	7.3	1.1	0.0	0.3	6.8	9.9	3.4
12/04/2006	1.5	1.1	1.6	0.6	1.1	0.1	0.0	0.0	0.3	0.5	0.4
13/04/2006	20.2	33.5	36.8	15.7	18.5	2.7	0.6	0.5	4.6	13.0	2.6
14/04/2006	6.9	14.5	16.4	4.3	11.1	0.3	0.0	0.2	1.6	3.5	4.4
Daily average ± SD	3.5 ± 8.0	4.6 ± 10.8	6.6 ± 20.6	2.2 ± 5.5	4.0 ± 11.5	0.4 ± 1.4	0.1 ± 0.4	0.1 ± 0.3	0.8 ± 1.8	1.8 ± 4.5	3.5 ± 8.0
Daily minimum	0.0	0.0	0.0	0.0	0.0	0.0	0.0	0.0	0.0	0.0	0.0
Daily maximum	38.0	71.6	156.5	37.8	69.2	10.5	2.3	1.8	8.6	31.1	38.0

Table 1.18 Daily average, minimum, and maximum levels for wet deposition (mg m^{-2} day^{-1}) of ionic, water-soluble components during the mid-summer campaign in 2006

Datum	**NO_3^-**	**SO_4^{2-}**	**Cl^-**	**NH_4^+**	**Na^+**	**K^+**	**Mg^{2+}**	**Ca^{2+}**	**N (NO_3^-)**	**N (NH_4^+)**	**Precipitation (mm day^{-1})**
13/06/2006	29.7	20.4	35.4	6.9	20.8	14.5	0.8	1.2	6.7	5.7	4.4
14/06/2006	5.2	7.7	8.1	2.5	9.3	2.1	0.0	0.0	1.2	2.0	2.2
15/06/2006	1.3	2.3	2.7	0.9	2.6	0.5	0.0	0.0	0.3	0.7	1.0
24/06/2006	26.7	17.7	7.7	9.5	7.1	0.8	0.7	2.3	6.0	7.8	2.0
04/07/2006	44.8	29.3	10.9	13.7	14.3	2.9	1.1	3.0	10.1	11.3	4.6
29/07/2006	0.6	4.1	2.4	1.8	5.2	0.1	0.0	0.0	0.1	1.5	4
01/08/2006	211	169	123	20.5	70.8	5.3	14.2	84.0	47.7	16.9	2.70
02/08/2006	78.4	94.7	98.9	8.4	52.6	3.8	8.8	47.3	17.7	6.9	1.70
03/08/2006	391	326	521	47.5	303	36.5	26.1	157	88.4	39.1	12.00
Daily average ± SD	14.1 ± 60	12 ± 50	14.5 ± 72.	1.99 ± 7.21	8.67 ± 41.83	1.19 ± 5.26	0.92 ± 4.08	5.26 ± 24.2	3.18 ± 13.5	1.64 ± 5.94	0.65 ± 1.91
Daily minimum	0.0	0.0	0.0	0.0	0.0	0.0	0.0	0.0	0.0	0.0	0.00
Daily maximum	391	326	521	47.5	303	36.5	26.1	157	88.4	39.1	12.00

Table 1.19 Average and representative individual (daily) oceanic and continental fluxes of inorganic nitrogen compounds during the autumn/ early winter campaign in 2004

	Deposition (mg/m^2 day)			**Ratio of fluxes**
	Average (over season)	Oceanic (21^{st} Sept., 2004.)	Continental (1^{st} Oct., 2004.)	(Continental to Oceanic)
Gaseous compounds –				
N (HNO_2)	0.17 ± 0.12	0.08	0.16	2.0
N (HNO_3)	0.05 ± 0.04	0.04	0.11	2.7
N (NH_3)	1.98 ± 0.83	1.72	2.94	1.8
Total gaseous N –	**2.12 ± 0.89**	**1.83**	**3.21**	**1.8**
Aerosols –				
Coarse (AD > 10 μm)				
N (NO_3^-)	0.40 ± 0.24	0.37	0.98	2.7
N (NH_4^+)	0.16 ± 0.14	0.03	0.33	11
total	*0.55 ± 0.36*	*0.40*	*1.32*	*3.3*
Medium (10μm>AD>2μm)				
N (NO_3^-)	0.14 ± 0.14	0.18	0.26	1.4
N (NH_4^+)	0.35 ± 0.34	0.03	0.85	28
total	*0.49 ± 0.45*	*0.21*	*1.11*	*5.3*
Fine (2 μm>AD>0.4 μm)				
N (NO_3^-)	0.01 ± 0.009	0.006	0.02	3.0
N (NH_4^+)	0.06 ± 0.03	0.035	0.14	4.0
total	*0.07 ± 0.03*	*0.04*	*0.16*	*4.0*
Total aerosol N –	**1.09 ± 0.76**	**0.65**	**2.6**	**4.0**
Total dry N flux –	**2.75 ± 1.60**	**2.5**	**5.8**	**2.3**
Ratio of aerosol to total dry N (%)	***40***	***26***	***45***	**-**
Total wet flux	**3.6 ± 2.9**	**0**	**0.92**	**-**
Ratio of wet to dry fluxes	**1.3**	**0**	**0.16**	**-**

Table 1.20 Overview of daily average deposition fluxes and fluctuations, expressed as standard deviation (±SD) of nitrogen compounds for the late summer campaign in 2005

	Deposition (mg N/m^2 day)			**Ratio of fluxes**	
	(a) UK/Atlantic/ Channel	(b) North Sea	(c) North Sea/ Continental	(a) to (b)	(a) to (c)
Gaseous –					
N (HNO_2) (denuder)	0.20 ± 0.05	0.12 ± 0.06	0.17 ± 0.06	1.6	1.14
N (HNO_3)	0.13 ± 0.06	0.19 ± 0.14	0.08 ± 0.003	0.7	1.73
N (NH_3)	4.48 ± 1.49	2.37 ± 1.97	0.77 ± 1.34	1.9	5.8
N (NO_2) (diffusion tube)	0.0002±0.00005	0.00025±0.00004	0.00031±0.00005	1.5	1.2
Total gaseous N –	***4.80 ± 1.45***	***2.68 ± 2.06***	***1.02 ± 1.37***	***1.8***	***4.7***
Aerosols –					
Coarse (AD > 10 µm)					
N (NO_3^-)	0.12 ± 0.07	0.39 ± 0.35	0.58 ± 0.08	0.3	0.20
N (NH_4^+)	1.47 ± 0.08	0.45 ± 0.72	0.11 ± 0.03	3.2	13.4
total coarse	*1.59 ± 0.14*	*0.84 ± 0.40*	*0.69 ± 0.06*	*1.9*	*2.3*
Medium (10µm>AD>2µm)					
N (NO_3^-)	0.74 ± 0.68	0.08 ± 0.04	0.55 ± 0.16	9.4	1.36
N (NH_4^+)	1.08 ± 0.87	0.11 ± 0.04	1.19 ± 0.23	10	0.90
total medium	*1.82 ± 1.55*	*0.19 ± 0.04*	*1.74 ± 0.38*	*9.8*	*1.04*
Fine (2 µm>AD>0.4 µm)					
N (NO_3^-)	0.09 ± 0.03	0.06 ± 0.02	0.15 ± 0.13	1.6	0.62
N (NH_4^+)	0.14 ± 0.05	0.07 ± 0.02	0.27 ± 0.24	2.0	0.52
total fine	*0.23 ± 0.08*	*0.13 ± 0.05*	*0.42 ± 0.36*	*1.8*	*0.56*
Total aerosol N –	***3.63 ± 1.72***	***1.16 ± 0.43***	***2.85 ± 0.40***	***3.1***	***1.3***
Total dry flux –	**8.44 ± 3.1**	**3.84 ± 2.47**	**3.87 ± 1.23**	**2.5**	**2.2**
Wet flux –					
N (NO_3^-)	12.2 ± 22.2	1.79 ± 2.84	0.0 ± 0.0	6.8	-
N (NH_4^+)	0.72 ± 0.92	1.89 ± 4.54	0.0 ± 0.0	0.4	-
Total wet flux	**13.1 ± 23**	**3.68 ± 7.38**	**0.0 ± 0.0**	**0.5**	**-**
Total flux	**21.5 ± 26**	**7.52 ± 9.8**	**3.87 ± 1.23**	**2.9**	**5.6**
Percent of aerosols in dry flux (%)	***43***	***30***	***74***		
Wet to dry ratio	**1.55**	**1.1**	**0**		

Table 1.21 Overview of daily average deposition fluxes and fluctuations (±SD) of nitrogen compounds for the early winter/spring campaign in 2006

		Deposition (mg N/m^2 day)				**Ratio of fluxes**	
		(a) Atlantic/ Channel*	(b) Continental	(c) North Sea		(b) to (a)	(b) to (c)
Gaseous –							
N (HNO_2) (denuder)		0.05 ± 0.04	0.11 ± 0.05	0.06 ± 0.05		2.3	2.0
N (HNO_3)		0.05 ± 0.04	0.07 ± 0.04	0.08 ± 0.04		1.2	0.85
N (NH_3)		1.12 ± 0.75	1.44 ± 1.46	1.35 ± 0.98		1.3	1.1
N (NO_2) (diffusion tube)		0.00014±0.0001	0.00008±0.00002	0.00007±0.00003		1.5	1.2
Total gaseous N –		***1.22 ± 0.77***	***1.62 ± 1.48***	***1.49 ± 1.02***		***1.3***	***1.1***
Aerosols –							
Coarse (AD > 10 µm)							
N (NO_3^-)		0.25 ± 0.16	0.08 ± 0.04	0.19 ± 0.11		0.34	0.43
N (NH_4^+)		0.28 ± 0.23	0.10 ± 0.07	0.24 ± 0.23		0.36	0.41
total coarse		*0.53 ± 0.32*	*0.18 ± 0.11*	*0.44 ± 0.34*		*0.35*	*0.42*
Medium (10µm>AD>2µm)							
N (NO_3^-)		0.19 ± 0.11	0.38 ± 0.21	0.23 ± 0.12		2.0	1.7
N (NH_4^+)		0.21 ± 0.18	0.67 ± 0.36	0.31 ± 0.21		3.0	2.2
total medium		*0.41 ± 0.26*	*1.05 ± 0.56*	*0.54 ± 0.32*		*2.5*	*2.0*
Fine (2 µm>AD>0.4 µm)							
N (NO_3^-)		0.10 ± 0.14	0.23 ± 0.20	0.15 ± 0.15		2.2	1.5
N (NH_4^+)		0.21 ± 0.21	0.35 ± 0.25	0.25 ± 0.14		1.7	1.4
total fine		*0.31 ± 0.34*	*0.58 ± 0.45*	*0.40 ± 0.29*		*1.9*	*1.5*
Total aerosol N –		***1.25 ± 0.70***	***1.81 ± 0.66***	***1.37 ± 0.53***		***1.5***	***1.3***
Total dry flux –		**2.5 ± 1.5**	**3.4 ± 2.1**	**2.9 ± 1.6**		**1.4**	**1.2**
Wet flux –							
N (NO_3^-)		1.00 ± 1.9	0.57 ± 1.2	0.56 ± 2.1		0.6	1.0
N (NH_4^+)		2.35 ± 5.5	1.25 ± 2.6	0.98 ± 3.2		0.5	1.3
DON		0.20 ± 0.6	0.36 ± 1.1	0.07 ± 0.3		1.8	5.2
Total wet flux		**3.50 ± 7.2**	**2.10 ± 3.7**	**1.61 ± 5.3**		**0.5**	**1.2**
Total flux		**6.0 ± 8.7**	**5.5 ± 5.8**	**4.5 ± 6.9**		**0.9**	**1.2**
Percent of aerosols in total dry flux (%)		***50***	***53***	***47***			
Wet to dry ratio		**1.4**	**0.62**	**0.56**			

Table 1.22 Overview of daily average deposition fluxes and fluctuations (±SD) of nitrogen compounds for the mid-summer campaign in 2006

		Deposition (mg N/m^2 day)				**Ratio of fluxes**	
		(a) Atlantic/ Channel*	(b) Continental	(c) North Sea		(b) to (a)	(b) to (c)
Gaseous –							
N (HNO_2) (denuder)		0.07 ± 0.05	0.08 ± 0.07	0.04 ± 0.05		1.2	2.0
N (HNO_3)		0.09 ± 0.05	0.14 ± 0.10	0.11 ± 0.04		1.5	1.3
N (NH_3)		1.20 ± 0.95	1.63 ± 1.13	1.63 ± 0.97		1.4	1.0
N (NO_2) (diffusion tube)		0.00018±0.00034	0.0002±0.00007	0.00023±0.00003		0.8	1.1
Total gaseous N –		***1.36 ± 0.96***	***1.85 ± 1.09***	***1.78 ± 0.99***		***1.4***	***1.0***
Aerosols –							
Coarse (AD > 10 μm)							
N (NO_3^-)		0.26 ± 0.19	0.24 ± 0.14	0.20 ± 0.16		0.9	1.2
N (NH_4^+)		0.20 ± 0.17	0.08 ± 0.12	0.17 ± 0.16		0.4	0.5
total coarse		*0.46 ± 0.30*	*0.32 ± 0.19*	*0.38 ± 0.16*		*0.7*	*0.8*
Medium (10μm>AD>2μm)							
N (NO_3^-)		0.09 ± 0.08	0.04 ± 0.03	0.05 ± 0.05		0.4	0.8
N (NH_4^+)		0.16 ± 0.20	0.23 ± 0.16	0.23 ± 0.25		1.4	1.0
total medium		*0.25 ± 0.26*	*0.27 ± 0.18*	*0.28 ± 0.26*		*1.1*	*0.9*
Fine (2 μm>AD>0.4 μm)							
N (NO_3^-)		0.08 ± 0.16	0.04 ± 0.05	0.07 ± 0.11		0.5	0.5
N (NH_4^+)		0.16 ± 0.14	0.24 ± 0.06	0.20 ± 0.15		1.1	1.2
total fine		*0.29 ± 0.28*	*0.27 ± 0.09*	*0.27 ± 0.23*		*0.9*	*1.1*
Total aerosol N –		***0.99 ± 0.65***	***0.86 ± 0.37***	***0.93 ± 0.52***		***0.9***	***0.9***
Total dry flux –		**2.4 ± 1.3**	**2.7 ± 1.5**	**2.7 ± 1.4**		**1.1**	**1.0**
Wet flux –							
N (NO_3^-)		6.67 ± 20	1.1 ± 2.8	0.0 ± 0.0		0.6	-
N (NH_4^+)		3.04 ± 8.6	1.2 ± 2.6	0.0 ± 0.0		0.5	-
DON		0.27 ± 0.9	3.5 ± 12	0.0 ± 0.0		12	-
Total wet flux		**10.0 ± 29**	**5.1 ± 15**	**0.0 ± 0.0**		**0.24**	**-**
Total (wet+dry) flux		**12.4 ± 29**	**7.8 ± 16.5**	**2.7 ± 1.4**		**0.63**	**2.9**
Percent of aerosols in total dry flux (%)		***41***	***32***	***35***			
Wet to dry ratio		**4.2**	**1.9**	**0**			

Table 1.23. Relative abundance (%) of the obtained particles types (combined groups) for the autumn/winter campaign in 2004

	AlSi	**NaCl**	**Org + S**	**FeOx**	**$NaNO_3$**	**SiOx**	**Biogenic**
September 22, 2004							
0.2 - 2.0 μm	52.1	9.4	14.1	9.0	9.8	3.4	2.1
2.0 - 8.0 μm	55.2	9.1	16.1	7.7	7.0	3.5	1.4
October 18, 2006							
0.2 - 2.0 μm	68.4	0.5	1.5	19.5	10.0		
2.0 - 8.0 μm	38.0	22.8	22.2	10.4	6.6		

Appendix 2

Inorganic nitrogen compounds
Figures

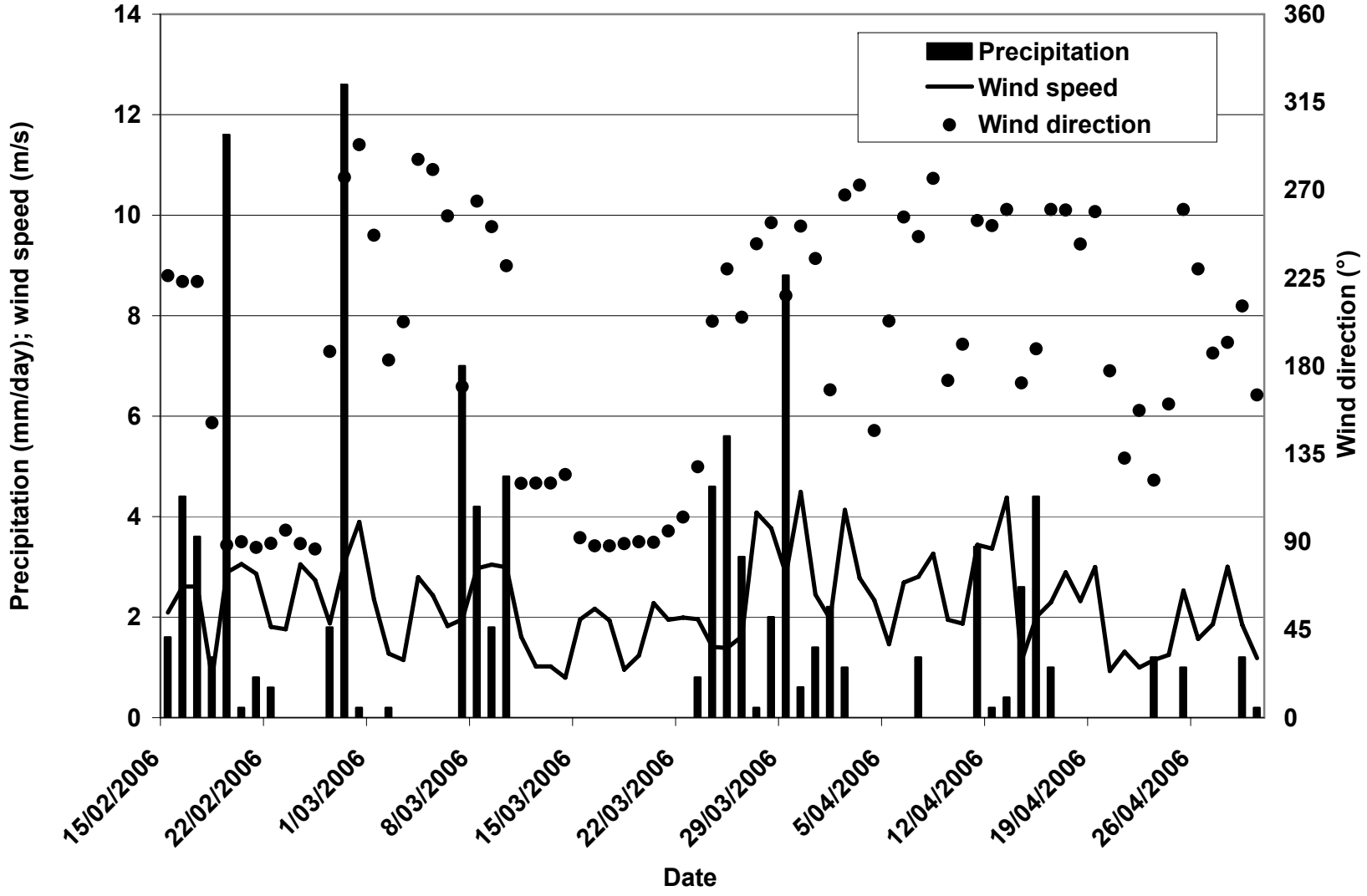

Figure 2.1 Variation of the meteorological parameters (precipitation, wind-speed, and wind-direction) during the 3rd campaign.

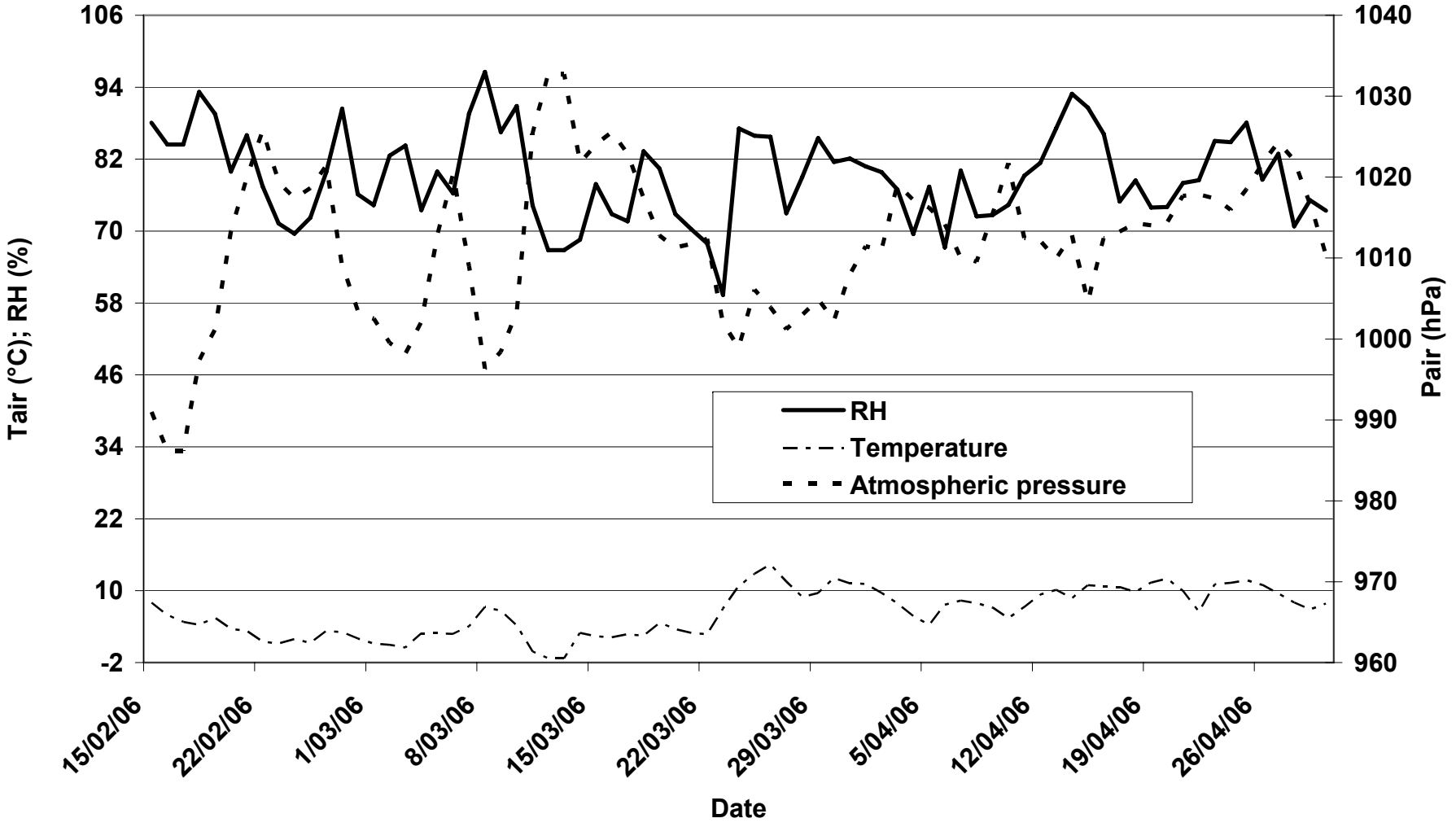

Figure 2.2 Variation of the meteorological parameters (RH, air-temperature, and air-pressure) during the 3rd campaign.

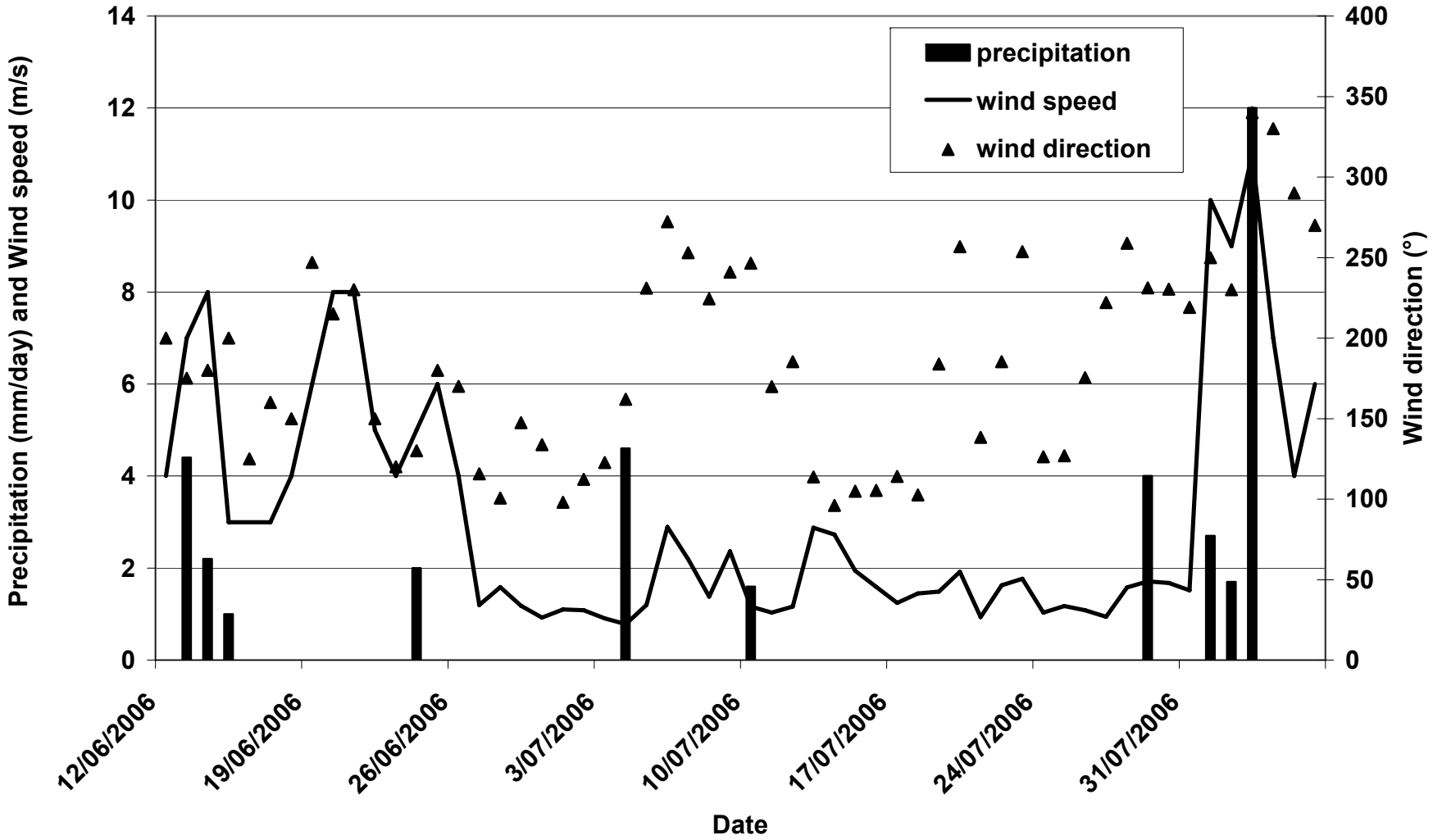

Figure 2.3 Variation of the meteorological parameters (precipitation, wind-speed, and wind-direction) during the 4th campaign.

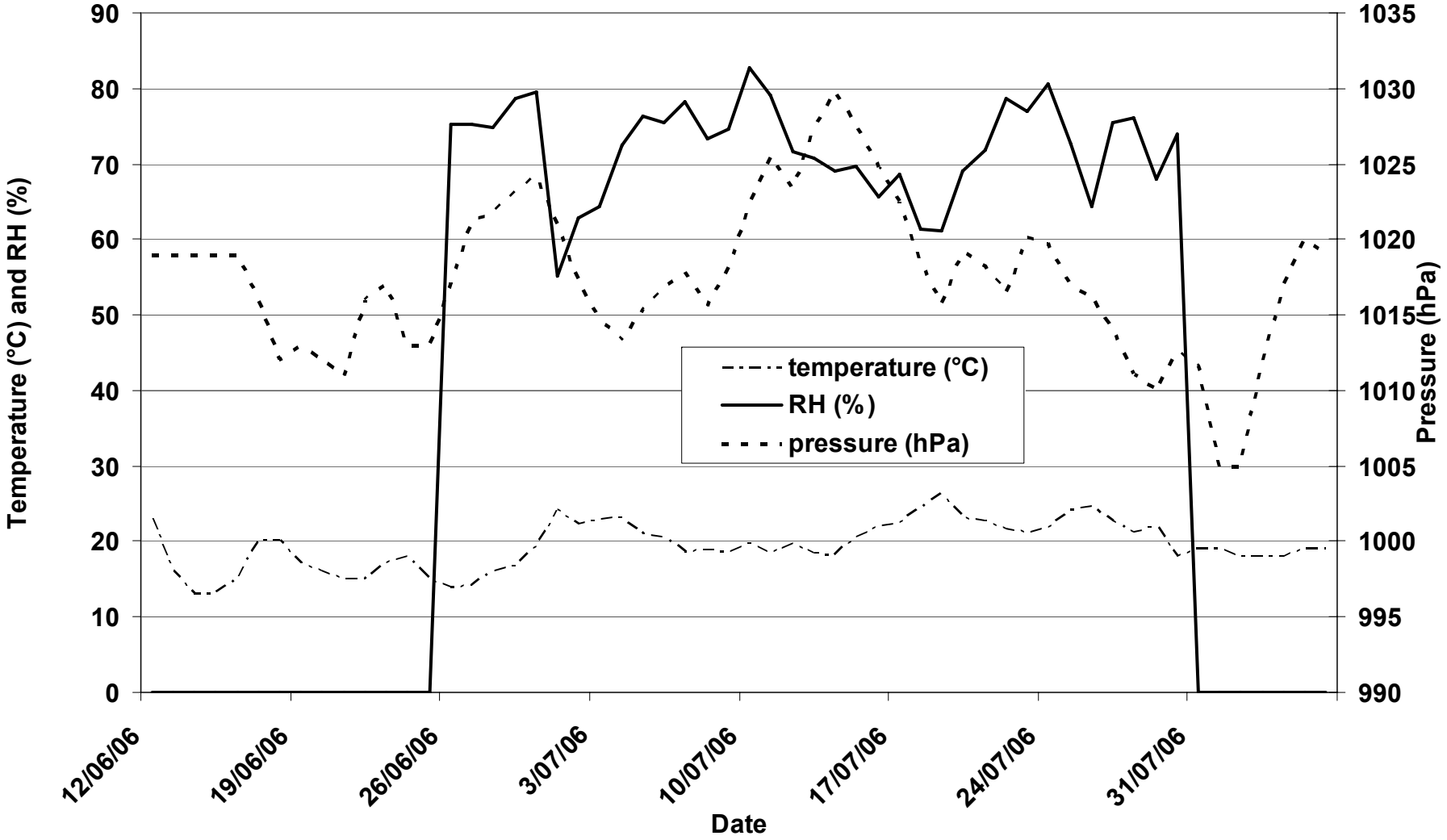

Figure 2.4 Variation of the meteorological parameters (RH, air-temperature, and air-pressure) during the 4th campaign.

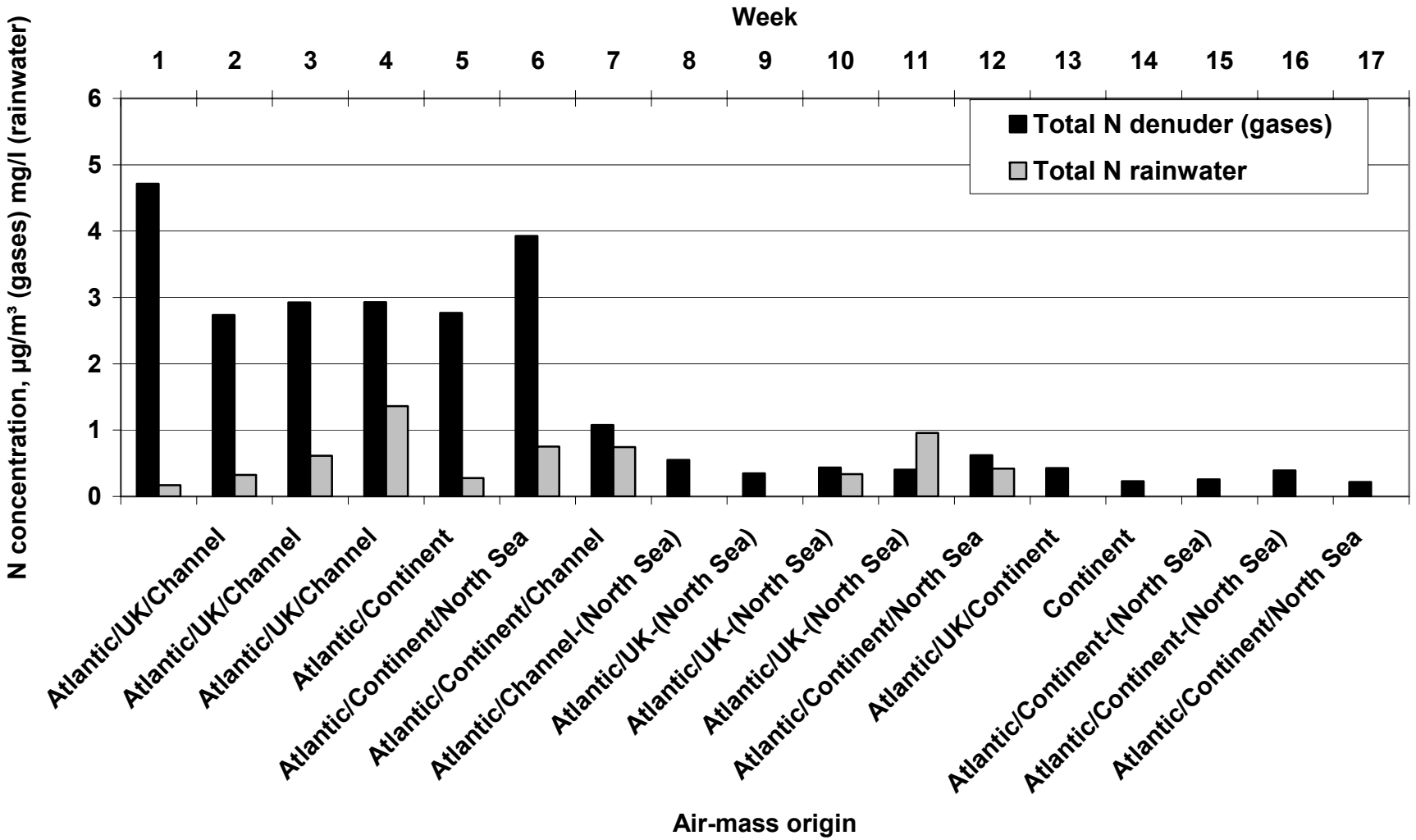

Figure 2.5 Variation of the weekly average total N concentrations for gases and rainwater during the 1st campaign.

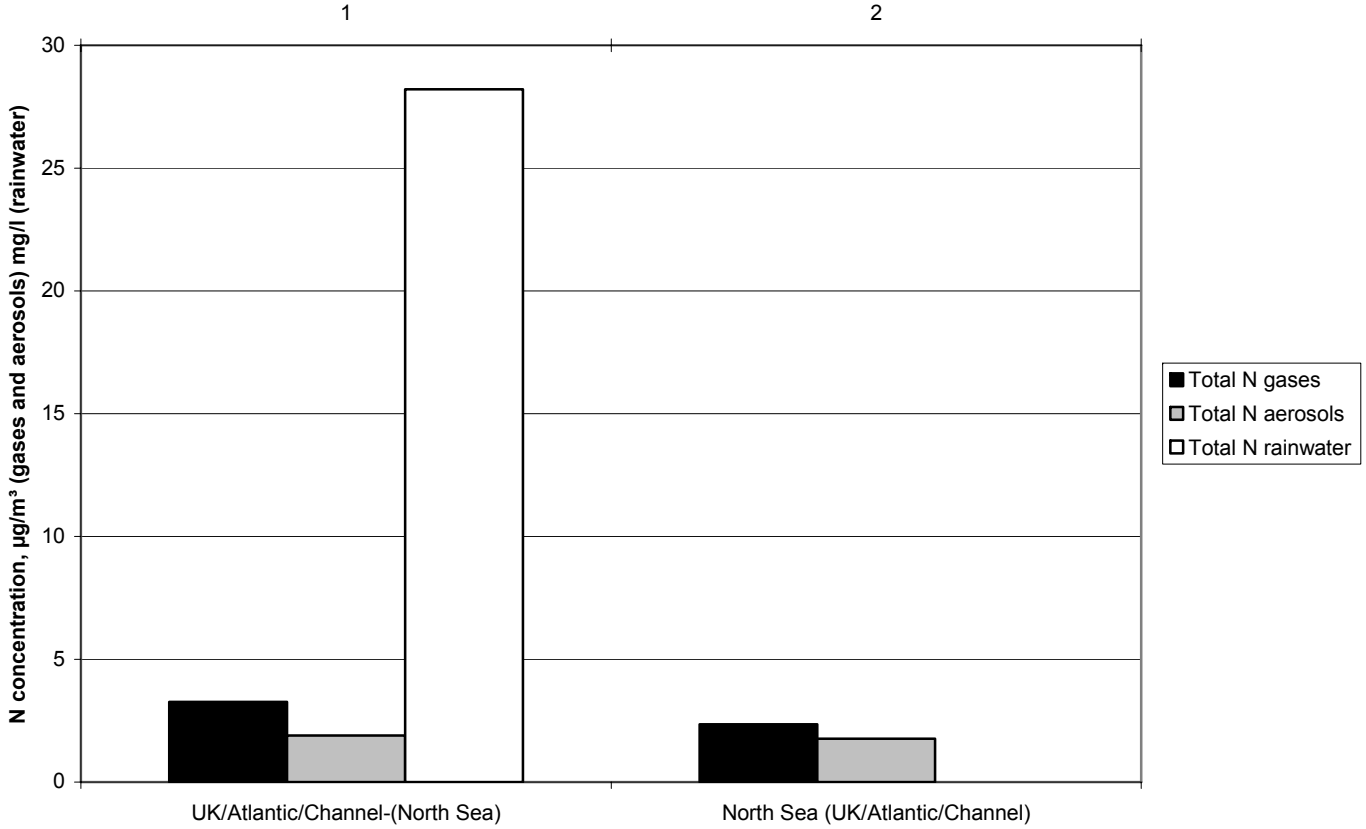

Figure 2.6 Variation of the weekly average total N concentrations for gases, aerosols, and rainwater during the 2nd campaign.

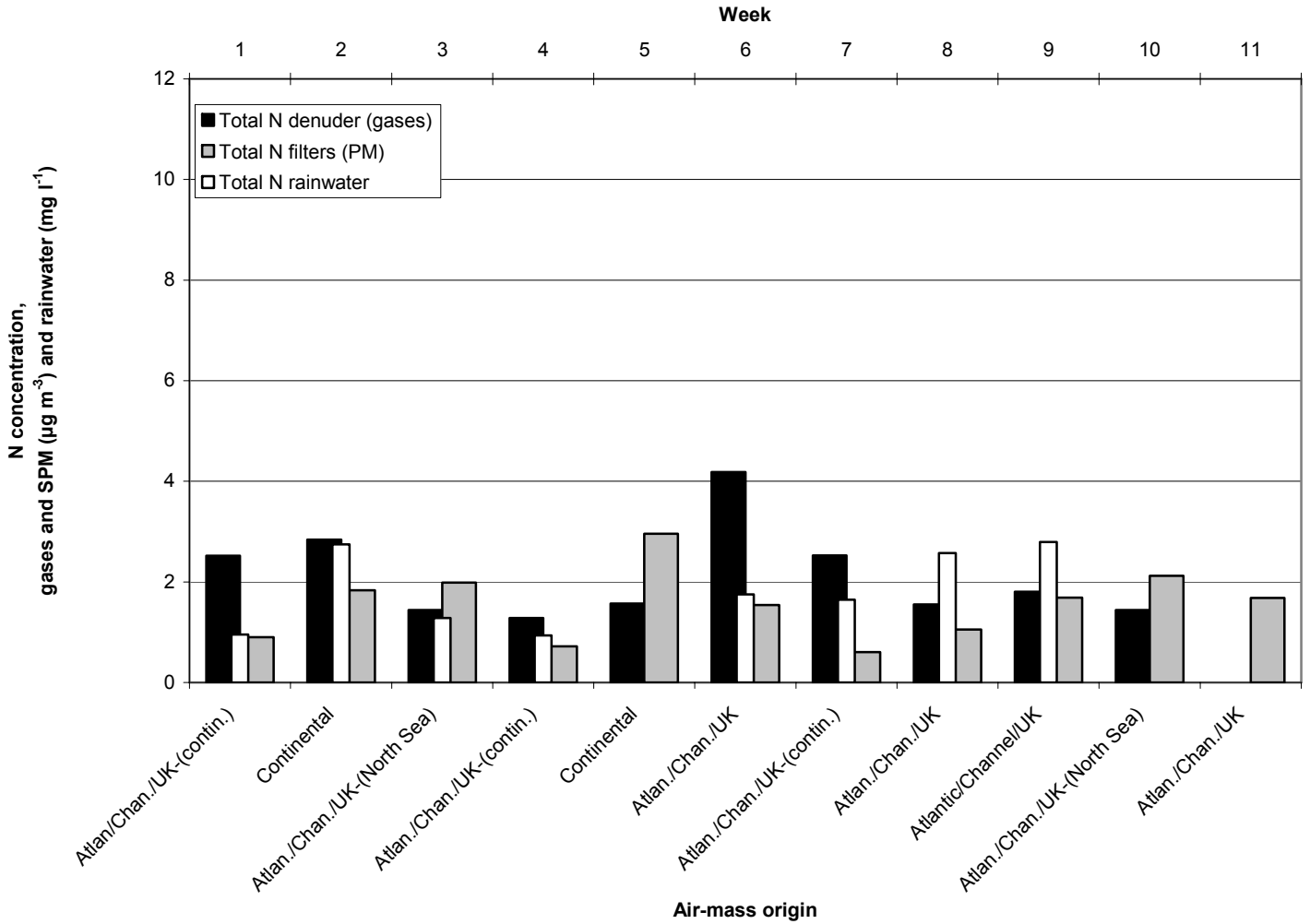

Figure 2.7 Variation of the weekly average total N concentrations for gases, aerosols, and rainwater during the 3rd campaign.

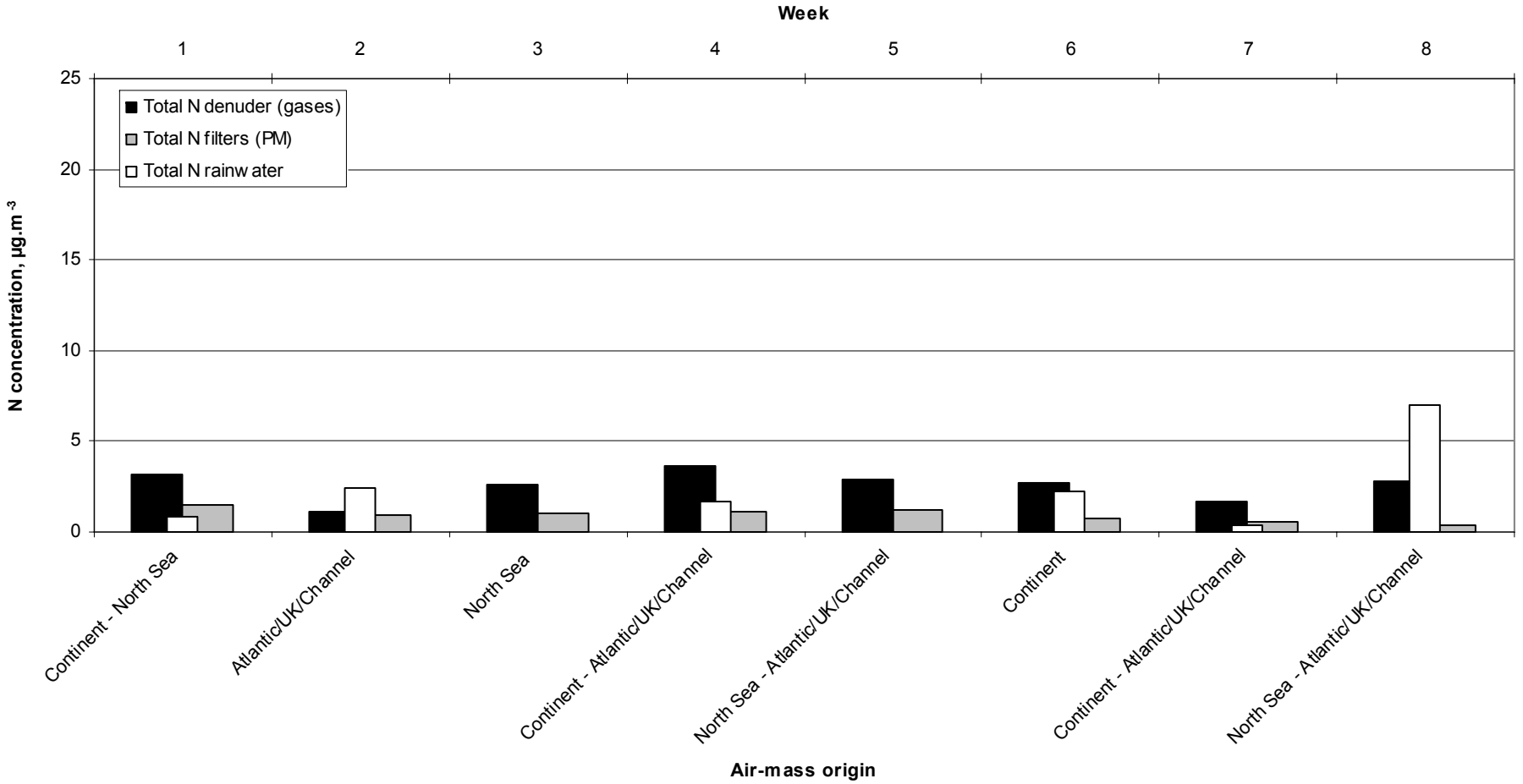

Figure 2.8 Variation of the weekly average total N concentrations for gases, aerosols, and rainwater during the 4th campaign.

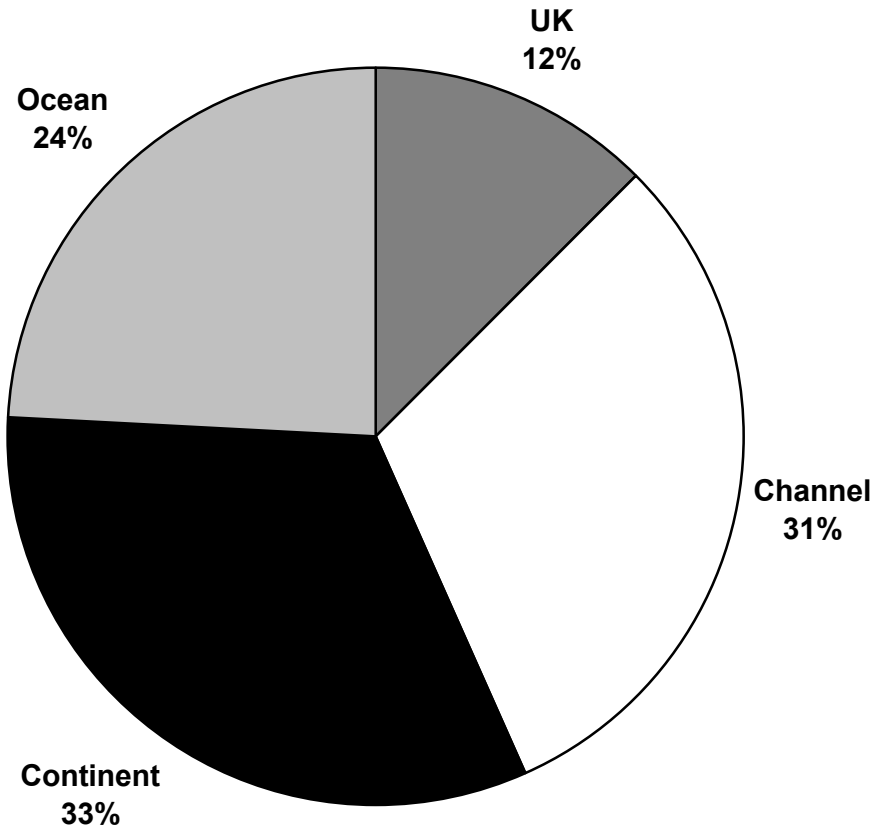

Figure 2.9 Relative contribution of air-masses (Oceanic, UK, Continental, and Channel) to the total level of gaseous N.

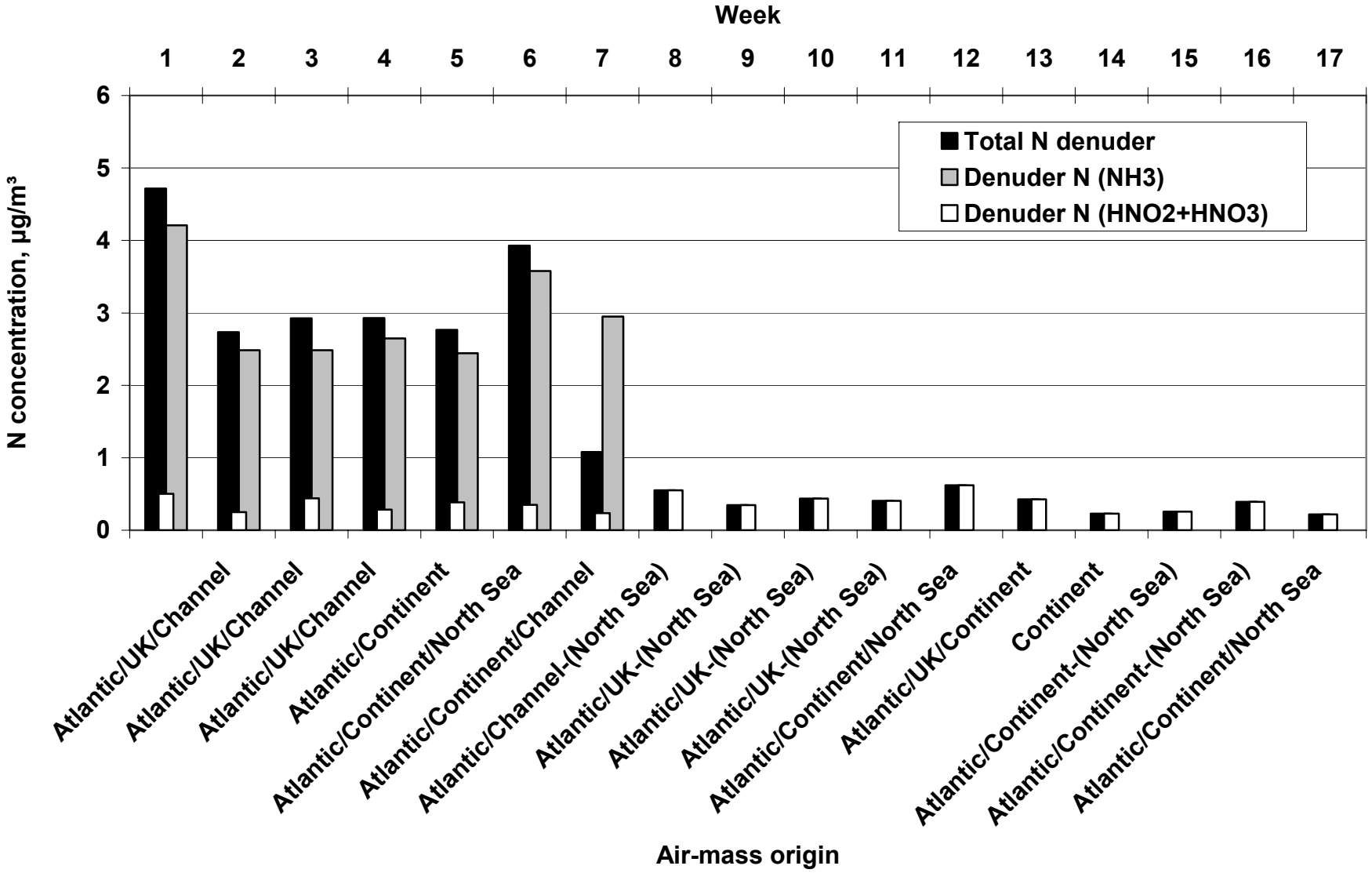

Figure 2.10 Variation of the weekly average gaseous N concentrations (NH_3, HNO_2 + HNO_3, and total) during the 1st campaign.

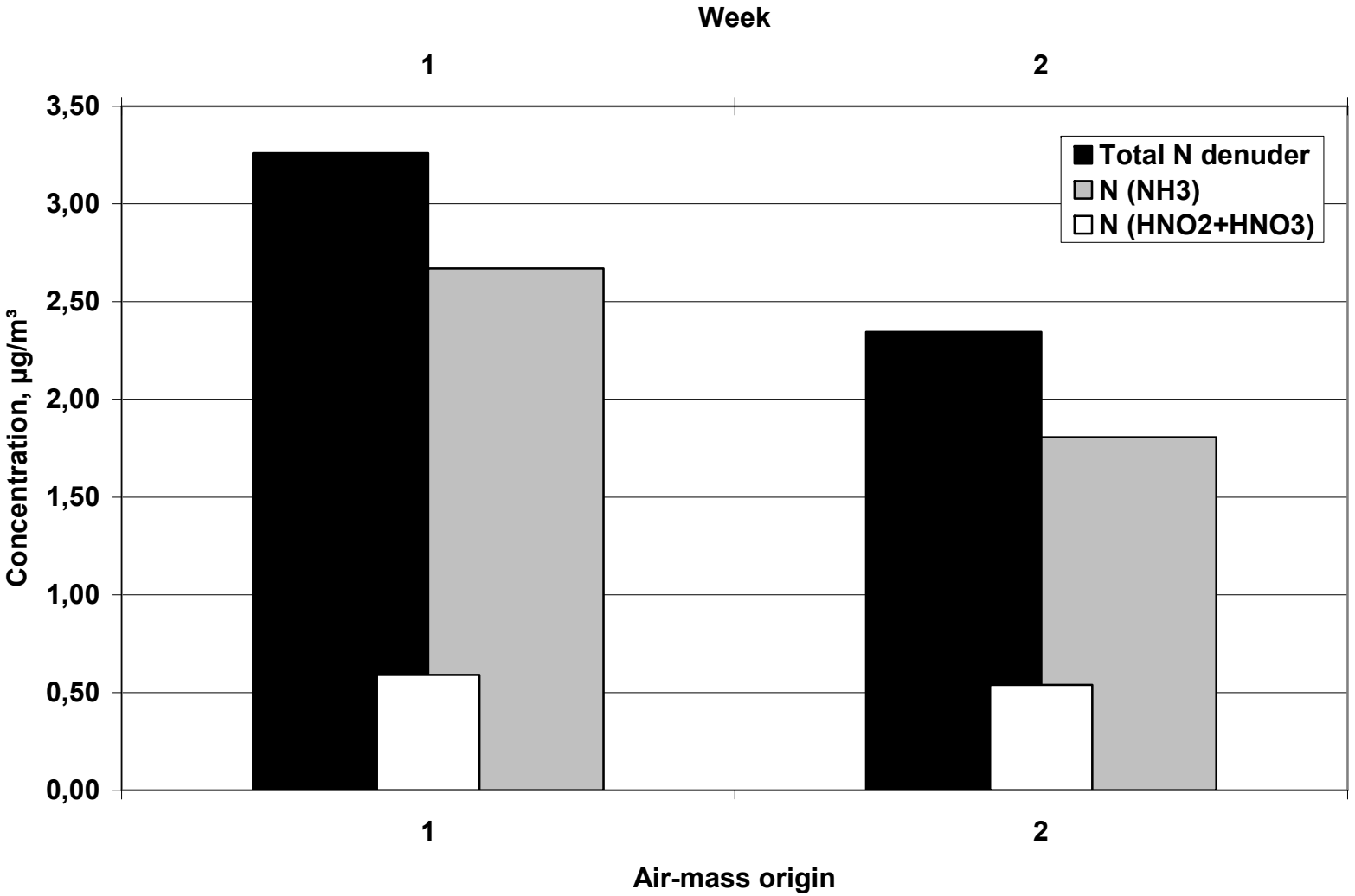

Figure 2.11 Variation of the weekly average gaseous N concentrations (NH_3, HNO_2 + HNO_3, and total) during the 2nd campaign.

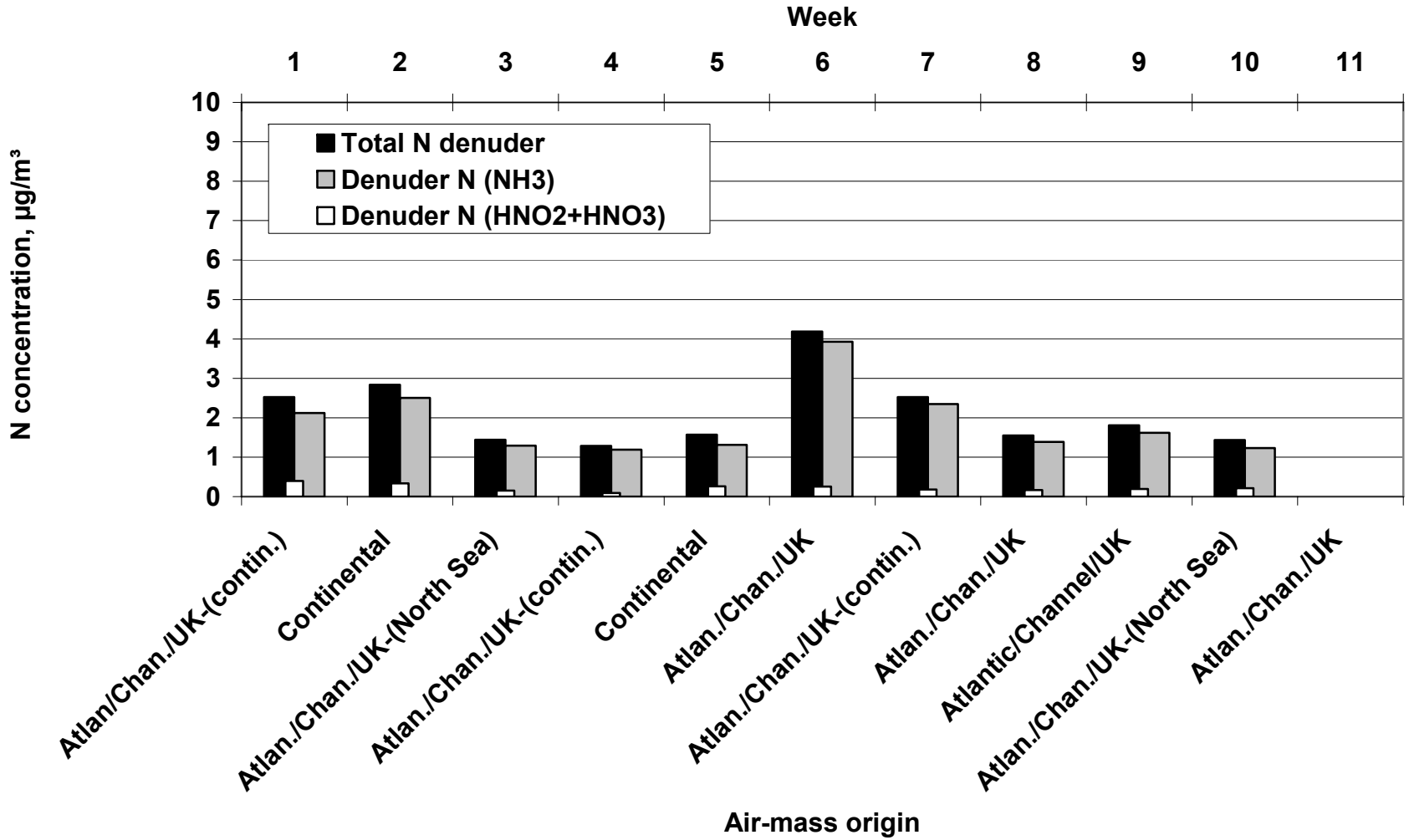

Figure 2.12 Variation of the weekly average gaseous N concentrations (NH_3, HNO_2 + HNO_3, and total) during the 3rd campaign.

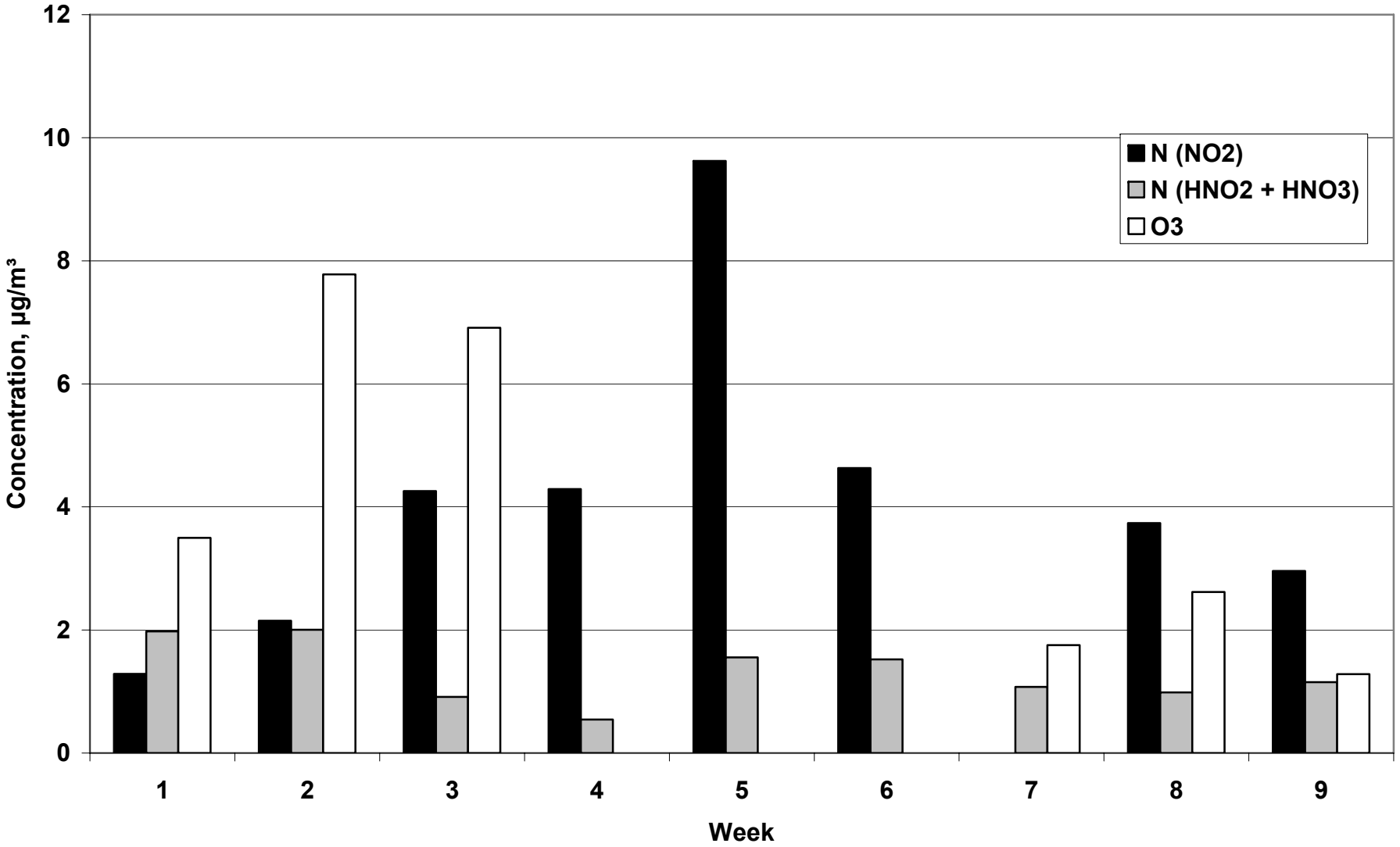

Figure 2.13 Variation of the weekly average concentrations of gaseous compounds (NO_2, O_3, and HNO_2 + HNO_3) during the 3rd campaign.

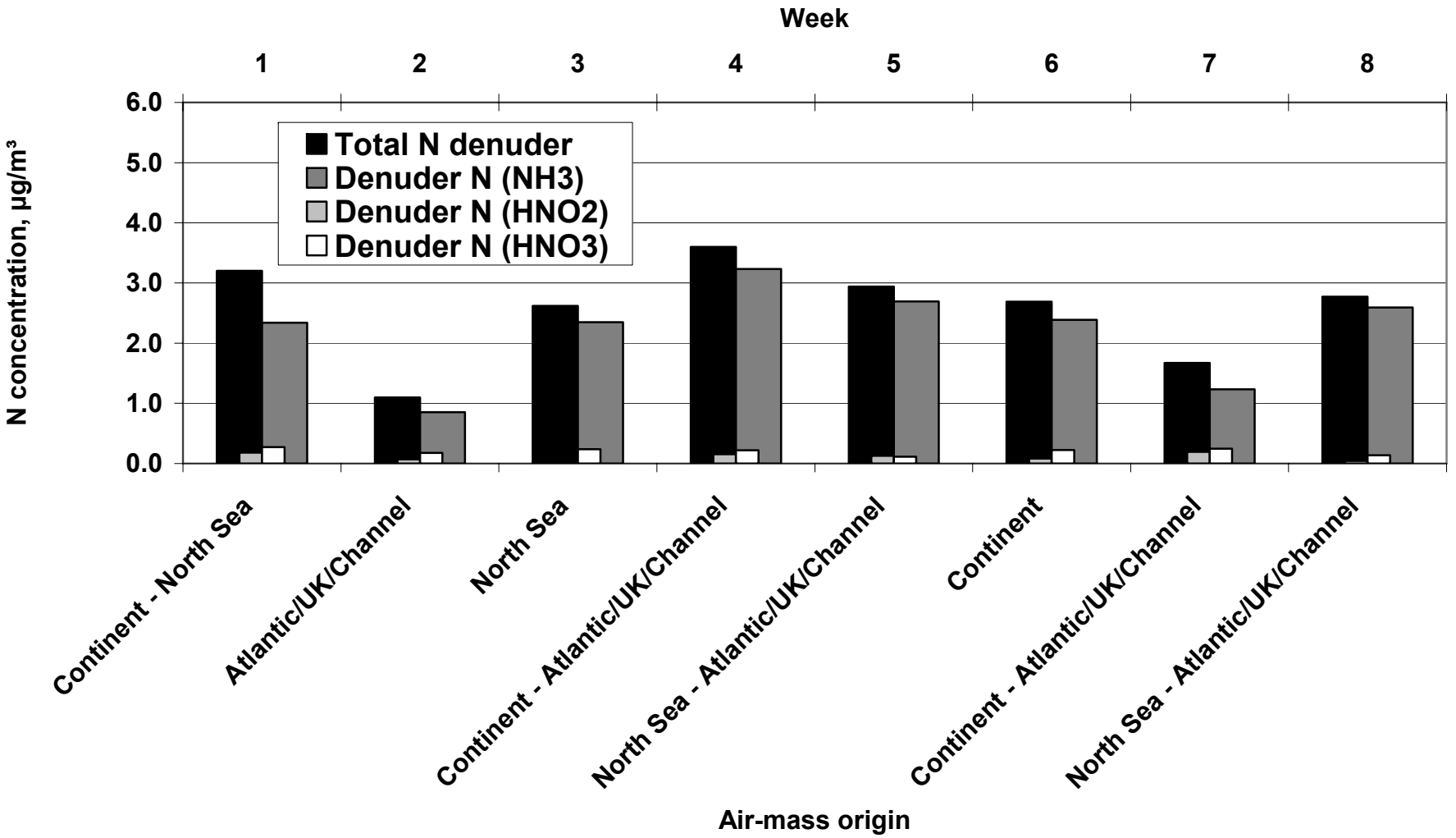

Figure 2.14 Variation of the weekly average gaseous N concentrations (NH_3, HNO_2 + HNO_3, and total) during the 4th campaign.

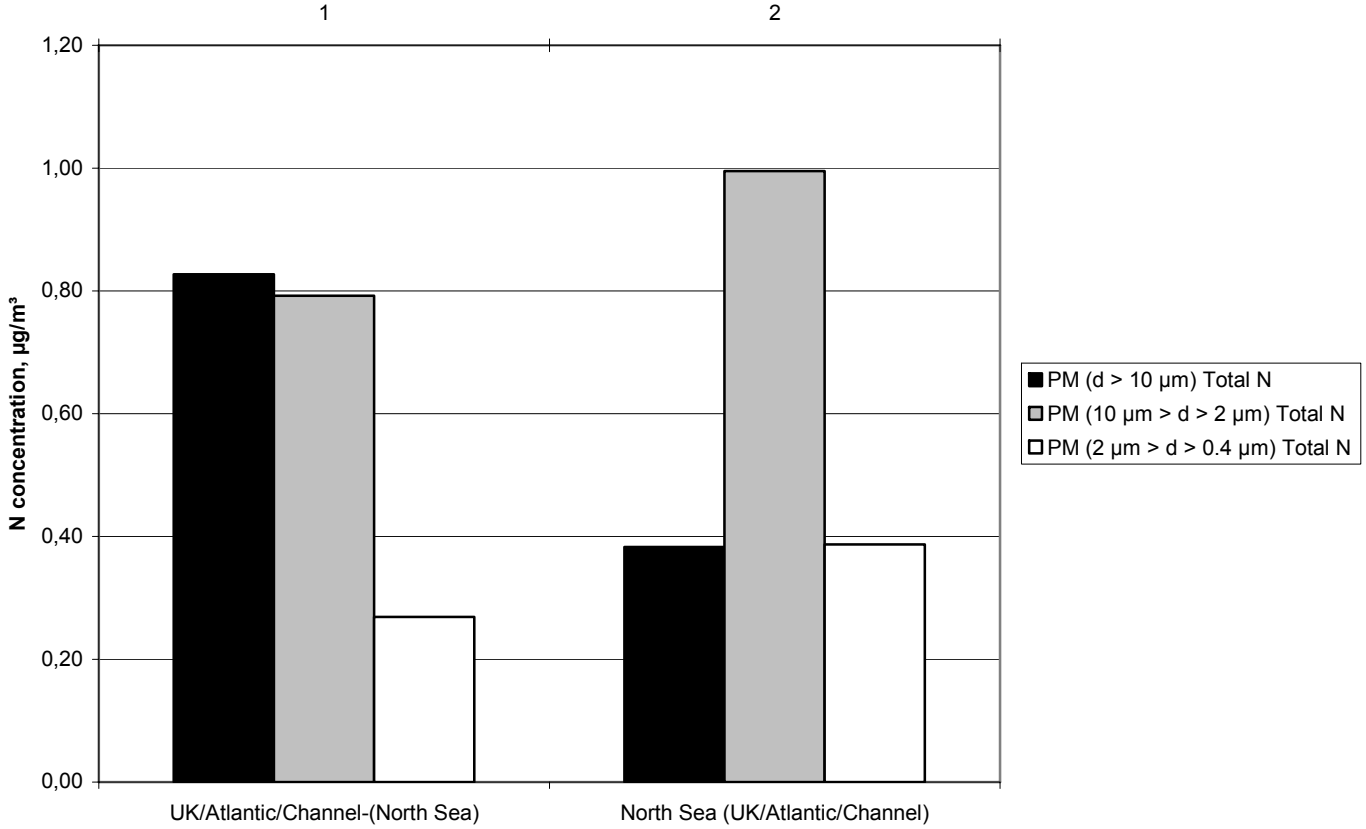

Figure 2.15 Variation of the weekly average N concentrations in the three size fractions (d > 10 µm, 10 µm > d > 2 µm, and 2 µm > d > 0.4 µm) during the 2nd campaign.

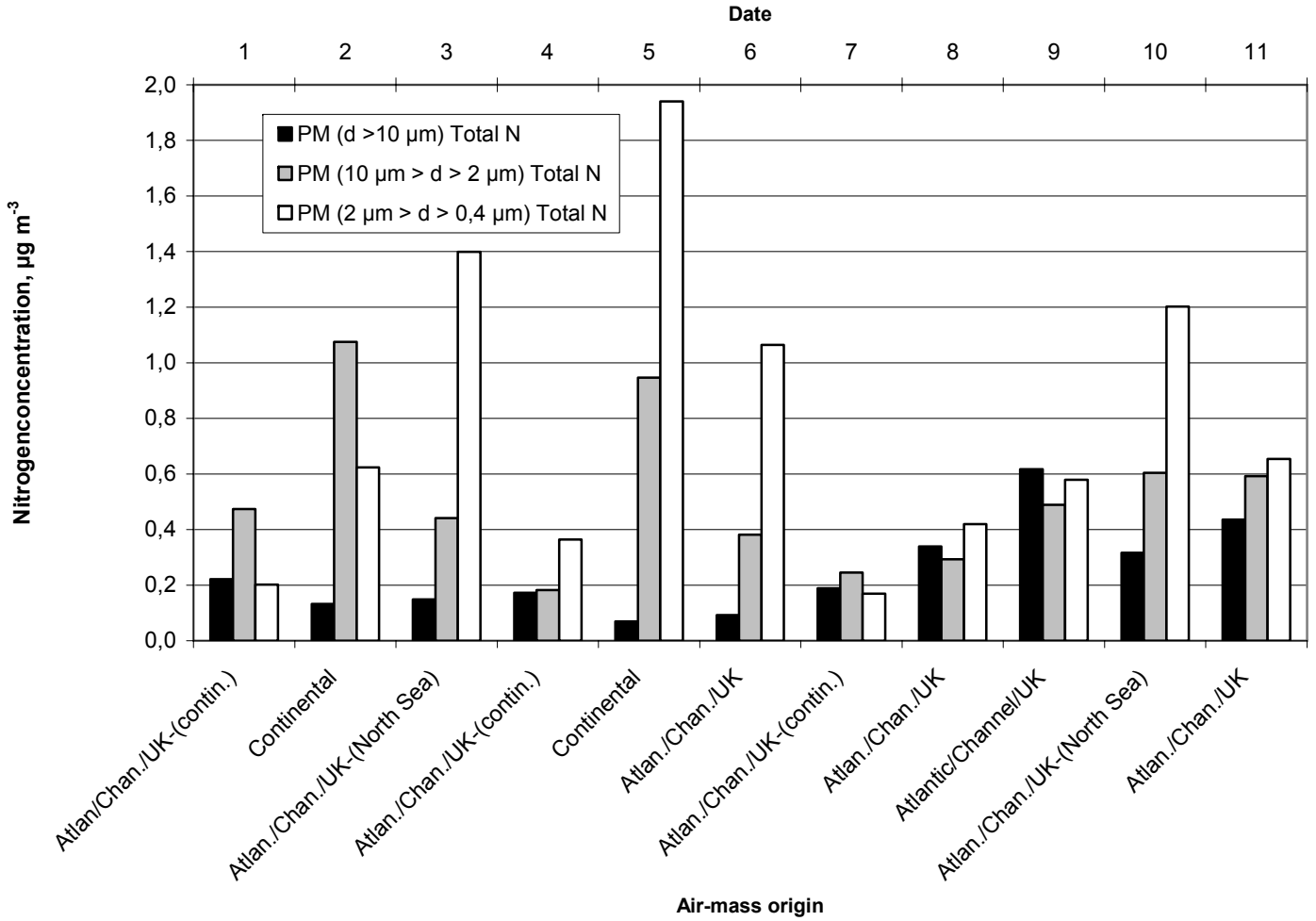

Figure 2.16 Variation of the weekly average N concentrations in the three size fractions (d > 10 µm, 10 µm > d > 2 µm, and 2 µm > d > 0.4 µm) during the 3rd campaign.

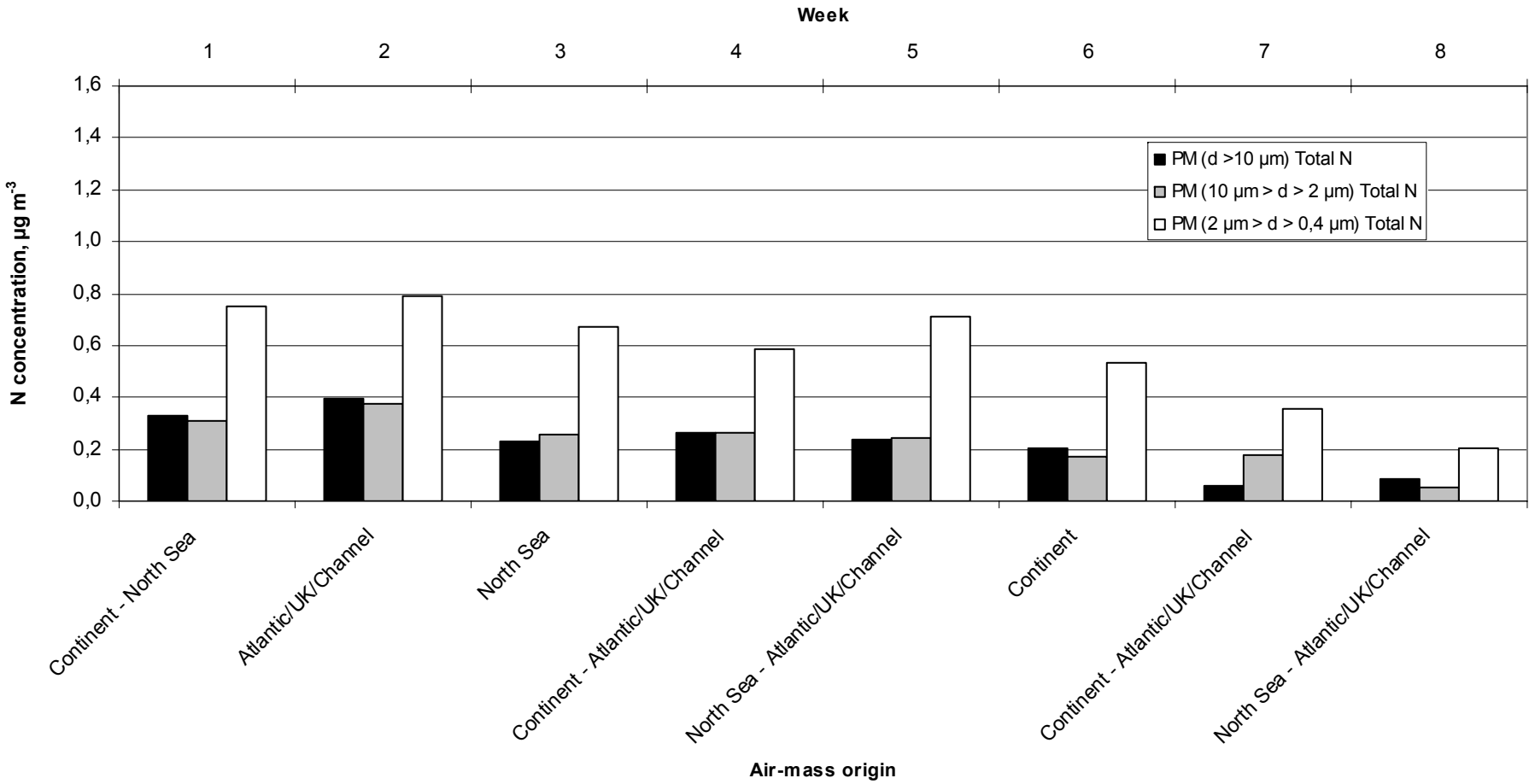

Figure 2.17 Variation of the weekly average N concentrations in the three size fractions ($d > 10$ µm, 10 µm $> d > 2$ µm, and 2 µm $> d > 0.4$ µm) during the 4th campaign.

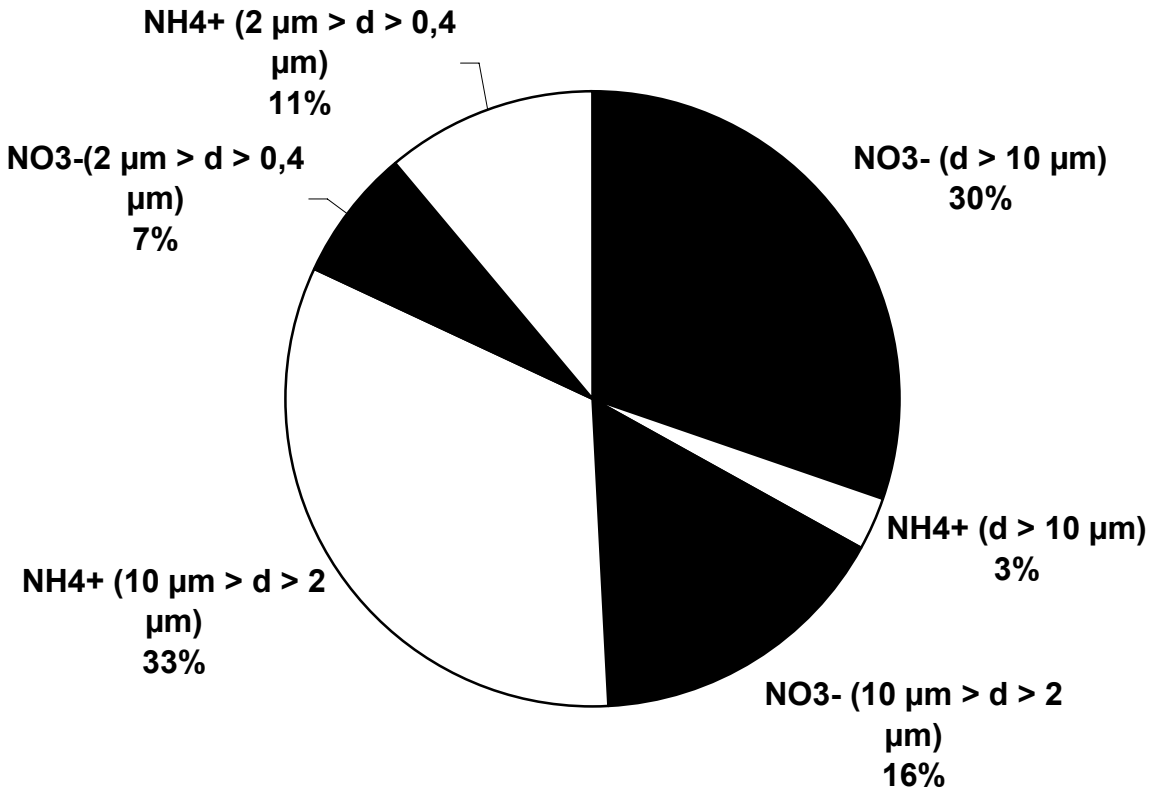

Figure 2.18 Relative contribution of the size-fractions (d > 10 µm, 10 µm > d > 2 µm, and 2 µm > d > 0.4 µm) to the total level of particulate N for the 2nd campaign.

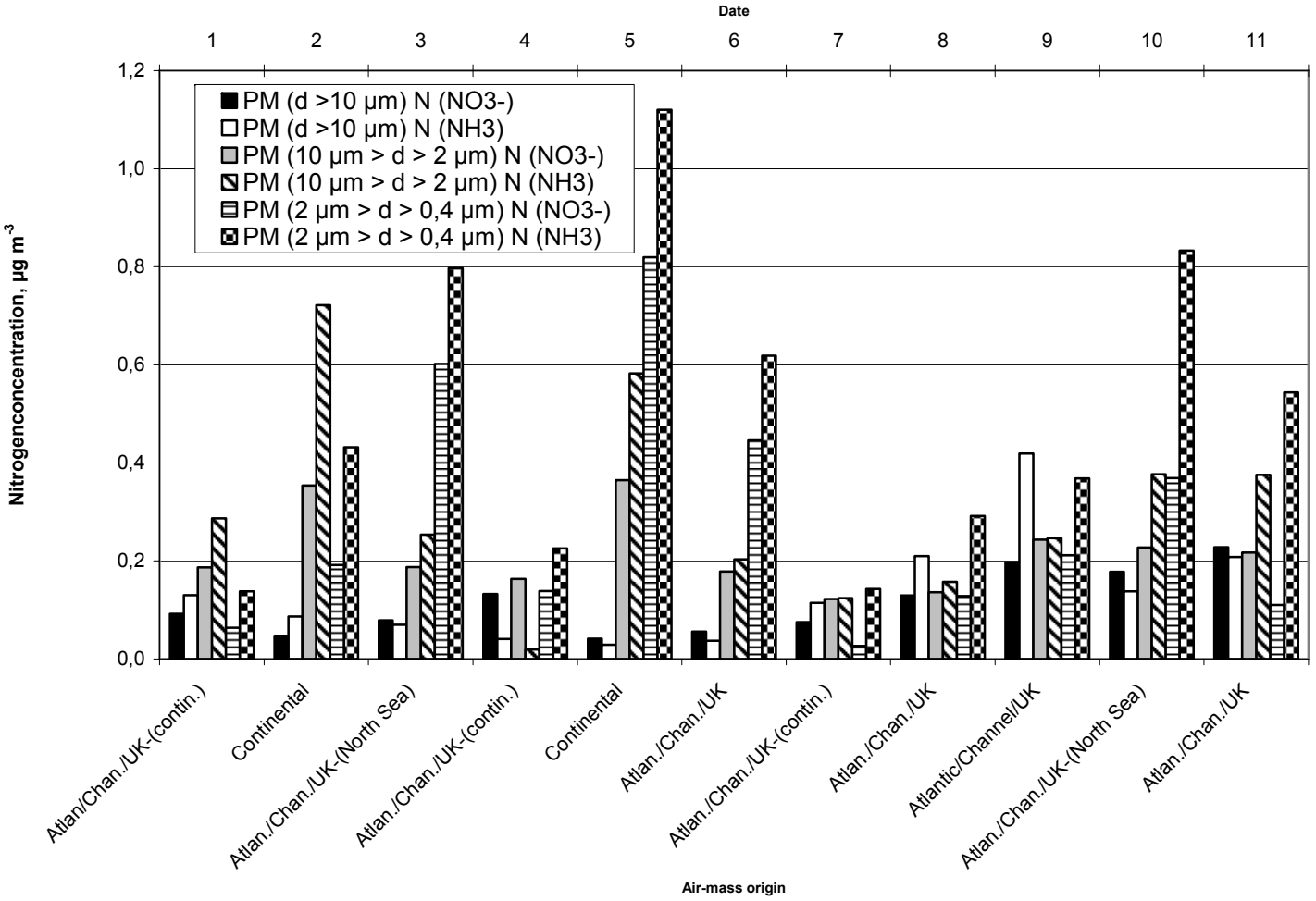

Figure 2.19 Variation of the weekly average concentrations of the nitrogen-containing compounds in aerosols during the 3rd campaign.

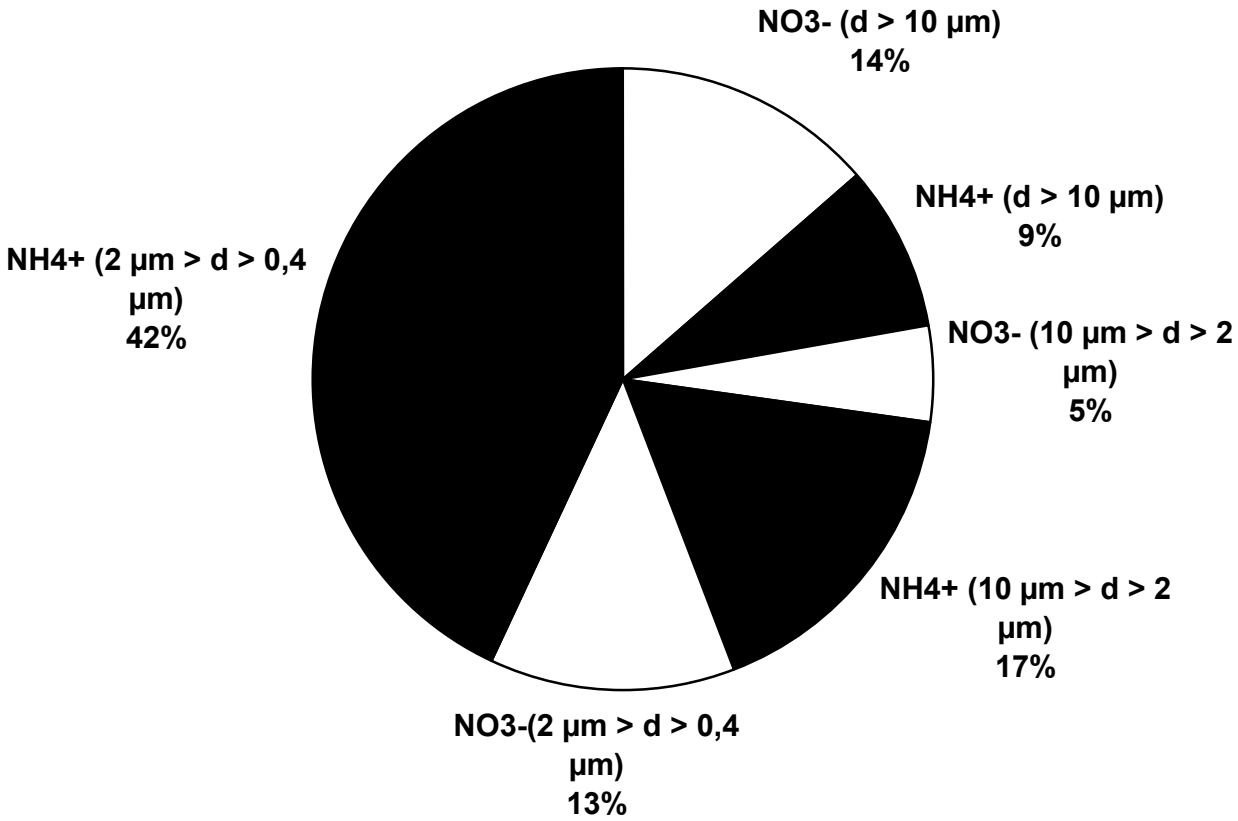

Figure 2.20 Relative contribution of the size-fractions (d > 10 µm, 10 µm > d > 2 µm, and 2 µm > d > 0.4 µm) to the total level of particulate N for the 4th campaign.

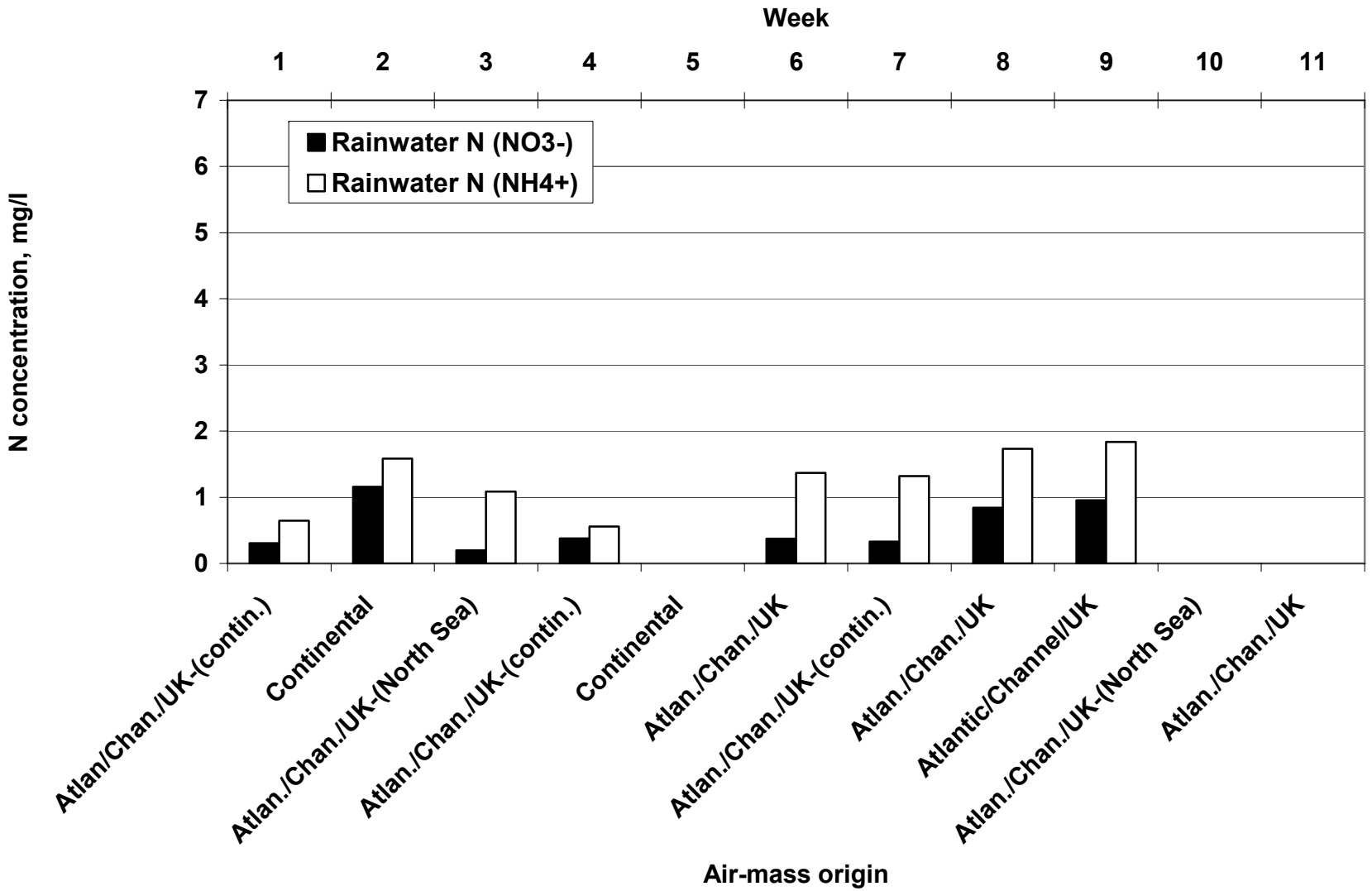

Figure 2.21 Variation of the weekly average concentrations of the nitrogen-containing compounds in rainwater during the 3rd campaign.

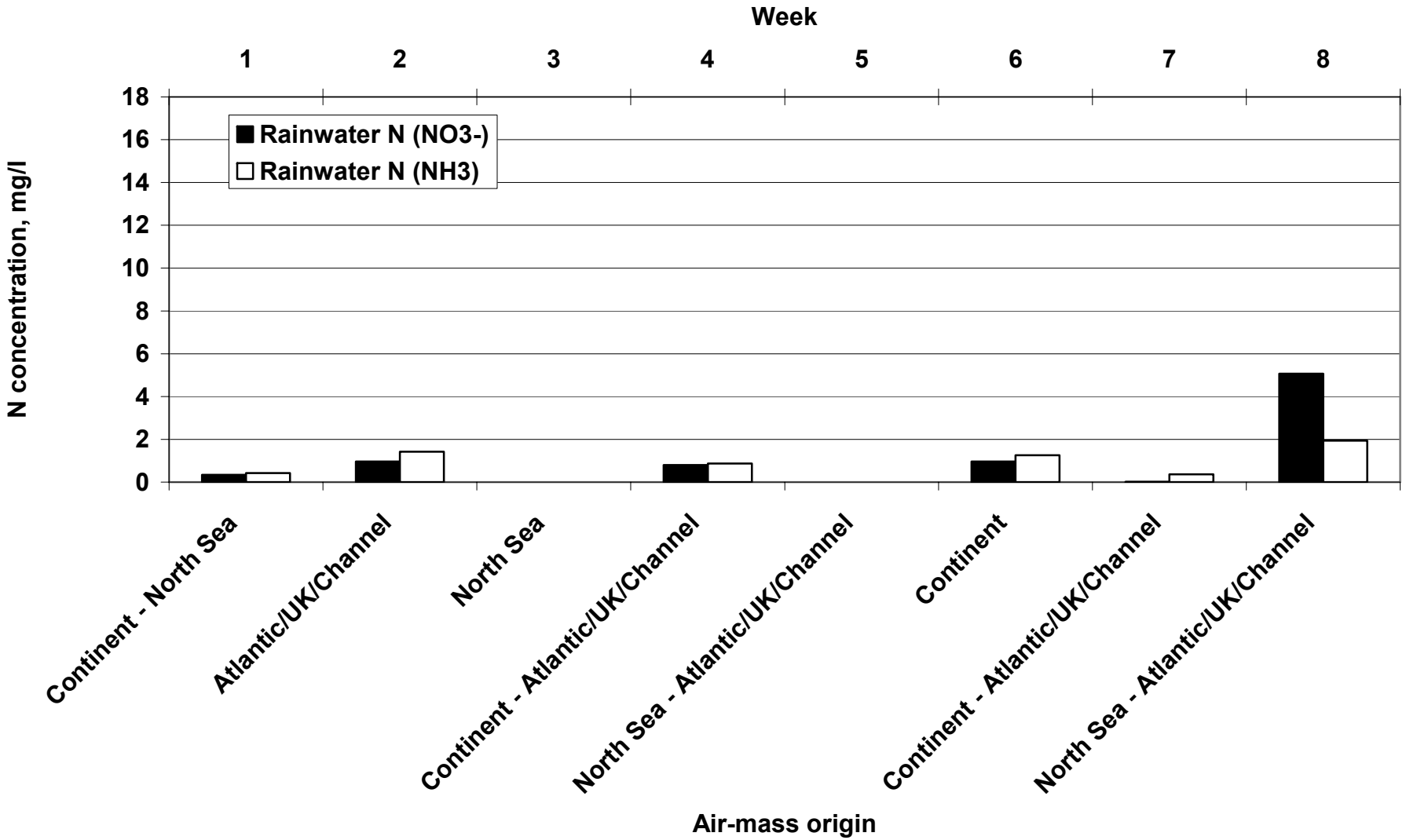

Figure 2.22 Variation of the weekly average concentrations of the nitrogen-containing compounds in rainwater during the 4th campaign.

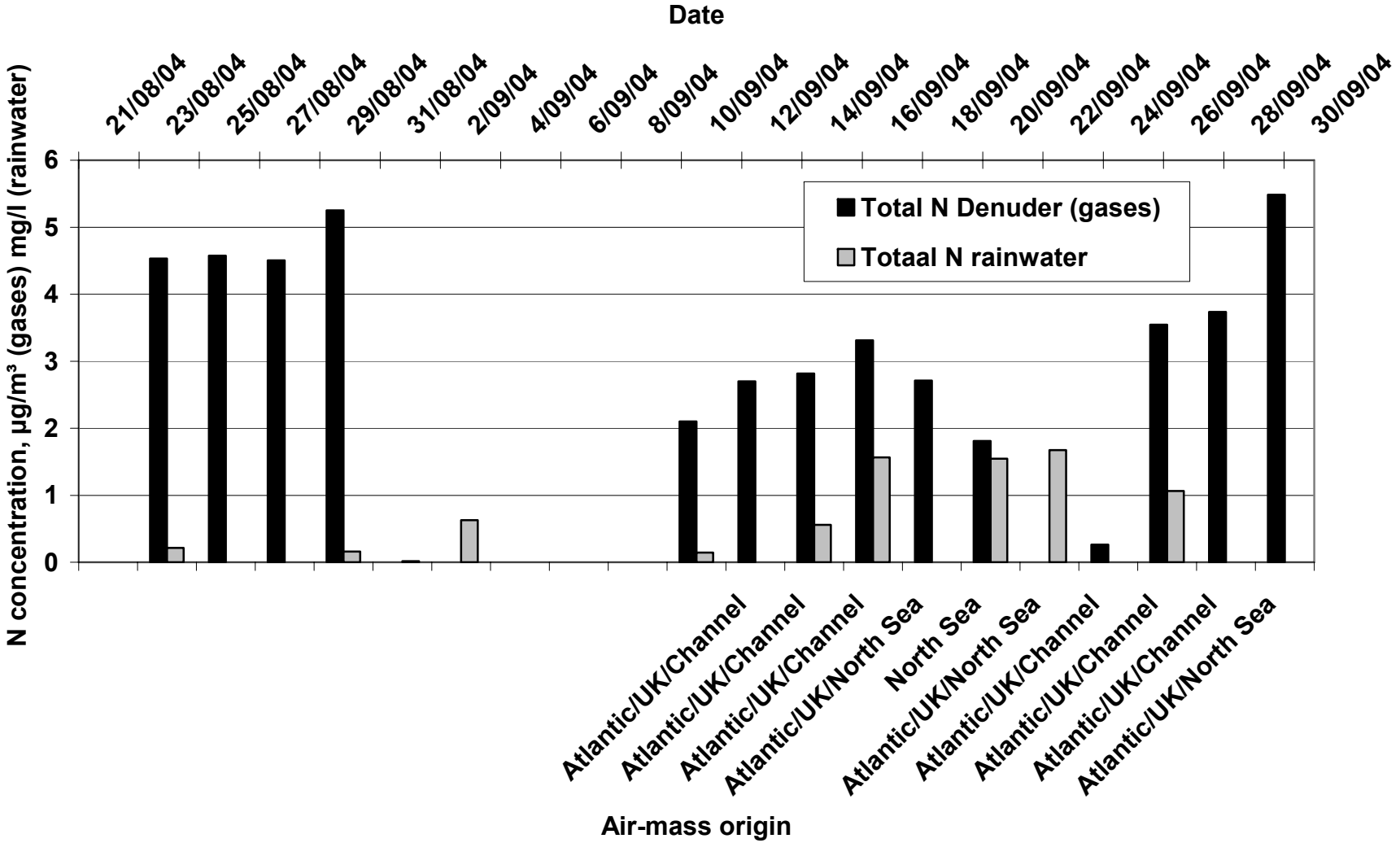

Figure 2.23 Daily variations of the total N concentrations for gases, aerosols, and rainwater during the 1st, 2nd, and 3rd week of the 1st campaign.

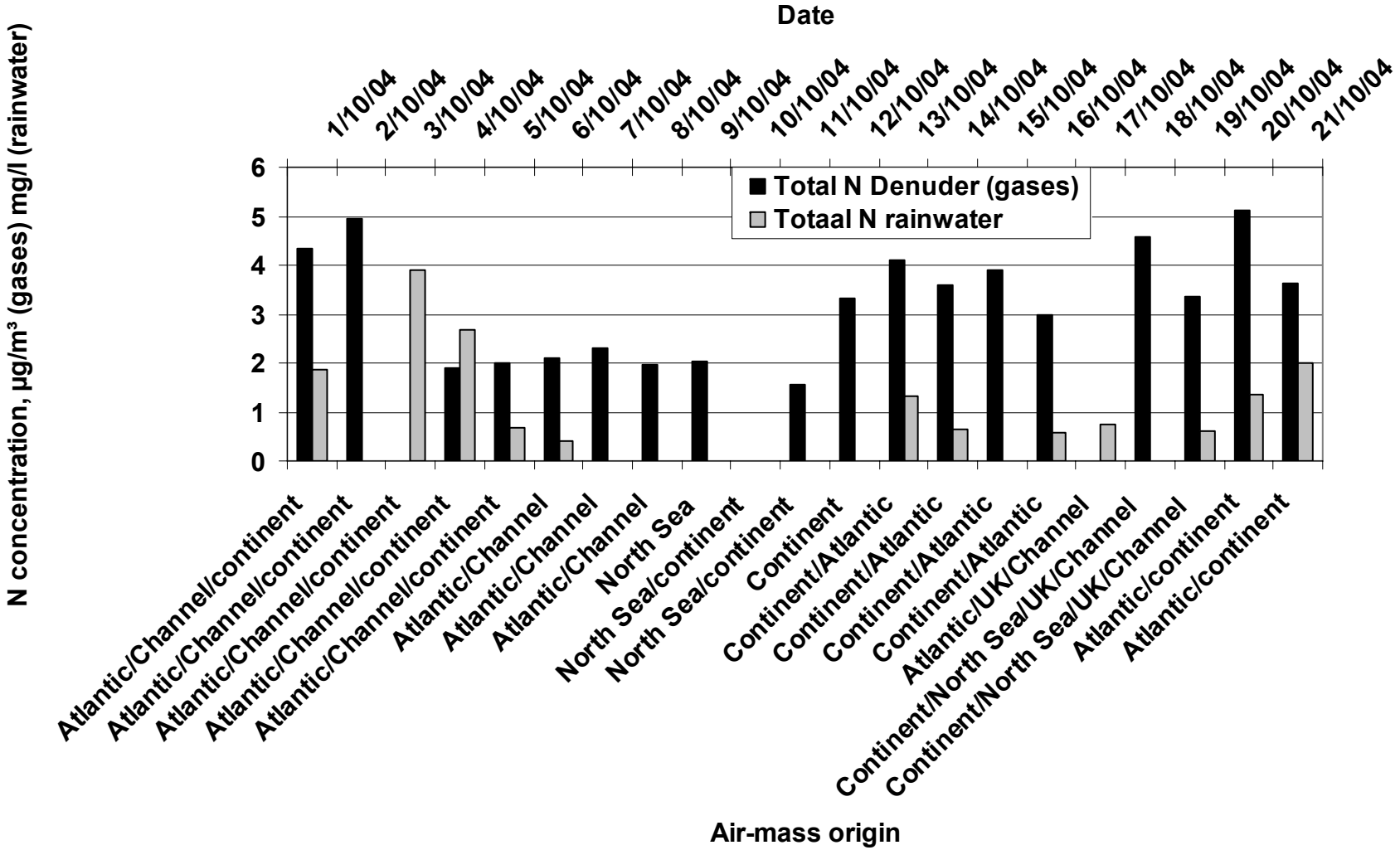

Figure 2.24 Daily variations of the total N concentrations for gases and rainwater during the 4th, 5th, and 6th week of the 1st campaign.

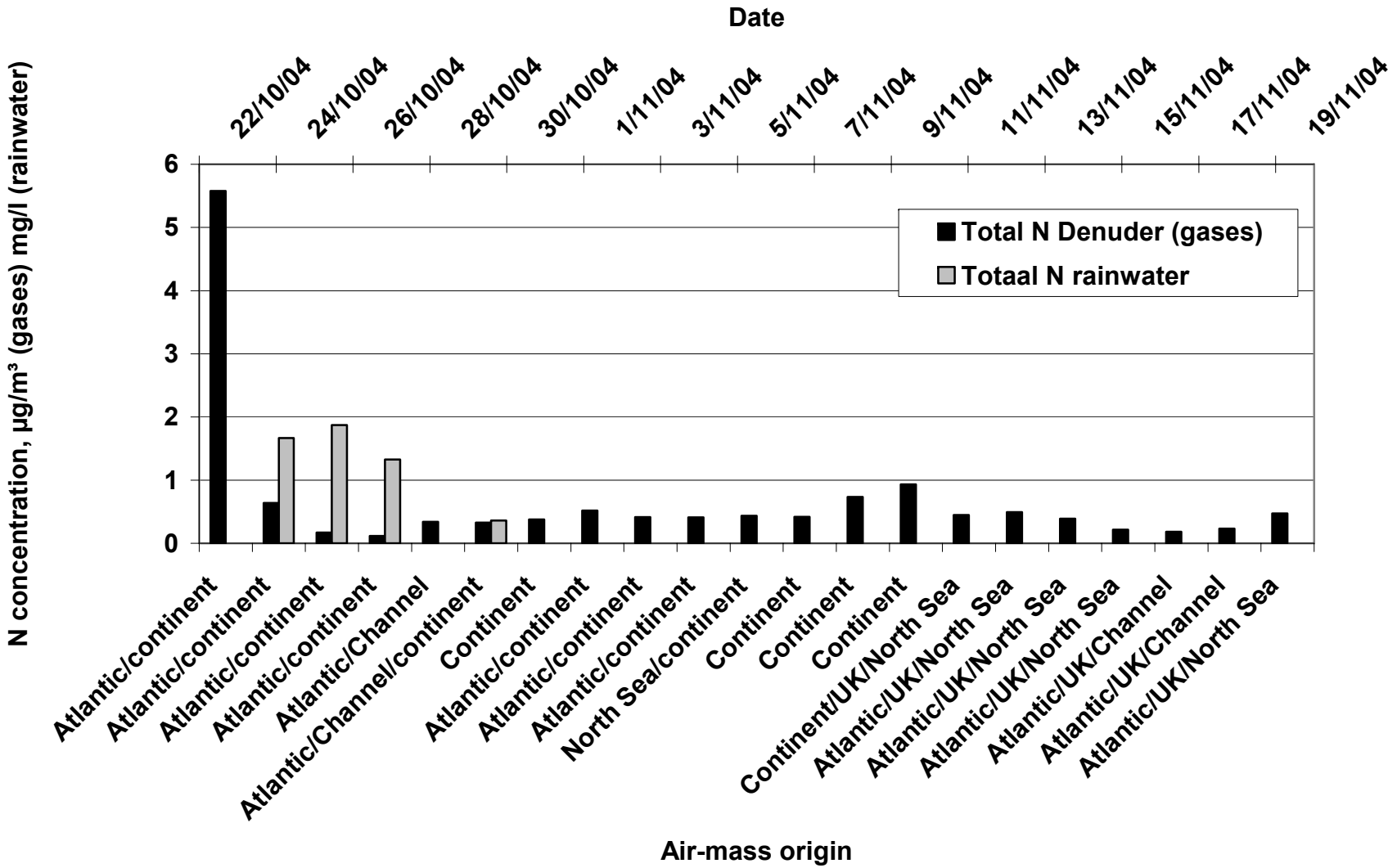

Figure 2.25 Daily variations of the total N concentrations for gases and rainwater during the 7th, 8th, and 9th week of the 1st campaign.

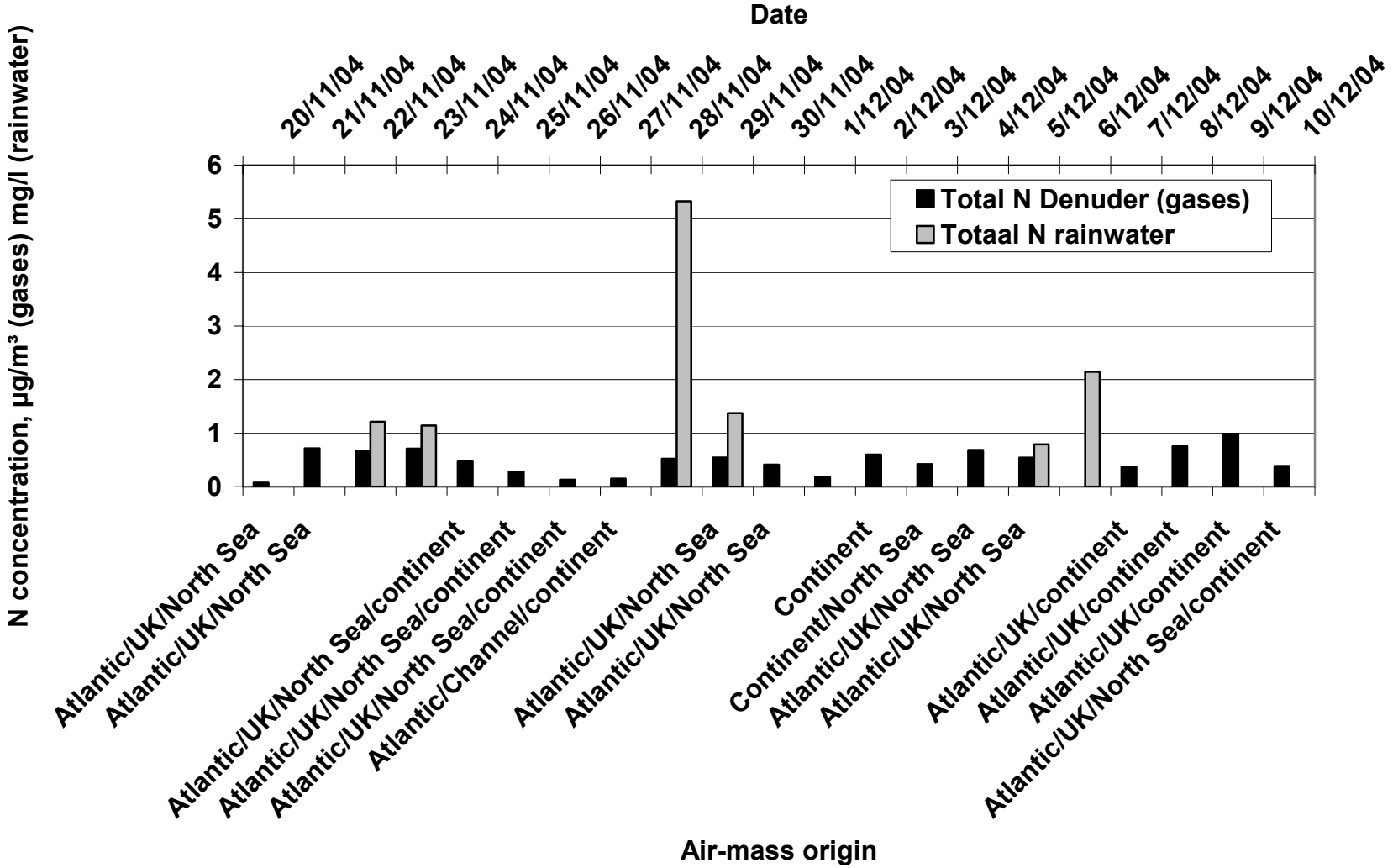

Figure 2.26 Daily variations of the total N concentrations for gases and rainwater during the 10th, 11th, and 12th week of the 1st campaign.

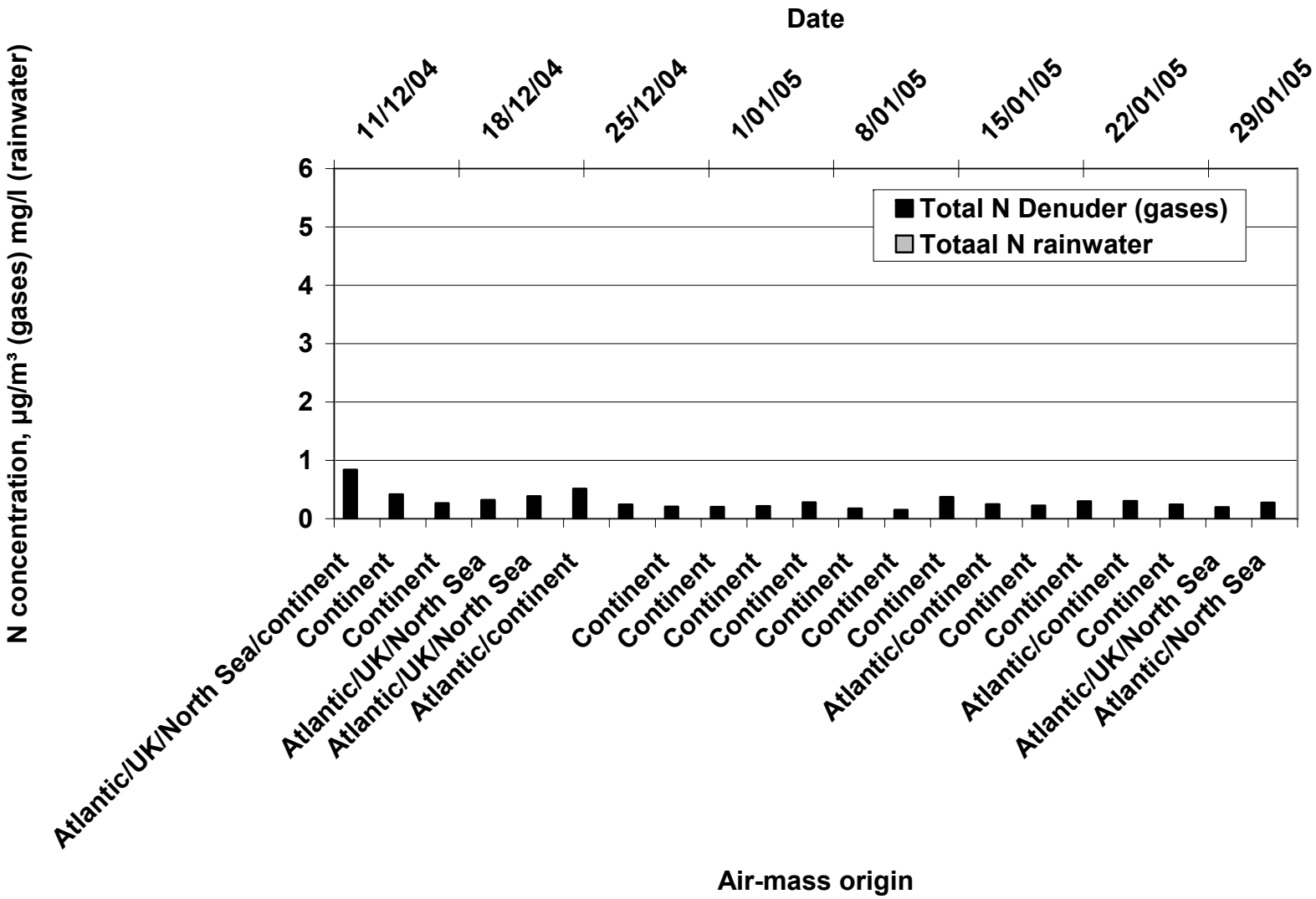

Figure 2.27 Daily variations of the total N concentrations for gases and rainwater during the 13th, 14th, and 15th week of the 1st campaign.

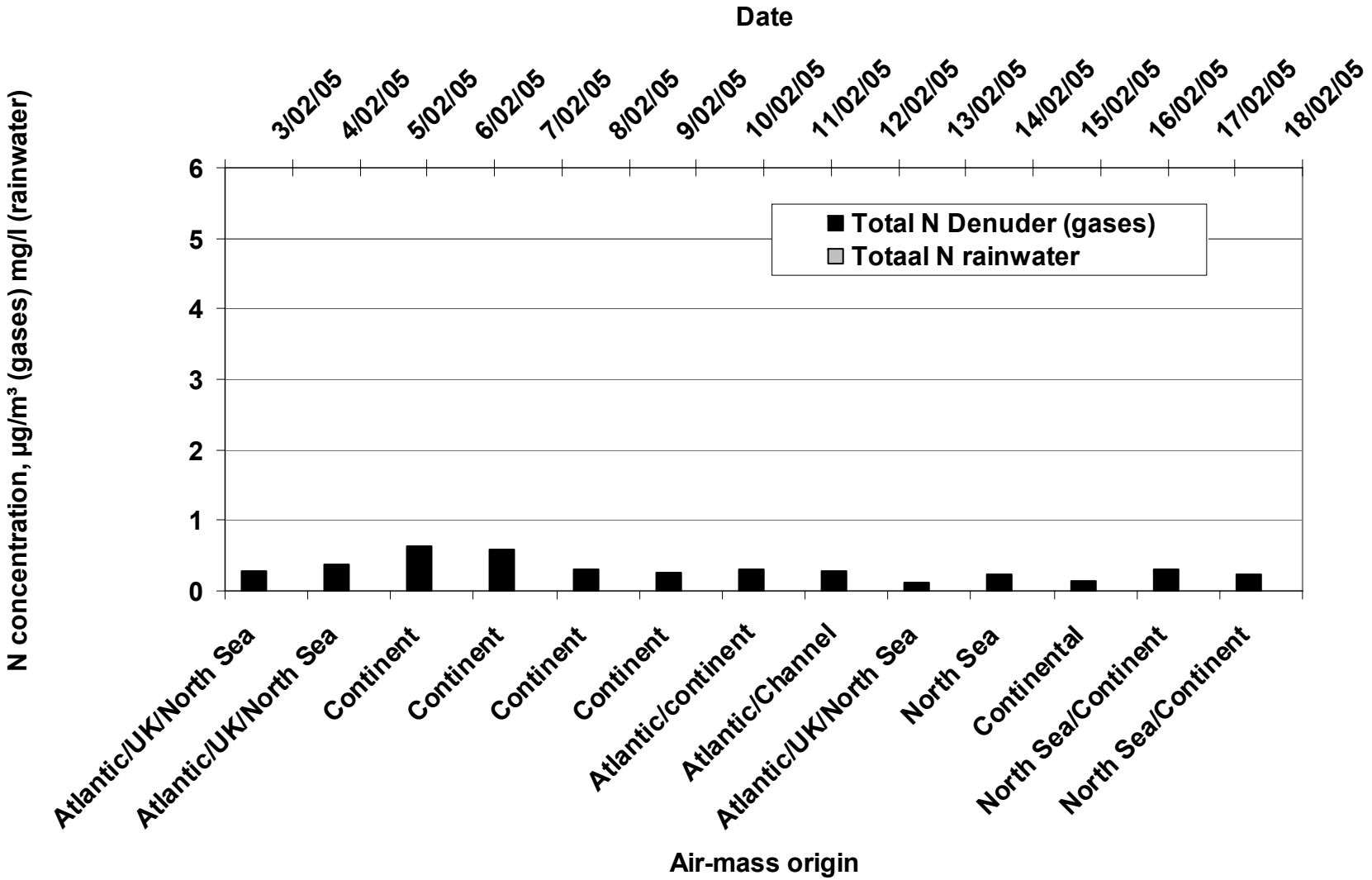

Figure 2.28 Daily variations of the total N concentrations for gases and rainwater during the 16th and 17th week of the 1st campaign.

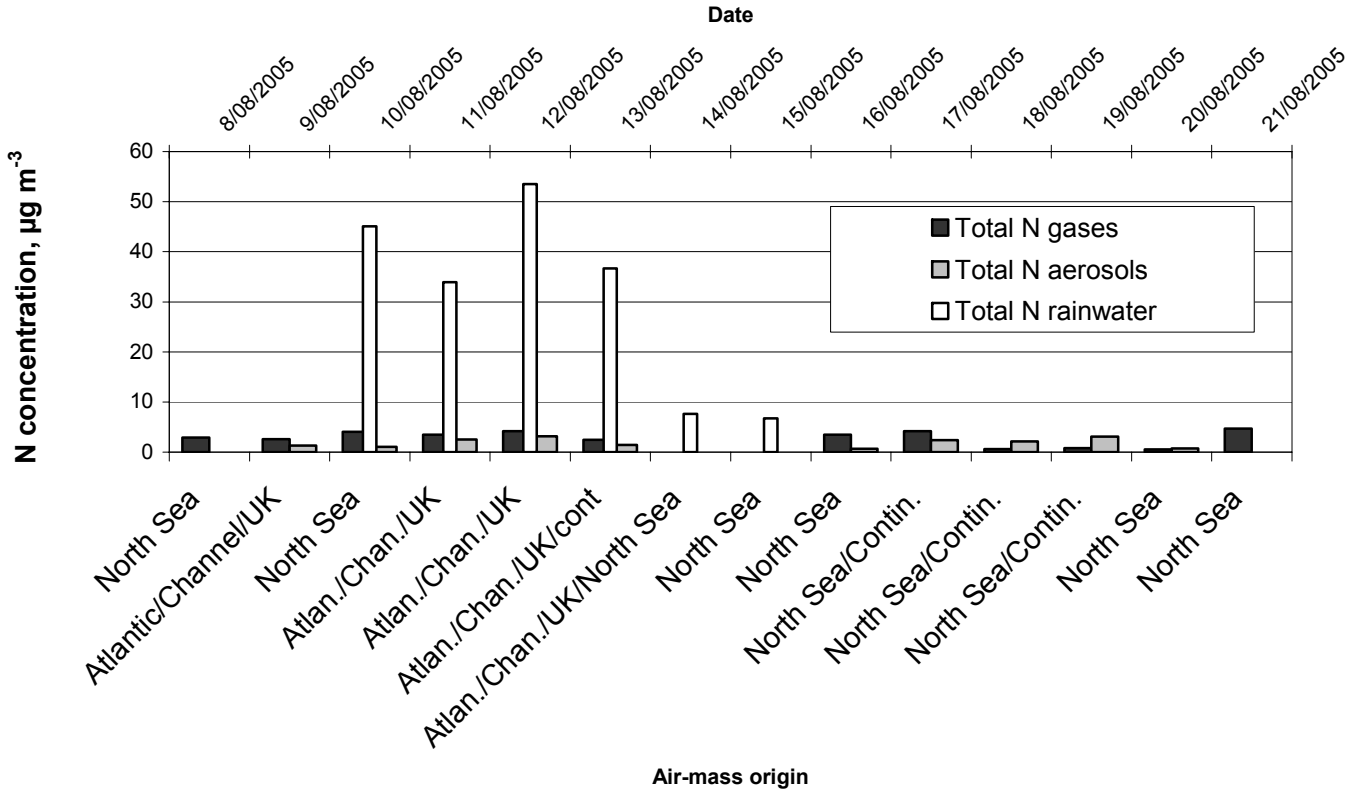

Figure 2.29 Daily variations of the total N concentrations for gases, aerosols, and rainwater during 2nd campaign.

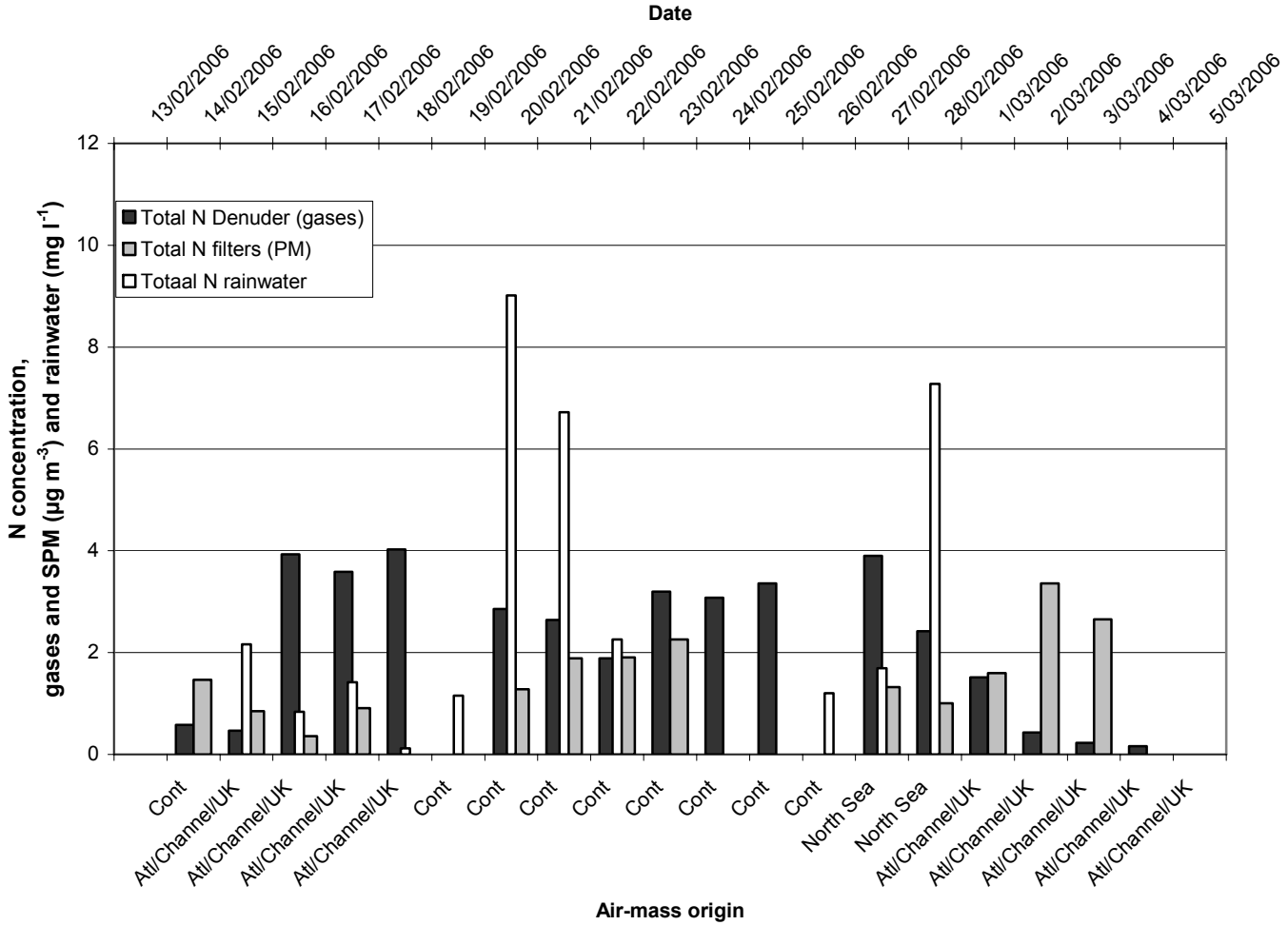

Figure 2.30 Daily variations of the total N concentrations for gases, aerosols, and rainwater during the 1st, 2nd, and 3rd week of the 3rd campaign

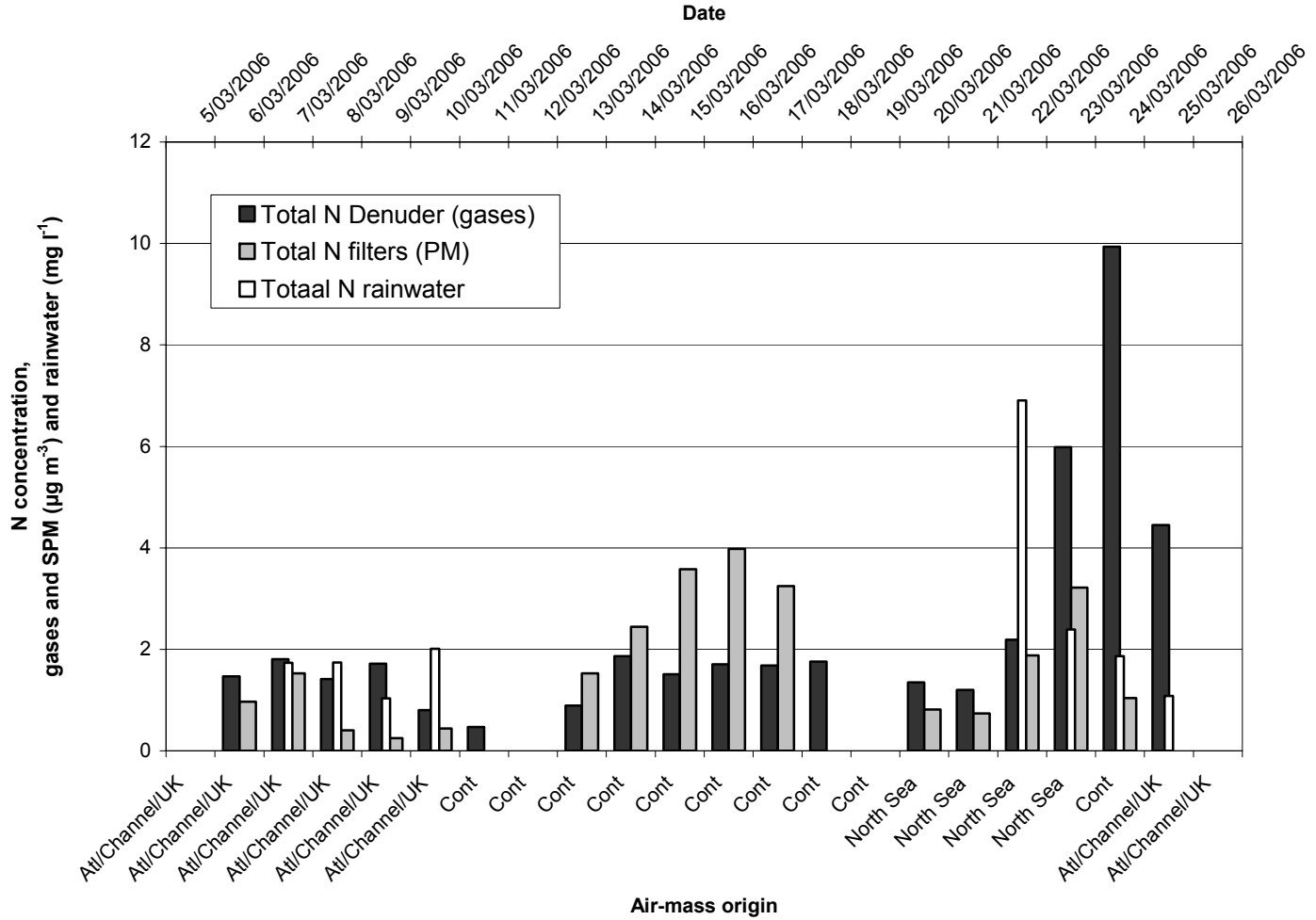

Figure 2.31 Daily variations of the total N concentrations for gases, aerosols, and rainwater during the 4th, 5th, and 6th week of the 3rd campaign.

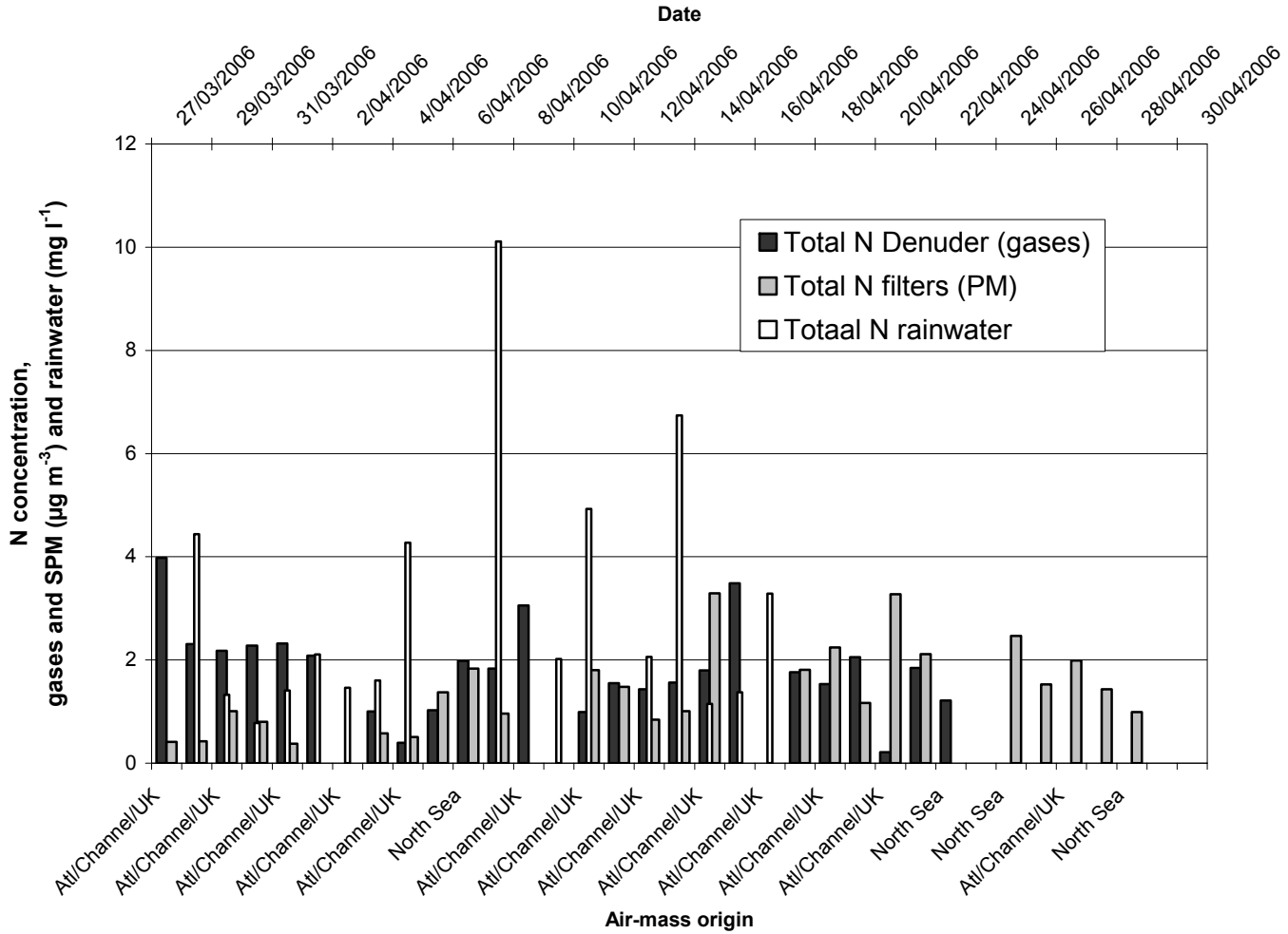

Figure 2.32 Daily variations of the total N concentrations for gases, aerosols, and rainwater during the 7th, 8th, 9th, 10th and 11th week of the 3rd campaign.

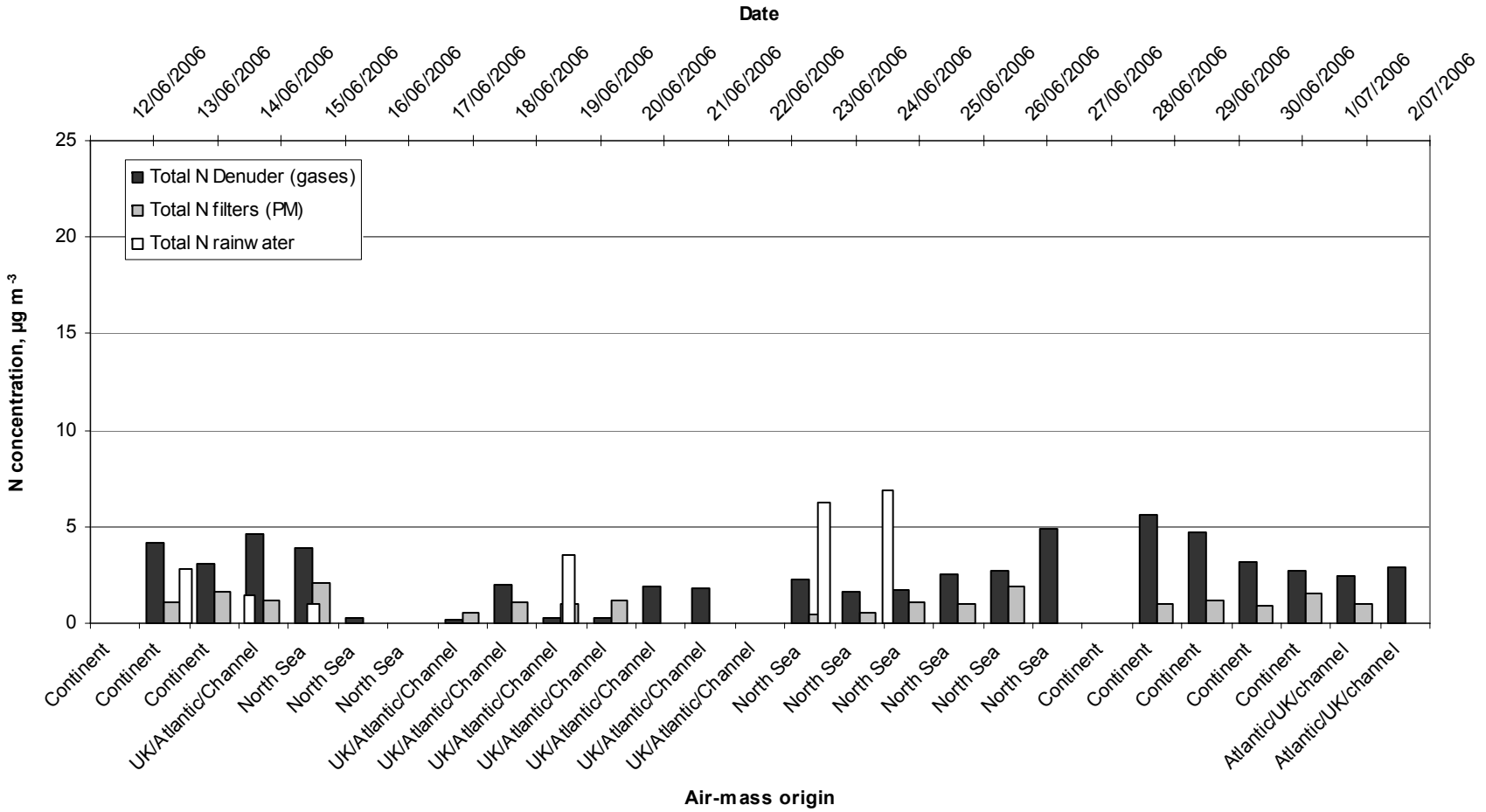

Figure 2.33 Daily variations of the total N concentrations for gases, aerosols, and rainwater during the 1st, 2nd, 3rd and 4th week of the 4th campaign.

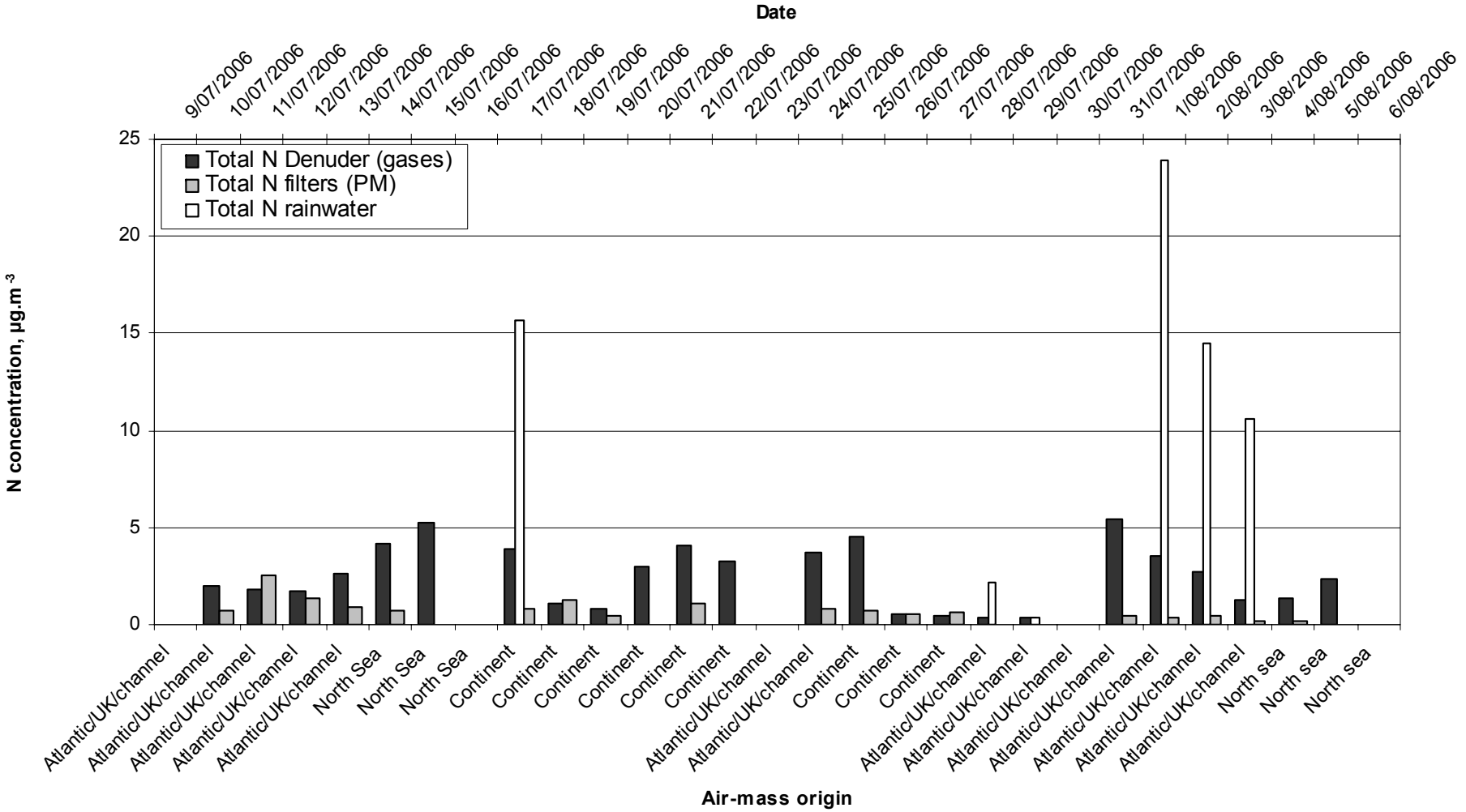

Figure 2.34 Daily variations of the total N concentrations for gases, aerosols, and rainwater during the 5th, 6th, 7th and 8th week of the 4th campaign.

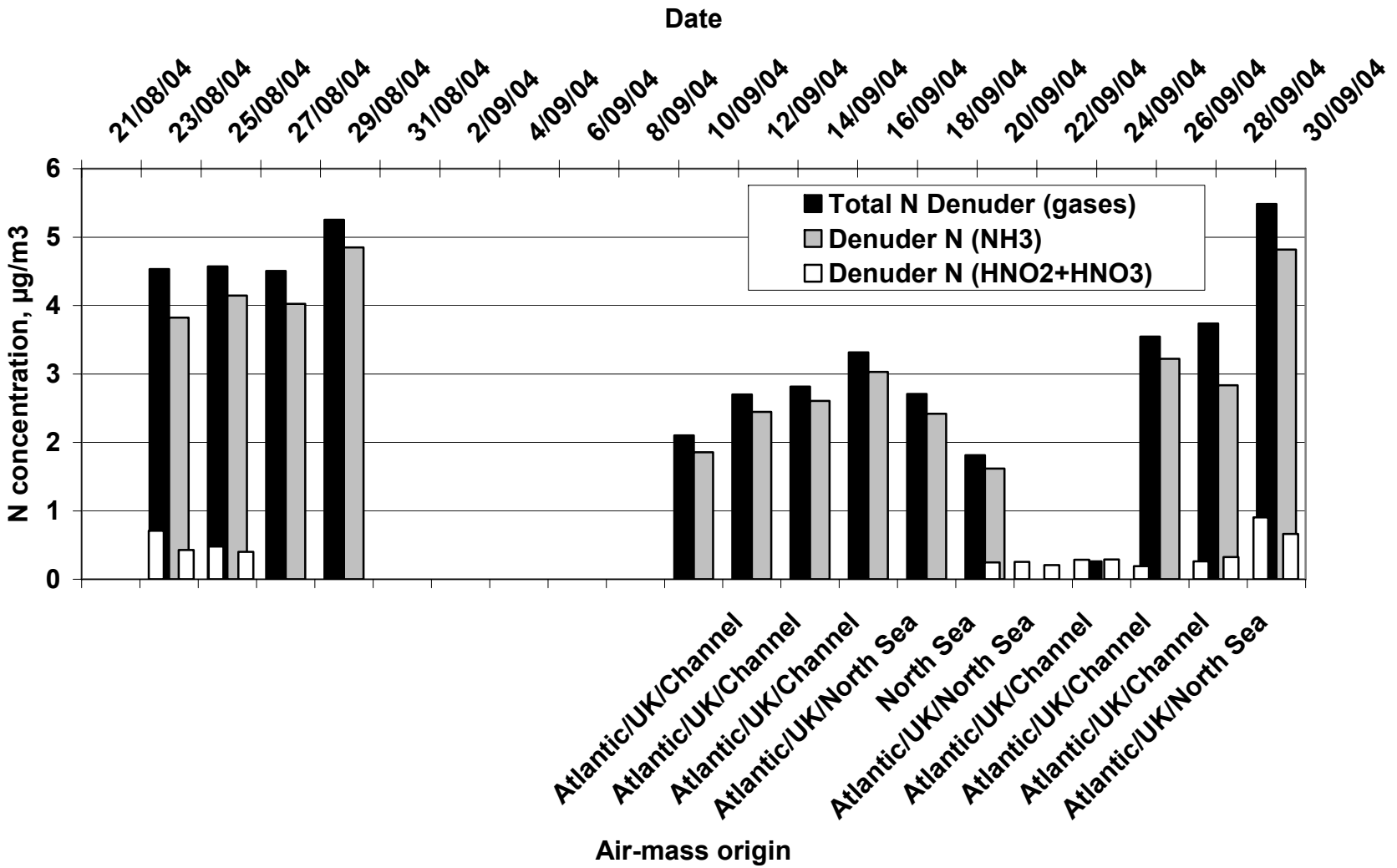

Figure 2.35 Daily variations of the concentrations of gaseous nitrogen-containing compounds during the 1st, 2nd and 3rd week of the 1st campaign.

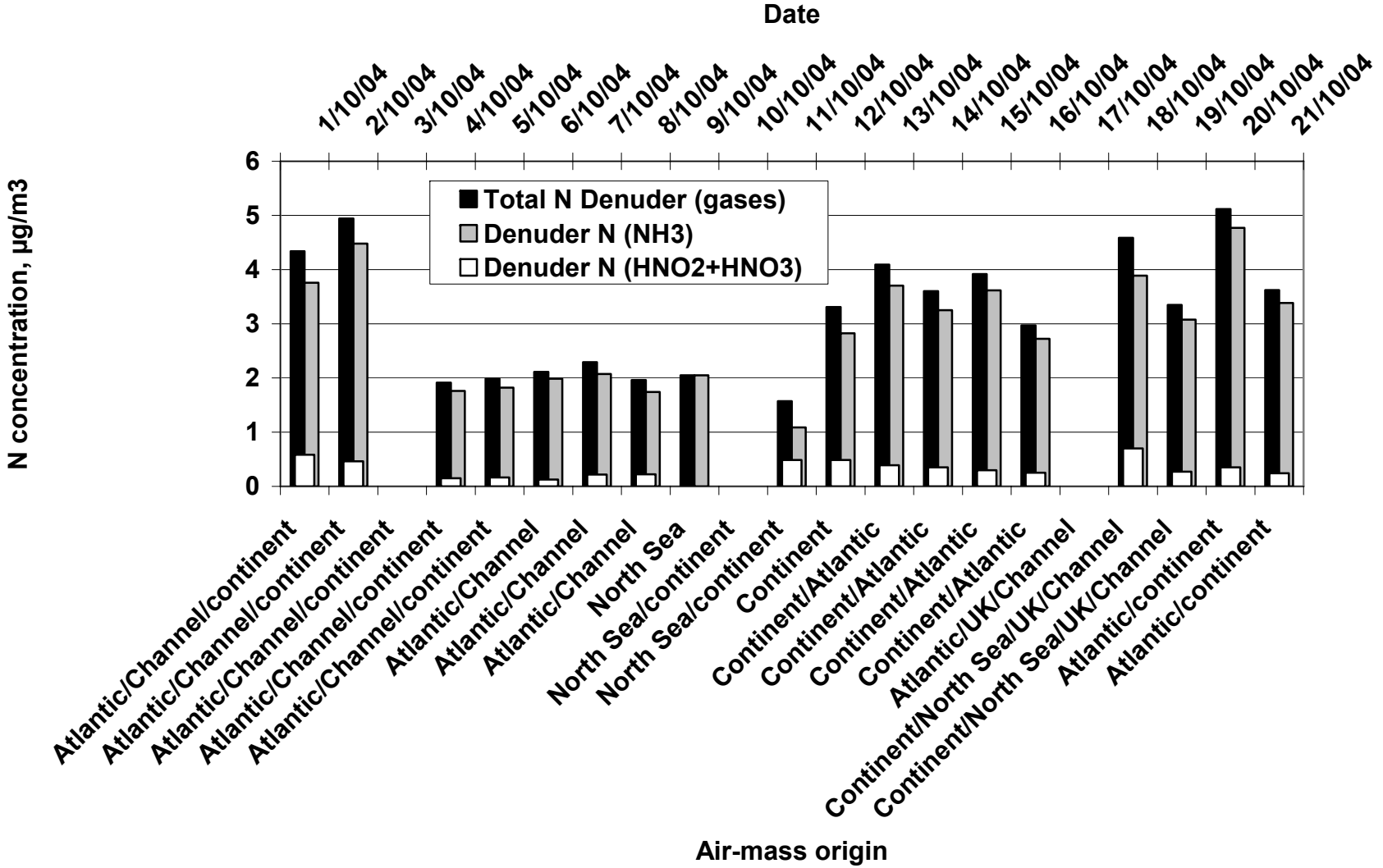

Figure 2.36 Daily variations of the concentrations of gaseous nitrogen-containing compounds during the 4th, 5th and 6th week of the 1st campaign.

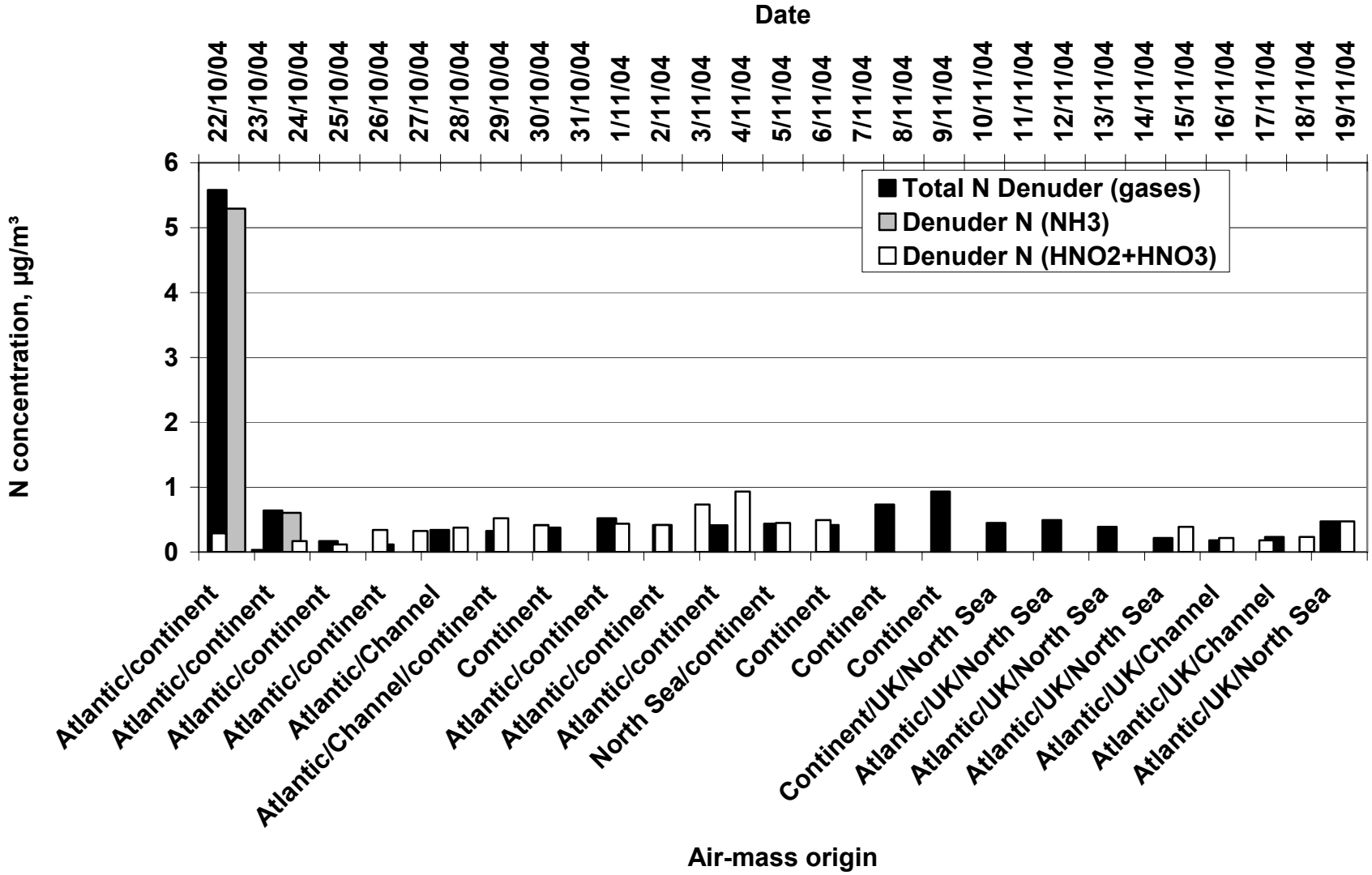

Figure 2.37 Daily variations of the concentrations of gaseous nitrogen-containing compounds during the 7th, 8th and 9th week of the 1st campaign.

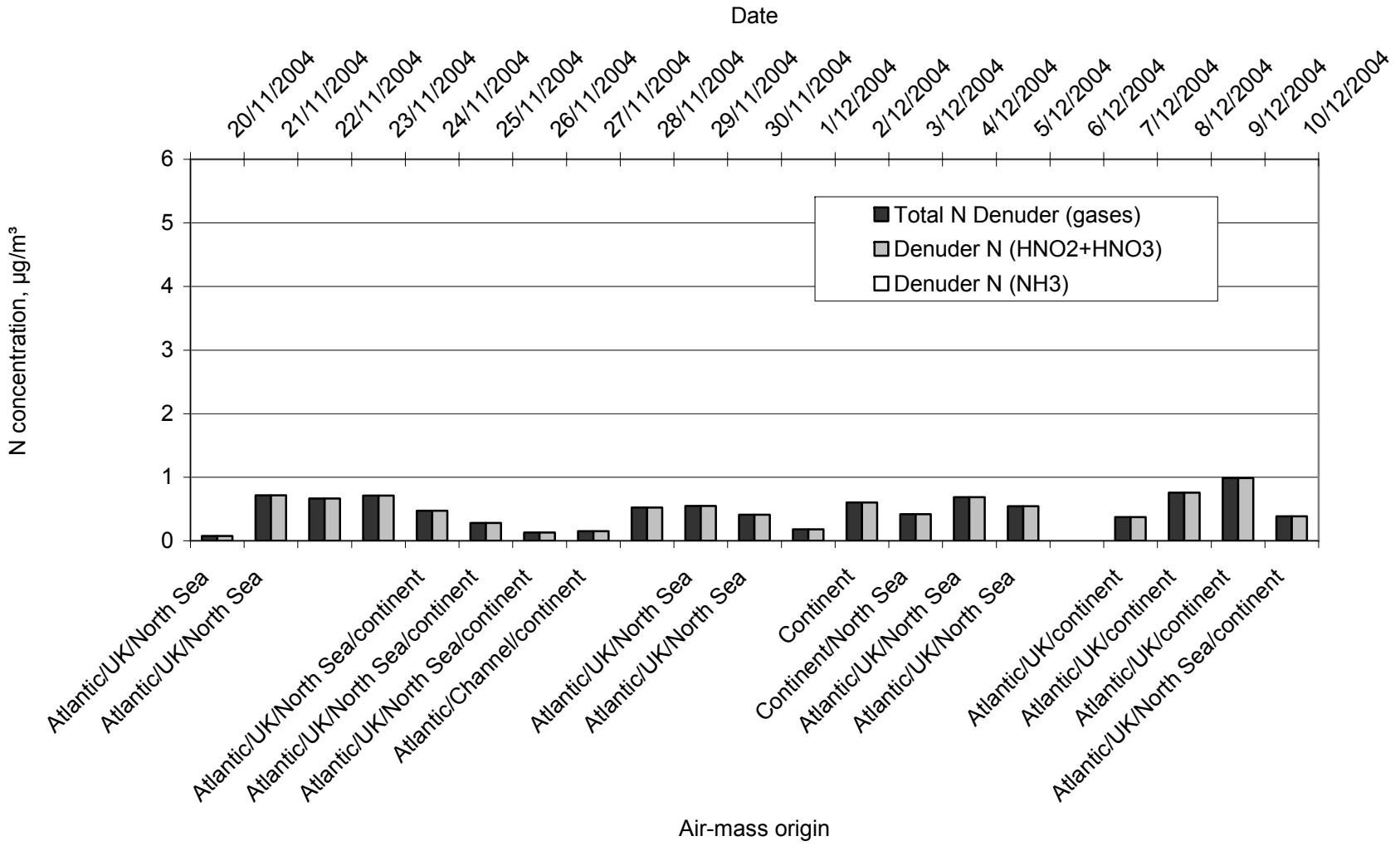

Figure 2.38 Daily variations of the concentrations of gaseous nitrogen-containing compounds during the 10th, 11th and 12th week of the 1st campaign.

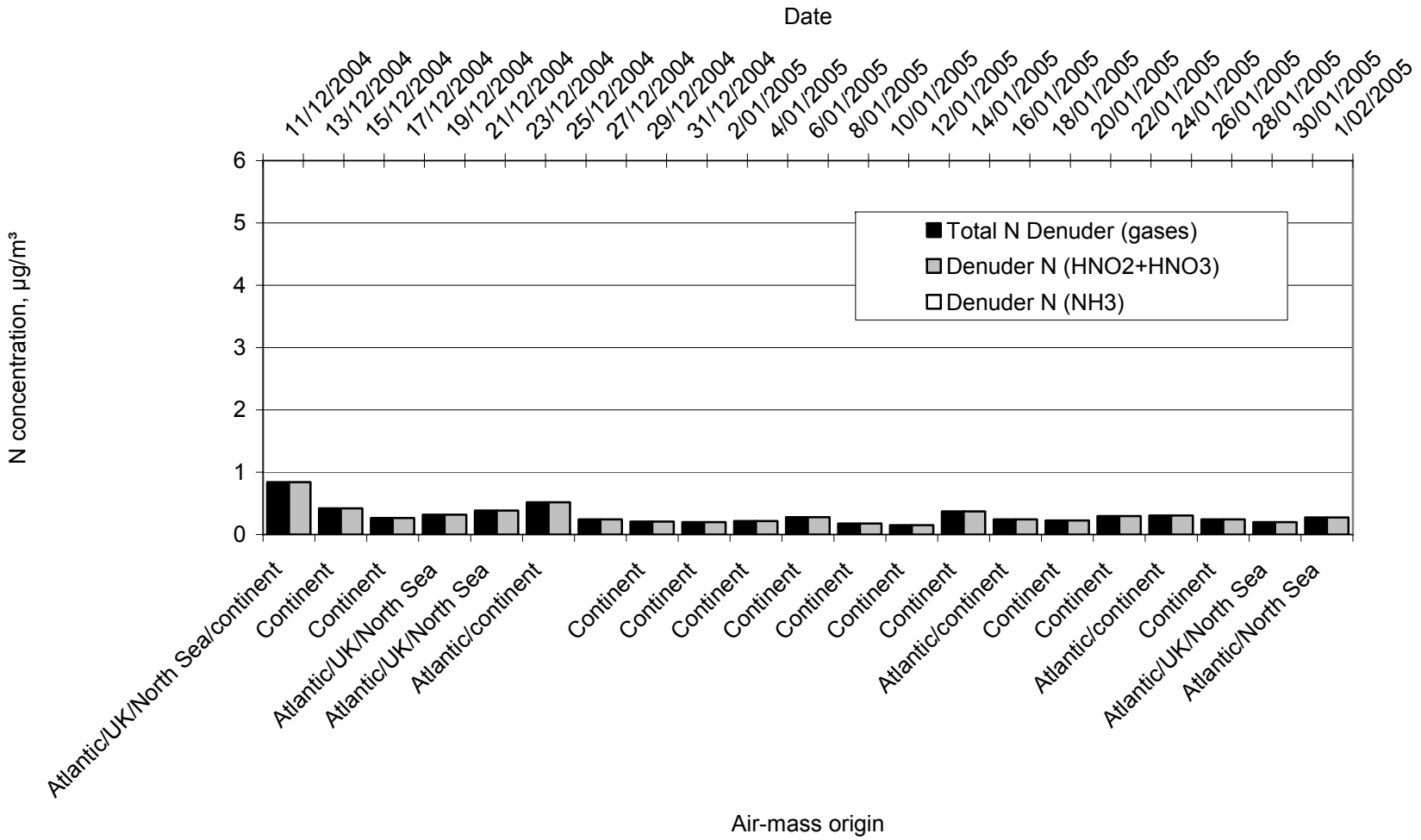

Figure 2.39 Daily variations of the concentrations of gaseous nitrogen-containing compounds during the 13th, 14th and 15th week of the 1st campaign.

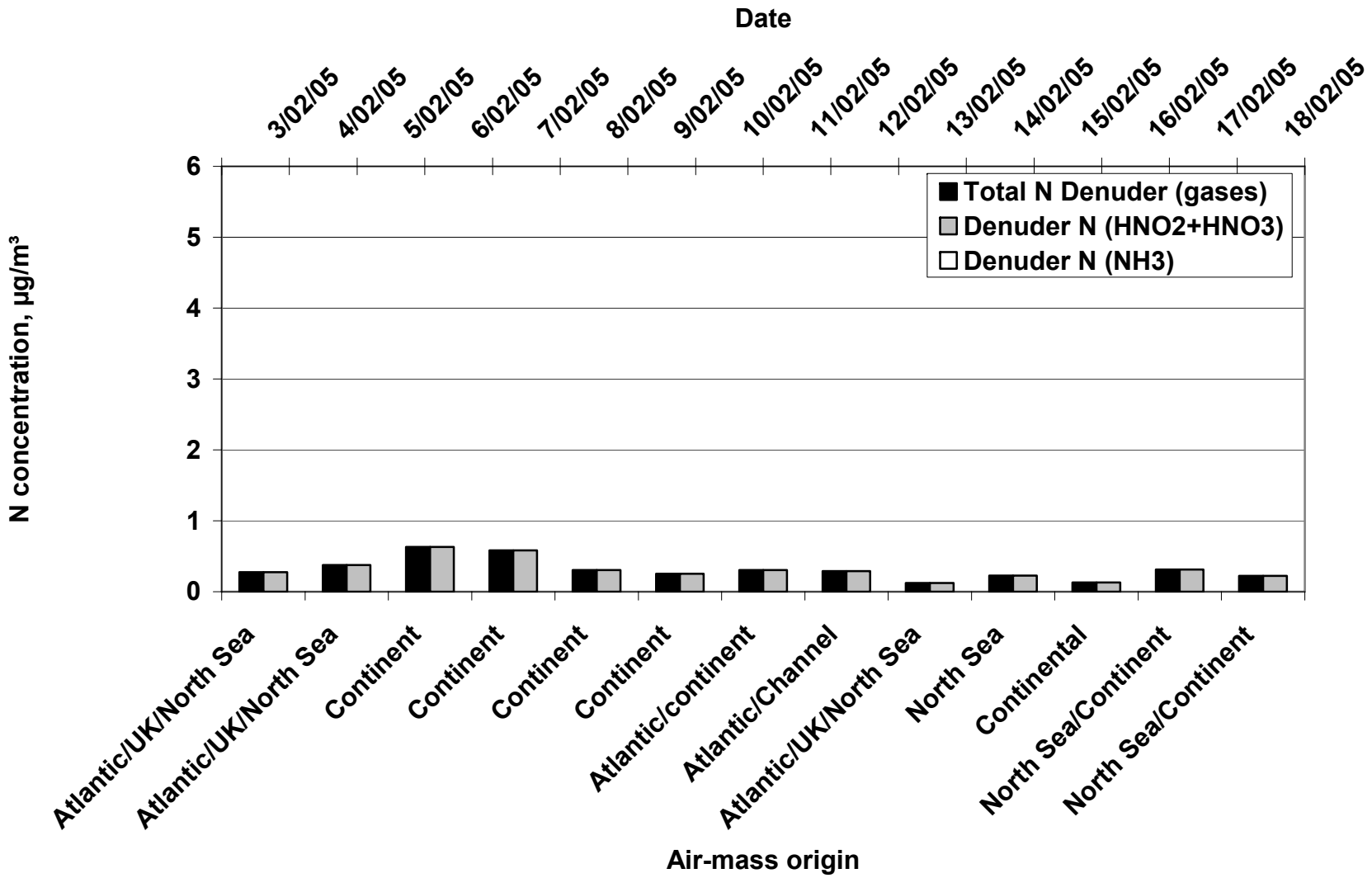

Figure 2.40 Daily variations of the concentrations of gaseous nitrogen-containing compounds during the 16th and 17th week of the 1st campaign.

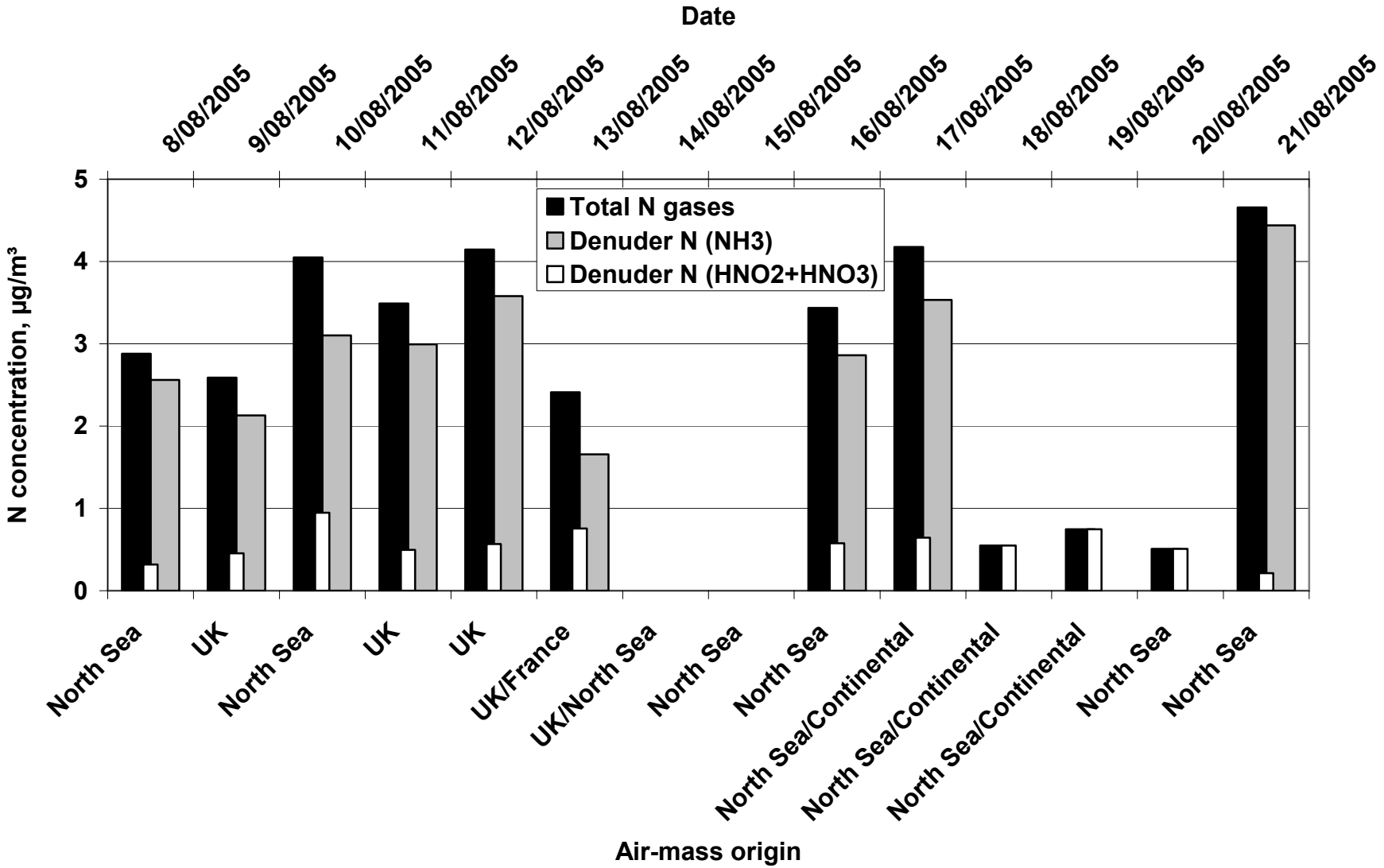

Figure 2.41 Daily variations of the concentrations of gaseous nitrogen-containing compounds during the 2nd campaign.

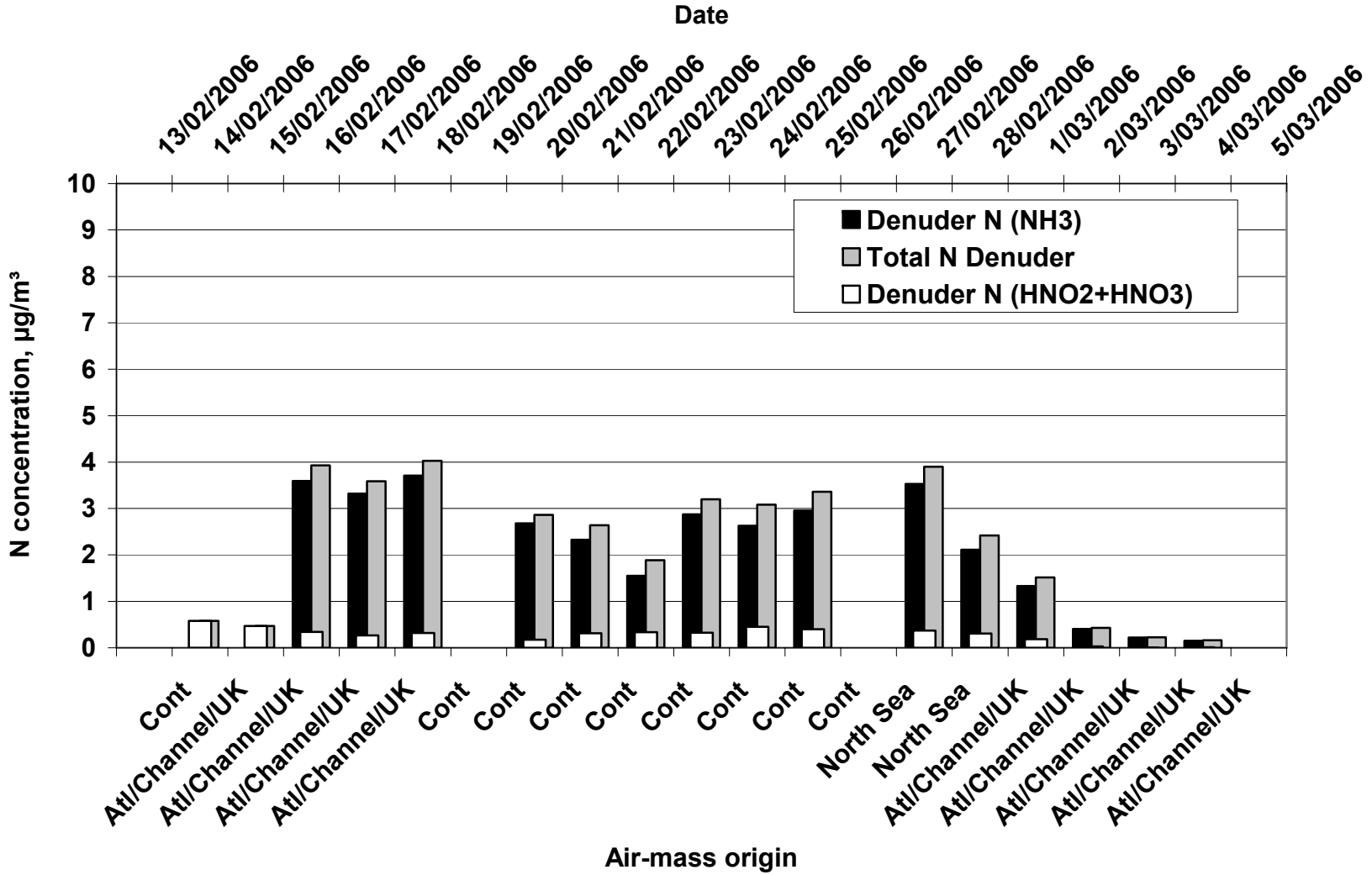

Figure 2.42 Daily variations of the concentrations of gaseous nitrogen-containing compounds during the 1st, 2nd and 3rd week of the 3rd campaign.

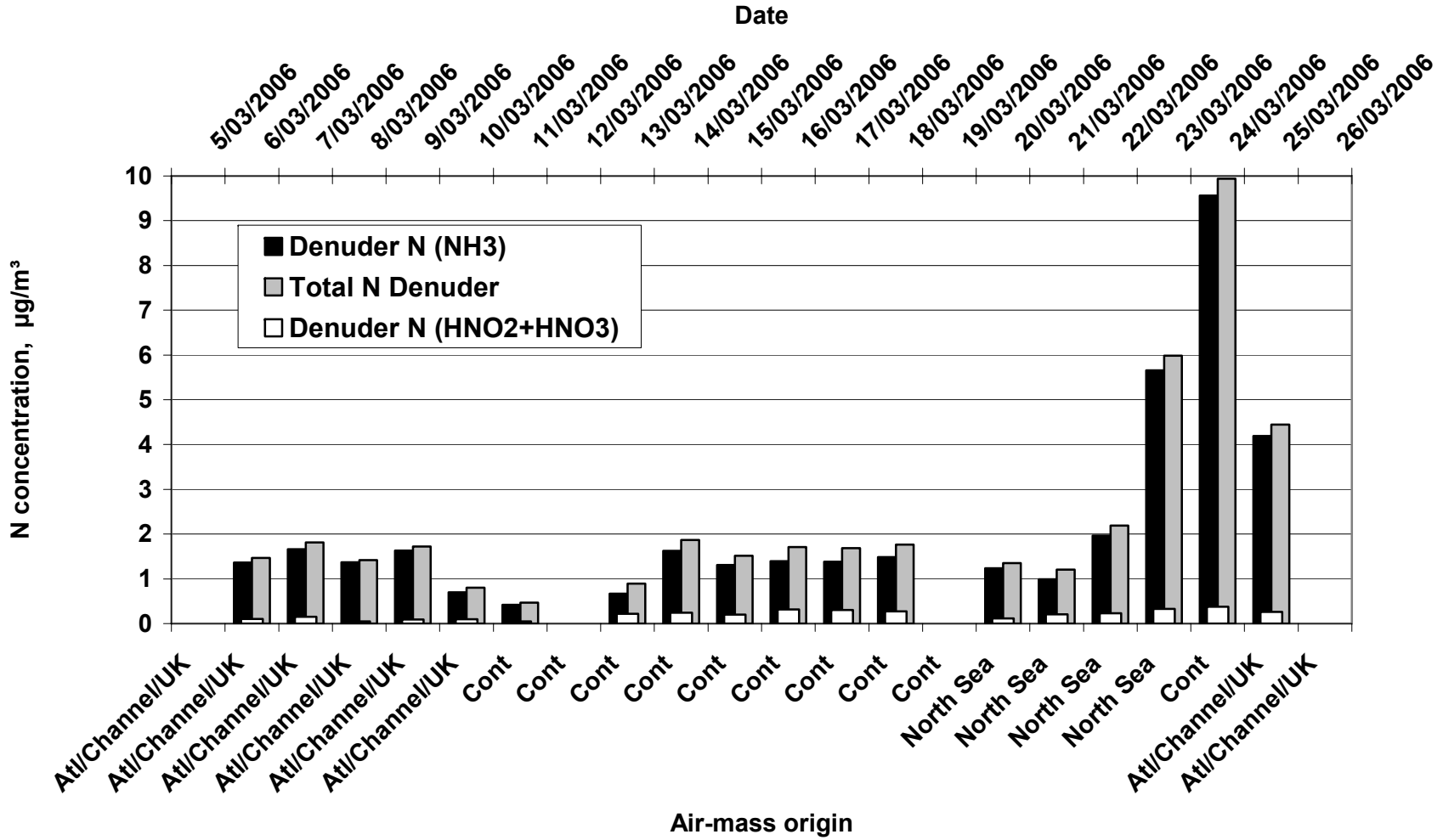

Figure 2.43 Daily variations of the concentrations of gaseous nitrogen-containing compounds during the 4th, 5th and 6th week of the 3rd campaign.

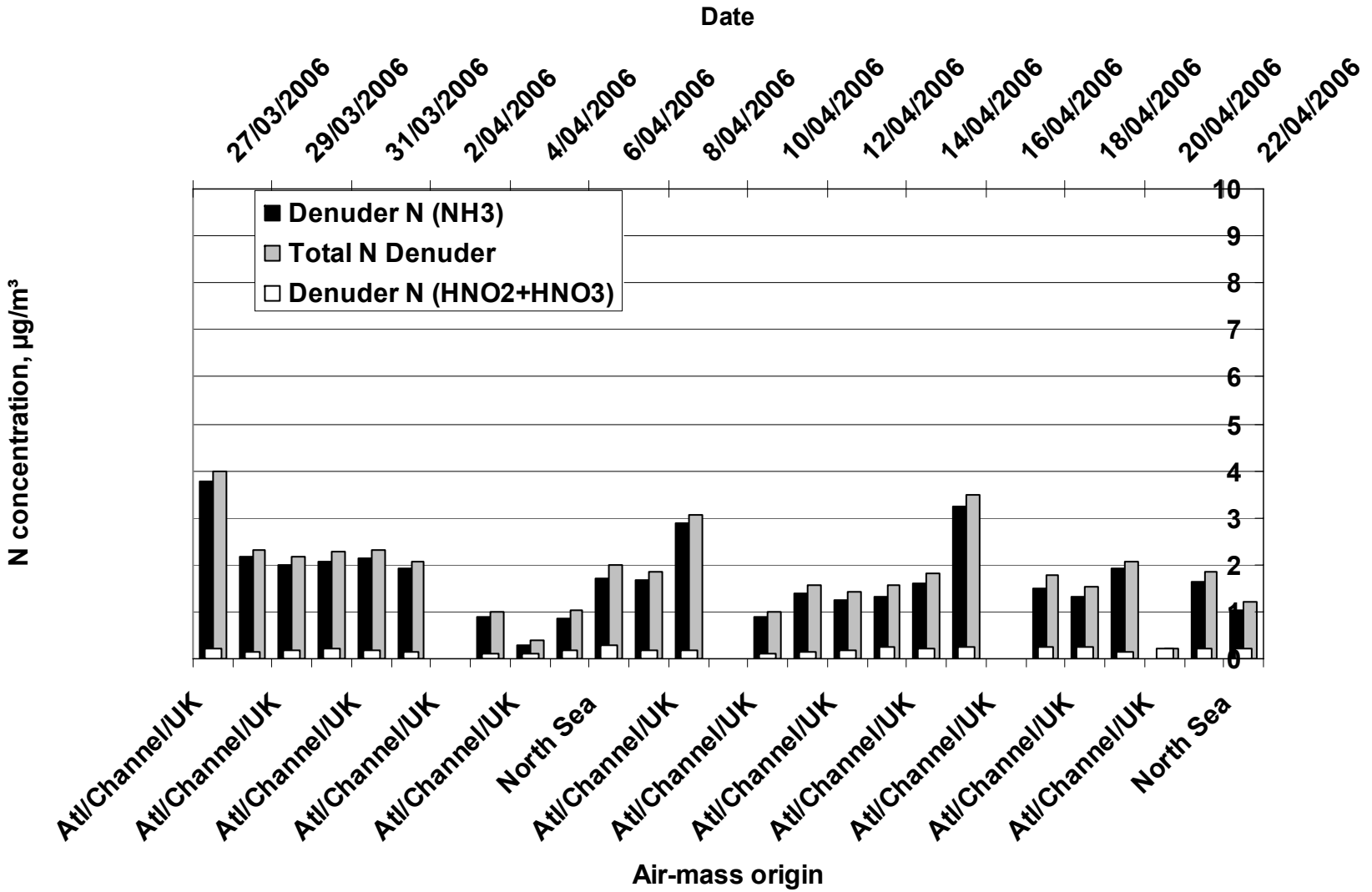

Figure 2.44 Daily variations of the concentrations of gaseous nitrogen-containing compounds during the 7th, 8th, 9th and 10th week of the 3rd campaign.

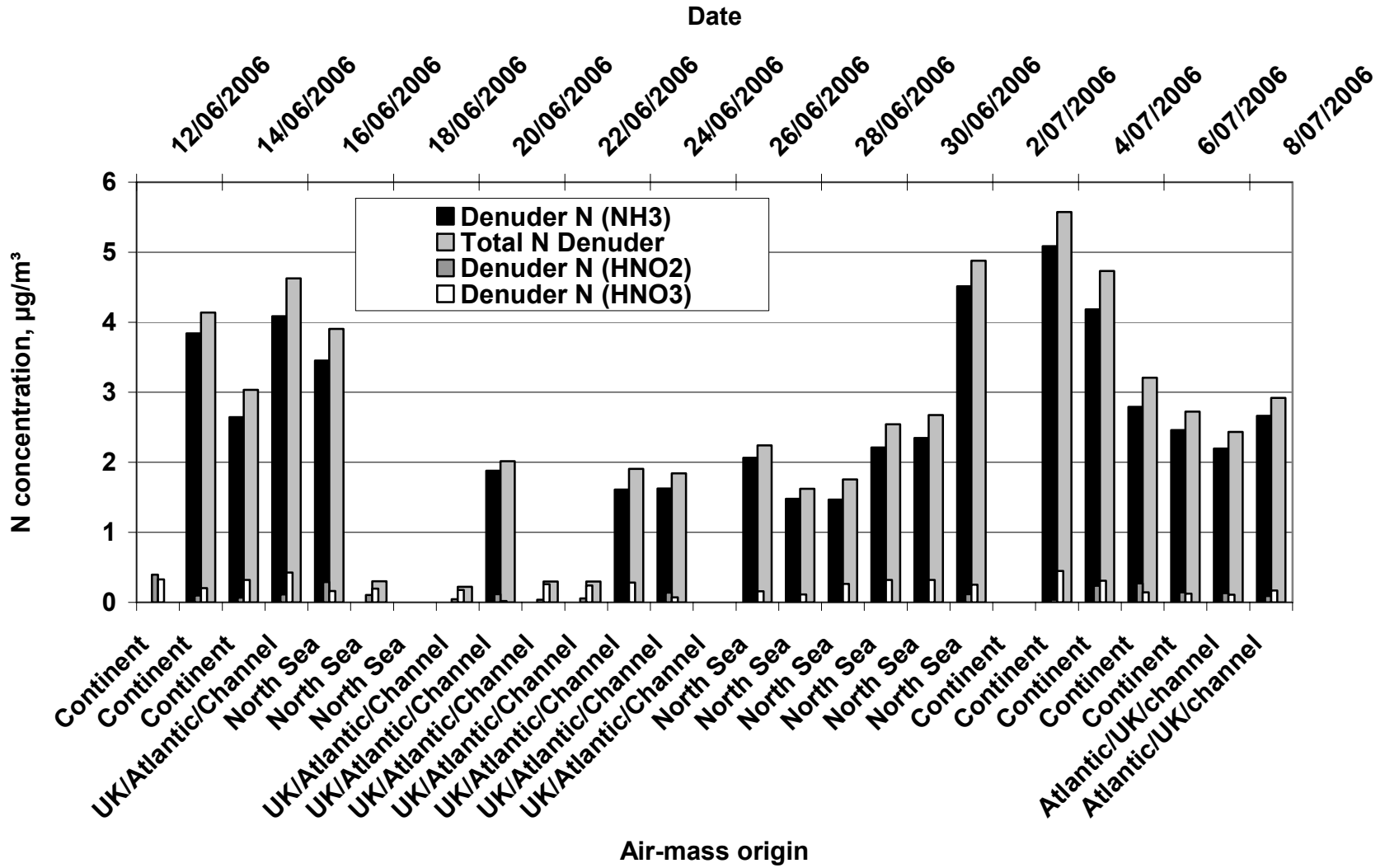

Figure 2.45 Daily variations of the concentrations of gaseous nitrogen-containing compounds during the 1st, 2nd, 3rd and 4th week of the 4th campaign.

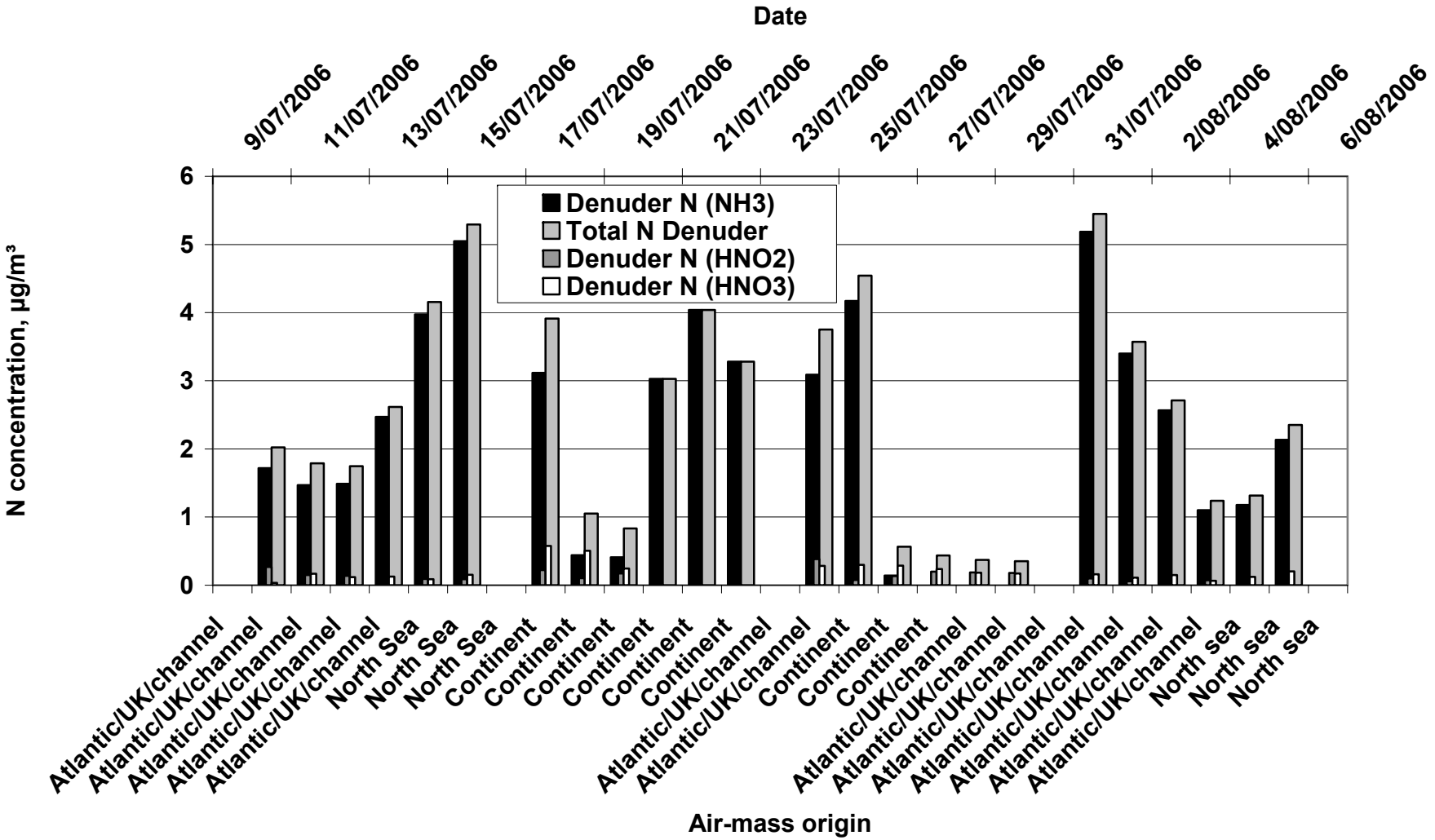

Figure 2.46 Daily variations of the concentrations of gaseous nitrogen-containing compounds during the 5th, 6th, 7th and 8th week of the 4th campaign.

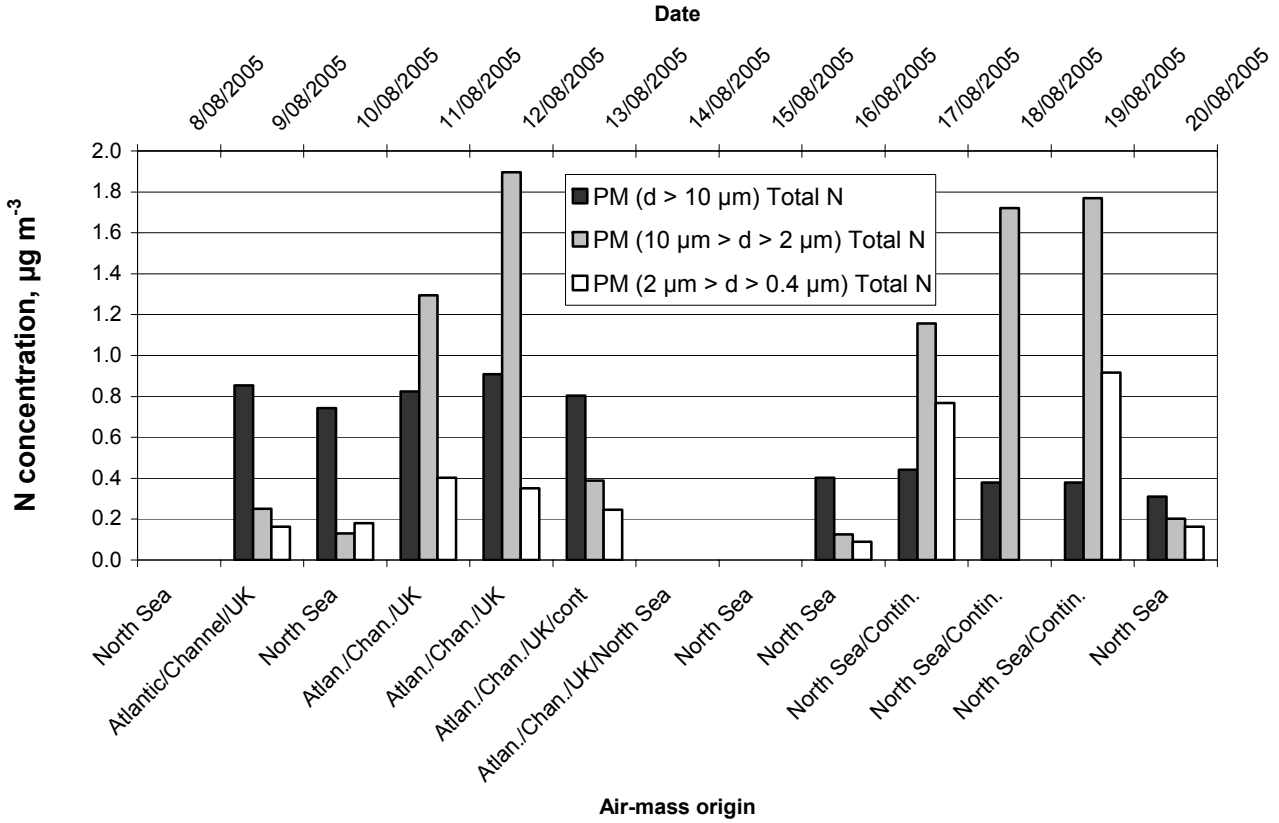

Figure 2.47 Daily variations of the concentrations of nitrogen-containing compounds in aerosols during the 2nd campaign.

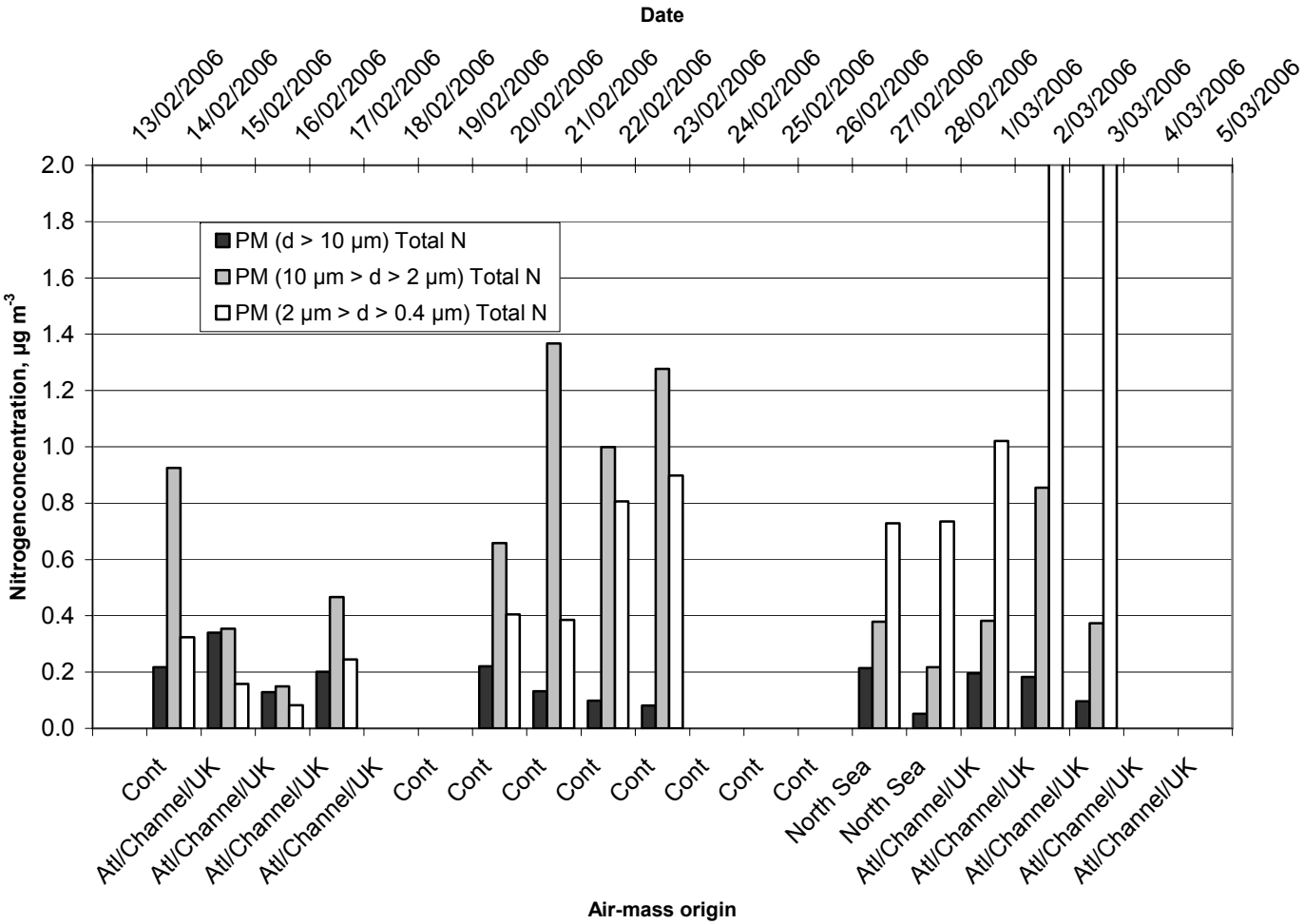

Figure 2.48 Daily variations of the concentrations of nitrogen-containing compounds in aerosols during the 1st, 2nd, and 3rd week of the 3rd campaign.

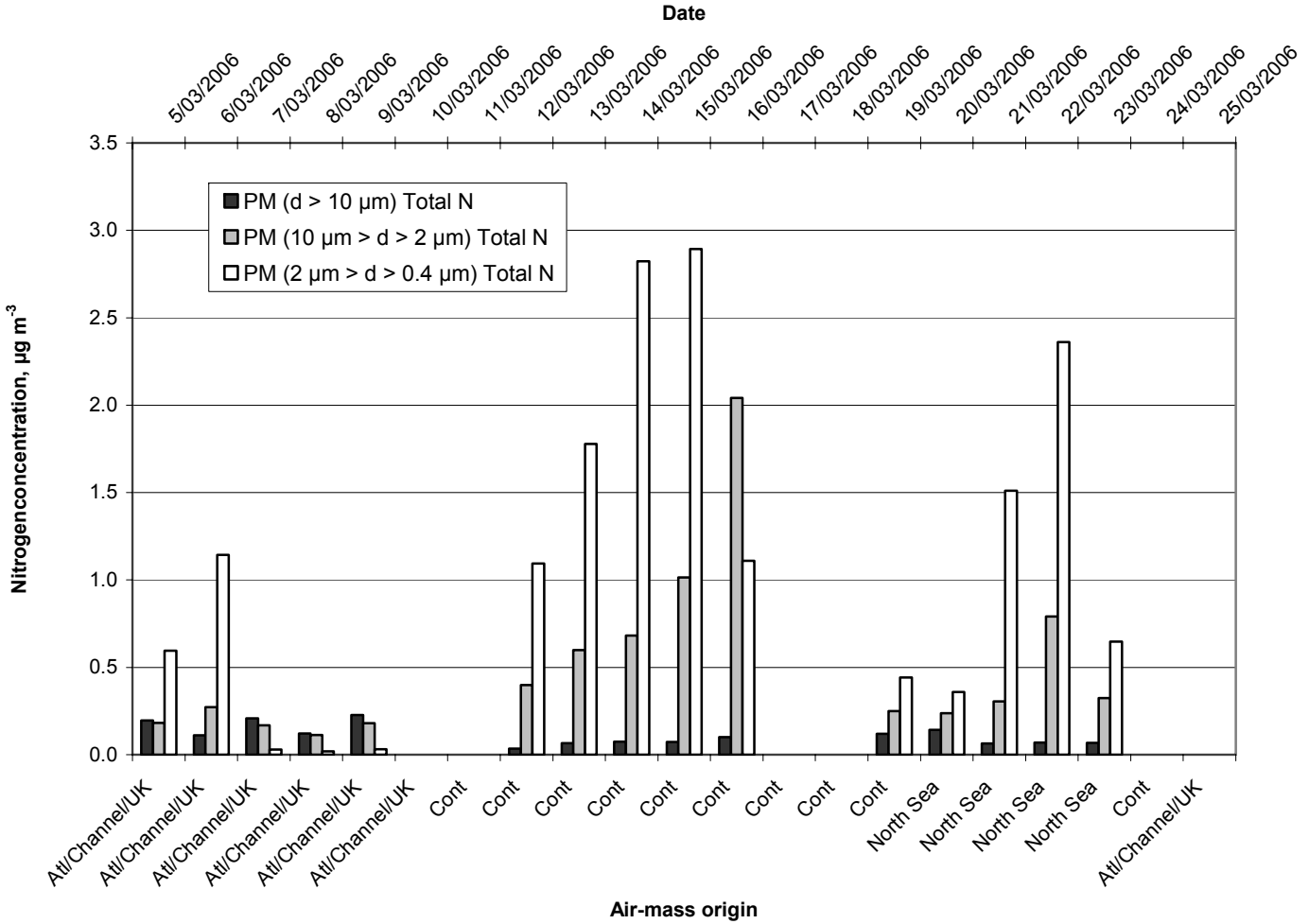

Figure 2.49 Daily variations of the concentrations of nitrogen-containing compounds in aerosols during the 4th, 5th and 6th week of the 3rd campaign.

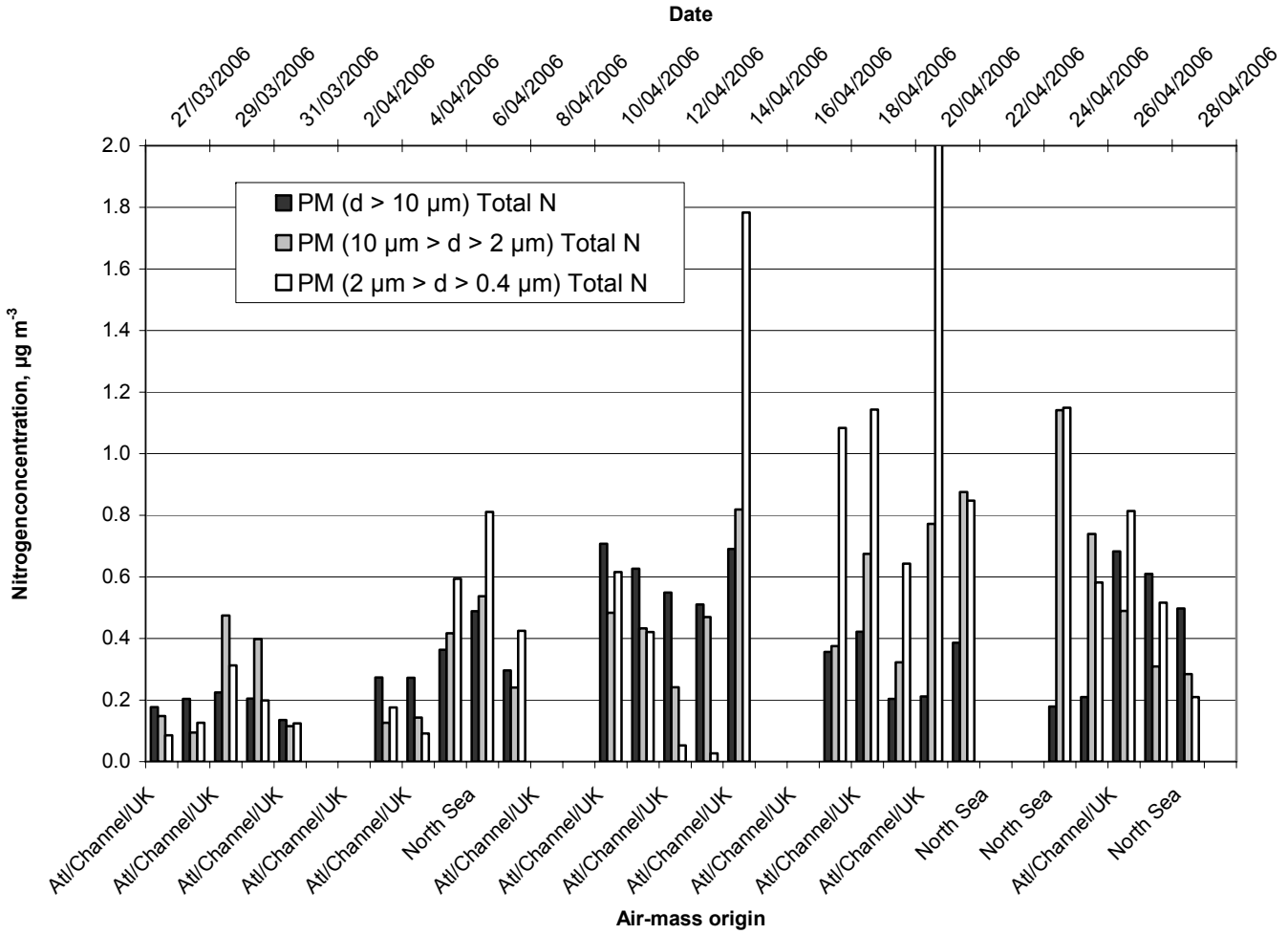

Figure 2.50 Daily variations of the concentrations of nitrogen-containing compounds in aerosols during the 7th, 8th, 9th, 10th and 11th week of the 3rd campaign.

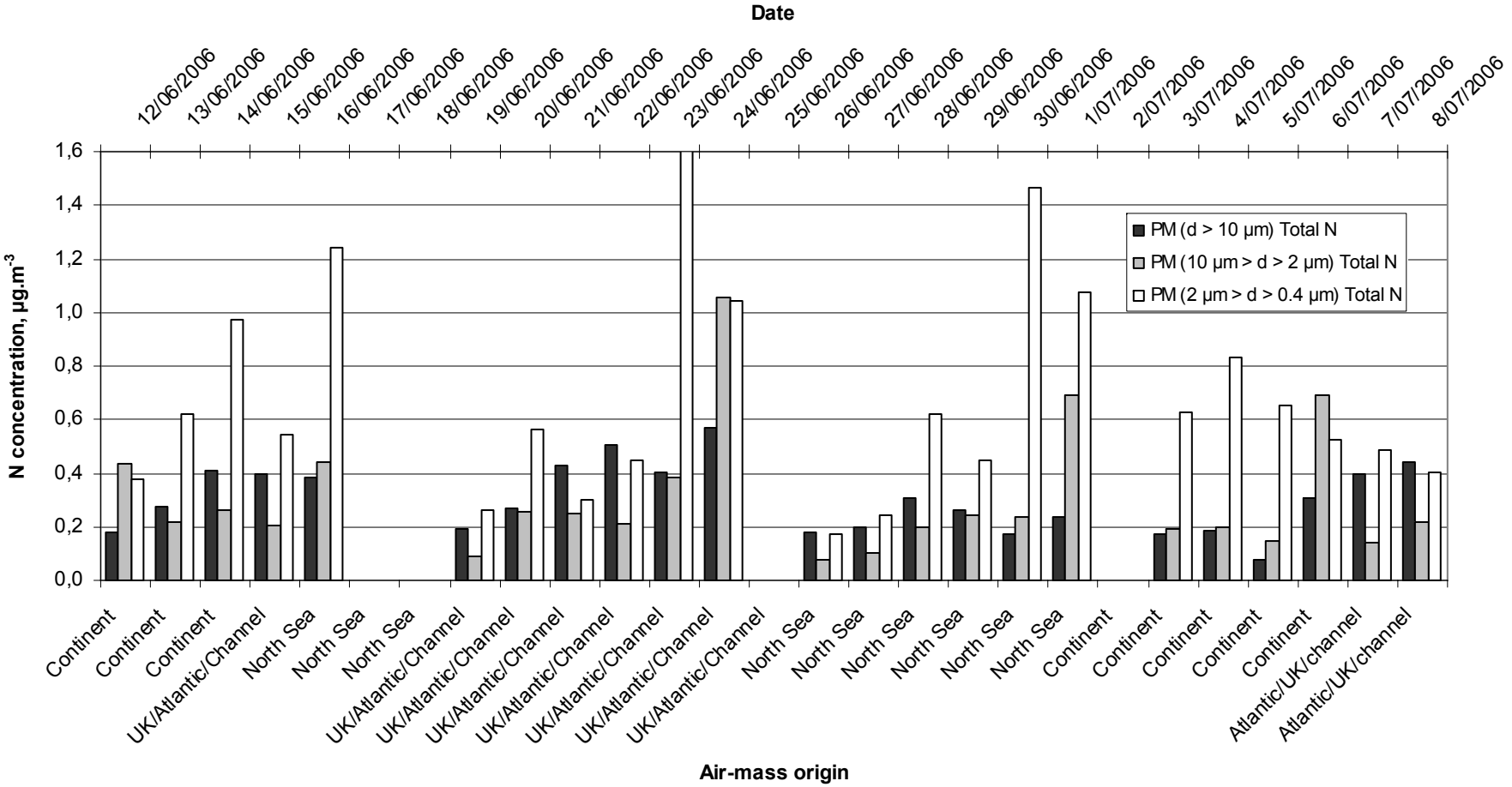

Figure 2.51 Daily variations of the concentrations of nitrogen-containing compounds in aerosols during the 1st, 2nd, 3rd, and 4th week of the 4th campaign.

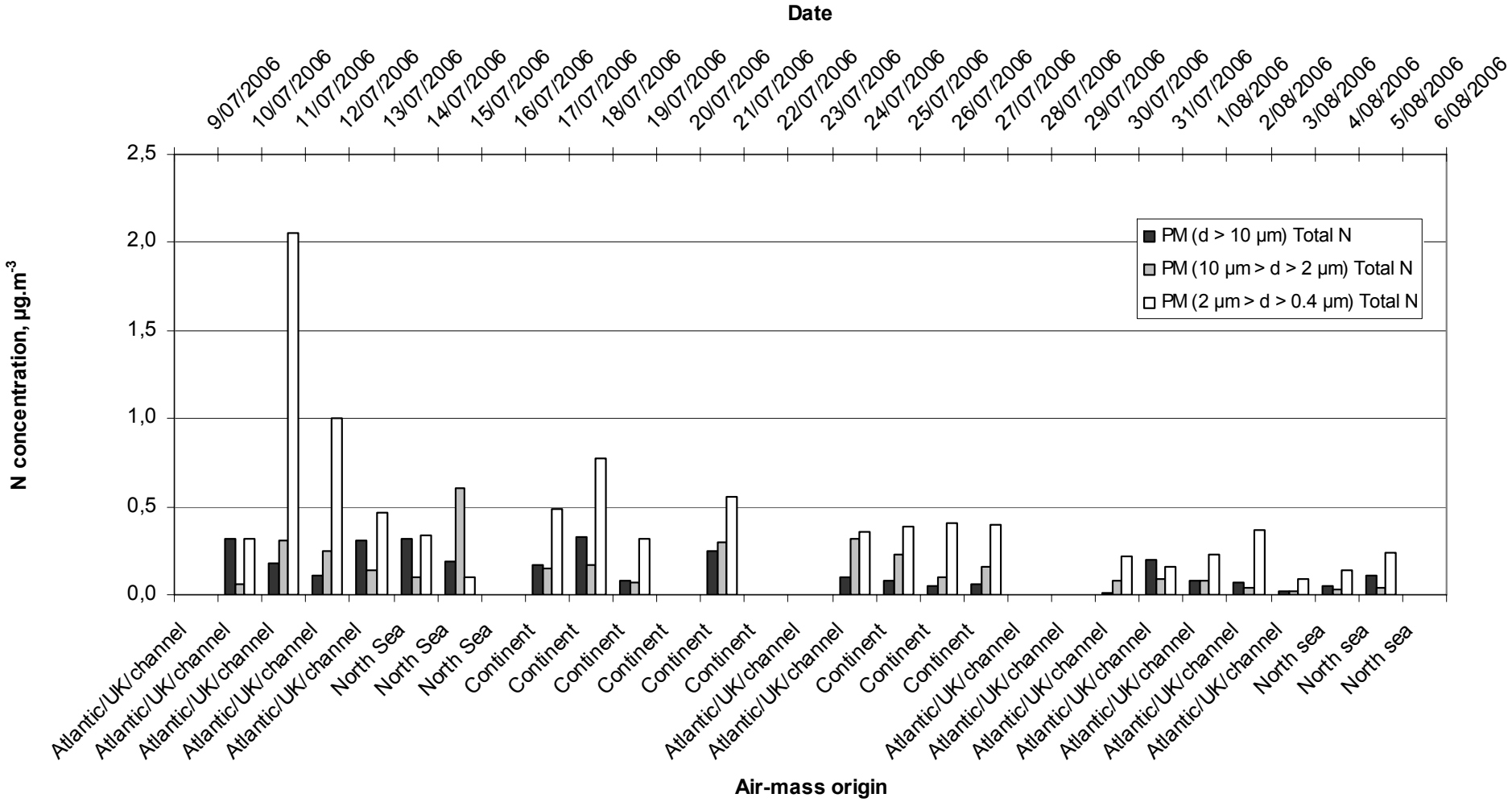

Figure 2.52 Daily variations of the concentrations of nitrogen-containing compounds in aerosols during the 5th, 6th, 7th, and 8th week of the 4th campaign.

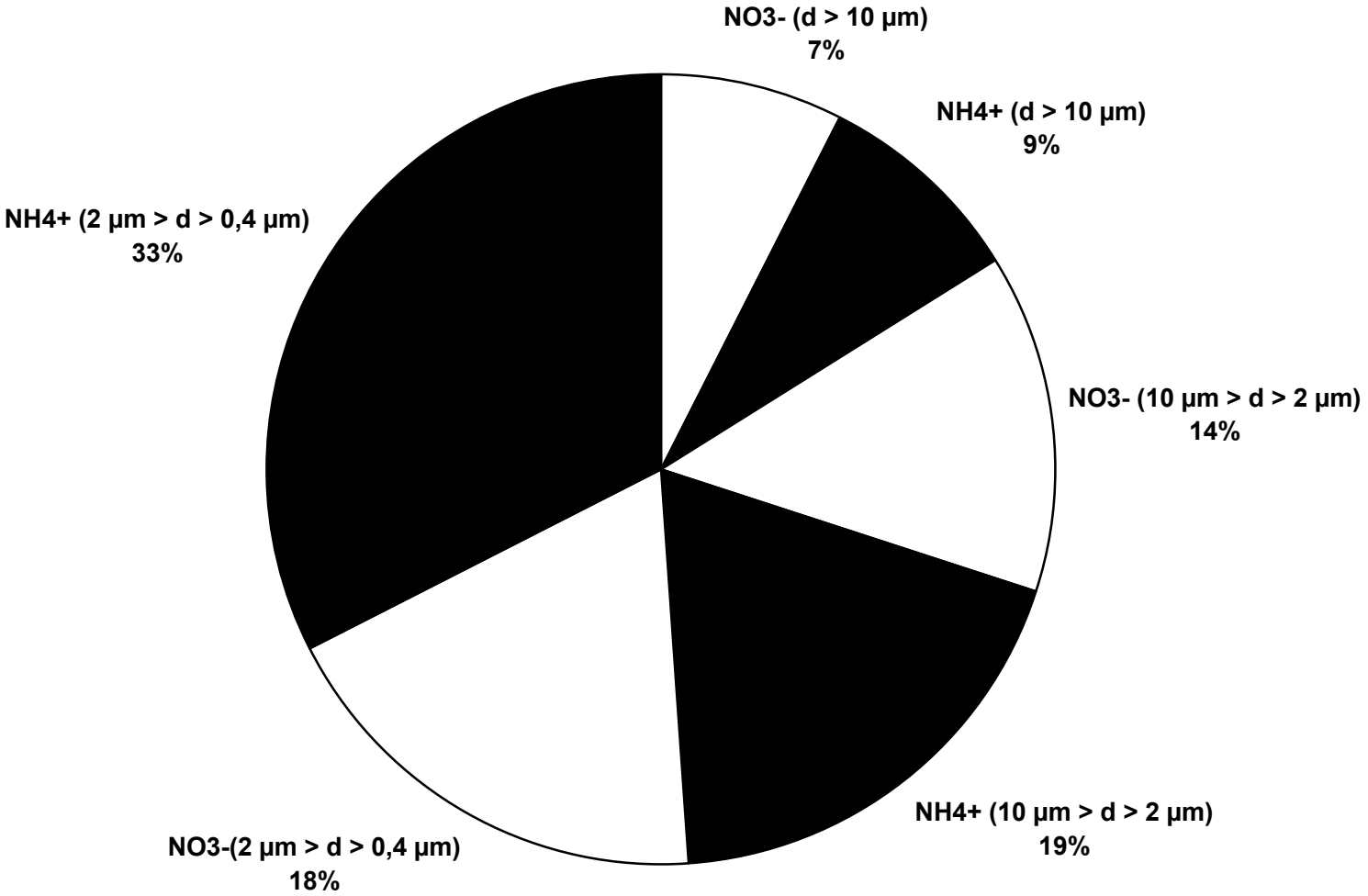

Figure 2.53 Relative contribution of the size-fractions (d > 10 µm, 10 µm > d > 2 µm, and 2 µm > d > 0.4 µm) to the total level of particulate N for the 3rd campaign.

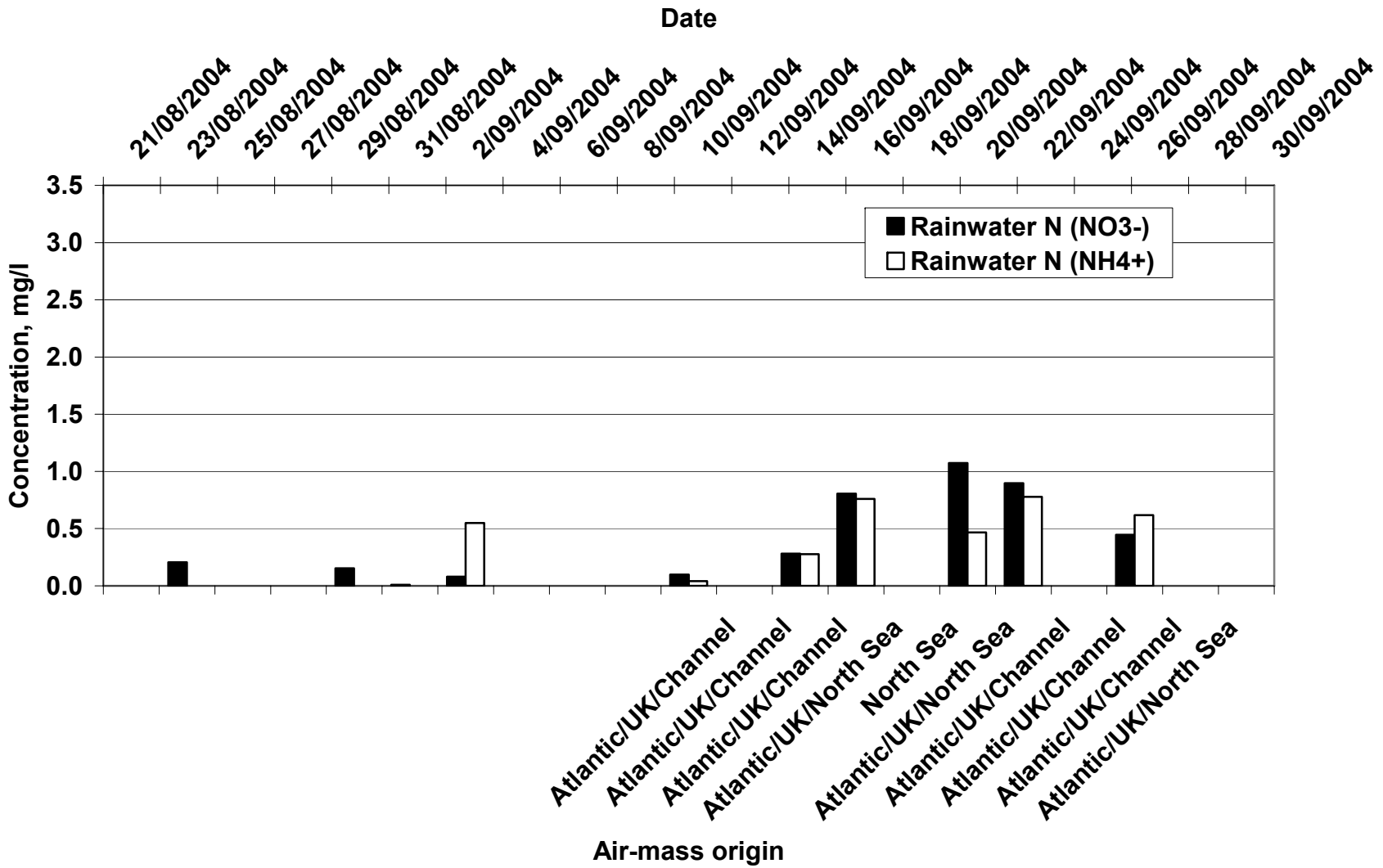

Figure 2.54 Daily variations of the concentrations of nitrogen-containing compounds in rainwater during 1st, 2nd, and 3rd week of the 1st campaign.

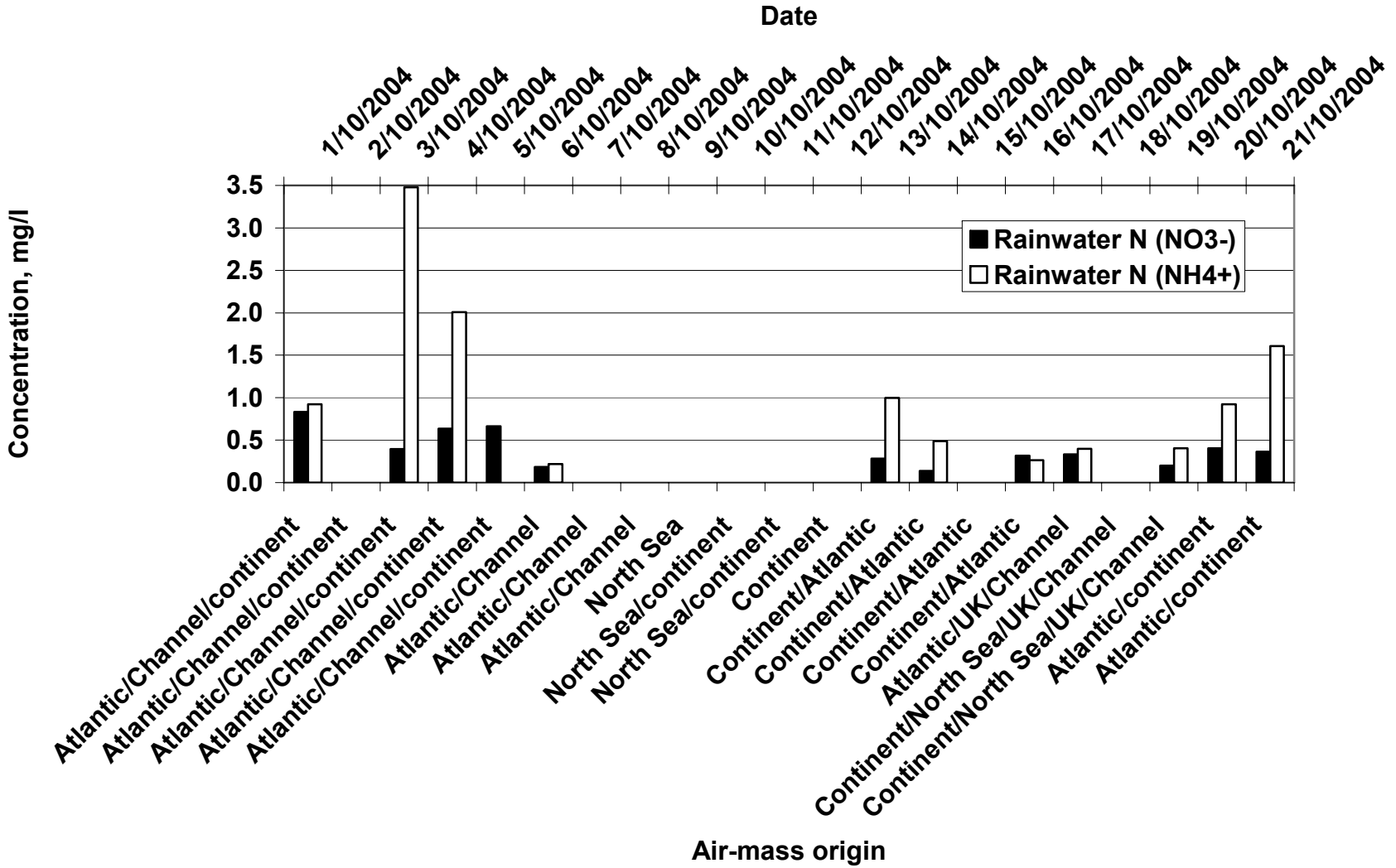

Figure 2.55 Daily variations of the concentrations of nitrogen-containing compounds in rainwater during 4th, 5th, and 6th week of the 1st campaign.

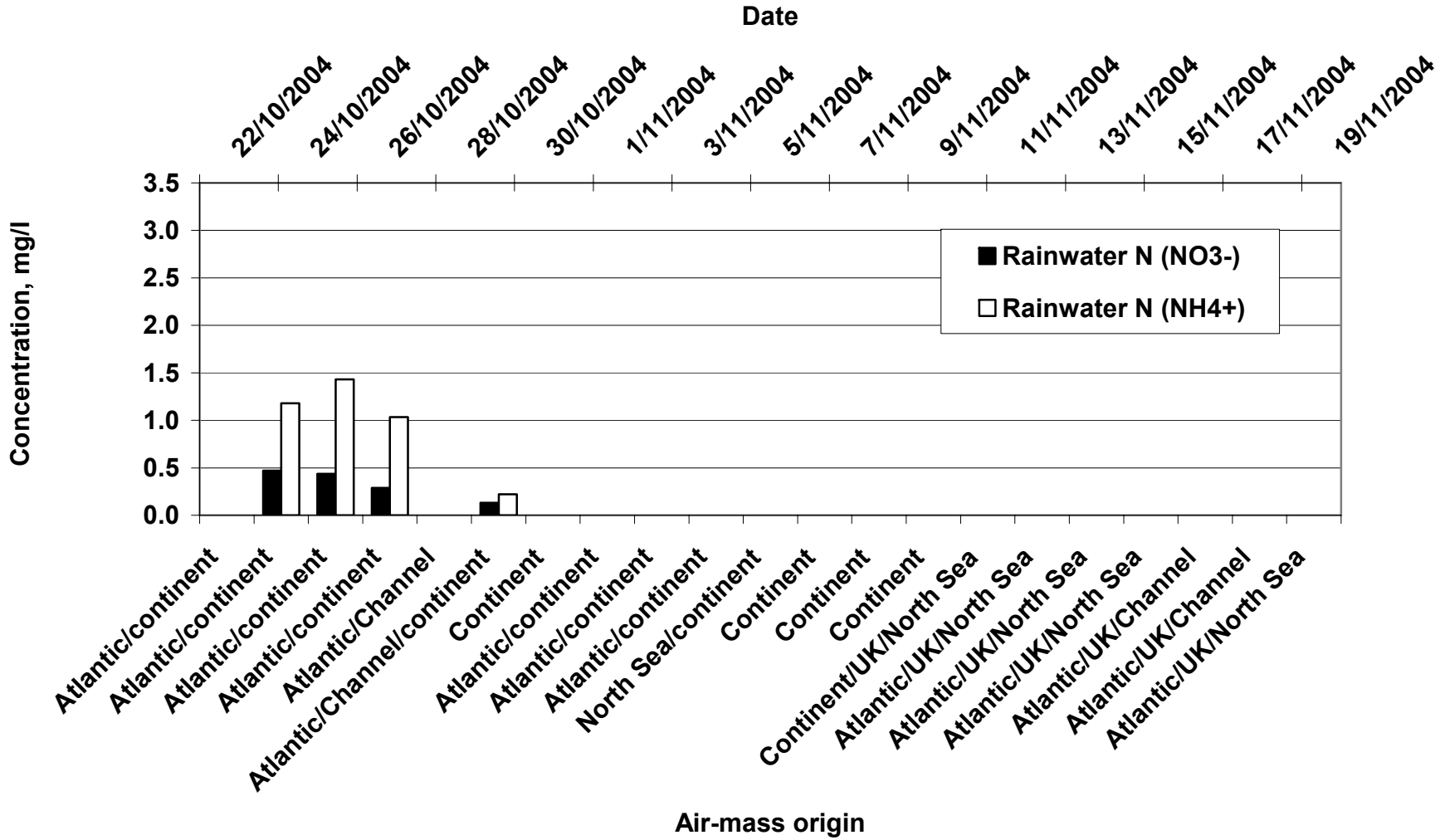

Figure 2.56 Daily variations of the concentrations of nitrogen-containing compounds in rainwater during 7th, 8th, and 9th week of the 1st campaign.

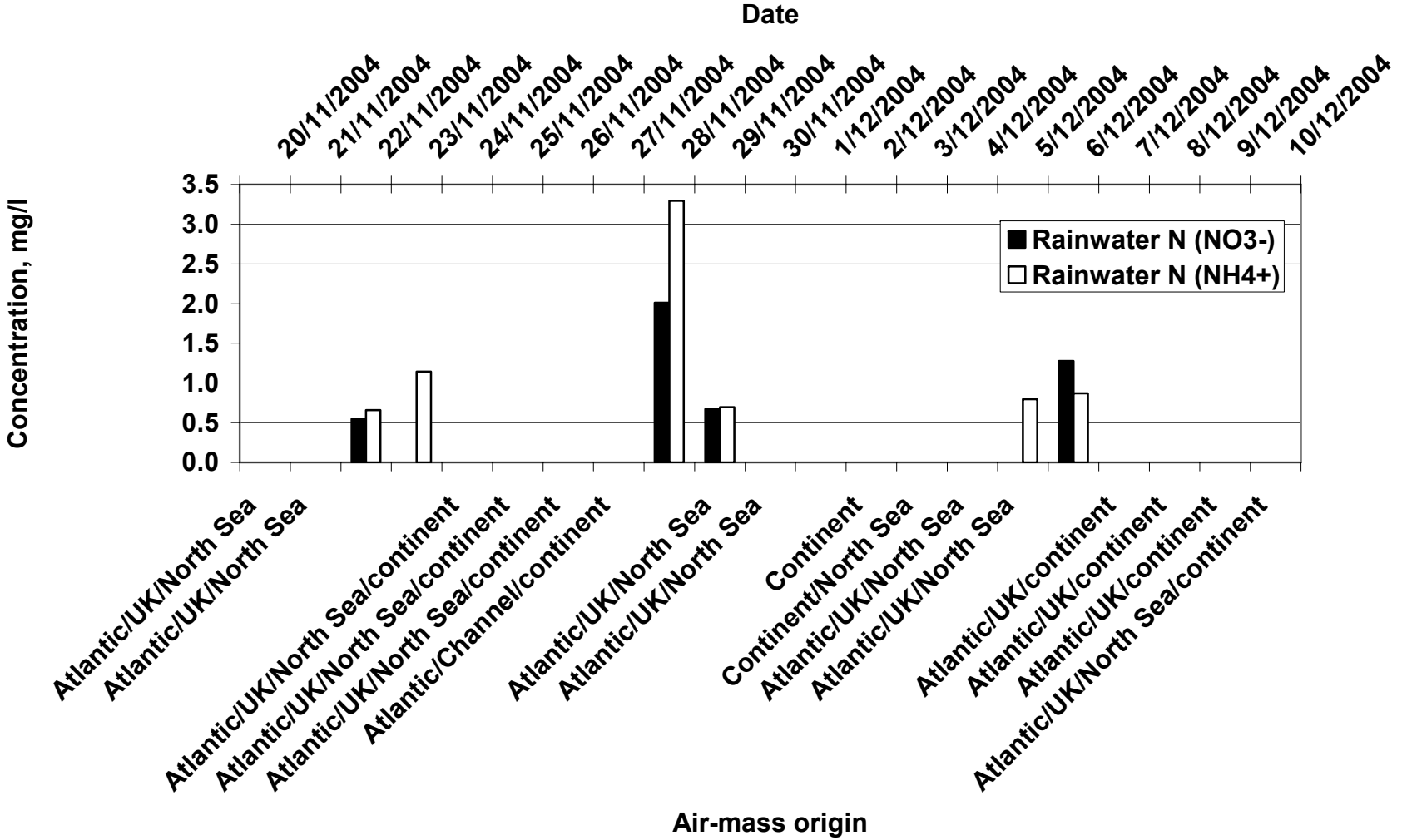

Figure 2.57 Daily variations of the concentrations of nitrogen-containing compounds in rainwater during 10th, 11th, and 12th week of the 1st campaign.

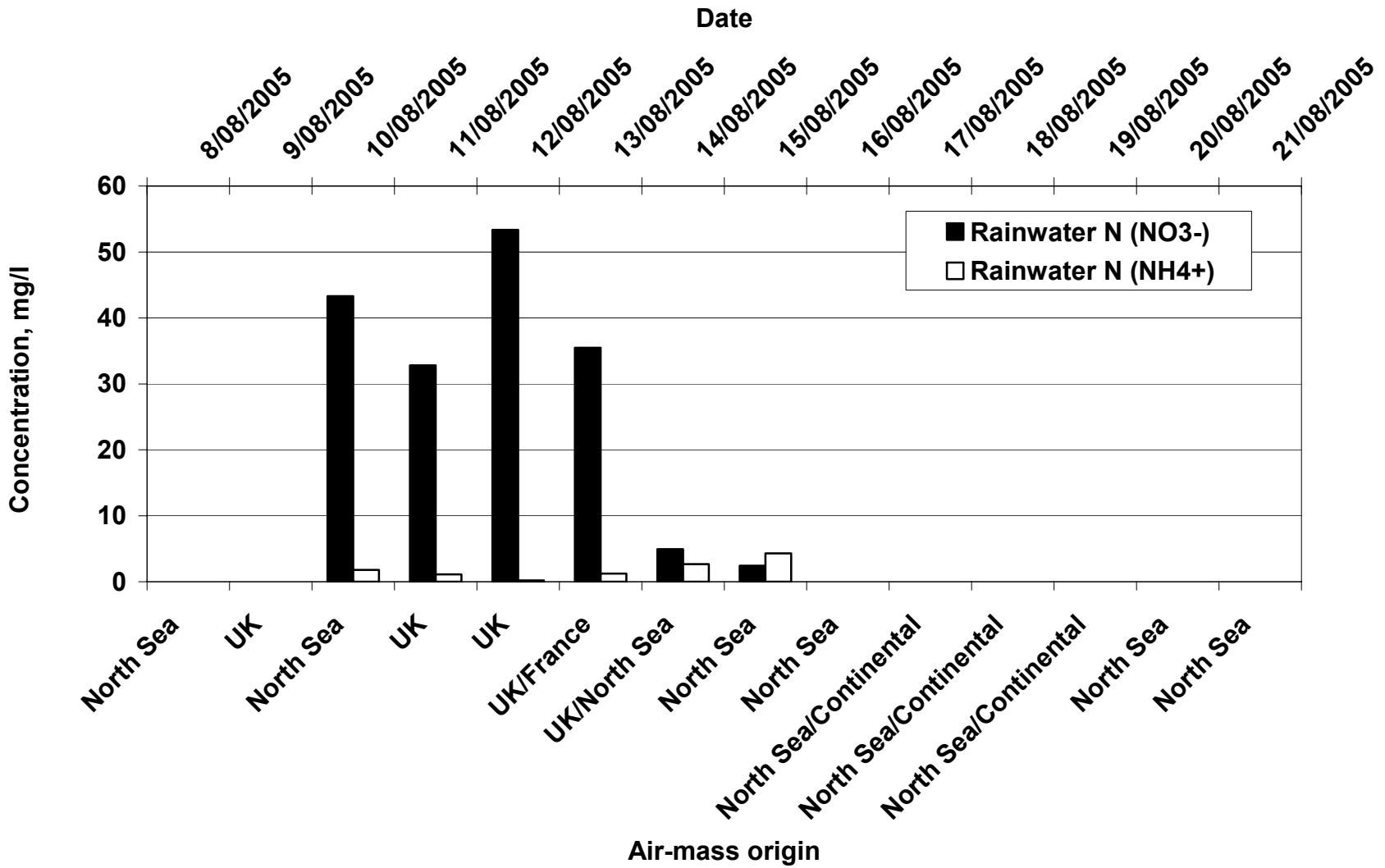

Figure 2.58 Daily variations of the concentrations of nitrogen-containing compounds in rainwater during 1st, 2nd, and 3rd week of the 2nd campaign.

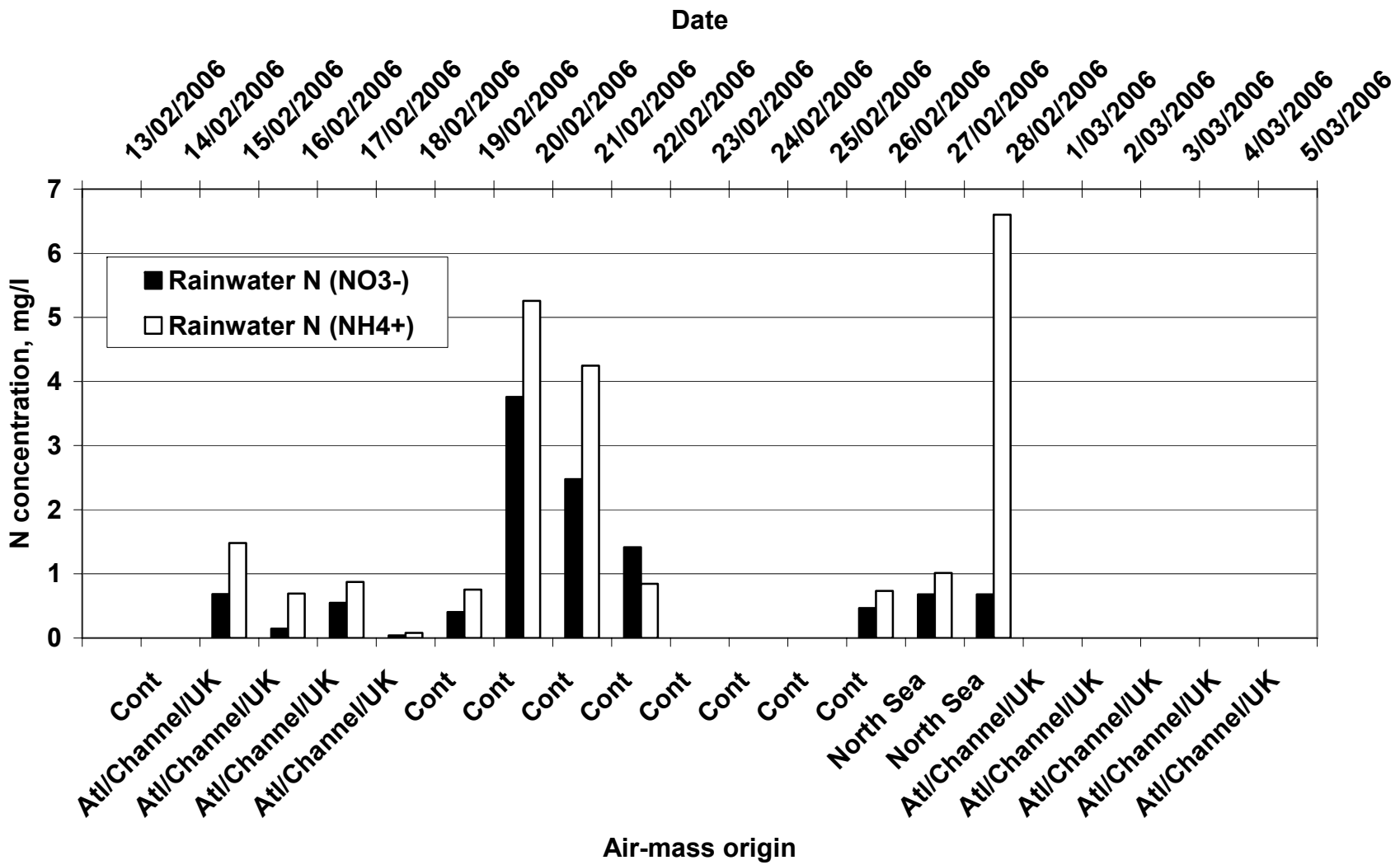

Figure 2.59 Daily variations of the concentrations of nitrogen-containing compounds in rainwater during 1st, 2nd, and 3rd week of the 3rd campaign.

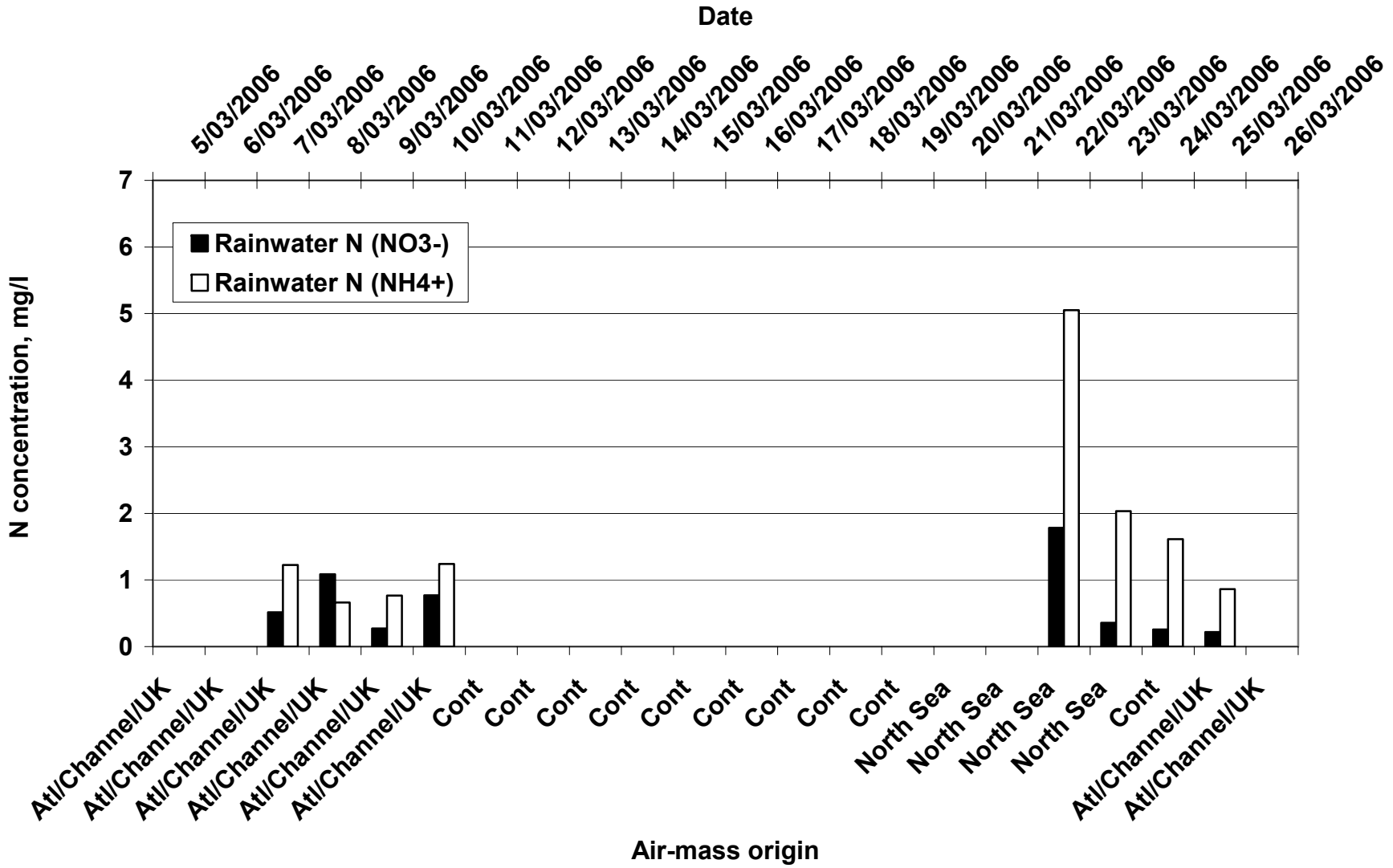

Figure 2.60 Daily variations of the concentrations of nitrogen-containing compounds in rainwater during 4th, 5th, and 6th week of the 3rd campaign.

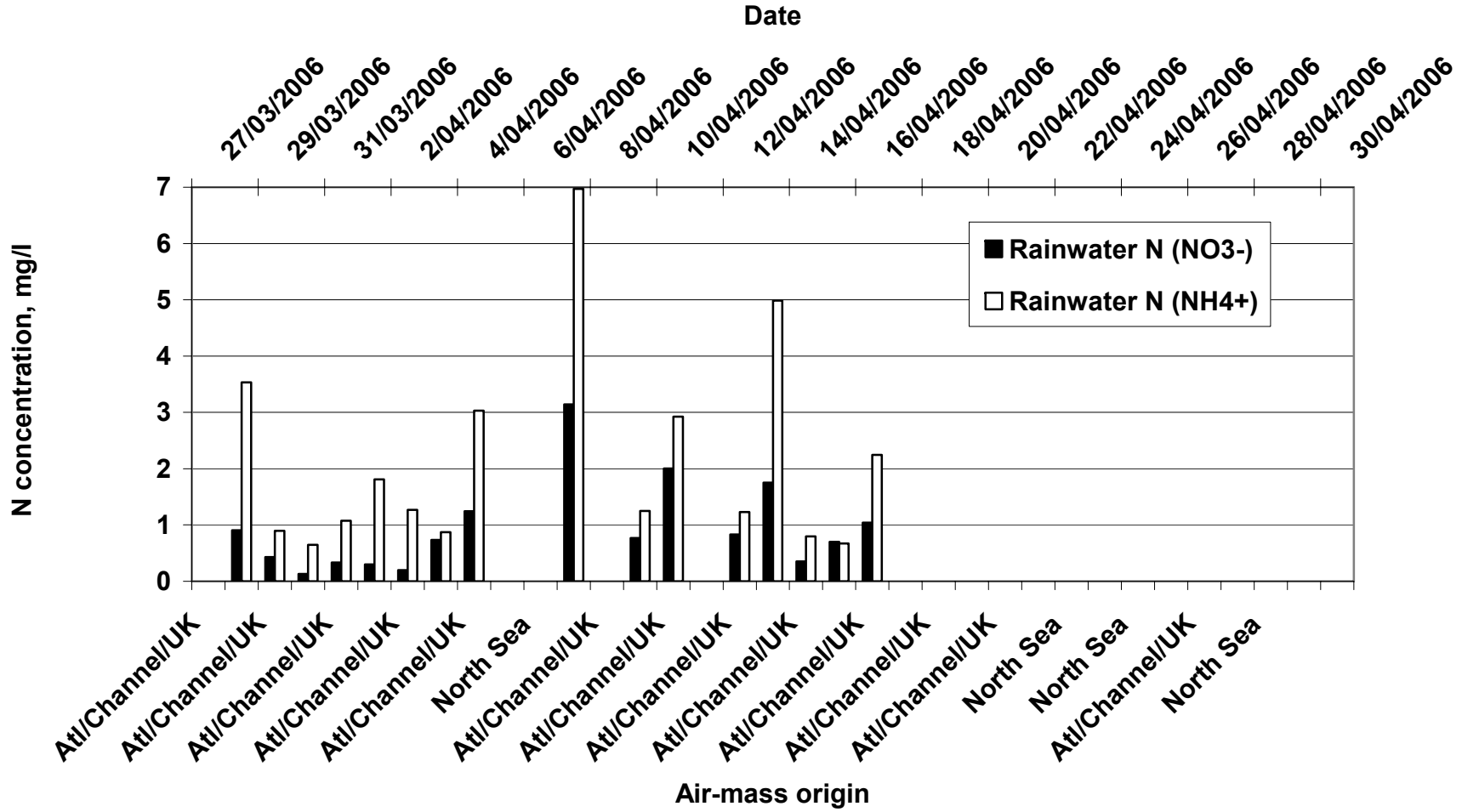

Figure 2.61 Daily variations of the concentrations of nitrogen-containing compounds in rainwater during 7th, 8th, 9th, 10th, and 11th week of the 3rd campaign.

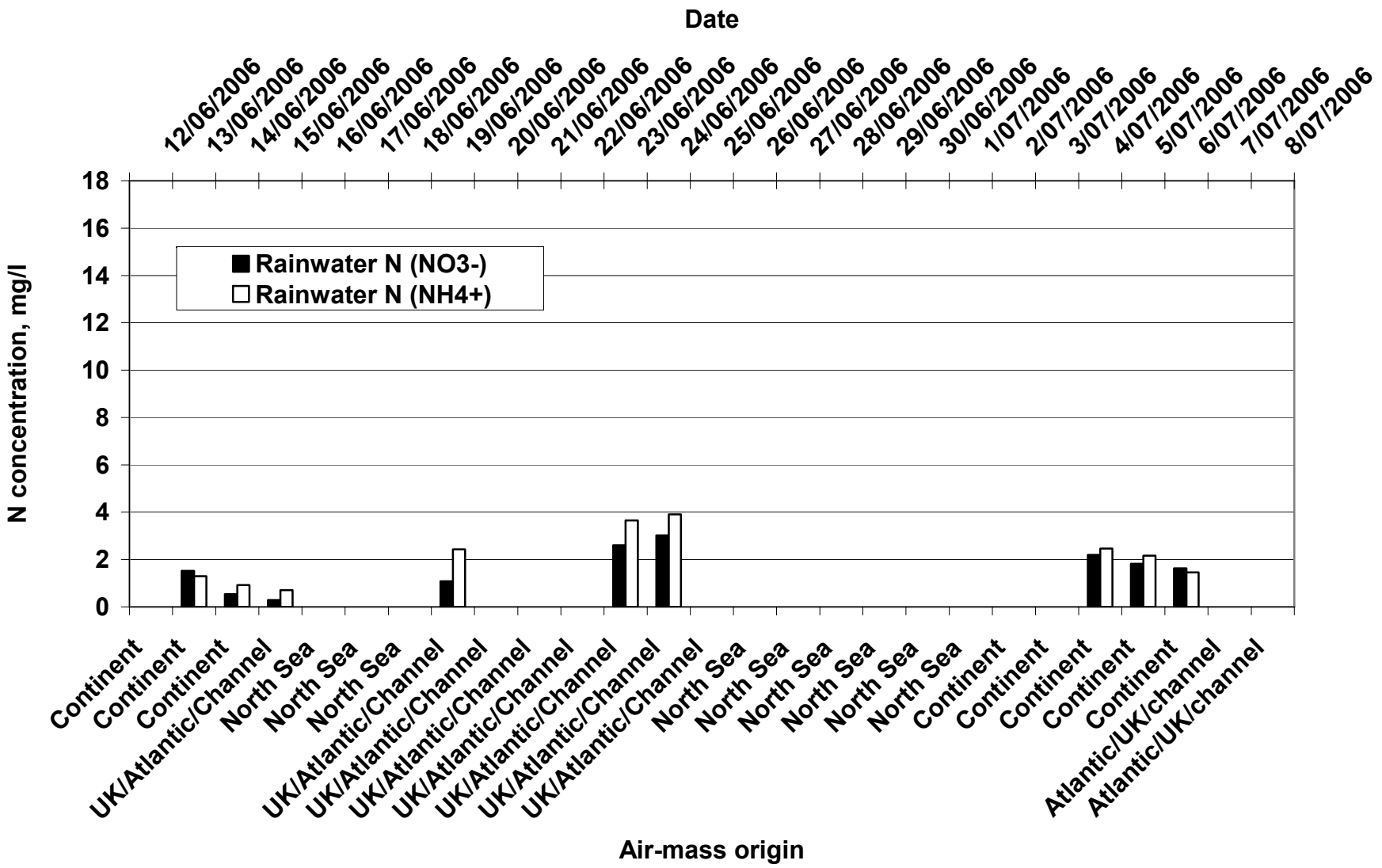

Figure 2.62 Daily variations of the concentrations of nitrogen-containing compounds in rainwater during 1st, 2nd, 3rd, and 4th week of the 4th campaign.

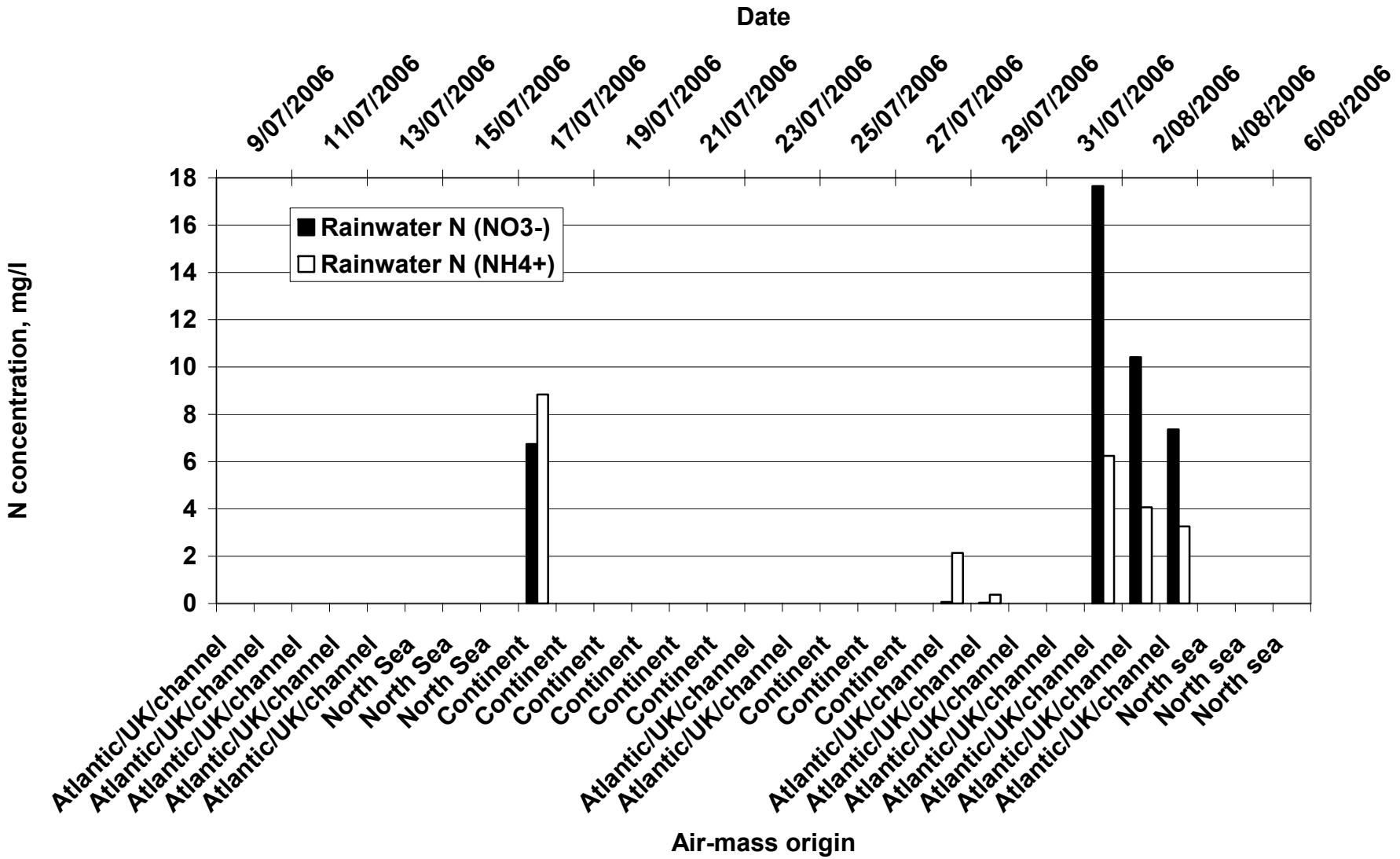

Figure 2.63 Daily variations of the concentrations of nitrogen-containing compounds in rainwater during 5th, 6th, 7th, and 8th week of the 4th campaign.

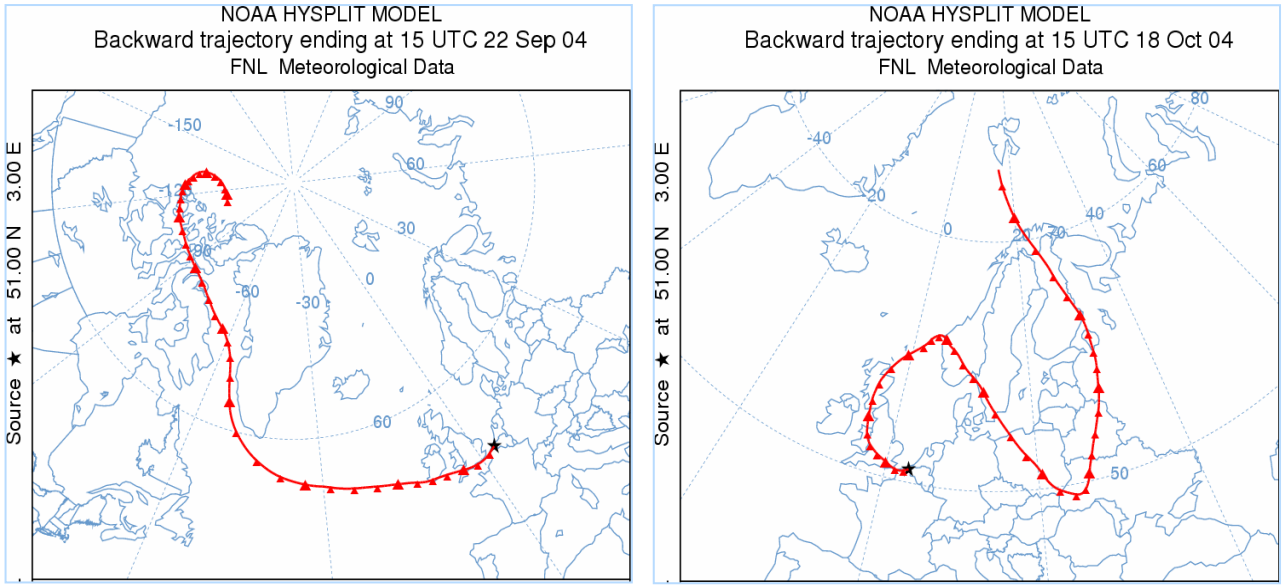

Figure 2.64. Air mass backward trajectories for different sampling days: (a) September 22 2004; (b) October 18 2004.

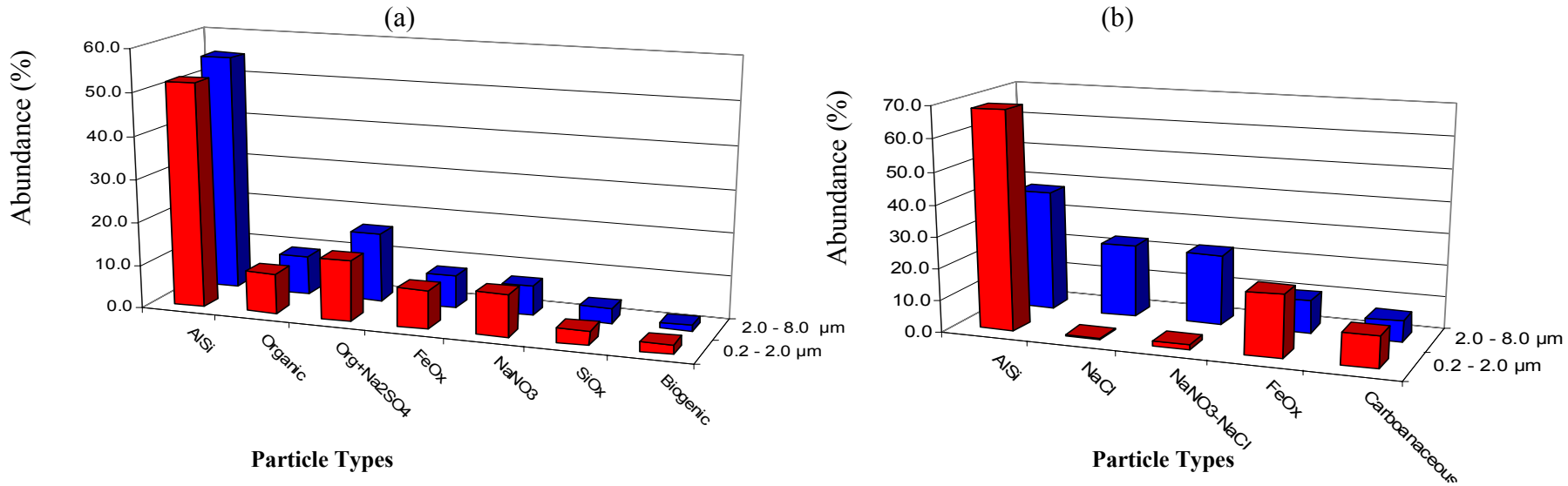

Figs. 2.65. EPMA results

Appendix 3

Organic Nutrient detection Tables and Figures

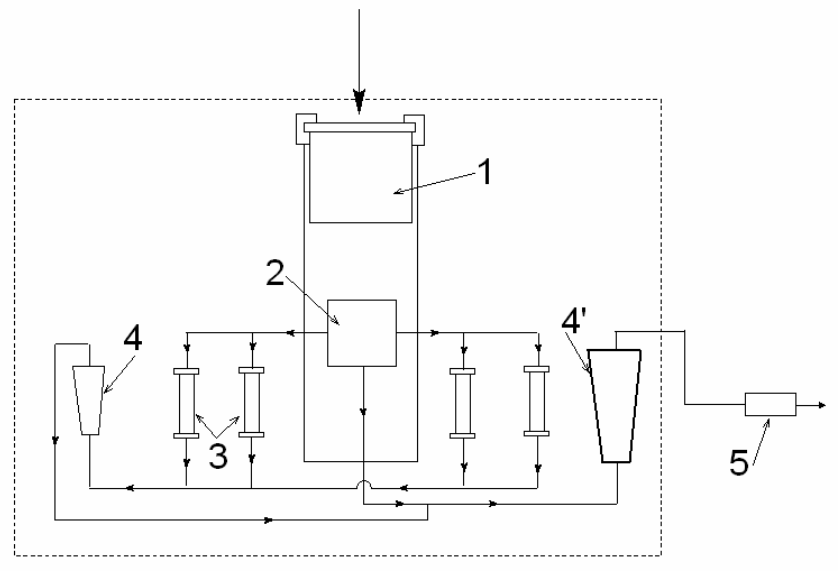

Figure 3.1 Scheme of sampler: 1 - adsorption trap, 2 - valve, 3 – traps for low volume air sampling, 4 and 4’ - rotameters, 5 - pump

(a) the sheltered inlet of the sampler

(b) overall view of the sampler
Figure 3.2 Photography of the sampler
Table 3.1 The nomenclature of alkyl nitrates and the corresponding halides used for synthesis and yields of the synthesis reactions

Alkyl nitrate		Yield (%)
Methyl*	1 C1	98
Ethyl	1 C2	96
1-Propyl	1 C3	97
1-Butyl	1 C4	96
2-Butyl*	2 C4	98
1-Pentyl	1 C5	96
2-Pentyl	2 C5	92
3-Pentyl	3 C5	96
1-Hexyl	1 C6	95
1-Heptyl	1 C7	98
1-Octyl	1 C8	99
1-Nonyl	1 C9	97

* - synthesized from RI; all the others from RBr

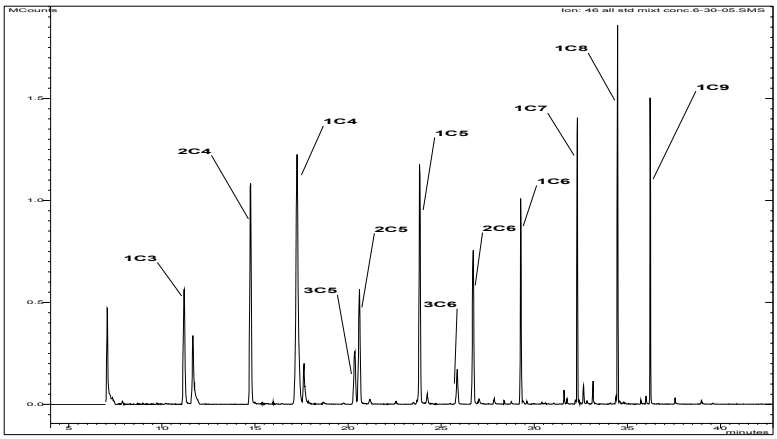

Figure 3.3a Mass chromatograms (m/z=46) for reference mixture

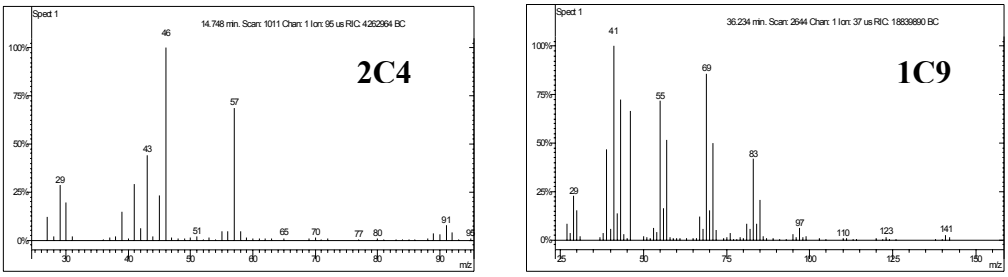

Figure 3.3b Mass spectrum for 2C4 and 1C9

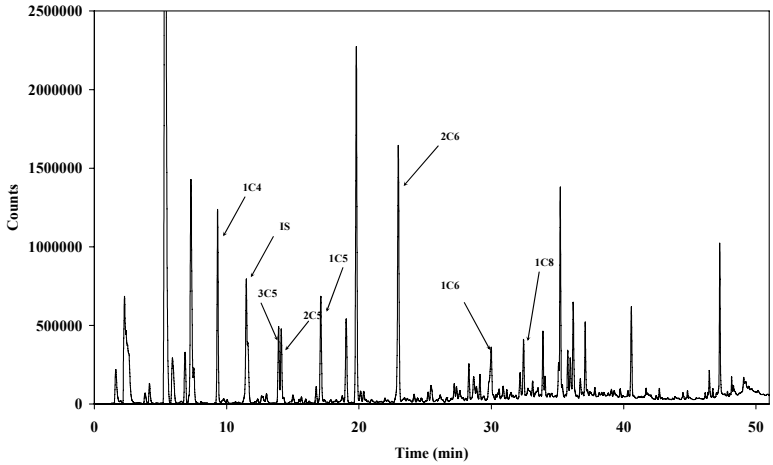

Figure 3.3c GC-ECD chromatogram for ambient sample

Table 3.2 Optimized temperature programs used for GC-MS and GC-ECD analysis of alkyl nitrates

		Temperature (^{o}C)	Rate (^{o}C min^{-1})	Hold (min)	Total time (min)
Column Oven	GC-MS	40		5.8	51
		51	3	2	
		75	5	3.5	
		96	5	2.5	
		260	10	8.13	
	GC-ECD	40		2	51
		100	3	1	
		180	5	1	
		260	10	3	

Table 3.3 Elution order and retention time (min) of alkyl nitrates on VF-1ms capillary column in GC-MS

Alkyl nitrate		Retention Time (min)
1-Propyl	1 C3	10.274
2-Butyl*	2 C4	13.932
1-Butyl	1 C4	16.393
3-Pentyl	3 C5	19.248
2-Pentyl	2 C5	19.500
1-Pentyl	1 C5	22.922
2-Hexyl	2 C6	25.617
1-Hexyl	1 C6	28.551
1-Heptyl	1 C7	31.766
1-Octyl	1 C8	33.973
1-Nonyl	1 C9	35.747

Table 3.4 Analytical performance characteristics

	GC-MS	GC-ECD
Detection limit (pg injected)	25-40	3-5
Detection limit (pg m^{-3})	15-24	1.8-3
Precision (%), n=5 (0.5 μg mL^{-1})	2-6	3-7.5
Dynamic linear range (μg mL^{-1})	0.25-7.5	0.03-0.6
R^2 for linear range	0.997-0.999	0.997-0.998

(a)

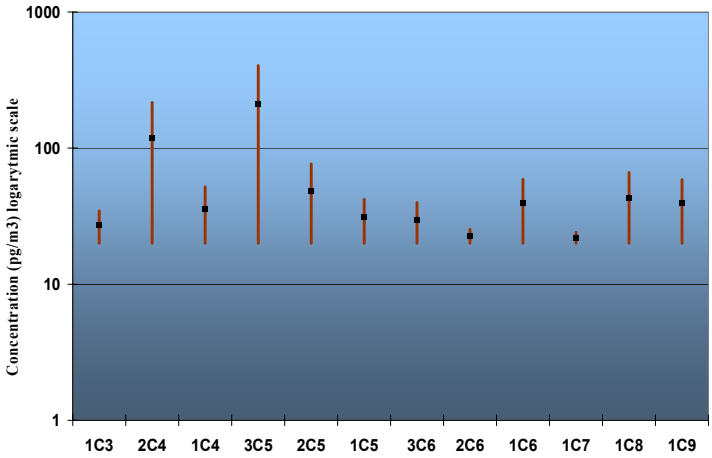

(b)

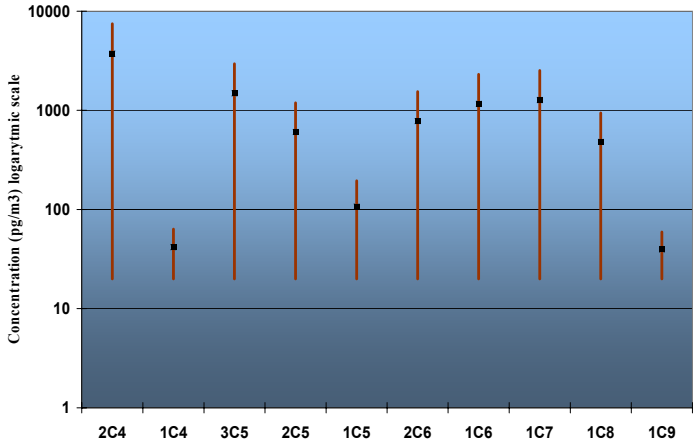

(c)

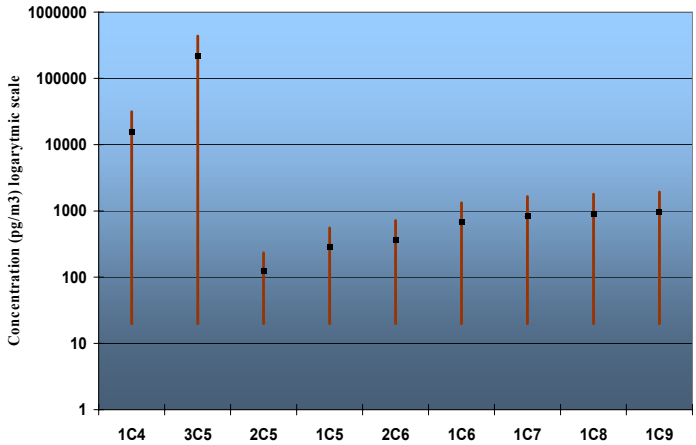

Figure 3.4 Distribution of ANs levels in summer 2005 samples (a), winter/spring 2006 (b), and summer 2006 (c) (range and middle of the range)

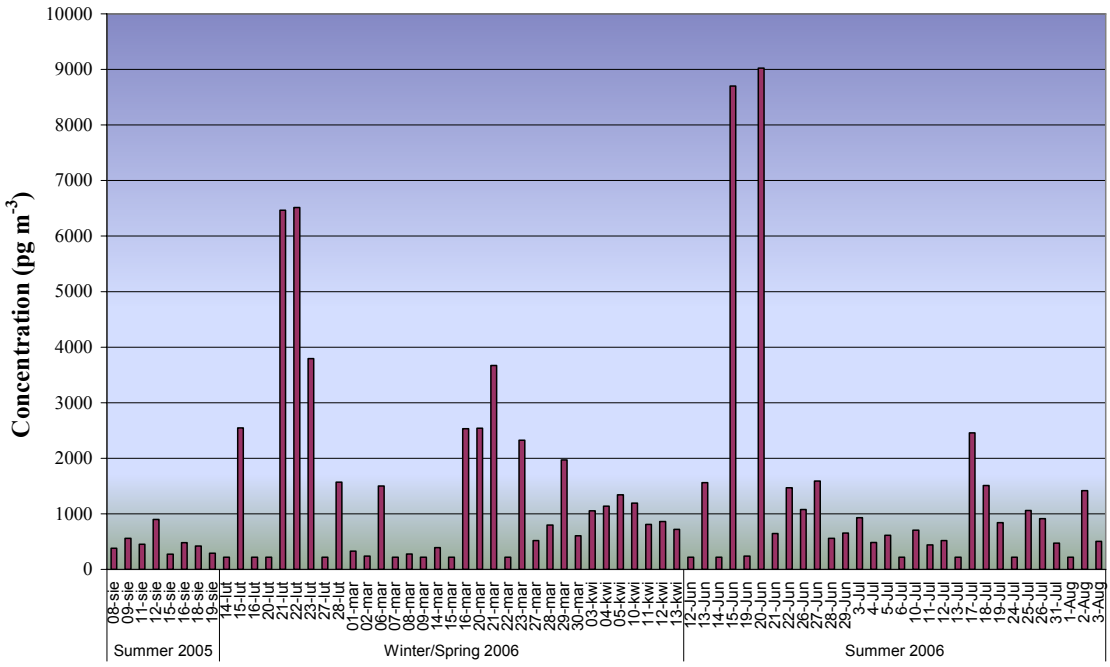

Figure 3.5 The variation of the sum of ANs concentrations during the sampling campaigns.

(a) 3C5

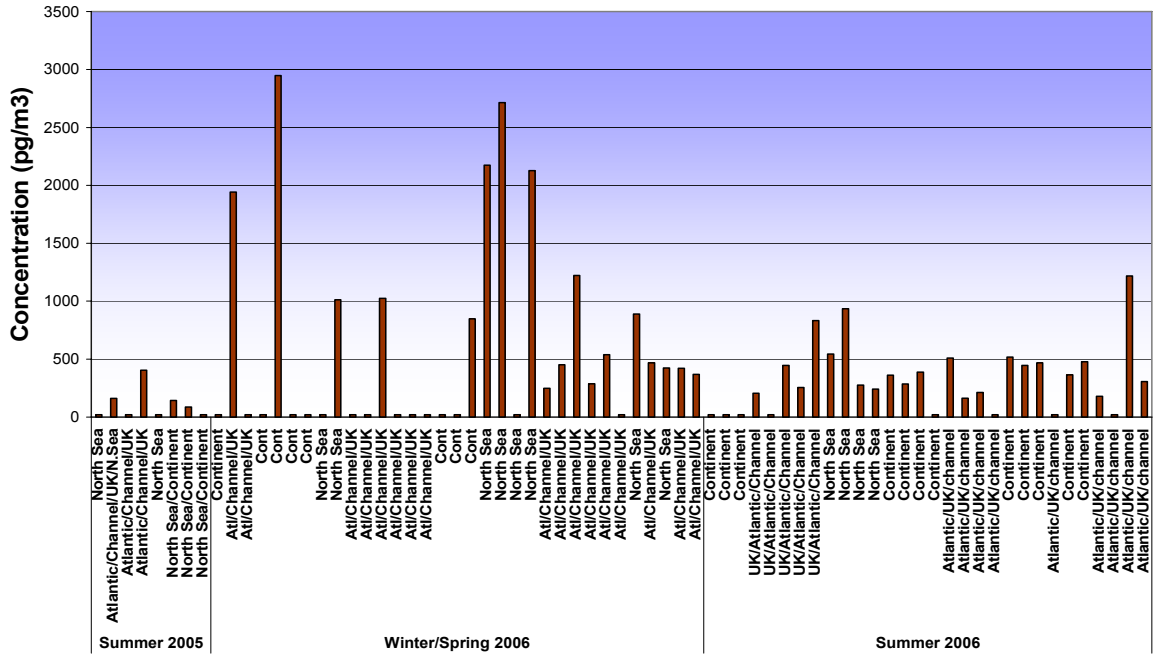

(b) 2C6

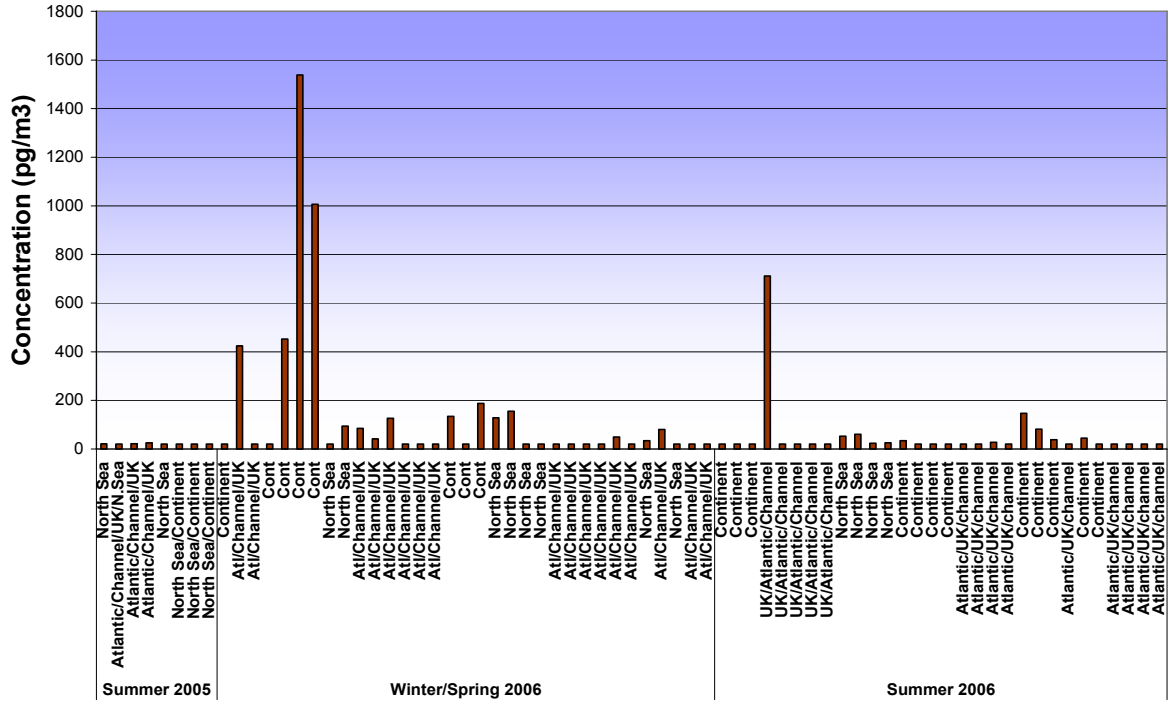

Fig. 3.6 The variation of the concentration of individual analoges during the sampling campaigns.

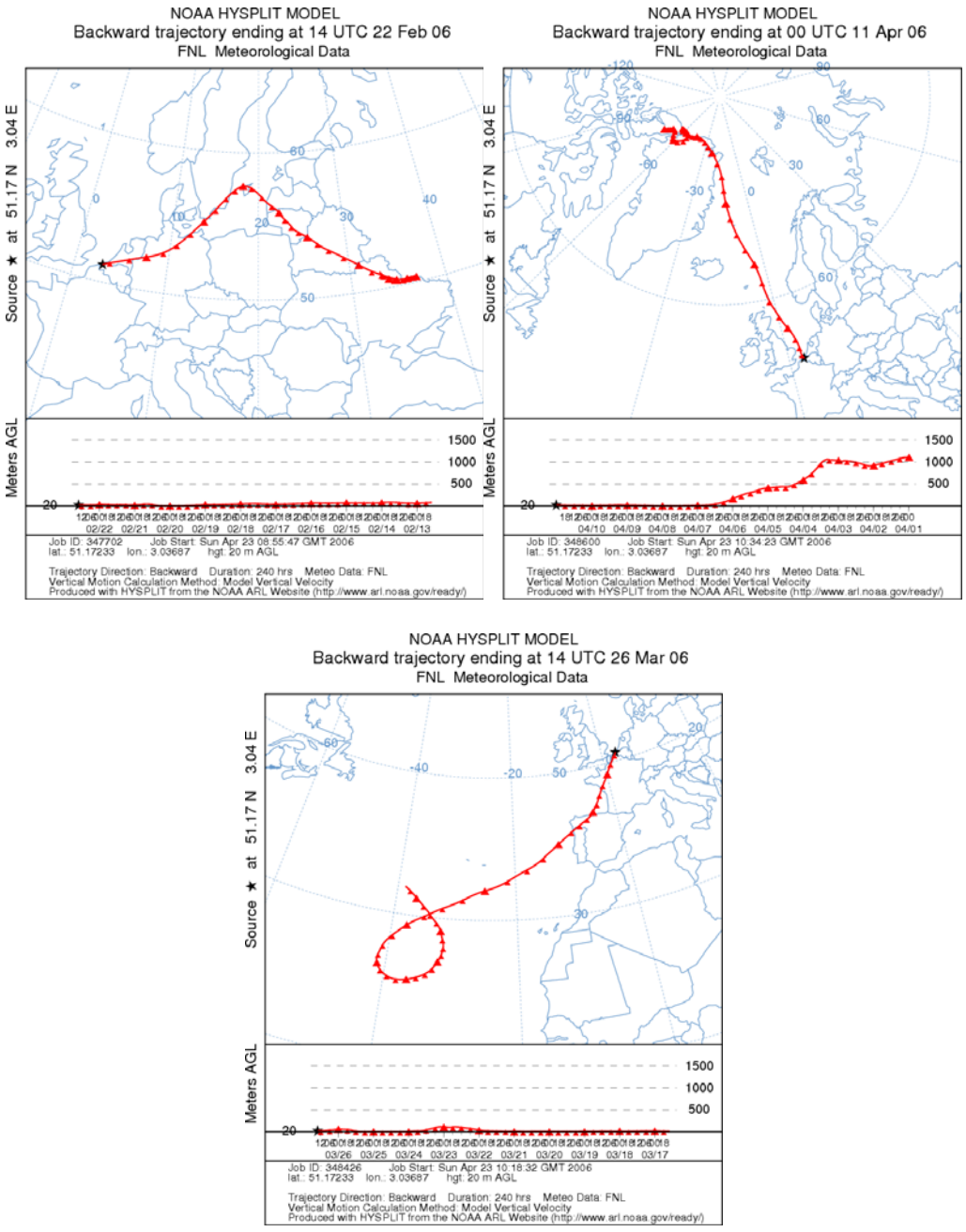

Figure 3.7 Representative air-mass backward trajectory calculated by Hybrid Single-Particle Lagrangian Integrated (HYSPLIT) Model

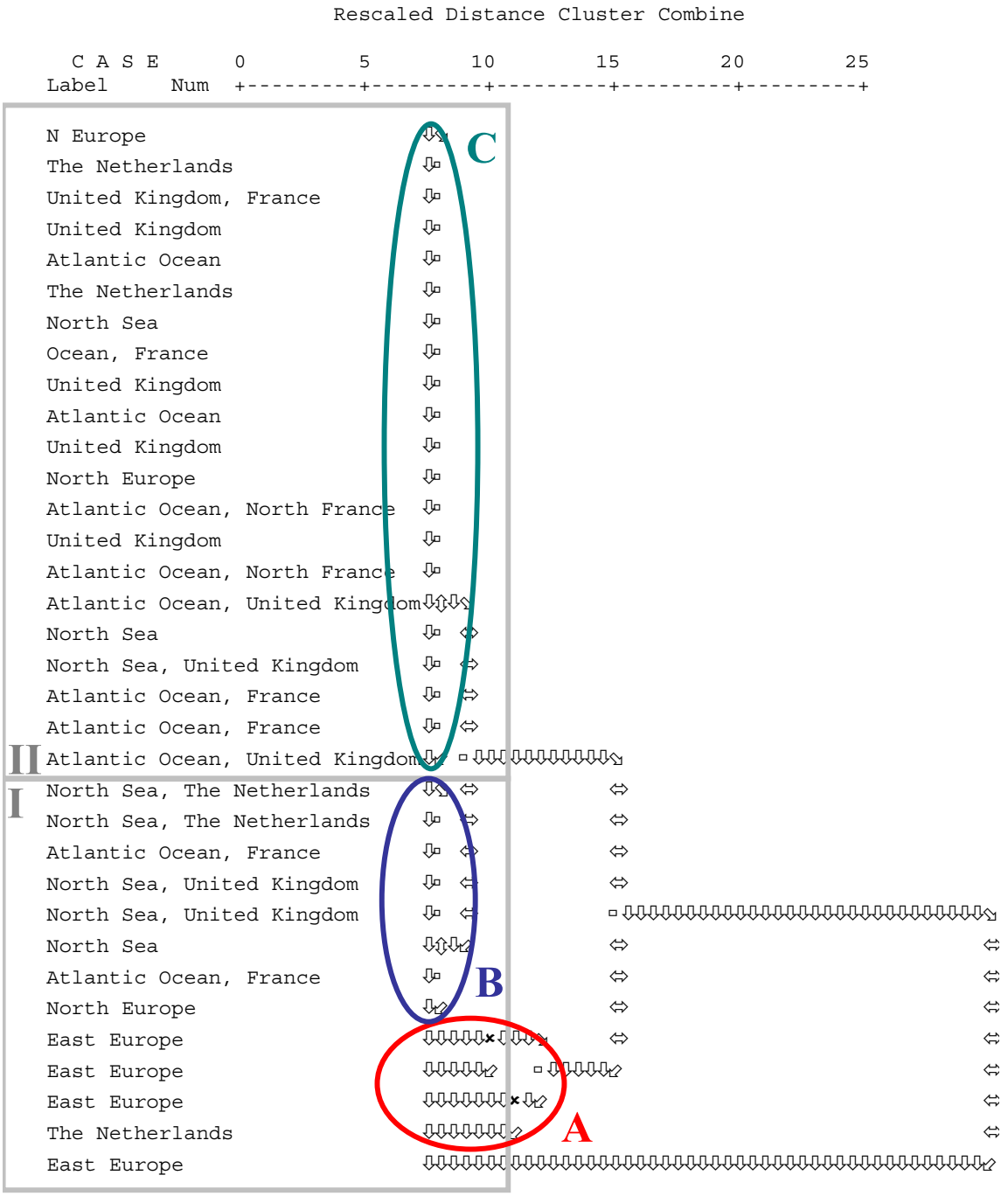

Figure 3.8 The dendrogram using average linkage (Between Groups) – I - low level of precipitation, II – high level of precipitation, Group A - East Europe influence, Group B - North Sea and North Europe influence, Group C - mostly Atlantic Ocean and France influence.

Appendix 4

X-ray Fluorescence Tables and Figures

Figure 4.1 The sampling arrangement

Table 4.1 The applied measurement conditions

Element	Secondary target	Accelerating Voltage (kV)	Current (mA)	Analyzed line
Al-Ca	Ti	35	17	K_α
Ti-V	Fe	50	12	K_α
Cr-Zn	Ge	100	6	K_α
Se, Pb	Zr	100	6	K_α, L_α
Sr	Mo	100	6	K_α
As	KBr	100	6	K_α
Cd	CsI	100	6	K_α
Sb	CeO_2	100	6	K_α

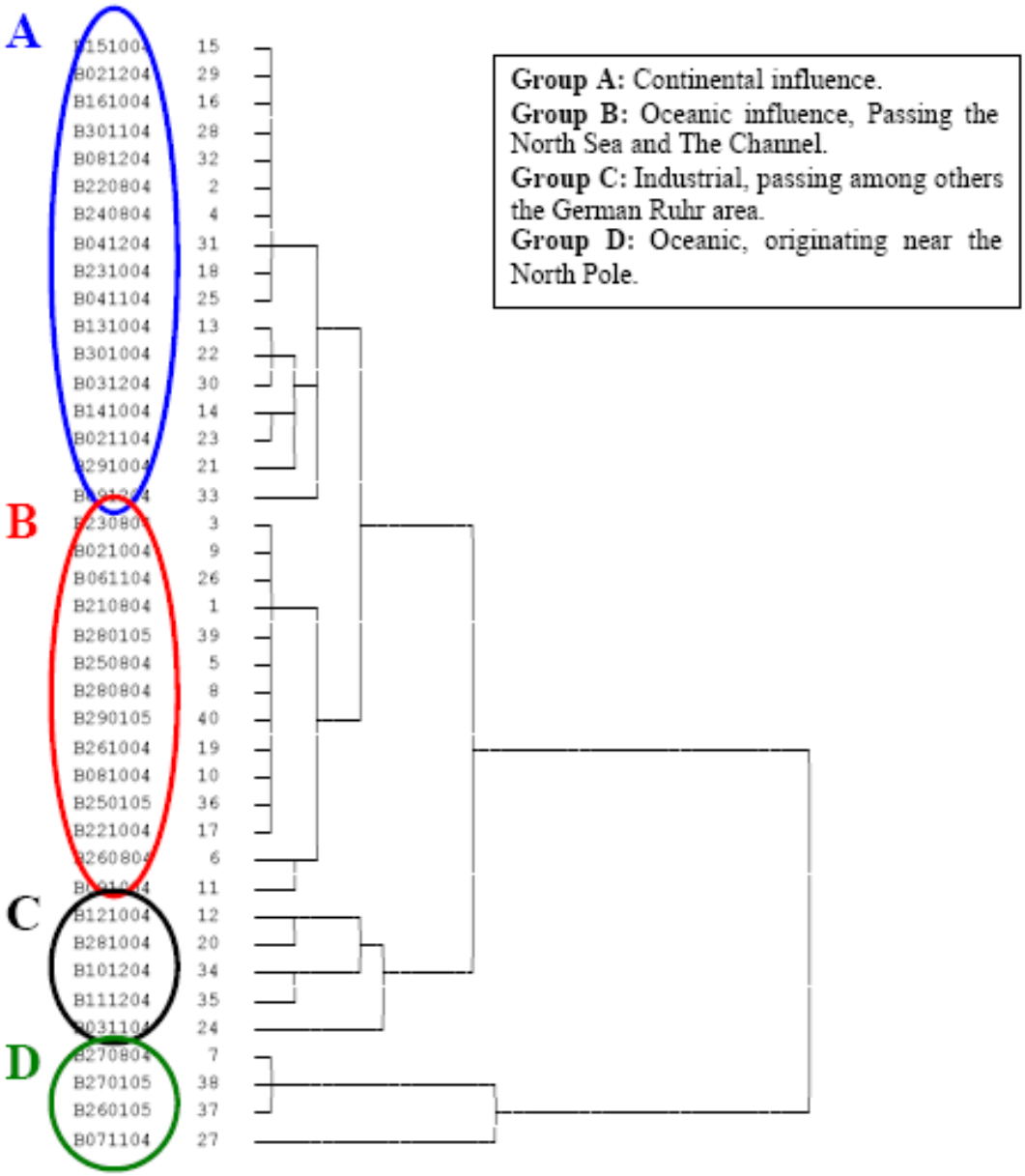

Figure 4.2 The clustering results for the coarse fraction

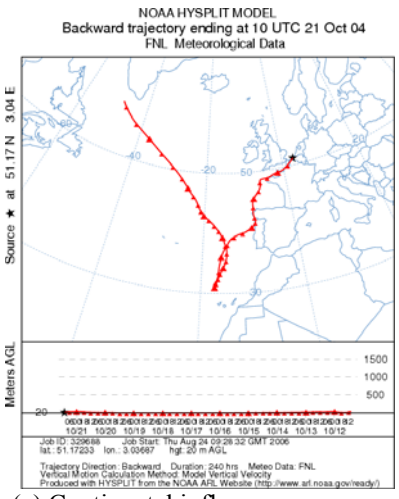

(a) Continental influence

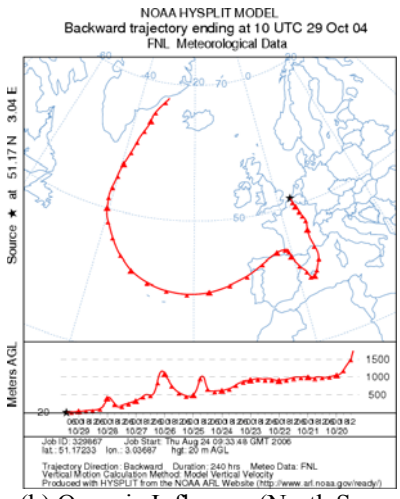

(b) Oceanic Influence (North Sea and The Channel)

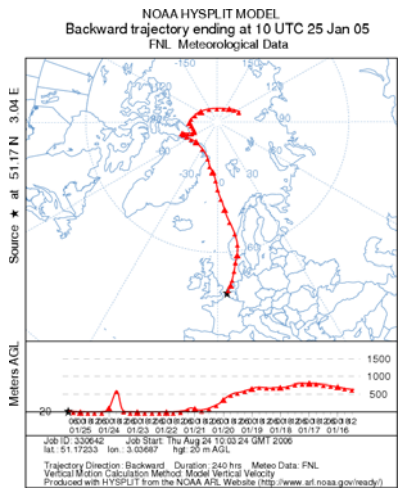

(c) Industrial influence (Ruhr area)

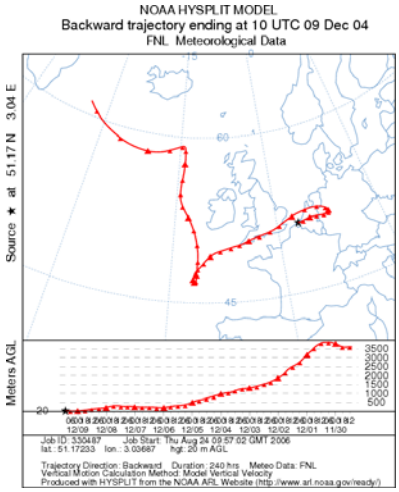

(d) Oceanic influence (North Pole)

Figure 4.3 The backward trajectories for the three samples chosen to represent the first campaign

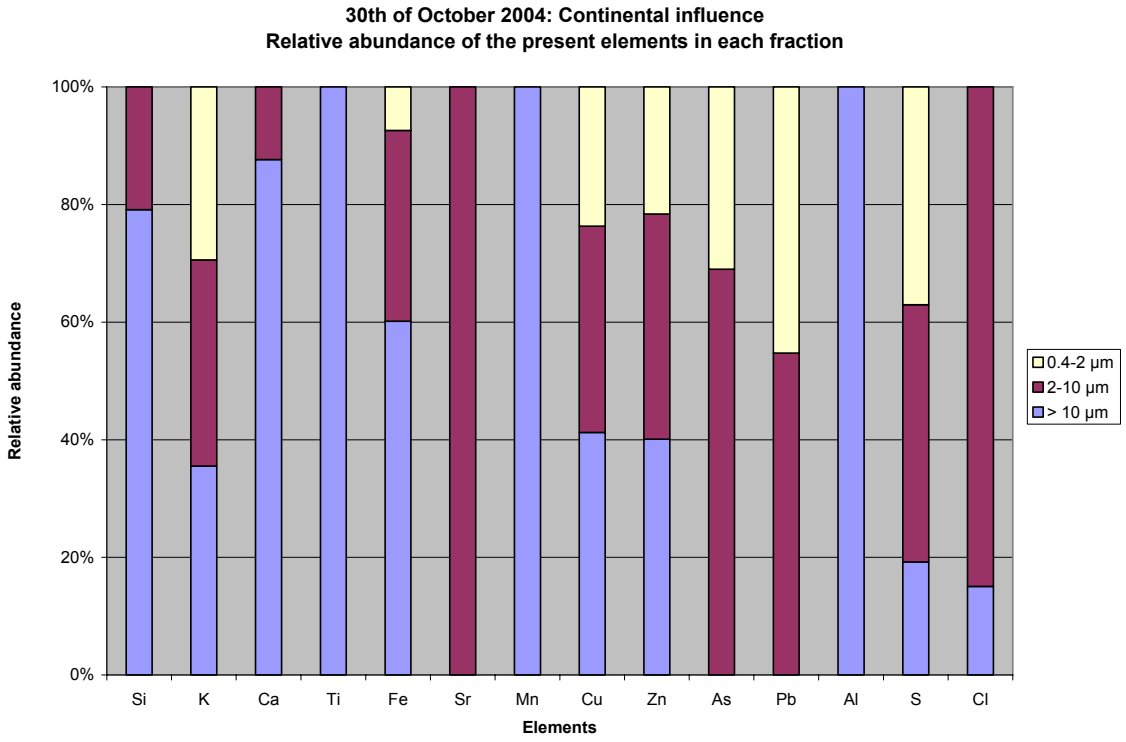

Figure 4.4: The relative abundance of the elements in the three fractions for the continental sample

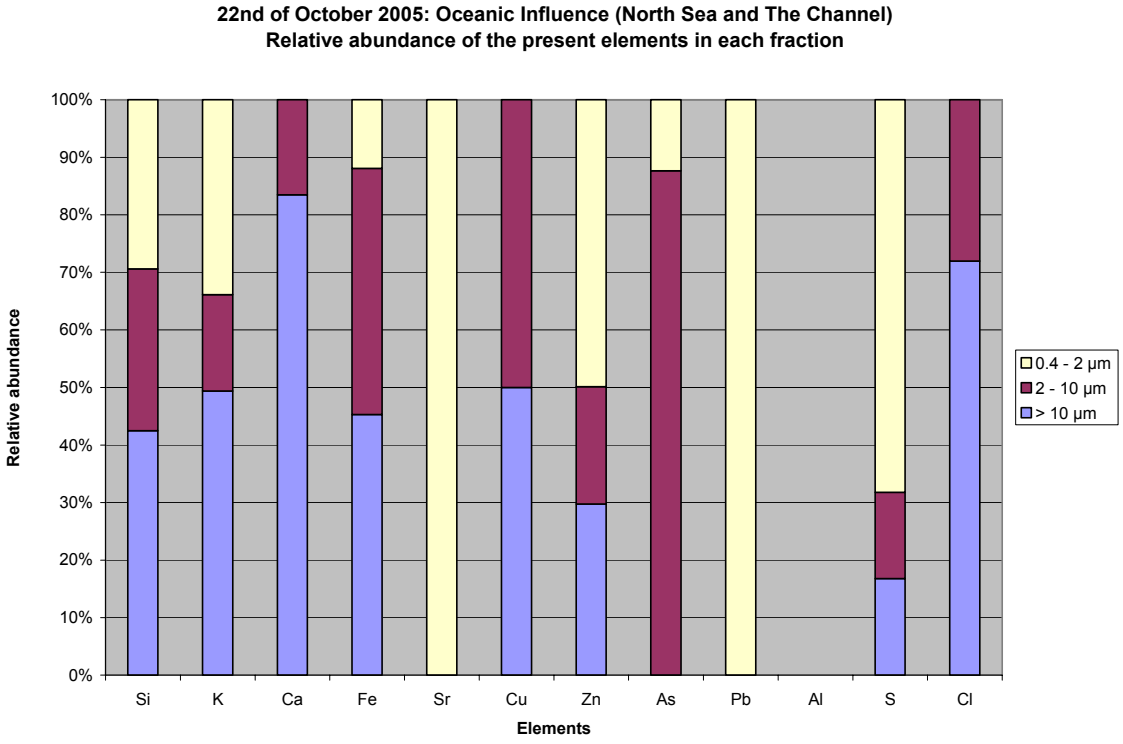

Figure 4.5 The relative abundance of the elements in the three fractions for the oceanic sample (North Sea and The Channel)

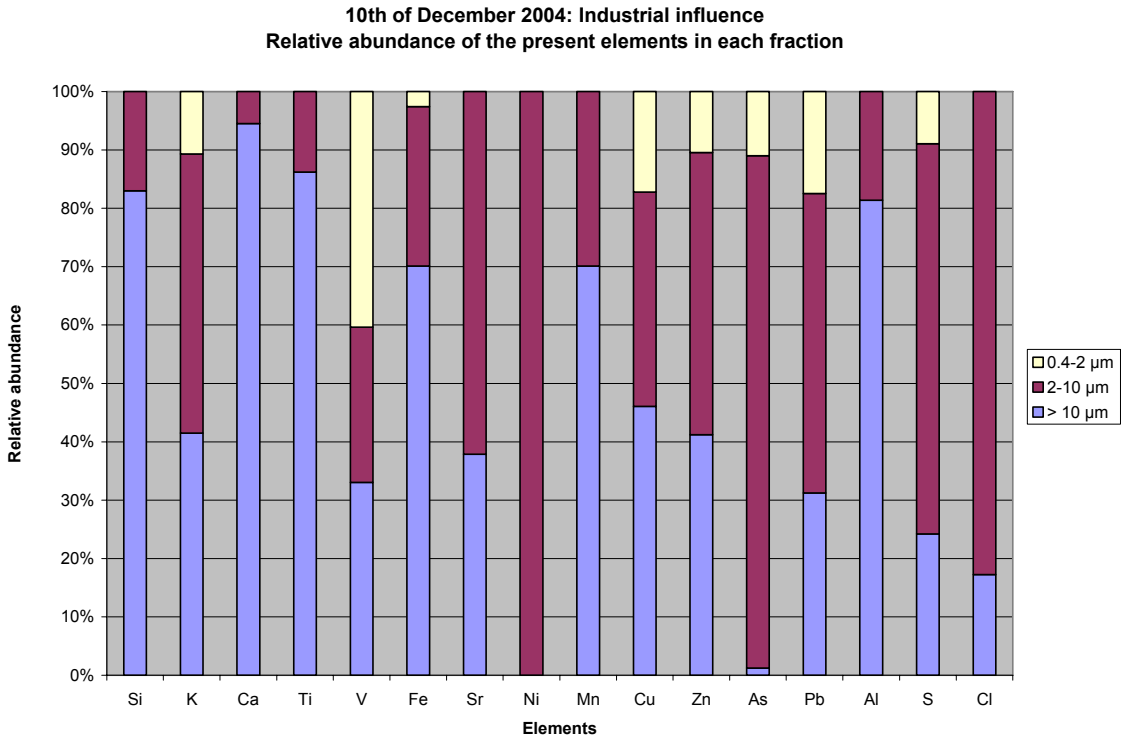

Figure 4.6 The relative abundance of the elements in the three fractions for the industrial sample

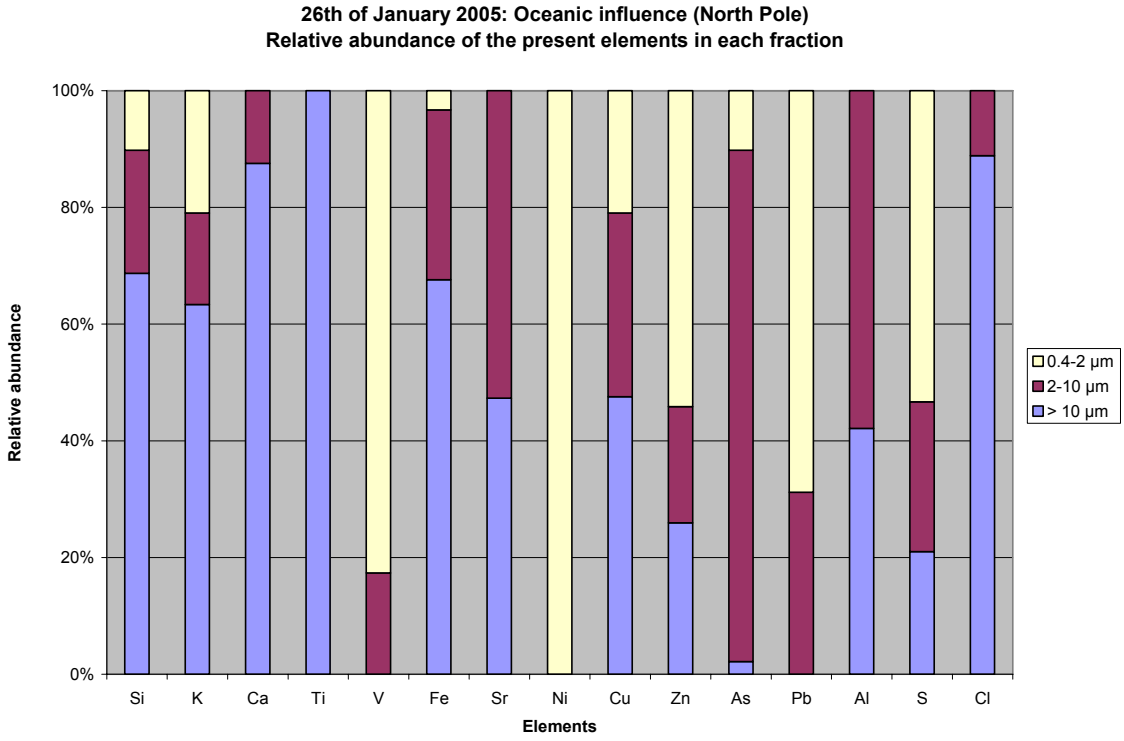

Figure 4.7 The relative abundance of the elements in the three fractions for the oceanic sample (North Pole)

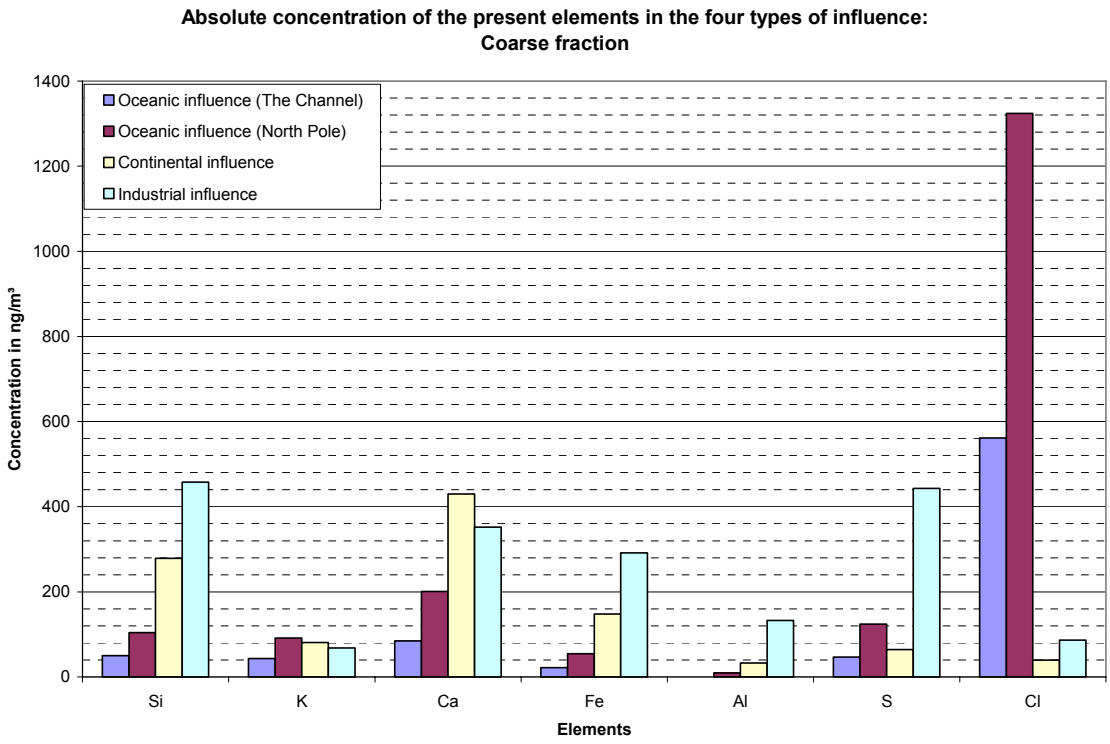

Figure 4.8 The absolute abundance of the elements Si, K, Ca, Fe, Al, S and Cl for the coarse fraction in function of the four influences.

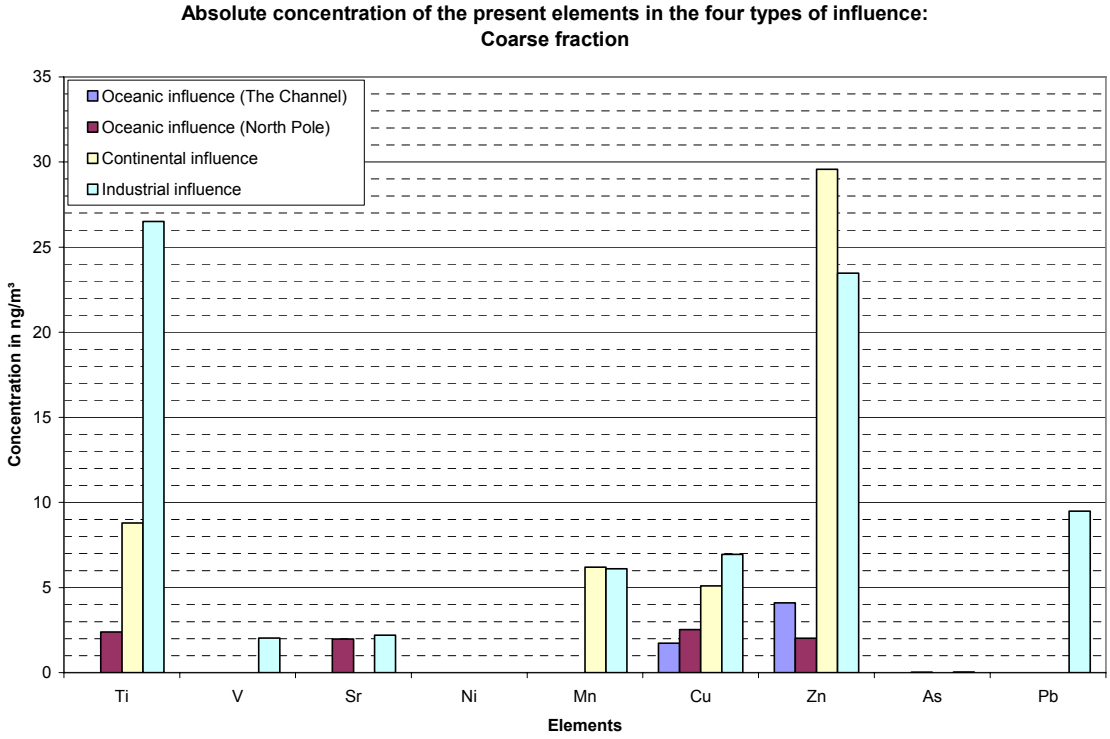

Figure 4.9 The absolute abundance of the elements Ti, V, Sr, Ni, Mn, Cr, Zn, As and Pb for the coarse fraction in function of the four influences.

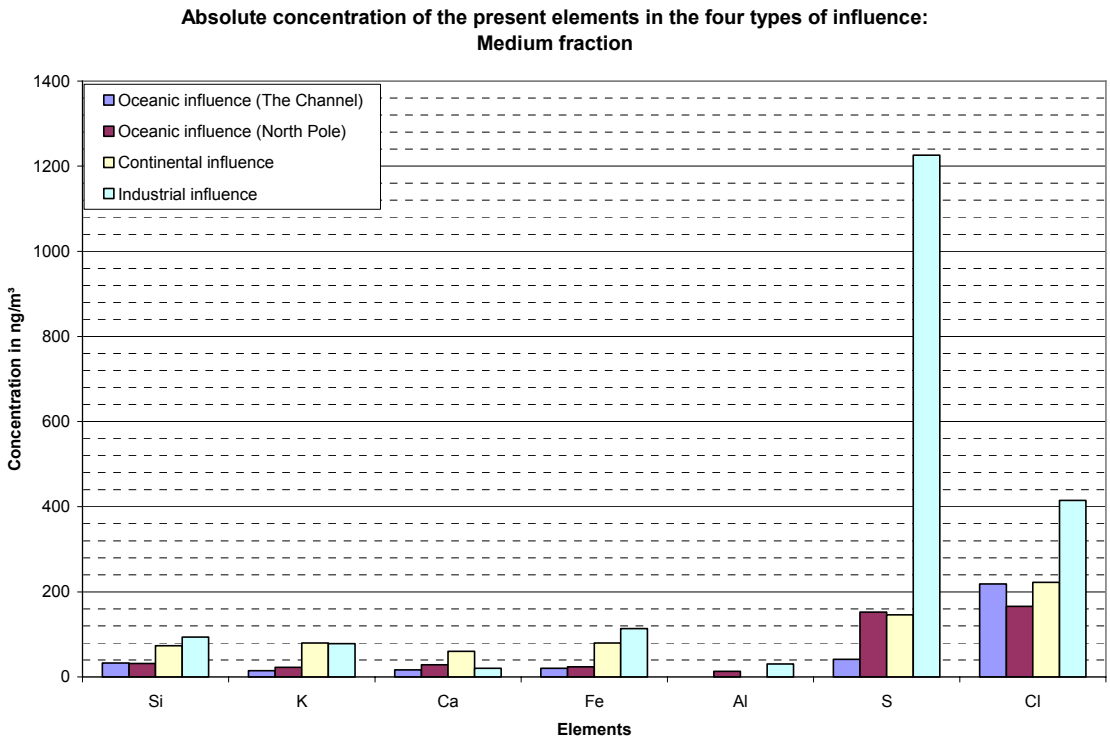

Figure 4.10 The absolute abundance of the elements Si, K, Ca, Fe, Al, S and Cl for the medium fraction in function of the four influences.

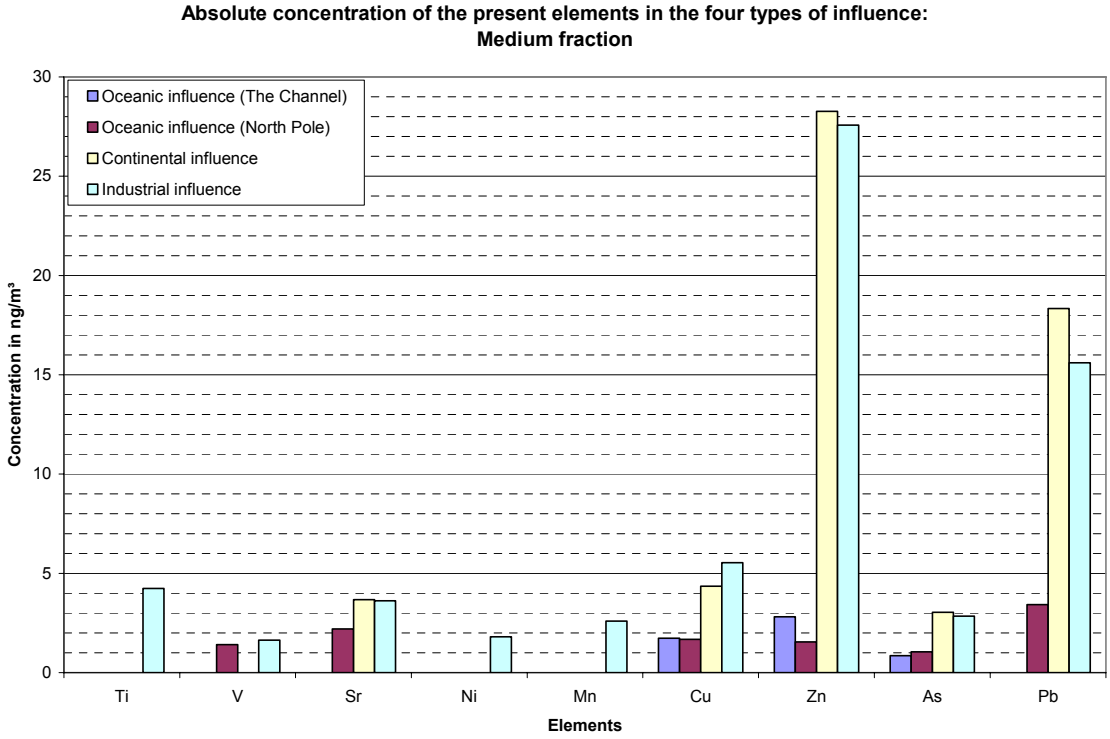

Figure 4.11 The absolute abundance of the elements Ti, V, Sr, Ni, Mn, Cr, Zn, As and Pb for the medium fraction in function of the four influences.

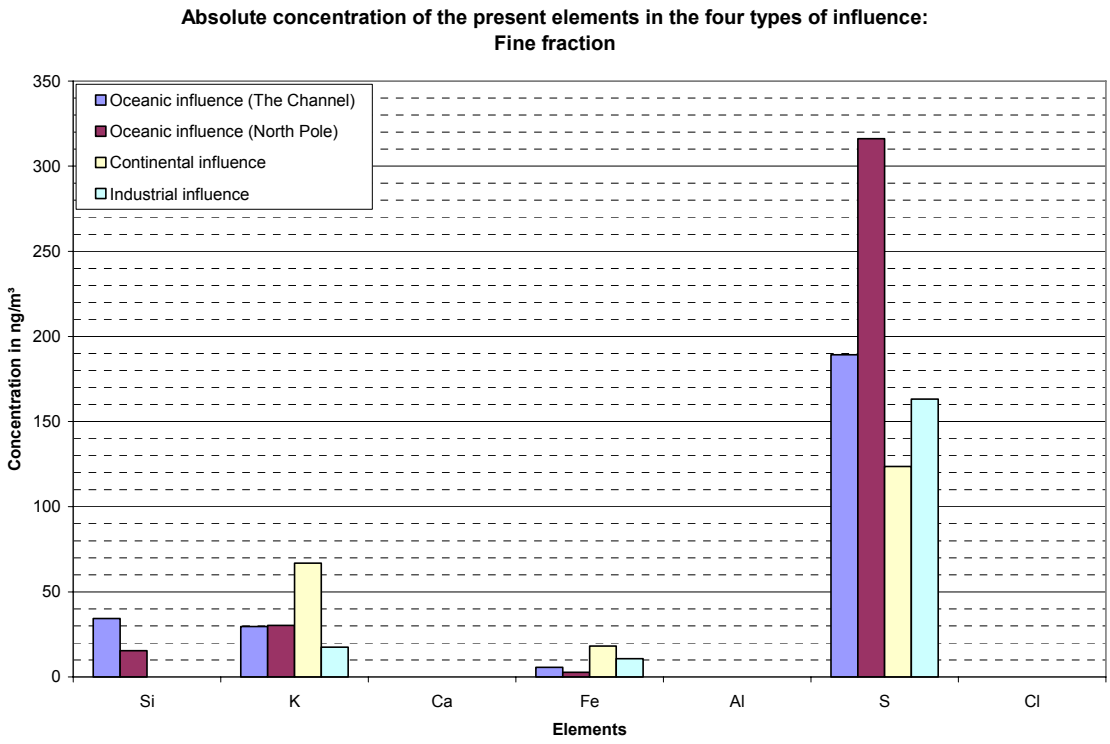

Figure 4.12 The absolute abundance of the elements Si, K, Ca, Fe, Al, S and Cl for the fine fraction in function of the four influences.

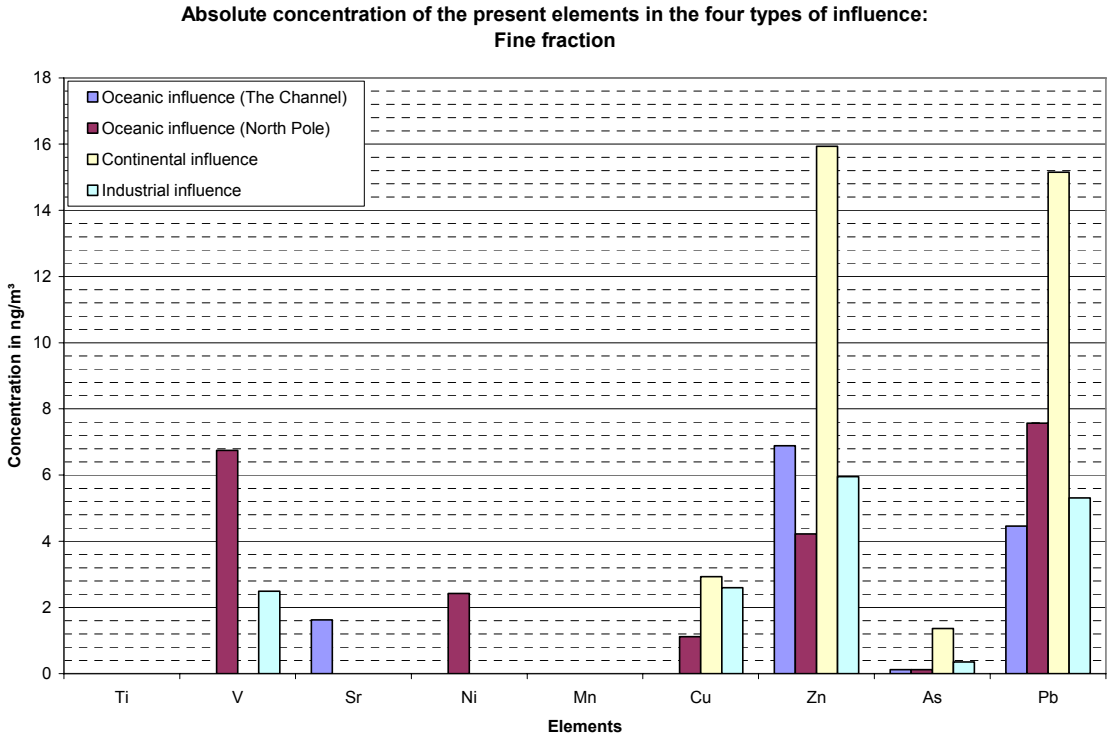

Figure 4.13 The absolute abundance of the elements Ti, V, Sr, Ni, Mn, Cr, Zn, As and Pb for the fine fraction in function of the four influences.

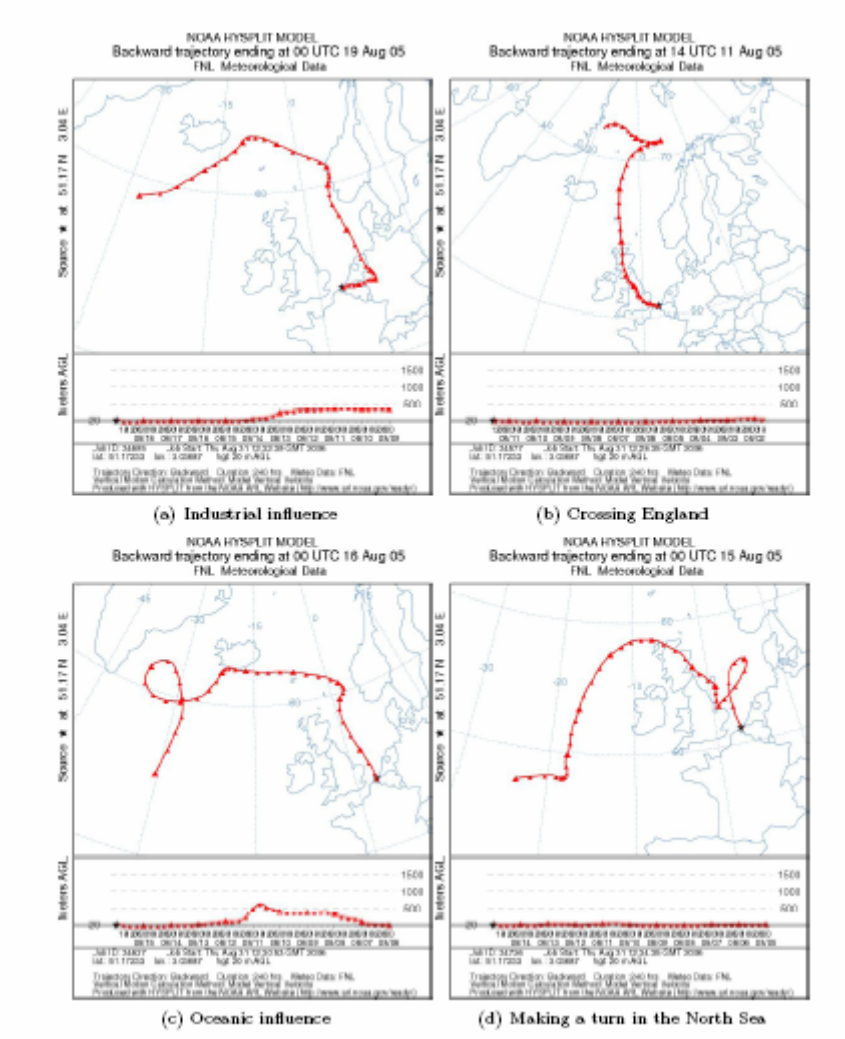

Figure 4.14 The backward trajectories for the four samples chosen to represent the second campaign

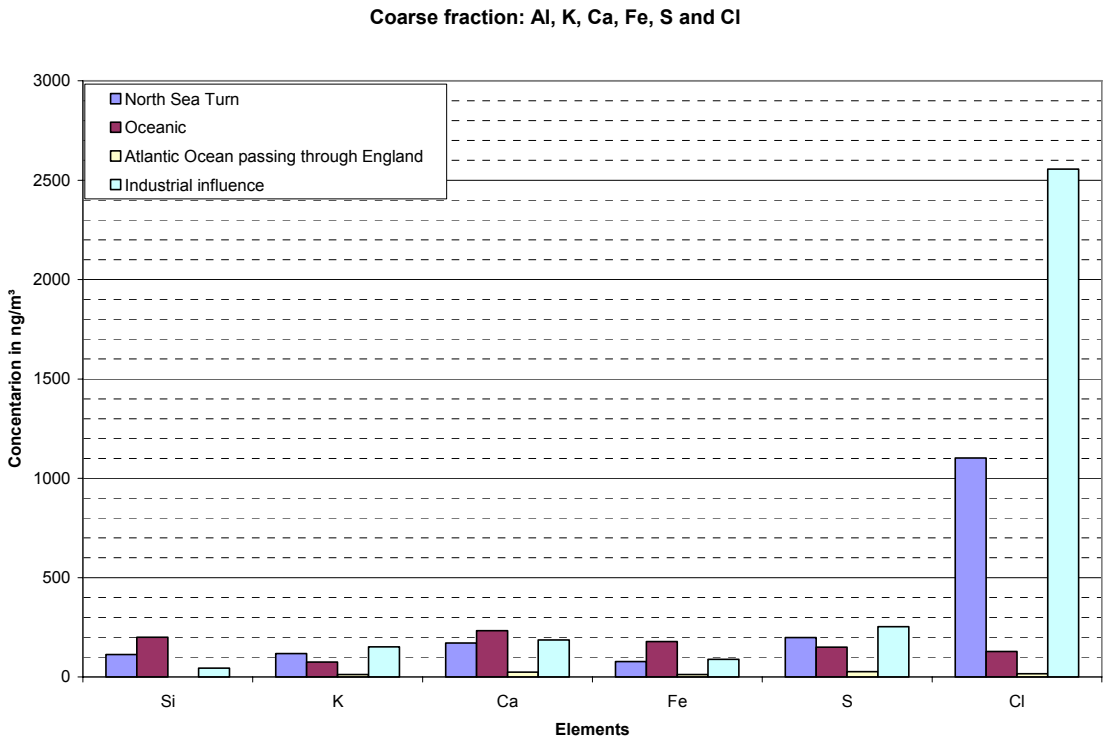

Figure 4.15 The absolute abundance of the elements Si, K, Ca, Fe, S and Cl for the coarse fraction in function of the four influences.

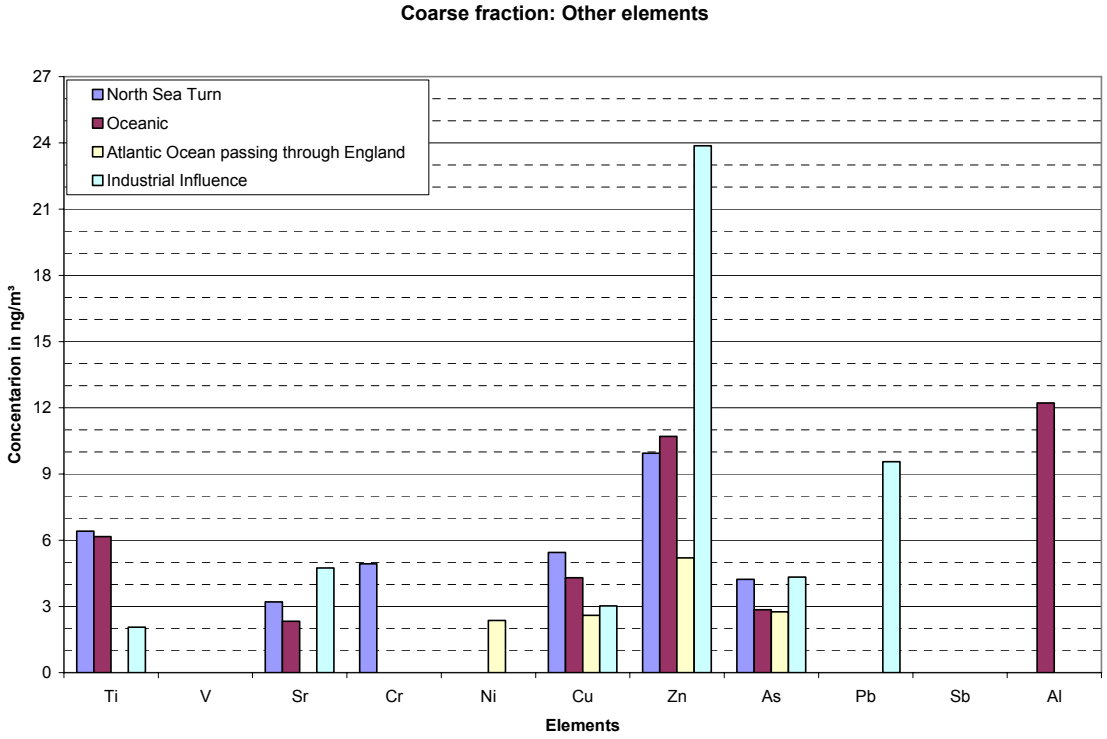

Figure 4.16 The absolute abundance of the elements Ti, V, Sr, Cr, Ni, Cu, Zn, As, Pb, Sb and Al for the coarse fraction in function of the four influences.

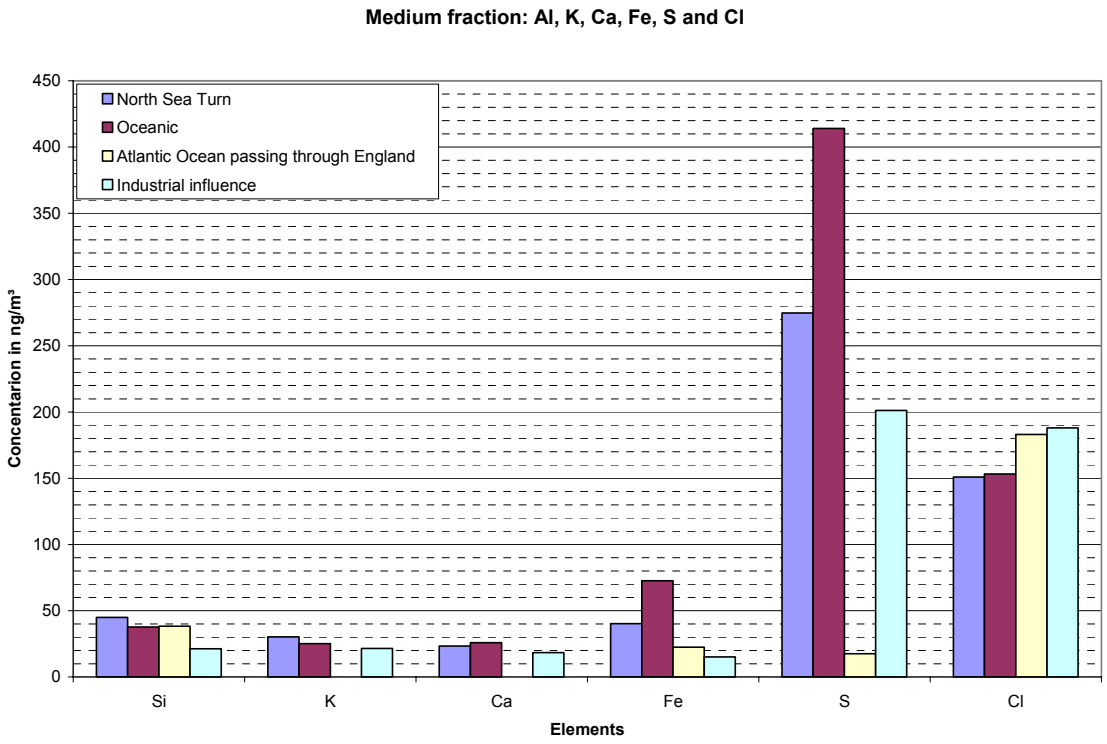

Figure 4.17 The absolute abundance of the elements Si, K, Ca, Fe, S and Cl for the medium fraction in function of the four influences.

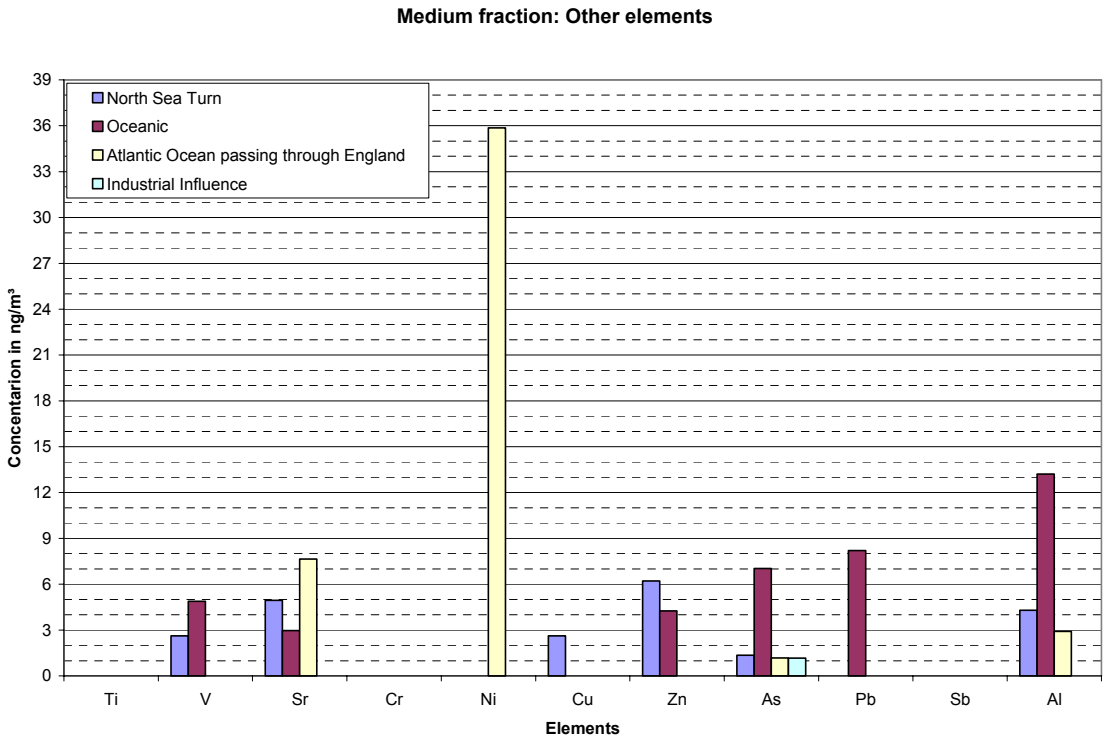

Figure 4.18 The absolute abundance of the elements Ti, V, Sr, Cr, Ni, Cu, Zn, As, Pb, Sb and Al for the medium fraction in function of the four influences.

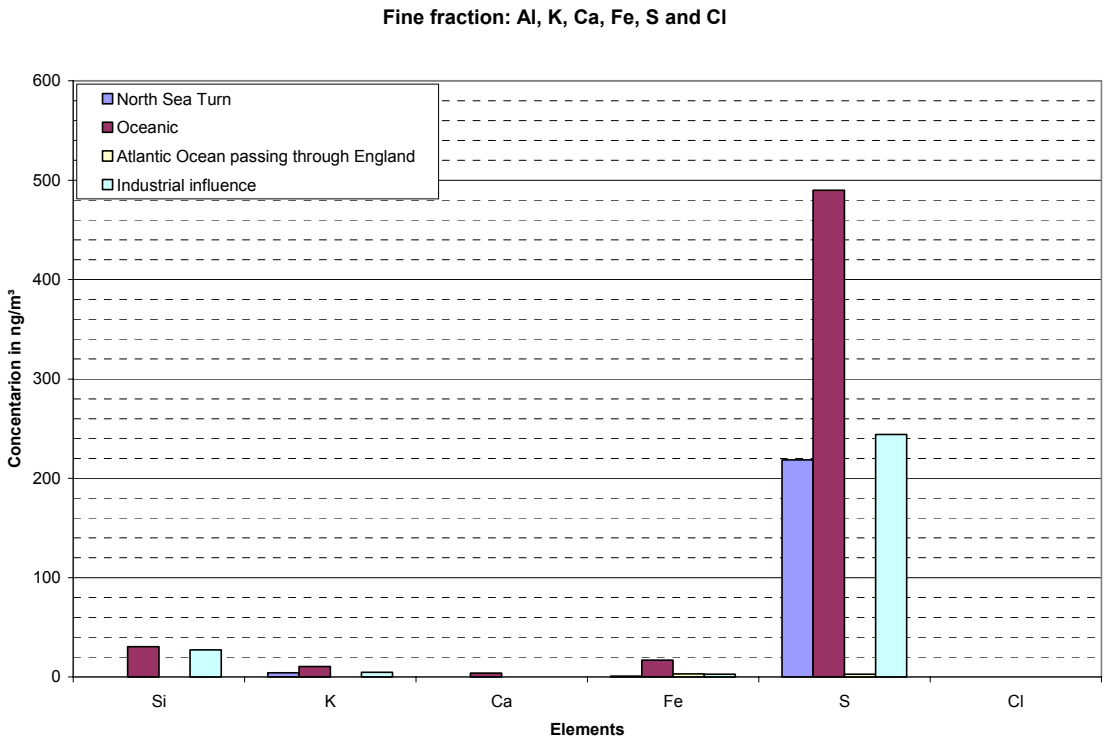

Figure 4.19 The absolute abundance of the elements Si, K, Ca, Fe, S and Cl for the fine fraction in function of the four influences.

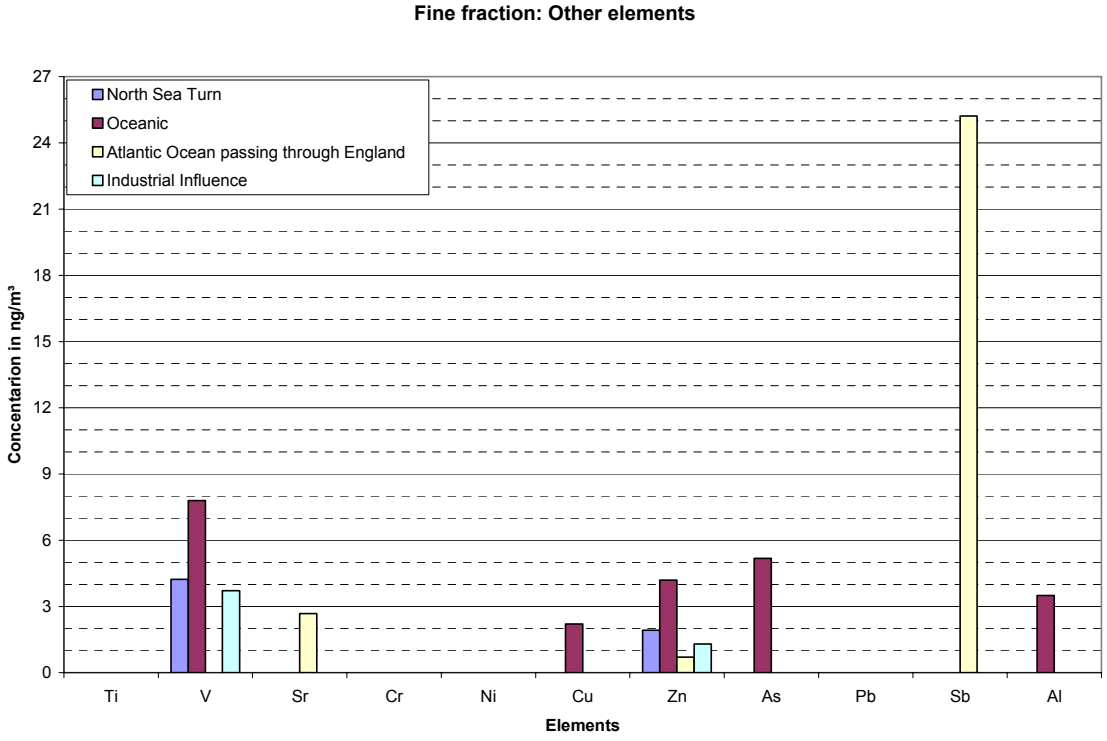

Figure 4.20 The absolute abundance of the elements Ti, V, Sr, Cr, Ni, Cu, Zn, As, Pb, Sb and Al for the fine fraction in function of the three influences.

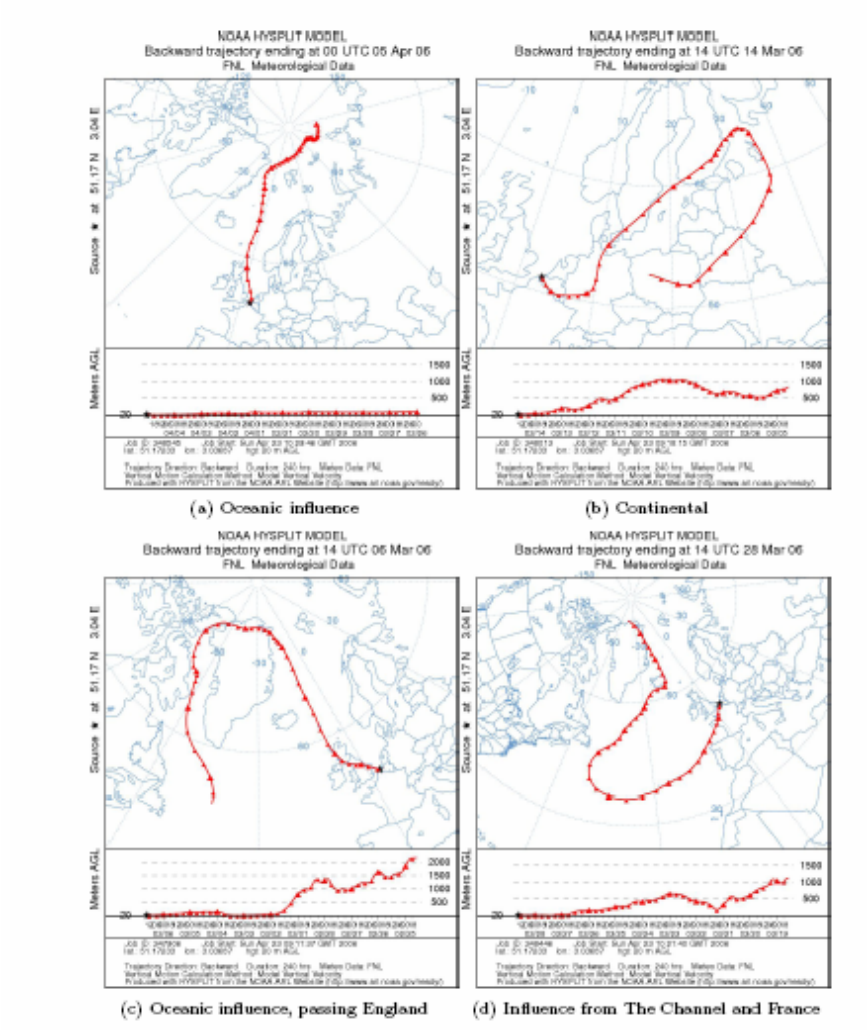

(a) Oceanic influence (b) Continental

(c) Oceanic influence, passing England (d) Influence from The Channel and France

Figure 4.21 The first part of backward trajectories for four of the six samples chosen to represent the third campaign

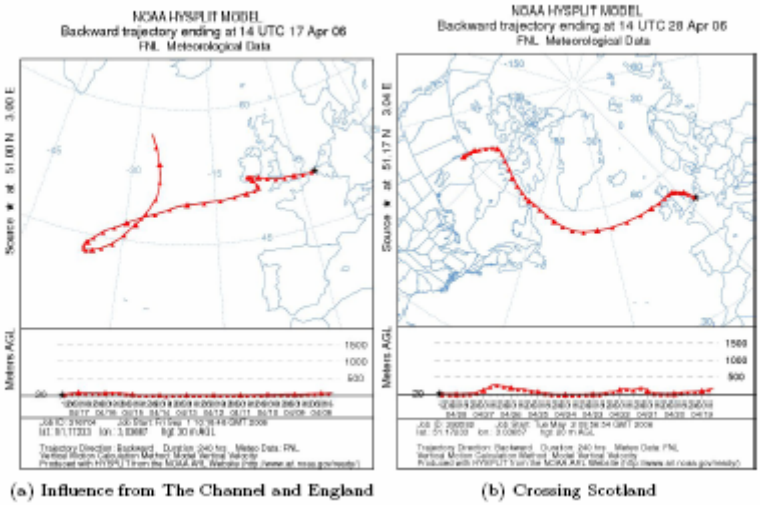

(a) Influence from The Channel and England (b) Crossing Scotland

Figure 4.22 The second part of the backward trajectories for two last samples chosen to represent the third campaign

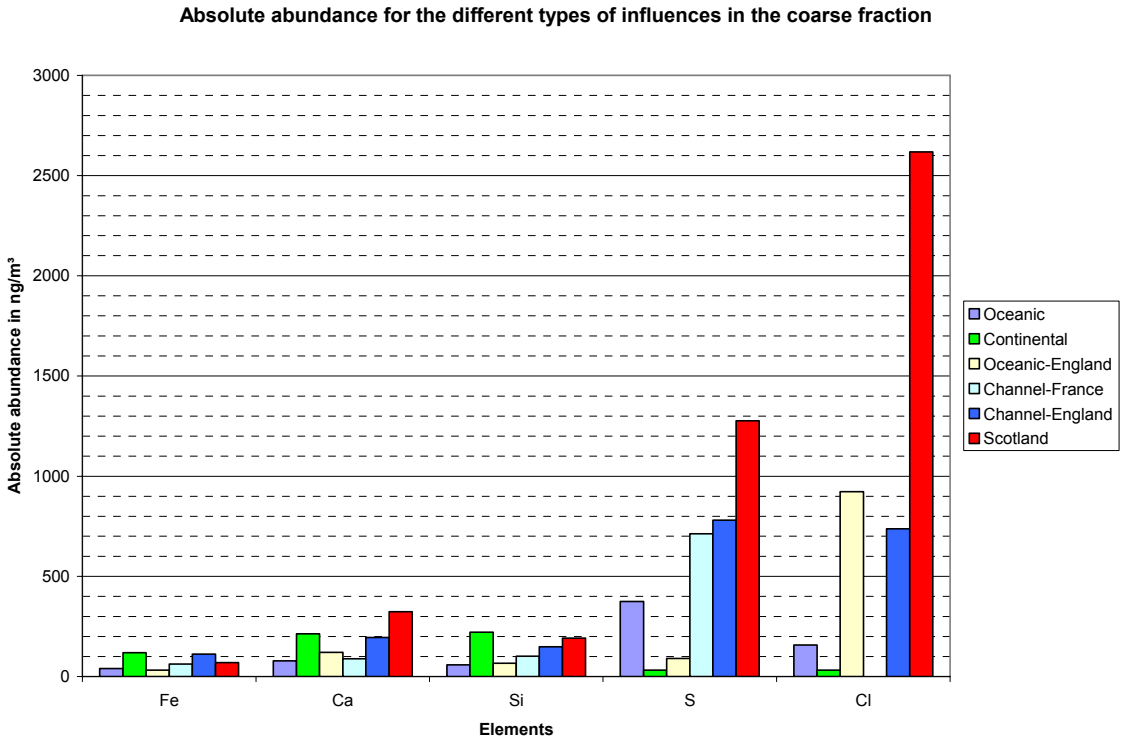

Figure 4.23 The absolute abundance in the coarse fraction of the elements Fe, Ca, Si, S and Cl for the different influences

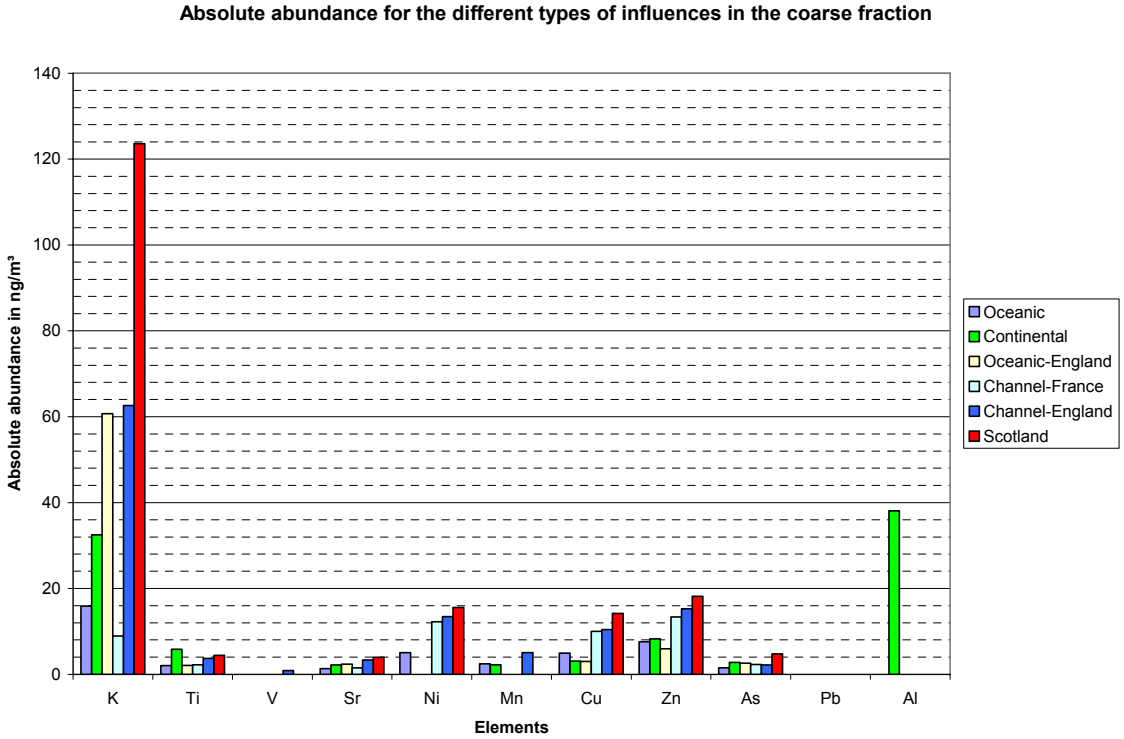

Figure 4.24 The absolute abundance in the coarse fraction of the elements K, Ti, V, Sr, Ni, Mn, Cu, Zn, As, Pb and Al for the different influences

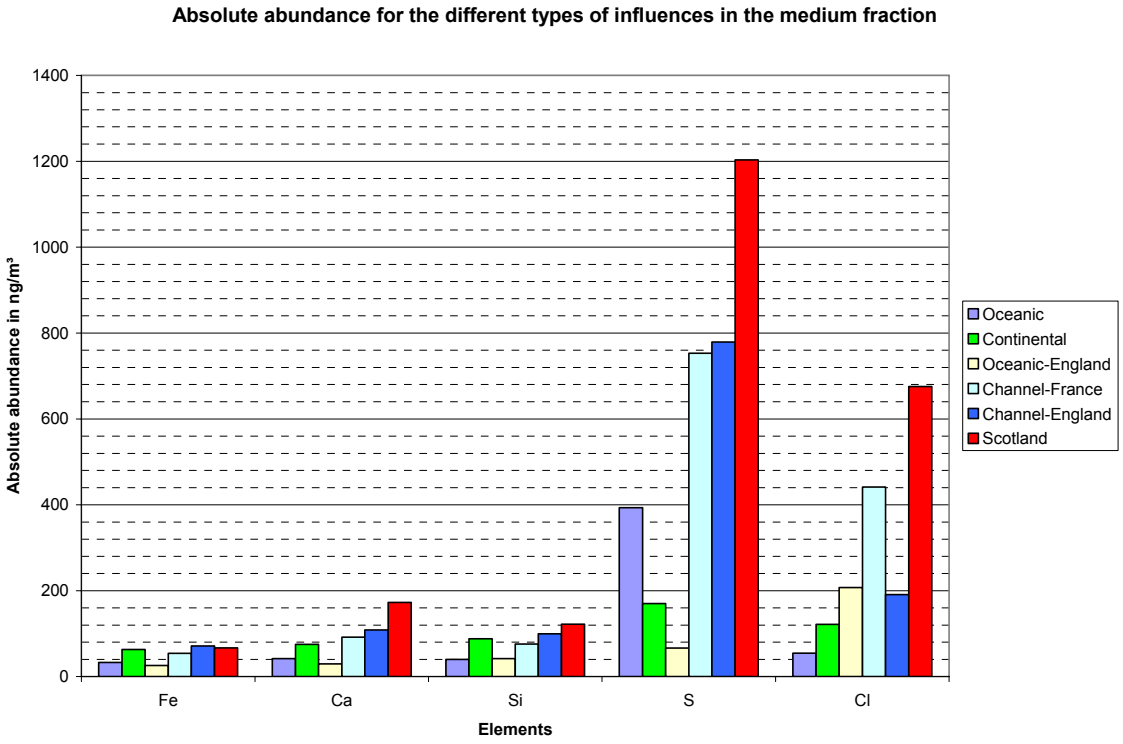

Figure 4.25 The absolute abundance in the medium fraction of the elements Fe, Ca, Si, S and Cl for the different influences

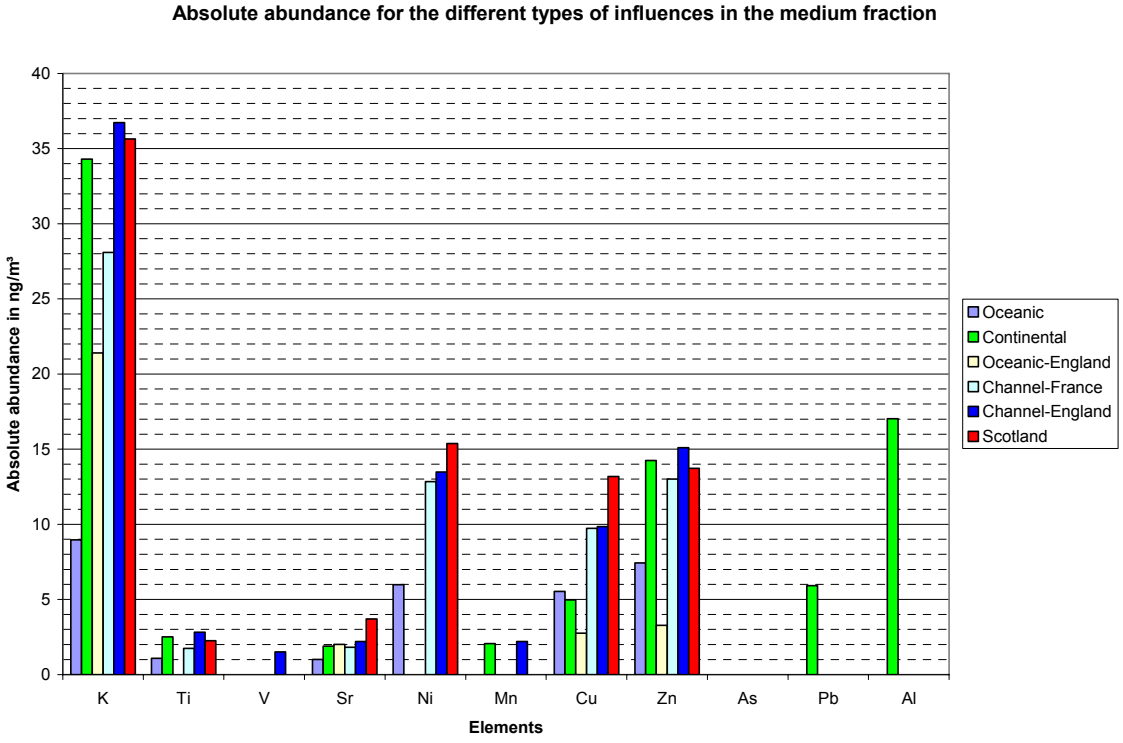

Figure 4.26 The absolute abundance in the medium fraction of the elements K, Ti, V, Sr, Ni, Mn, Cu, Zn, As, Pb and Al for the different influences

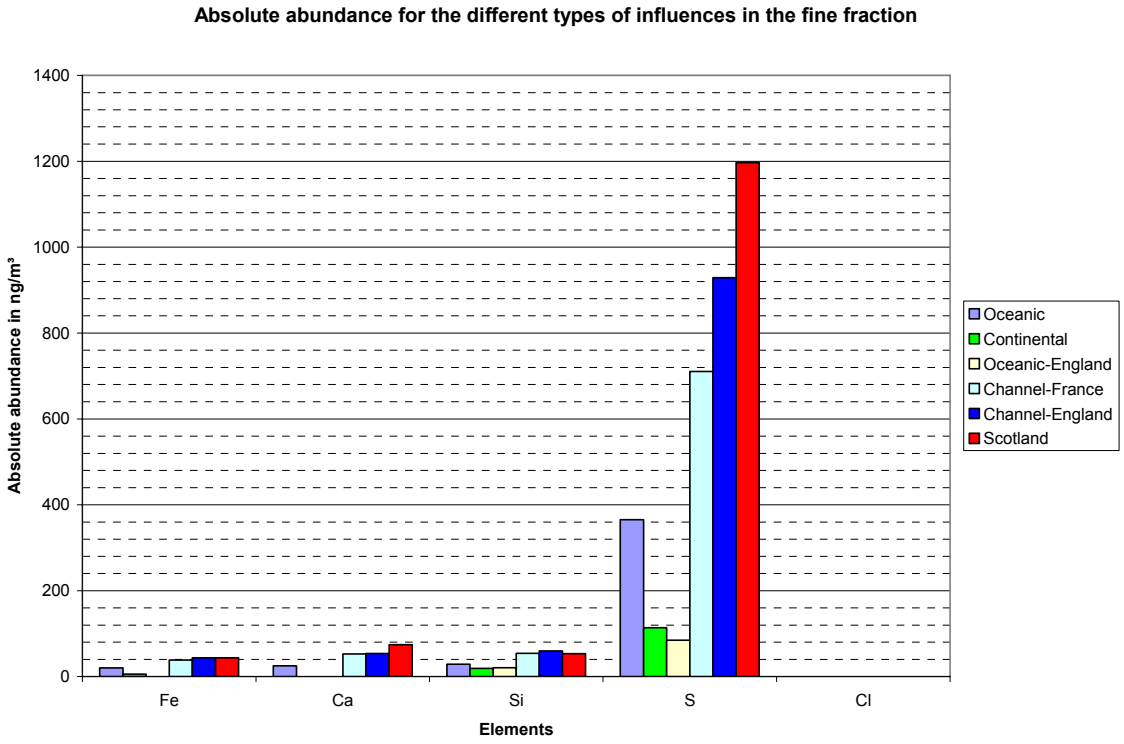

Figure 4.27 The absolute abundance in the fine fraction of the elements Fe, Ca, Si, S and Cl for the different influences

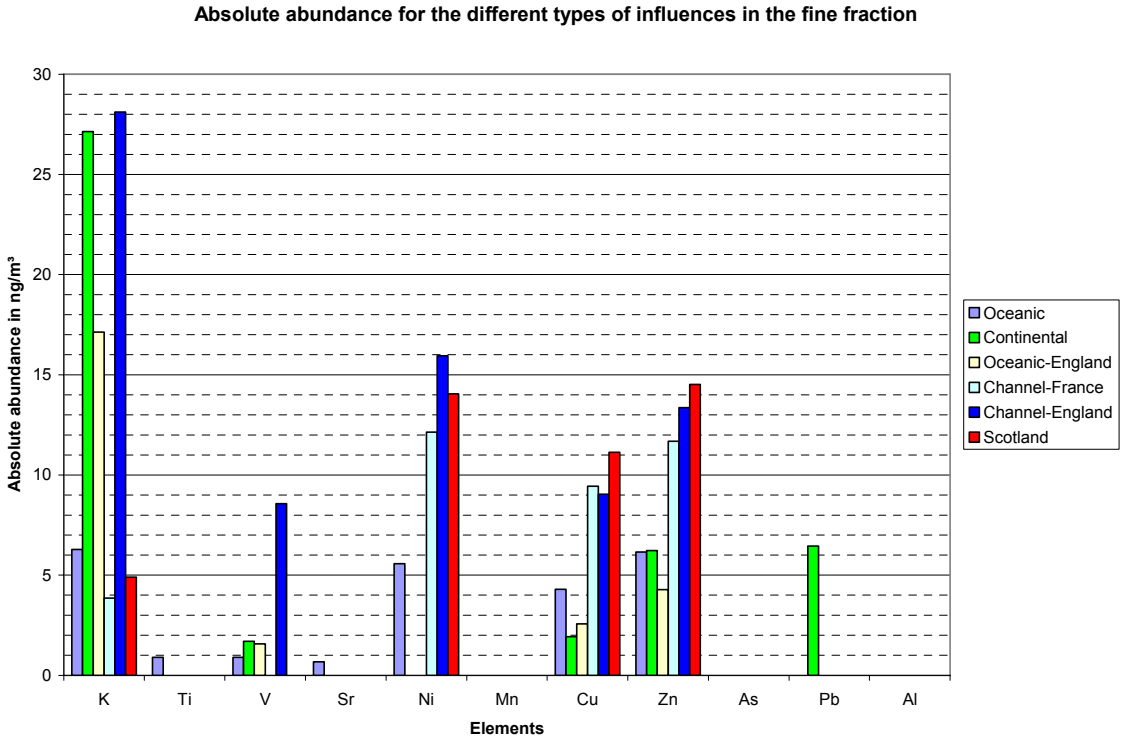

Figure 4.28 The absolute abundance in the fine fraction of the elements K, Ti, V, Sr, Ni, Mn, Cu, Zn, As, Pb and Al for the different influences

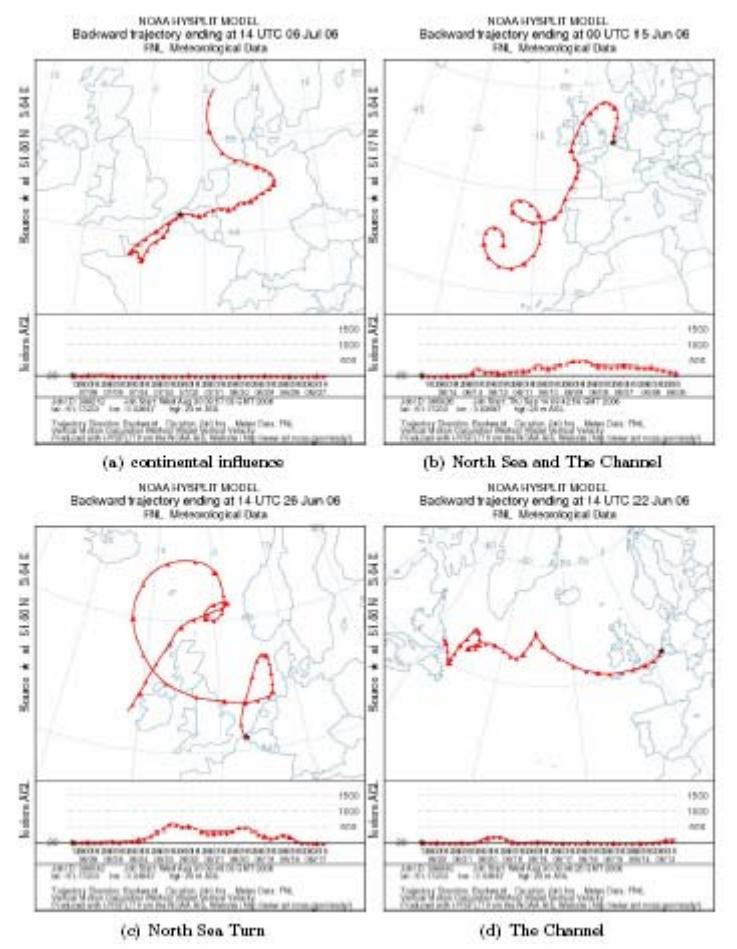

Figure 4.29 The first part of backward trajectories for four of the six samples chosen to represent the fourth campaign

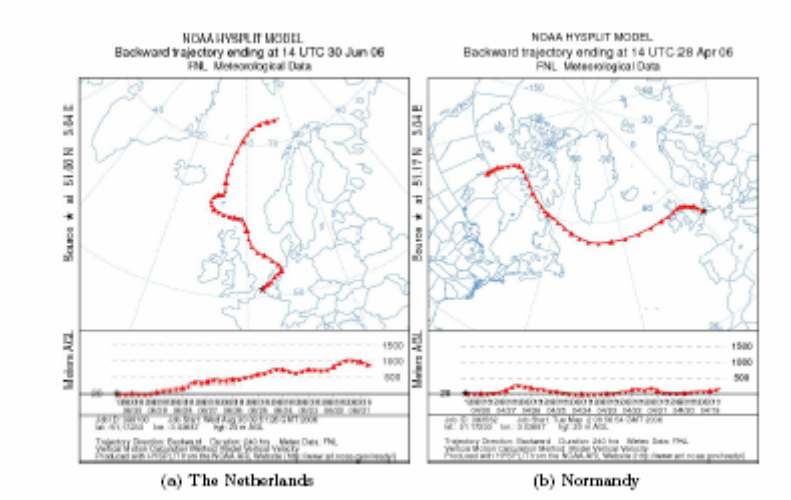

Figure 4.30 The second part of the backward trajectories for two last samples chosen to represent the fourth campaign

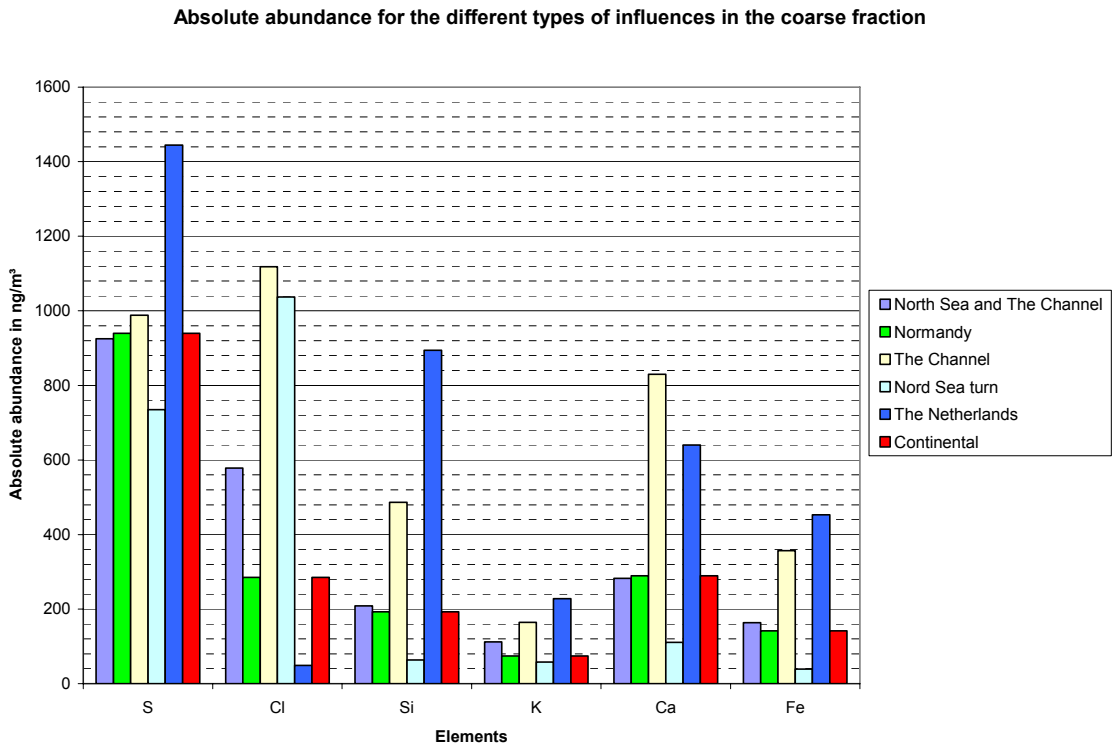

Figure 4.31 The absolute abundance in the coarse fraction of the elements S, Cl, Si, K, Fe and Ca for the different influences

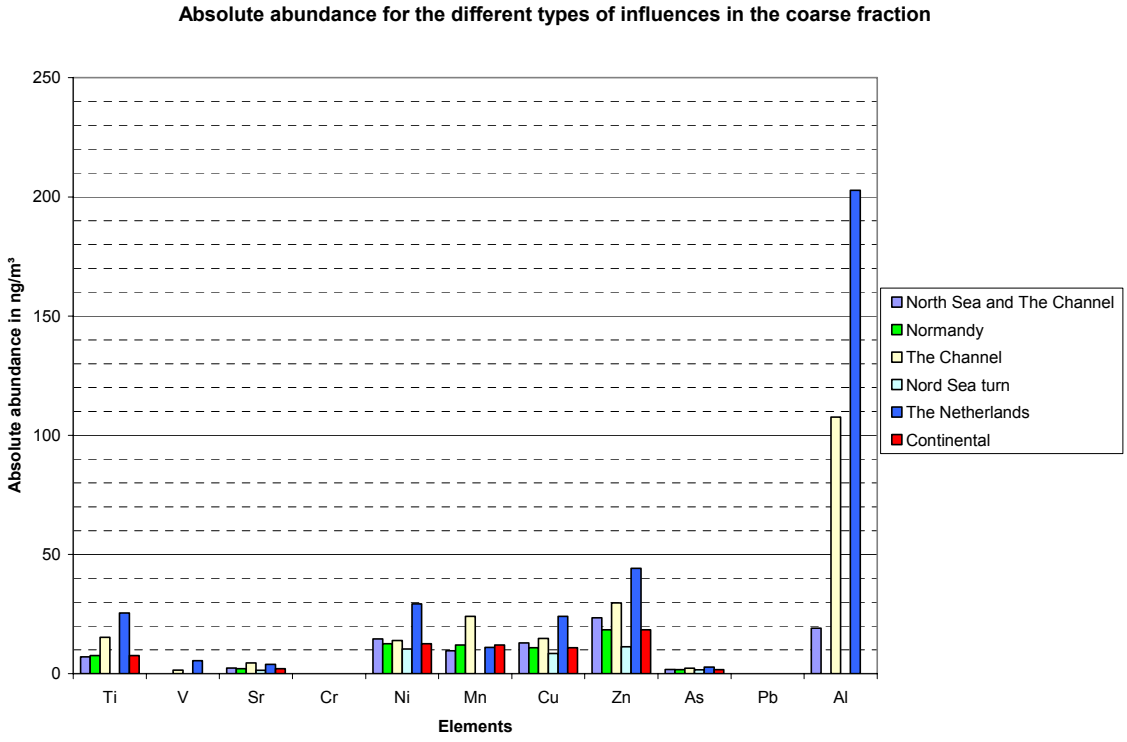

Figure 4.32 The absolute abundance in the coarse fraction of the elements Ti, V, Sr, Cr, Ni, Mn, Cu, Zn, As, Pb and Al for the different influences

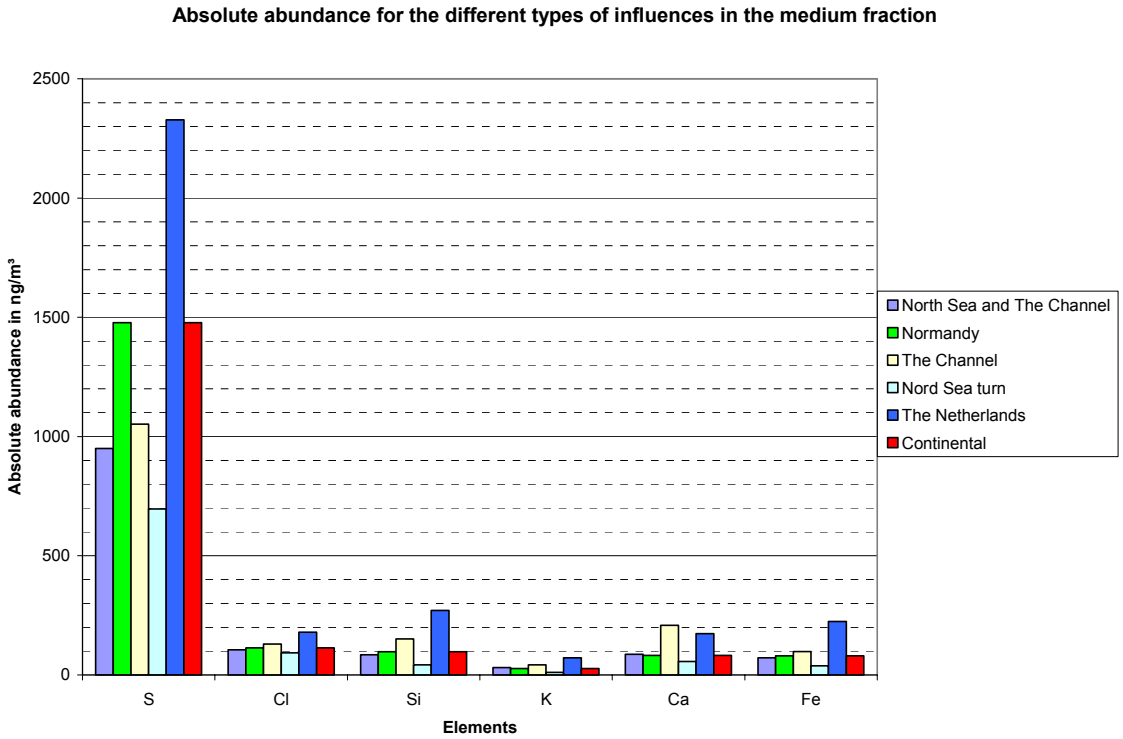

Figure 4.33 The absolute abundance in the fine fraction of the elements S, Cl, Si, K, Fe and Ca for the different influences

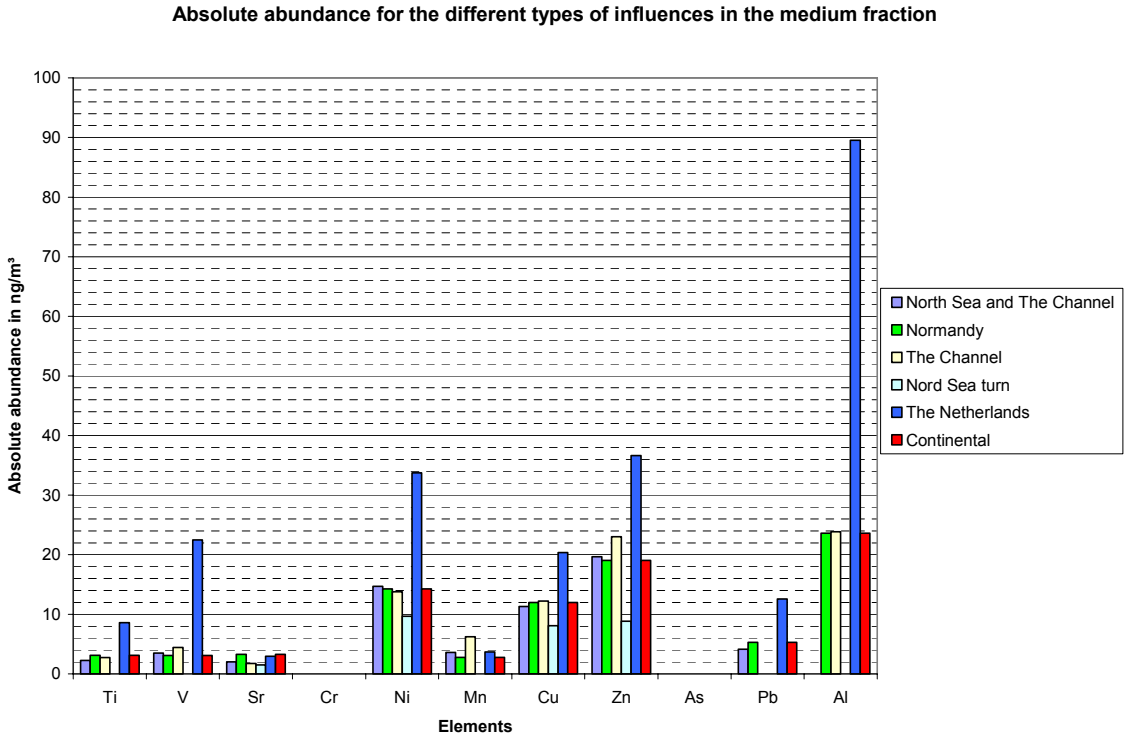

Figure 4.34 The absolute abundance in the fine fraction of the elements Ti, V, Sr, Cr, Ni, Mn, Cu, Zn, As, Pb and Al for the different influences

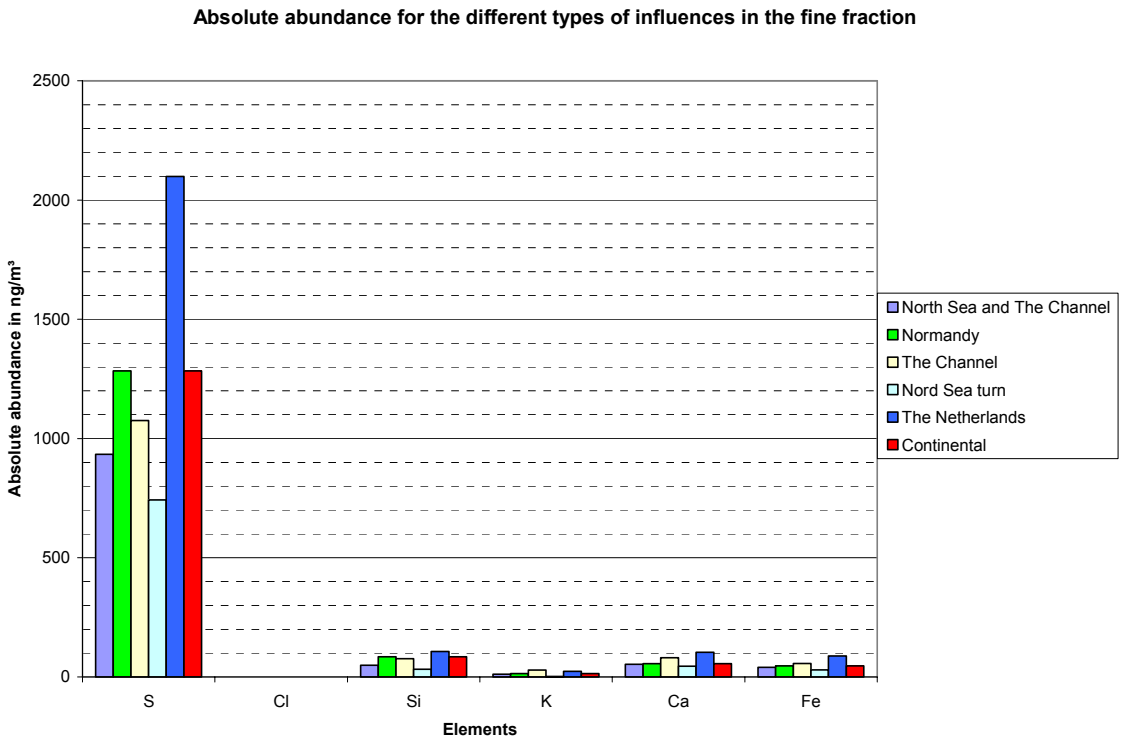

Figure 4.35 The absolute abundance in the ultra fine fraction of the elements S, Cl, Si, K, Fe and Ca for the different influences

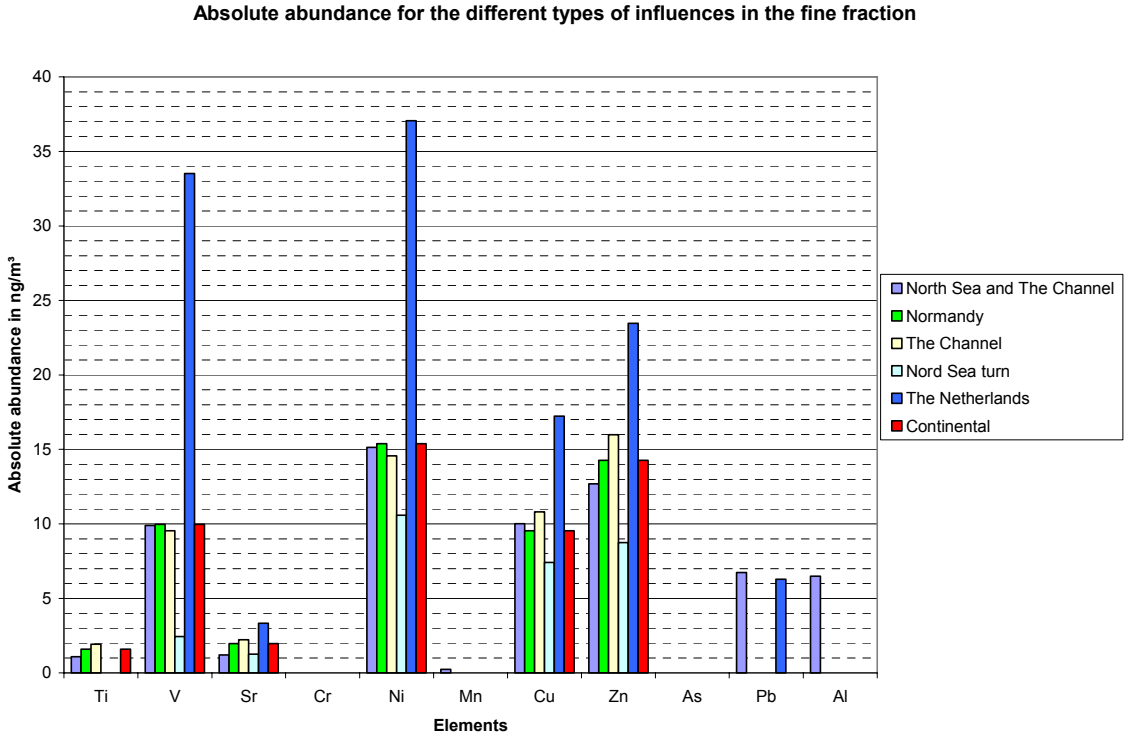

Figure 4.36 The absolute abundance in the fine fraction of the elements Ti, V, Sr, Cr, Ni, Mn, Cu, Zn, As, Pb and Al for the different influences